Charles University in Prague
Faculty of Science
Department of Experimental Plant Biology

Institute of Experimental Botany
Academy of Sciences of the Czech Republic
Laboratory of Hormonal Regulation in Plants

Martin Kubeš

The importance of plant proteins from ABCB subfamily in auxin transport

PhD Thesis

Prague 2011

Supervisor
Doc. RNDr. Eva Zažímalová, CSc.
Institute of Experimental Botany ASCR, Prague, Czech Republic
Department of Experimental Plant Biology, Faculty of Science, Charles University, Prague, Czech Republic

Consultants
Ing. Klára Hoyerová, PhD.
Institute of Experimental Botany ASCR, Prague, Czech Republic

RNDr. Jan Petrášek, PhD.
Institute of Experimental Botany ASCR, Prague, Czech Republic
Department of Experimental Plant Biology, Faculty of Science, Charles University, Prague, Czech Republic

Acknowledgements

First and foremost, I would like to thank to my supervisor Doc. RNDr. Eva Zažímalová, CSc. for leading and financial support during my PhD study.

I would like to thank to Ing. Klára Hoyerová, PhD. for her personal encouragement and support during my PhD study.

I would like to thank to RNDr. Jan Petrášek, PhD. for his inspiring ideas and support during my PhD study.

I wish to acknowledge all my colleagues from the Laboratory of Hormonal Regulation in Plants for help and pleasant working atmosphere.

My acknowledgement belongs also to my family (particularly to my parents) and my friends.

This PhD thesis can not originate without all co-authors of the original articles included in this thesis. Thanks a lot!

This work was supported by several local and international grant projects. Their numbers are specified in headings of respective chapters.

Statement

I hereby declare that the work presented in this thesis is my own and was carried out entirely with help of literature and aid cited in the thesis. This thesis is not a subject of any other defending procedure.

Prague, Czech Republic
July 18th, 2011 Mgr. Martin Kubeš

On behalf of the co-authors of the papers published, I hereby confirm the agreement with inclusion of the papers below into the dissertation thesis of Martin Kubeš. The papers were produced as a team work and the particular contribution of Martin Kubeš is specified at the beginning of relevant chapters of the thesis.

Prague, Czech Republic
July 18th, 2011 doc. RNDr. Eva Zažímalová, CSc.

Content

Abbreviations

1-NOA	1-naphthoxyacetic acid
2-NOA	2-naphthoxyacetic acid
2,4-D	2,4-dichlorophenoxyacetic acid
4-Cl-IAA	4-chloroindole-3-acetic acid
AAP	amino acid permeases
ABC	ATP-binding cassette
ABP1	auxin binding protein 1
ANT	aromatic and neutral amino acid transporter
Arabidopsis	*Arabidopsis thaliana* (L.) Heynh.
ARF	auxin response factor
ATF	amino acid transporter family
ATIs	auxin transport inhibitors
AUX1	AUXIN RESISTANT 1
AuxRE	auxin response element
AVP1	ATPase/ hydrogen-translocating pyrophosphatase (AVP1)
AXR4	AUXIN RESISTANT 4
BeA	benzoic acid
BFA	brefeldin A
BRET	bioluminescence resonance energy transfer
BUM	2-[4-(diethylamino)-2-hydroxybenzoyl] benzoic acid
BY-2	*Nicotiana tabacum* L. cv. Bright Yellow-2 cell suspension culture
CHPAA	3-chloro-4-hydroxyphenylacetic acid
CPD	2-carboxylphenyl-3-phenylpropan-1,3-dione
DEX	dexamethasone, (8*S*,9*R*,10*S*,11*S*,13*S*,14*S*,16*R*,17*R*)-9-Fluoro-11,17-dihydroxy-17-(2-hydroxyacetyl)-10,13,16-trimethyl-6,7,8,9,10,11,12,13,14,15,16,17-dodecahydro-3*H*-cyclopenta[*a*]phenanthren-3-one
DMSO	dimethyl sulfoxide
doxorubicin	(8*S*,10*S*)-10-(4-amino-5-hydroxy-6-methyl-tetrahydro-2*H*-pyran-2-yloxy)-6,8,11-trihydroxy-8-(2-hydroxyacetyl)-1-methoxy-7,8,9,10-tetrahydrotetracene-5,12-dione
ER	endoplasmic reticulum
EST	estradiol

FKBD	FK506-binding domain
FKBP	FK506-binding protein
FRAP	fluorescence recovery after photobleaching
gravacin	3-(5-[3,4-dichlorophenyl]-2-furyl) acrylic acid
HUGO	Human Genome Organization http://www.hugo-international.org/
IAA	indole-3-acetic acid
IAAld	indole-3-acetaldehyde
IBA	indole-3-butyric acid
LAX	LIKE AUXIN RESISTANT
LHTS	lysine histidine transporters
MDR	multidrug resistance
MRP	multidrug resistance associated
NAA	1-naphthaleneacetic acid
NAA-Glc	NAA glucosyl ester
NBD	nucleotide binding domain
NPA	1-naphthylphthalamic acid
NRT 1.1	nitrate transmembrane transporter
PAT	polar auxin transport
PDR	pleiotropic drug resistance
PGP	P-glycoprotein
P_i	inorganic phosphate
PM	plasma membrane
PPIase	peptidyl-prolyl cis-trans isomerase
ProT	proline transporters
ROS	reactive oxygen species
TIBA	2,3,5-triiodobenzoic acid
TMD	transmembrane domain
TWD1	twisted dwarf 1
verapamil	*(RS)*-2-(3,4-dimethoxyphenyl)-5-{[2-(3,4-dimethoxyphenyl)ethyl]-(methyl)amino}-2-prop-2-ylpentanenitrile
Xanthi	*Nicotiana tabacum* L. cv. Xanthi XHFD8 cell suspension culture

Summary

Polar auxin transport provides essential directional and positional information for many developmental processes in plants. At the cellular level, it is realized by both the passive diffusion and the active transport through the membrane proteins - AUX1/LAXes, PINs and ABCBs. The aim of this thesis was to characterize the role of ABCB1, ABCB4 and ABCB19 proteins in polar auxin transport using transformed tobacco BY-2 cell lines. It was shown that localization of the ABCB1, 4 and 19 is not polar on the plasma membrane (PM). The ABCB4 was also more stable on PM after the treatment with auxin influx inhibitors 1-NOA, 2-NOA and CHPAA; making use of ABCB4-cell line helped to uncover new characteristics of markers of endocytosis – the FM-dyes. The induction of ABCB19 has led to the decrease in ^{3}H-NAA accumulation with characteristic cell phenotype (cells ceased to divide, started to elongate and there was formed an increased amount of starch granules), similar to the PIN7 overexpressing cell line. Thus, also the ABCB-based enhanced auxin efflux resulted in depletion of auxin from cells, and concomitantly changed their developmental program. The auxin starvation phenotype in the cell line with induced overexpression of PIN7 could be rescued by application of the auxin efflux inhibitor NPA; however, the accumulation of auxin in the ABCB19-overexpressing cell line was less sensitive to NPA, and the rescue of the auxin starvation phenotype was ineffective there. Importantly, the unique property of the ABCB4 was demonstrated: It displayed the dual, auxin-concentration-dependent auxin transport activity in *Arabidopsis* roots, tobacco BY-2 and yeast cells. The results also suggested that the non-competitive inhibition of the ABCB4-mediated auxin efflux contributes to the herbicidal effects of the synthetic auxin analogue 2,4-D. Besides intercellular transport, there is another process with the potential to modify auxin level, the metabolism. Auxin metabolic profiles together with data from auxin transport assays were produced, and they allowed mathematical modelling of auxin transport on the cellular level by utilizing real quantitative experimental data. It was shown that NAA is strongly and rapidly metabolized in BY-2 cells and the predominant metabolite was identified as NAA glucosyl ester. This metabolite was retained in cells, thus raising apparent intracellular concentration of NAA previously measured during auxin accumulation experiments. This might lead to serious underestimation of auxin efflux carriers transport capacity for NAA as well as IAA measured in the past. The mathematical modelling using both experimental data on accumulation of auxins together with metabolic profiling is currently in progress.

Souhrn

Polární transport auxinu poskytuje základní informaci o směru a poloze pro řadu vývojových procesů v rostlinách. Na buněčné úrovni je uskutečňován jak pasivní difuzí tak aktivním transportem prostřednictvím membránových proteinů – AUX1/LAX, PIN a ABCB. Hlavním cílem této disertační práce bylo charakterizovat roli ABCB1, ABCB4 a ABCB19 proteinů v polárním transportu auxinu s využitím transformovaných tabákových BY-2 buněčných linií. Ukázalo se, že lokalizace ABCB1, 4 a 19 proteinů na plazmatické membráně je nepolární. Také ABCB4 protein na plazmatické membráně byl po ošetření inhibitory auxinového vtoku do buňky 1-NOA, 2-NOA a CHPAA více stabilní; navíc využití ABCB4 buněčné linie pomohlo odhalit nové vlastnosti endocytotických markerů – FM barviv. Indukce ABCB19 proteinu vedla ke snížení akumulace ^{3}H-NAA s charakteristickým buněčným fenotypem (buňky se přestávaly dělit, začaly se prodlužovat a docházelo k vytváření a zvětšování škrobových zrn), podobně jako u PIN7 overexprimované buněčné linie. Proto také zvýšený výtok auxinu způsobený overexpresí ABCB genů vedl k vyčerpání auxinu z buněk a současně ke změně jejich vývojového programu. Projev fenotypu auxinového hladovění v overexprimované buněčné linii PIN7 mohl být zvrácen aplikací inhibitoru auxinového výtoku NPA, zatímco v případě k NPA méně citlivé ABCB19 overexprimující buněčné linii ke zvrácení tohoto fenotypu nedošlo. Za důležité lze považovat, že se podařilo prokázat jedinečnou vlastnost ABCB4 proteinu: byla naznačena jeho duální koncentračně závislá funkce při transportu auxinu v kořenech *Arabidopsis*, tabákových BY-2 a kvasinkových buňkách. Výsledky také poukázaly na fakt, že nekompetitivní inhibice ABCB4 zprostředkovaného auxinového výtoku přispívá k herbicidním účinkům syntetického auxinového analogu 2,4-D. Kromě mezibuněčného transportu je zde metabolismus jako další proces s potenciálem měnit hladiny auxinu. Získané metabolické profily auxinů společně s údaji z auxinových transportních esejí nám umožnili modelovat auxinový transport na buněčné úrovni s využitím reálných kvantitativních experimentálních dat. Ukázalo se, že na úrovni BY-2 buněk je NAA silně a rychle metabolizována a převládající metabolit byl identifikován jako NAA glukosyl ester. Tento metabolit byl zadržován v buňkách, čímž dříve při auxinových akumulačních experimentech docházelo ke zdánlivému zvyšování naměřené intracelulární koncentrace NAA. To by mohlo vést k vážnému podcenění transportní kapacity auxinových přenašečů pro NAA, ale i IAA u dat naměřených v minulosti. V současné době probíhá matematické modelování využívající experimentální data z akumulací auxinů společně s daty z metabolických profilů.

Nomenclature of ABC genes and proteins

Naming of plant ABC genes proceeded initially on a gene-by-gene basis until the completion of the first drafts of the *Arabidopsis thaliana* and *Oryza sativa* genomes, which led to the publication of several partial and near-complete inventories of plant ABC genes (Sánchez-Fernández et al., 2001a; Martinoia et al., 2002; van den Brûle and Smart, 2002; Jasinski et al., 2003; Garcia et al., 2004; Crouzet et al., 2006; Sugiyama et al., 2006).

Although these publications have proved to be extremely useful, the independent identification of the same genes by several groups and the use of different naming systems by different authors have introduced several conflicting names into the literature. It was confusing to follow the ABC research field and so, together with accelerating completion of plant genome sequencing, the work on unified system of ABC genes nomenclature was initiated.

Verrier et al. (2008) proposed a simple naming system that provides a unique, systematic identifier for each gene. Currently, plant ABC subfamilies are usually named after their human or microbial prototypes (e.g. multidrug resistance (MDR), multidrug resistance associated protein (MRP) and pleiotropic drug resistance (PDR)) as prescribed by Sánchez-Fernández et al. (2001b). Therefore, Verrier et al. (2008) unified plant and animal ABC naming systems and proposed to adopt the Human Genome Organization (HUGO)-approved subfamily designations, which the vertebrate and invertebrate ABC communities used widely (Dean et al., 2001; Dean and Annilo, 2005). Aligning amino acid sequences of NBDs and performing phylogenetic analysis group most eukaryotic ABC proteins into eight major subfamilies (A–H) and prokaryotic ABC proteins into one subfamily (I), regardless of the species of origin. These subfamilies are largely defined by domain organization (configuration of domains in the protein) and content (presence of additional domains; half-size versus full-size transporters).

In this thesis, new nomenclature proposed by Verrier et al. (2008) is used but in some cases usage of old synonyms for ABCB genes like ABCB1/PGP1, ABCB19/MDR1/PGP19 and ABCB4/PGP4 could not be avoided. The “old” names were used mainly in papers published before the year 2008 and in all references from the same period. In those cases all relevant names for given gene/protein are used.

1. Introduction

The plant hormone auxin has a unique position among other plant growth regulatory substances. A wide spectrum of developmental processes in plants is controlled by the differential distribution of its molecules (Benjamins and Scheres, 2008). Moreover, mutual proportion between endogenous auxins and cytokinins is crucial for regulation of plant cell division, elongation and differentiation (Davies, 2004).

Various levels of auxins in plant tissues or organs are created in response to both exogenous stimuli and the internal developmental program, and thus they provide interconnection between environmental or endogenous signals and signalling pathways, resulting in particular developmental events. In principle, there are two processes that have the potential to modify the level of any compound in a cell: metabolism and intercellular transport. Indeed, in the case of auxin, both metabolic changes of auxin (reviewed by Normanly et al., 2010; Ludwig-Müller, 2011) as well as its transport (reviewed by Petrášek and Friml, 2009; Vanneste and Friml, 2009; Zažímalová and Murphy et al., 2010) have been shown to be involved in modulation of plant development.

The native auxin such as indole-3-acetic acid (IAA) mediates interactions between cells, tissues and organs over both short distances (e.g. between adjacent cells) and over long ones (e.g. between the shoot apex and sites of lateral root initiation) (Morris et al., 2004). The auxin cell-to-cell movement contributing to both short and long distance auxin flow is unique compared to other plant hormones; at the cellular level it is realized by both passive diffusion and active translocation across PM and it is mostly polar (Rubery and Sheldrake, 1974; Raven, 1975; Goldsmith, 1977). IAA transport plays a crucial role in the initiation and/or maintenance of cell and tissue polarity and axiality, upon which pattern formation depends (Morris et al., 2004). Generally, auxin determines - mostly via its polar transport - the shape of the plant (Friml, 2003).

The *Arabidopsis thaliana* genome encodes one AUX1 and three Like AUX1 (LAX1, LAX2 and LAX3) proteins (Parry et al., 2001a, b). As mentioned above, auxin molecules can enter cells passively; however, they can also be transported into cells via the H^+ - symport activity of this AUX1/LAX family of PM permeases (reviewed by Kerr and Bennett, 2007).

Previous studies have demonstrated that the polarized movement of auxin is dependent on the action of polarly localized and constitutively cycling PIN auxin efflux proteins (reviewed by Petrášek and Friml, 2009; Friml, 2010). In *Arabidopsis thaliana*, the PIN family consists of eight members and it divides into two basic subclades, differing in the length of a hydrophilic loop localized in the middle of their polypeptide chain (reviewed by Křeček and Skůpa et al., 2009).

Another proteins playing role in auxin influx and efflux are plant orthologs of mammalian ABC transporters from the ABCB (MDR/PGP) protein subfamily (Noh et al., 2001; Geisler et al., 2005). ABCB1 (PGP1) and ABCB19 (MDR1/PGP19) have been shown to act as auxin efflux carriers (reviewed by Geisler and Murphy, 2006; Titapiwatanakun and Murphy, 2009), whereas ABCB4 (PGP4) exhibits more complex auxin transport characteristics. Santelia et al. (2005) and Terasaka et al. (2005) showed that ABCB4 is involved in auxin transport processes controlling lateral root and root hair development in *Arabidopsis thaliana*, and it also functions in the basipetal redirection of auxin flow from the root tip. ABCB4 expression in tobacco BY-2 cells was shown to mediate NAA efflux (Cho et al., 2007), and the authors speculated about ABCB4 efflux activity which reduces auxin levels in the root hair cells and consequently inhibits root hair elongation. On the other hand, heterologous expression of ABCB4 in mammalian HeLa cells resulted in net increase of IAA retention indicating ABCB4 function in auxin uptake (Terasaka et al., 2005). The uptake activity of ABCB4 is not unexpected because it exhibits sequence homology with the berberine alkaloid uptake transporter CjMDR1/ABCB1 from *Coptis japonica* (Shitan et al., 2003). Moreover ABCB4 expression in *Schizosaccharomyces pombe* cells displayed a concentration-dependent reversal of IAA transport (Yang and Murphy, 2009). These facts have pointed to inconsistencies related to auxin transport activity and function of the plant ABCB4 protein.

Beside these PM-localised auxin transporters (AUX1/LAX, PINs and ABCBs) there are other proteins able to transport auxin. For instance, as recently published, *Arabidopsis thaliana* NRT1.1 nitrate transporter (reviewed by Gojon et al., 2011), which acts as a nitrate sensor and is crucial for nitrate signalling governing root growth, not only transports and senses nitrate but it also facilitates auxin uptake (Krouk et al., 2010, 2011). Moreover, nitrate inhibits the NRT1.1-dependent auxin uptake, suggesting that transduction of nitrate signal by NRT1.1 is associated with a modification of auxin transport. Similar properties could be expected also for other anion transporters, such as malate etc. (discussed in Zažímalová and Murphy et al. 2010).

Anyway, in spite of recent fast progress in understanding auxin transport, there are still a lot of open questions related to the mechanism of action of all types of auxin transporters and their role in plant development.

2. Outlines of the thesis

The first reviews touched the problematics of plant ABC proteins from the side of knowledge about their animal or human counterparts (Dudler and Hertig, 1992; Higgins, 1995). The main inspiration came from the multidrug resistance protein (MDR1), which was connected with a phenomenon described in mammalian tumor cells and their resistance to chemotherapeutics where tumor cells initially sensitive to a cytotoxic drug could evolve into a state in which they were not only resistant against the same drug but also against a wide variety of structurally unrelated drugs (reviewed by Endicott and Ling, 1989; Van der Bliek and Borst, 1989; Pastan and Gottesman, 1991). First information about plant ABC proteins structure and function were published at the beginning of this century (Davies and Coleman, 2000; Theodoulou, 2000; Sánchez-Fernández et al., 2001a, b; Martinoia et al., 2002; Rea et al., 2002). Simultaneously, Jasinski et al. (2003) and Garcia et al. (2004) indicated phylogenetic relationship between *Arabidopsis thaliana* and *Oryza sativa* ABC genes inside three main subfamilies (*ABCB/MDR*, *ABCC/MRP* and *ABCG/PDR*). *Arabidopsis thaliana* proteins from ABCC/MRP and ABCG/PDR subfamilies were more minutely described by Kolukisaoglu et al. (2002) and van den Brûle and Smart (2002).

In the collaboration with the laboratory of Dr. Jiří Friml, I have started the work by the successful transformation of inducible constructs carrying *ABCB1* and *ABCB19* genes into BY-2 cells. After the western blot verification of recombinant protein production and cell phenotype characterization I used these cell lines for auxin accumulation experiments. Results are shown in Chapter 1 of this thesis and published in Petrášek et al. (2006).

Besides the auxin accumulation experiments I have also tested some inhibitors of ABC proteins used in microbiology and human biology (like doxorubicin, vanadate, verapamil). Vanadate was shown to inhibit ATPase activity of ABC transporter for maltose (MalFGK2) of *Salmonella typhimurium* (Hunke et al., 1995) or ABC transport complex in *Escherichia coli* (Davidson et al., 1996). Later, Fetsch and Davidson (2002) described that vanadate catalyzes photocleavage of the signature motif LSGGQ and the nucleotide-binding (Walker A) motif of ABC maltose transport complex in *Escherichia coli*. Consecutively Terasaka et al. (2003) showed that vanadate-induced nucleotide trapping technique could be applicable to plant cells for characterizing ABC proteins expressed in berberine-producing cell cultures (*Thalictrum minus* and *Coptis japonica*). Loe et al. (2000) demonstrated that verapamil stimulates glutathione transport by MRP1 in tumor cells. Correspondigly, multidrug resistance is the most widely studied manifestations of tumor cells resistance to doxorubicin (Bradley et al., 1988). My goal was according to already mentioned drug effects to interfere with the intracellular localization or

the activity of ABCB19. Unfortunately, on the level of cell phenotype and viability no significant differences between treated and untreated cells were observed.

While ABCB1 and ABCB19 inducible lines of BY-2 were not stable, for later experiments it was necessary to repeatedly transform new BY-2 cells and work with freshly established lines. The other set of results that is presented in Chapter 2 of this thesis and published in Mravec et al. (2008) shows the phenotypical comparisons between inducible lines carrying various PIN genes with ABCB19 cells.

Apart from new BY-2 cell transformations I started together with Dr. Klára Hoyerová the accumulation assays in short and long stems (inflorescence) segments of *Arabidopsis thaliana* plants transformed with inducible *ABCB1* and *ABCB19* genes. We used partially modified methods of Goldsmith (1982) and Parry et al. (2001a). The importance of ABCB1 and ABCB19 for long-distance auxin transport in *Arabidopsis* plants was showed, while in induced ABCB1 and ABCB19 short stem segments the ^{3}H-NAA retention was enhanced comparing to wild-type control and non-induced variants. Moreover both used inhibitors gravacin and NPA increased net ^{3}H-NAA retention. Preliminary results were presented as a poster at the ACPD conference in Prague 2009.

As the continuation of my effort to address the auxin transporting role of ABCB proteins, I have moved my interest to the functionaly enigmatic ABCB4 protein. Despite several contrary results about ABCB4 auxin transport directionality (Terasaka et al., 2005; Santelia et al., 2005; Cho et al., 2007) together with indication of possible ABCB4 dual transport function (Yang and Murphy, 2009), nobody has provided conclusive evidence on the auxin transport directionality through this protein. I started with transformation of BY-2 cells with *ABCB4-YFP* from Dr. Hyung-Taeg Cho, but it was not successful. Therefore, I have contacted Dr. Angus Murphy for providing me with *ABCB4-GFP* gene construct under native and constitutive promoter. Transformation with this construct was successful and the localization of ABCB4 was characterized in terms of its membrane stability and helped to uncover new characteristics of FM endocytic dyes (Chapter 3 of this thesis; Jelínková and Malínská et al., 2010) as well as auxin influx inhibitors 1-NOA, 2-NOA and CHPAA (Chapter 4 of this thesis; Laňková et al., 2010). Concurrently I have initiated first ABCB4 auxin accumulation experiments. On ACPD conference in Prague 2009 I discussed with Dr. Angus Murphy my actual results and we started collaboration on ABCB4 dual transport function. We continued on BY-2 cell level and they contributed with *Arabidopsis thaliana* roots data and data from yeast IAA accumulation, where they confirmed ABCB4 concentration dependent dual transport function. Results are presented in the Chapter 5 of this thesis and manuscript is resubmitted in the Plant Journal.

Before starting ABCB4 story, I was welcomed to the project of my colleague Sibu Simon, where he was interested in the action of auxin and auxin analogues. The manuscript is submitted in the Chemistry&Biology journal. This manuscript is not included in submitted thesis but it is available electronically on the attached CD together with my contribution and specification of my results. During this project we were suspicious about the contamination or degradation of our radiolabeled auxins stocks. Thus I have started fruitful collaboration with Dr. Petre Dobrev. He did analysis of ^{3}H-2,4-D, ^{3}H-IAA and ^{3}H-NAA stocks used also by other colleagues in the lab and confirmed our suspicious in case of ^{3}H-IAA, where nearly 35% of IAA itself was degradated, in case of ^{3}H-NAA and ^{3}H-2,4-D it was about 5%. Later I found out that the reason for ^{3}H-IAA degradation was coming from the side of our suppliers and instability of this compound. From the auxin purity analysis on HPLC system, it was only small step to the routine metabolic profiling in cell cultures and plants.

Based on the ^{3}H-2,4-D, ^{3}H-IAA and ^{3}H-NAA metabolic profiles in BY-2 cells and cultivation media it was soon very clear that it is not possible to separate transport and metabolism, but it is necessary to think about both processes together. Moreover, combination of results from accumulation and metabolism in BY-2 cells allowed us to prepare mathematical model of auxin transport on the cellular level. This project was great challenge for all team members because it required teamwork between biologists and mathematicians. Our joint effort is presented in emerging interdisciplinary manuscript, presented as Chapter 6 of this thesis.

3. Objectives of the thesis

The main objective of this thesis was to contribute to understanding the role of ABCB1, ABCB4 and ABCB19 proteins (members of ATP-binding cassette (ABC) family of transporters) in polar auxin transport.

Particular objectives were:

1) To clarify the role of these proteins in polar auxin transport and to determine their intracellular localization.
2) To reveal possible interactions between ABCB and PIN proteins in plants.
3) To understand the kinetics of auxin transport by the ABCB4 protein.
4) To determine auxin metabolic profiles in tobacco BY-2 and Xanthi cell cultures as one of the prerequisites for the creation of mathematical model of auxin transport on the cellular level.
5) To optimize and assess the method of extraction and purification, suitable for determination of auxins by means of HPLC-tandem mass spectrometry, including identification of the main auxin metabolites in BY-2 cell culture.

4. Literature overview

4.1. The plant growth regulator - auxin

Although plants do not have typical animal long distance signalling mechanisms like nervous system, they developed alternative ways to establish cell-to-cell communication. One of them is transport of plant hormone auxin which represents an outstanding intercellular communication system in plants. Polarized auxin transport provides essential directional and positional information for developmental processes, such as vascular differentiation, apical dominance, patterning, organ polarity, embryogenesis, organogenesis, phyllotaxis or tropisms (Benková et al., 2003; Blancaflor and Masson, 2003; Blilou et al., 2005; Pekker et al., 2005; Weijers and Jurgens, 2005). Disruption of directional auxin movement by genetic or pharmacological manipulations results in severe developmental defects (reviewed by Friml, 2003). Although a detailed understanding of the molecular basis for the complexity of auxin activity has not yet emerged, progress during the past 15 years has led to identification of critical components of auxin signalling and provided a framework for addressing how auxin regulates diverse developmental processes.

4.2. Historical overview

The idea of plant hormones initially originated in the 19th century as Julius von Sachs supposed that plant organ-forming substances move directionally within the plant, including a root-forming substance produced in leaves that moves downward (Sachs, 1868). Concurrently Charles Darwin in his work "The power of movement in plants" described the phototropic experiments with canary grass (*Phalaris canariensis* L.) coleoptiles, and suggested the existence of a mobile substance which transmits the light sensing at the tip of the coleoptiles into differential growth at the base of the coleoptiles (Darwin, 1880). Five years later Salkowski isolated indole-3-acetic acid (IAA) from fermentation media (Salkowski, 1885) but the concept of the hormone itself, its isolation, purification from plants and characterization took another 50 years (Went, 1926; Went and Thimann, 1937). Went used small agar blocks on which he placed the coleoptiles tips of oat (*Avena sativa* L.) stems. The compound accumulated in the agar block resumed the growth of decapitated stems. Kogl and Haagen-Smit (1931) called the new compound an auxin. This name comes from the Greek word "auxein" which means to grow.

4.3. Auxin metabolism – biosynthesis, conjugation and catabolism

A key missing link in our understanding of auxin-regulated developmental processes in plants is that the molecular mechanisms of auxin biosynthesis are not known completely.

Without this knowledge it is difficult to understand the exact mechanism of auxin movement and how auxin gradients are created and maintained. The most abundant form of native auxin is IAA but plants produce also indole-3-butyric acid (IBA) (Cooper, 1935), phenyl acetic acid (PAA) (Koepfli et al., 1938) and 4-chloroindole-3-acetic acid (4-Cl-IAA) (Porter and Thimann, 1965). Because of the relative instability of natural auxins, the stable synthetic auxin analogues 1-naphthaleneacetic acid (NAA) and 2,4-dichlorophenoxyacetic acid (2,4-D) are used in most of the experiments (reviewed by Woodward and Bartel, 2005).

The synthesis of auxin in *Arabidopsis thaliana* occurs mainly in leaves, cotyledons and roots (Ljung et al., 2001; Ljung et al., 2005). Although multiple pathways including three tryptophan-dependent routes (with indole-3-pyruvic acid, indole-3-acetamide, indole-3-acetaldoxime, and tryptamine as main intermediates) and one tryptophan-independent route (with either indole-3-glycerol or indole as auxin precursors) are proposed to synthesize auxin in plants, the molecular details and the physiological roles of each pathway are not known (Bartel, 1997; Cohen et al., 2003; Woodward and Bartel, 2005). Also due to the high functional redundancy of auxin biosynthetic genes and the complexity of auxin synthesis it is difficult to fully characterize these pathways (Fig. 1; reviewed by Woodward and Bartel, 2005).

Research of auxin biosynthesis in plants appears to be very difficult, and no auxin-deficient mutant has ever been identified. However, there are several auxin overproduction *Arabidopsis thaliana* mutants including *yucca* (Zhao et al., 2001), *sur1* (Boerjan et al., 1995; King et al., 1995), *sur2* (Delarue et al., 1998), or overexpressing lines CYP79B2 and CYP83B1 (Delarue et al., 1998; Barlier et al., 2000; Zhao et al., 2002).

All three tryptophan-dependent pathways converge at indole-3-acetaldehyde (IAAld), which is oxidized by IAAld oxidase to IAA. Interestingly, an aldehyde oxidase is also involved in the final step of abscisic acid biosynthesis. IAAld oxidase activity has been measured in plants, and the small aldehyde oxidase gene family in *Arabidopsis thaliana* has been described (Sekimoto et al. 1998; Seo et al., 1998).

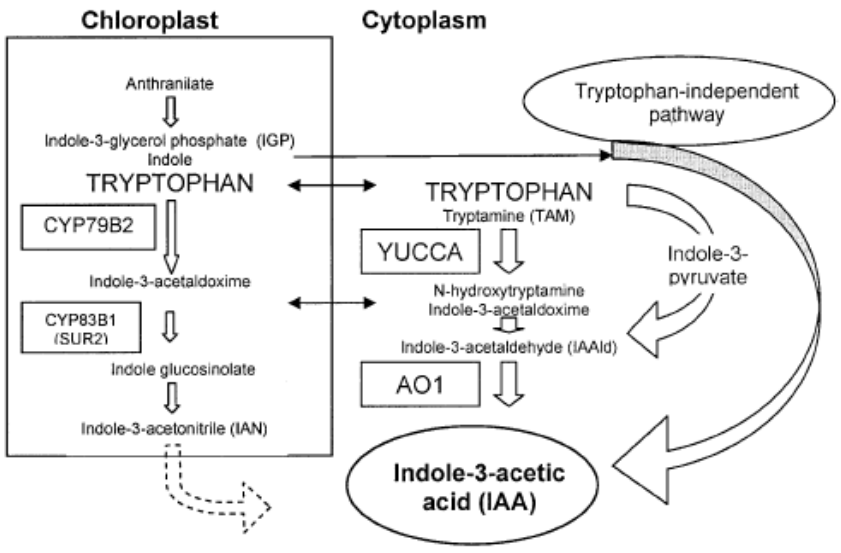

Figure 1. Parallel pathways for auxin biosynthesis
The dashed arrow illustrates the glucosinolate pathway restricted to few plant families. The long arrow on the right indicates the non-described tryptophan-independent pathway (adopted from Zažímalová and Napier, 2003).

Auxin conjugation and catabolism are other important players in auxin metabolism beside biosynthesis. Generally, active phytohormones are changed into multiple forms by range of chemical reactions like acylation, esterification or glycosylation. It seems that conjugated compounds can serve as a pool of inactive forms that can be converted to active forms by de-conjugation reactions. The concept of reversible conjugation of auxins suggests that under changeable conditions these compounds can be a source of free hormones. Auxin catabolism results in a loss of activity and decreases the size of the auxin bioactive pool. All catabolic steps are in principle irreversible, except for some processes such as the formation of ester, glucoside and amide conjugates in some plants (reviewed by Woodward and Bartel, 2005; Bajguz and Piotrowska, 2009; Ludwig-Müller, 2011).

For example, conjugation of IAA with amino-acids or sugars can follow after its synthesis probably as the way of storage or inactivation. IAA can be released after oxidation or hydrolysis of its conjugates (reviewed by Cohen and Bandurski, 1982). Free IAA is biologically inactivated by oxidation (e.g. to 2-oxindole-3-acetic acid) or by conjugation. Some of IAA conjugated to indole-3-acetyl-*N*-aspartic acid is further catabolized; however, conjugates are also used as storage compounds. IAA is conjugated in a variety of ways – as amides to amino acids, peptides and proteins, and to sugars through both ester and N-linkages. Conjugate hydrolysis releases free IAA, and such hydrolysis is the principal source of auxin in germinating seeds. It seems that conjugates are also transported within the plants (Zažímalová and Napier, 2003).

The molecular details (e.g. molecular mechanisms of auxin biosynthesis, conjugation and degradation together with the action of particular enzymes), physiological roles of each biosynthetic pathway and evolutionary context are the subjects of intensive study (reviewed by Cooke et al., 2002; Normanly 2010; De Smet et al., 2011; Ludwig-Müller 2011).

4.4. Auxin signalling

Proper auxin signalling is indispensable for plant growth and development (reviewed by Santner et al., 2009; Santner and Estelle, 2009) and in plant cells auxin triggers specific genomic and non-genomic responses. The identification and characterization of plant mutants defective in response to auxin led to the disclosure of downstream components of genomic auxin signalling (reviewed in Mockaitis and Estelle, 2008; Calderon-Villalobos et al., 2010). It turned out, that regulated protein degradation is the main factor in auxin transcriptional regulation (reviewed by Paciorek and Friml, 2006). Genome-wide studies indicate that the transcriptional response to auxin is rapid and broad, influencing the expression of a large and diverse set of genes within minutes (Tian et al., 2002; Goda et al., 2004; Overvoorde et al., 2005; Nemhauser et al., 2006).

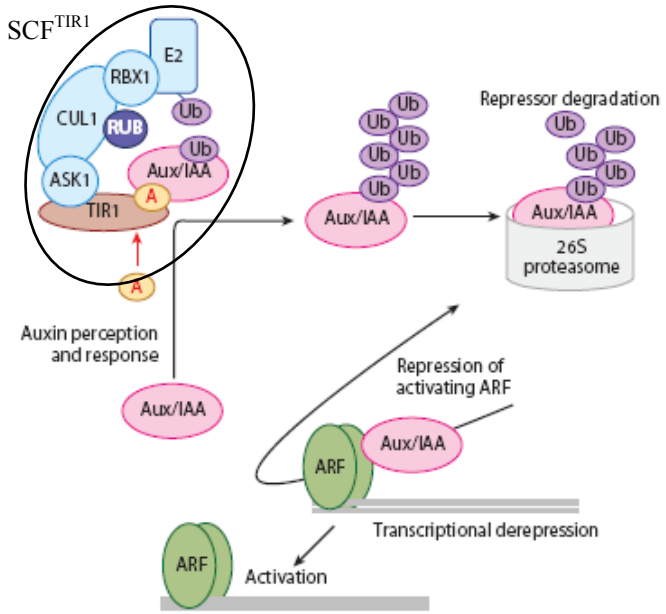

Figure 2. Auxin regulates transcription by promoting ubiquitin (Ub)-mediated degradation of Aux/IAA repressors
Auxin (A) binds to the F-box protein TIR1 in SCF^{TIR1} and stabilizes the interaction between TIR1 and an Aux/IAA substrate. The repressor is polyubiquitinated and degraded by the 26S proteasome. Loss of the Aux/IAA permits auxin response factor (ARF)-dependent transcription of auxin regulated genes. E2, (Ub)-conjugating enzyme (adopted from Mockaitis and Estelle, 2008).

TIR1 F-box protein is the auxin receptor (Dharmasiri et al., 2005a, b; Kepinsky and Leyser, 2005) which forms SKP1-like protein and CULLIN1 into the E3 ligase complex known as SCF^{TIR1} (Fig. 2; Gray et al., 1999; reviewed in Mockaitis and Estelle, 2008; Calderon-Villalobos et al., 2010). After auxin binding to TIR1, this complex promotes substrate ubiquitination and following proteasome-based degradation. The specific targets for this complex are Aux/IAA proteins (Conner et al., 1990; Abel et al., 1995; Gray et al., 2001). Aux/IAA proteins serve as the repressors of transcription factors called auxin response factors (ARFs) (Tiwari et al., 2001; Tiwari et al., 2003). After degradation of the Aux/IAA, the free ARFs can promote the transcription from specific promoters containing small conservative sequence TGTCTC called auxin response elements (AuxRE) (reviewed by Guilfoyle and Hagen, 2007). The huge amount of possible specific interactions among Aux/IAAs (29 genes) and ARFs (23 genes) suggest the way how autonomous auxin responses are mediated (reviewed in Weijers and Jurgens, 2004; Weijers et al., 2005).

However, auxin signalling does not include only transcriptional (genomic) regulation. For example, auxin efflux from the cells is also regulated via inhibition of endocytosis of auxin efflux carriers (and also other PM proteins) by unknown auxin-dependent and BIG-protein-dependent pathway (Paciorek et al., 2005).

A possible component of non-genomic auxin signalling is auxin binding protein 1 (ABP1), which was for the first time detected in membrane fractions from maize (*Zea mays* L.) etiolated coleoptiles (Hertel et al., 1972; Venis, 1977a, b). Later data revealed that ABP1 is targeted to ER and extracellular matrix (Leblanc et al., 1999; Bauly et al., 2000). Other studies demonstrated that ABP1 is involved in auxin binding at the PM and consecutively initiates a transduction pathway, including activation of the proton pump ATPase, acidification of the extracellular space and activation of inward rectifying K^+ channels (reviewed in Goldsmith,

1993; Timpte, 2001; Napier et al., 2002). Interestingly, mutant in *ABP1* gene in *Arabidopsis thaliana* is embryo lethal (Chen et al., 2001a), which suggests its important function in development. Recently, the function of ABP1 in auxin mediated cell division was proposed (David et al., 2007), but the precise role and the involvement in auxin signalling is still unclear. Tromas et al. (2010) reviewed the role of ABP1 in mediating growth and developmental responses together with phylogenetic analysis which revealed that ABP1 is an ancient protein that was already present in various algae and has acquired a motif of retention in ER only recently. Recently, Robert and Kleine-Vehn et al. (2010) demonstrated that ABP1 mediates a nontranscriptional auxin signalling that regulates the evolutionarily conserved process of clathrin-mediated endocytosis and they suggested that this signalling may be essential for the developmentally important feedback of auxin on its own transport.

4.5. Auxin transport - physical and chemical background

To perform its signalling function in plant, auxin must be spatio-temporally distributed and establishment of auxin concentration gradients depends on a tightly regulated transport. Long-distance auxin transport may be typically split in two ways: rapid auxin translocation through vascular system from source tissues to the roots and carrier mediated, slower cell-to-cell polar auxin transport (PAT) which mainly contributes to formation of auxin gradients in meristems (reviewed by Tanaka et al., 2006). The transport of auxin at the cellular level is realized by both passive diffusion and actively through the membrane proteins known as auxin carriers.

The key to understanding how auxin can move across the PM between two adjacent cells in polar orientation lies in the physical-chemical nature of auxin molecules and it was proposed by chemiosmotic hypothesis (Rubery and Sheldrake, 1974; Raven, 1975; Goldsmith, 1977). Because all native auxins are weak acids with amphipathic properties, their ability to penetrate through the PM depends on pH. In acidic apoplast the pH is approximately 5.5 as a result of protons extruded by PM H^+-ATPases and thus only non-dissociated and relatively lipophilic auxin molecules can passively enter the cell by diffusion across the PM. In the neutral cytoplasm (pH = 7.0) almost all auxin molecules are dissociated and trapped inside the cell, and they must be actively exported from the cell by specialized efflux carriers. The asymmetric distribution of auxin efflux carriers then can establish the polarity of auxin flow (Fig. 3; recently reviewed by Zažímalová and Murphy et al., 2010). This hypothesis was tested in the experiment, where decreased apoplastic pH in *Arabidopsis thaliana* overexpressing H^+- pyrophosphatase *AVP1* resulted in increased auxin transport (Li et al., 2005).

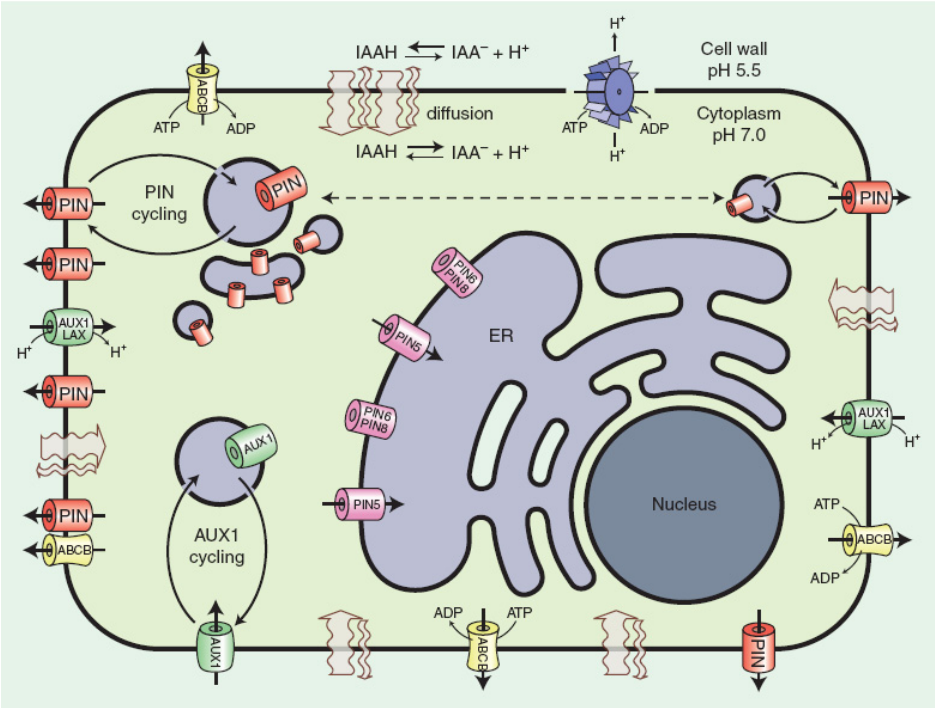

Figure 3. The scheme shows the organization of proteins involved in auxin transport PIN efflux carriers depicted in red represent "long" PINs (PIN1-4, 7), whereas PINs marked in pink represent "short" PINs (PIN5-6, 8) (see below). ER marks endoplasmic reticulum, pale blue structures represent ER and endosomes, curved bold full arrows show constitutive protein cycling, and dashed arrows symbolize the process of transcytosis. Possible collaboration between ABCBs and PINs is suggested by placing the symbols close to each other (adopted from Zažímalová and Murphy et al., 2010).

4.6. Auxin transporters

The previously described physical-chemical background implies the need for active transport of auxin out from the cells. Surprisingly, there are at least two protein families, members of which possess auxin-exporting activity. These are from the plant-specific PIN family (recently reviewed by Křeček and Skůpa et al., 2009, Petrášek and Friml, 2009) and from the B subfamily of ABC transporters (reviewed by Geisler and Murphy, 2006, Titapiwatanakun and Murphy, 2009). PINs are gradient-driven secondary transporters (carriers) while ABCBs are ATP-driven transporters (pumps). As mentioned previously, auxin molecules can enter cells passively; however, they can also be transported into cells via the H^+ symport activity of the AUX1/LAX family of PM permeases (reviewed by Kerr and Bennett, 2007).

The activities of the auxin influx and efflux carriers were described by measuring the cellular accumulation of ^{3}H-IAA, ^{3}H-NAA and ^{14}C-2,4-D in tobacco cell culture (*Nicotiana tabacum* L. cv. Xanthi XHFD8) (Delbarre et al., 1996) or in tobacco protoplasts (Delbarre et al., 1994). It was shown that NAA enters cells by passive diffusion and has its accumulation level controlled by the efflux carrier. In contrast, 2,4-D uptake is mostly driven by the influx carrier but, at least in tobacco cells, 2,4-D is a poor "substrate" for auxin-efflux carriers (Delbarre et al., 1996). Both auxin carriers, as well as passive diffusion into cells contribute to IAA accumulation. The relative contributions of diffusion and carrier-mediated influx and efflux to the membrane transport of 2,4-D, NAA and IAA have been quantified, and the data indicate that plant cells are able to modulate their auxin content by modifying the activity of each carrier (Delbarre et al., 1996).

4.6.1. Auxin influx carriers – AUX1/LAX family

Auxin influx carriers (AUX1/LAX), which mediate the uptake of auxin into the cell, belong to the ATF (amino acid transporter) family of proteins contain five distinct subclasses, AUX1/LAX, the amino acid permeases (AAP), the lysine histidine transporters (LHTs), the proline transporters (ProT) and the new aromatic and neutral amino acid transporter class (ANT) (Young et al., 1999; Ortiz-Lopez et al., 2000). The *Arabidopsis thaliana* genome encodes one AUX1 and three Like AUX1 (LAX1, LAX2, and LAX3) proteins, which amino acid sequence similarity is approximately 80% (Parry et al., 2001b). Chen et al. (2001b) reported that expression of ANT1 in yeast cells facilitates the uptake of both 2, 4-D and IAA, indicating its potential role also as an auxin carrier.

The first identified mutation in auxin influx carrier at the molecular level was presented by Maher and Martindale (1980) who identified the *aux1* mutation in screen for *Arabidopsis thaliana* seedlings less sensitive to 2,4-D. Later AUX1 was characterized at the molecular level in *Arabidopsis thaliana* by Bennett et al. (1996) and its transport function was confirmed by Yang et al. (2006). The *aux1* mutants exhibit reduced root gravitropism and decreased IAA transport in roots and young leaf primordia; further, *aux1* mutants are resistant to inhibitory concentrations of IAA and 2,4-D, but not to more lipophilic NAA (Marchant et al., 1999; Swarup et al., 2001). Because NAA diffuses into cells easily and it is a good substrate for auxin efflux carriers, gravitropic growth in *aux1* mutants is restored by treatment with NAA, but not with 2,4-D, which is taken up only actively - presumably via AUX1 - and it is a poor efflux carrier substrate (Marchant et al., 1999). The growth phenotypes of *aux1* mutants are phenocopied by treatment with the auxin influx inhibitors 1-NOA and CHPAA, which do not affect polar auxin efflux or sensitivity to NAA (Parry et al., 2001a). AUX1 functions in both root basipetal and acropetal auxin transport in a phloem-based auxin transport stream (Swarup et al., 2001). Consistent with this, AUX1 exhibits a basal PM localization in root protophloem cells, where it appears to function in conjunction with apically localized efflux carriers (Marchant et al., 1999; Swarup et al., 2001). Kramer and Bennett (2006) indicated that AUX1 together with other auxin efflux carriers plays a major role in redirection of polar auxin stream in the lateral root cap. Although AUX1 exhibits polar localization on the apical PM in some cells, in others, AUX1 exhibits a non-polar membrane distribution and is also accumulated at the Golgi apparatus and endosomal compartments. The connections between these PM and intercellular localizations have been shown to be dependent on actin filaments and the membrane sterols (Kleine-Vehn et al., 2006). Moreover, the apical localization of AUX1 on the PM of protophloem and epidermal cells requires the presence of AUXIN RESISTANT4 (AXR4), which is found in the ER (Dharmasiri et al., 2006).

Recently Laňková et al. (2010) examined the mechanism of action of the auxin influx inhibitors 1-naphthoxyacetic acid (1-NOA), 2-naphthoxyacetic acid (2-NOA) and 3-chloro-4-hydroxyphenylacetic acid (CHPAA) in transgenic BY-2 cell cultures. The mode of action of these inhibitors has been shown to be linked with the dynamics of the PM. The most potent inhibitor, 1-NOA, blocked the activities of both auxin influx and efflux carriers, whereas 2-NOA and CHPAA at the same concentration preferentially inhibited auxin influx. Laňková et al. (2010) also highlighted the importance of the rate of the particular vesicle trafficking process that may determine the extent of 1-NOA, 2-NOA, and CHPAA action on the PM dynamics.

The importance of AUX1/LAX carriers could be clearly demonstrated in many developmental processes. They are involved in embryogenesis (Ugartechea-Chirino et al., 2010), hypocotyl apical hook development (Vandenbussche et al., 2010), hypocotyl phototropism (Stone et al., 2008), root gravitropism (Bennett et al., 1996), lateral root development (Swarup et al., 2001; Swarup and Benková et al., 2008), root hair development (Jones et al., 2009), phloem loading and unloading (Marchant et al., 2002), and phyllotaxis (Bainbridge et al., 2008). Generally, the importance of auxin uptake carriers lies mainly in their role in the pumping of auxin against its concentration gradient. Mathematical modelling further supports the role of AUX1/LAX proteins in the creation of local auxin maxima as demonstrated for phyllotaxis (Smith et al., 2006).

4.6.2. Auxin efflux carriers - PIN family

The PIN-FORMED (PIN) proteins are plant specific secondary transporters (carriers) acting mostly in the efflux of auxin outside from cells. They are asymmetrically localized within cells and their polarity determines the directionality of intercellular auxin flow.

The first auxin efflux carriers were identified on the base of several *Arabidopsis thaliana* mutants: *agravitropic 1* (*agr1*) (Bell and Maher, 1990), *wavy roots 6* (*wav6*) (Okada and Shimura, 1990), *ethylene insensitive root 1* (*eir1*) (Roman et al., 1995), *pin-formed1* (*pin1*) (Okada et al., 1991). Later was proved, that PIN1 is a plant specific protein with characteristic structure (Gälweiler et al., 1998) and *AGR1*, *WAV6*, *EIR1* genes encode a homologous protein PIN2 (Chen et al., 1998; Luschnig et al., 1998; Müller et al., 1998; Utsuno et al., 1998). Okada et al. (1991), Müller et al. (1998) and Benková et al. (2003) confirmed that all these phenotypes can be phenocopied by exogenous application of auxin efflux inhibitor NPA.

In *Arabidopsis thaliana*, the PIN family consists of eight members and divides into two basic subfamilies according to the length of a hydrophilic loop in the middle of their polypeptide chain.

The “long” PINs (PIN1-4, and 7) are characteristic with the distinct central hydrophilic loop separating two hydrophobic domains (reviewed by Tanaka et al., 2006; Vieten et al., 2007; Křeček and Skůpa et al., 2009). The PIN1-4 and PIN7 proteins act as auxin efflux carriers and are localized at the PM where their polar localization determines the direction of auxin flow (Petrášek et al., 2006; Wisniewska et al., 2006). These “long” PINs have roles in many auxin-dependent processes in plant development (Luschnig et al., 1998; Friml et al., 2002a; 2002b; Blilou et al., 2005; Scarpella et al., 2006; Sauer et al., 2006; Xu et al., 2006). They do not stay statically in their PM domains, but undergo constitutive cycling between the PM and endosomal compartments (Geldner et al., 2001; Dhonukshe et al., 2007). The cycling is relatively fast between various parts of the cell using transcytosis-like mechanism (Kleine- Vehn et al., 2008). The polar localization of the “long” PINs and directional auxin flow are required for embryo development, organogenesis, tropisms, and other developmental processes (Friml et al., 2002b; Friml et al., 2003; Benková et al., 2003; Reinhardt et al., 2003; Blakeslee et al., 2005).

The “short” PINs (PIN5-6 and PIN8) have their central hydrophilic loop either partly (PIN6) or significantly (PIN5 and PIN8) reduced (Křeček and Skůpa et al., 2009). PIN5 has been proved as a functional auxin transporter and its localization on the ER suggests a role in intracellular auxin distribution or regulation of cellular auxin homeostasis, thus controlling availability of active auxin for various subcellular and cellular actions (Mravec et al., 2009). However, even though Mravec et al. (2009) showed PIN5 and PIN8 localization in ER, Ganguly et al. (2010) proposed that PIN8 also localizes in the PM. They showed that PIN8 catalyzes auxin efflux from tobacco BY-2 cells, that PIN8-GFP signal overlaps with FM4-64-labeled plasma membranes in *Arabidopsis thaliana* root hair and tobacco BY-2 cells (while the PIN5-GFP signal does not), that BFA causes the formation of PIN8-containing internal compartments both in *Arabidopsis thaliana* root hair and tobacco cells, and that PIN8 targets to the cell plate in dividing cells (while ER-localized PIN5-GFP does not). So, the mode of action of „short“ PINs is not fully understood yet.

PIN homologs in other plants have also been identified (Křeček and Skůpa et al., 2009), and some of them have been functionally characterized (reviewed by Petrášek and Friml, 2009).

4.6.2.1. Regulation of PIN function and polar targeting

The formation of auxin gradients depends mainly on the regulation of direction of auxin flow by differential AUX1/LAX, PIN and ABCB PM targeting. All of these transporters have been shown to be constitutively recycled between the PM and endosomal compartments.

PINs activity inside the cells is regulated at different levels: transcription (Blilou et al., 2005; Vieten et al., 2005), protein degradation (Abas et al., 2006), protein

phosphorylation/dephosphorylation (Friml et al., 2004; Lee and Cho, 2006; Michniewicz et al., 2007; Zhang et al., 2010) and vesicle trafficking (Steinmann et al., 1999; Geldner et al., 2001, 2003; Paciorek et al., 2005).

There are two possible regulators of the PIN polar localization, the Ser/Thr protein kinase PINOID (PID; Christensen et al., 2000; Benjamins et al., 2001; Friml et al., 2004; Sukumar et al., 2009) and the protein phosphatase 2A (PP2A; Zhou et al., 2004; Michniewicz et al., 2007). High levels of PIN phosphorylation caused by overexpression of *PID* or inhibition of *PP2A* lead to a preferential apical PIN targeting, whereas low phosphorylation levels in the *pid* mutants result in a preferential basal PIN targeting (Friml et al., 2004; Treml et al., 2005). Importantly, PID has been shown to directly phosphorylate the hydrophilic loop of PIN proteins while PP2A phosphatase has been shown to antagonize this (Michniewicz et al., 2007).

PIN proteins seem to be delivered originally in a non-polar orientation after *de novo* synthesis, and their polarity is established by internalization from the PM and polar recycling (Dhonukshe et al., 2008). Therefore, the secretion, clathrin-dependent endocytosis (Dhonukshe et al., 2007), and subsequent recycling are important processes in the PIN polar localization. On the contrary, in dividing cells, PIN proteins are delivered to the forming cell plate by the microtubule-dependent pathway (Geldner et al., 2001; Dhonukshe et al., 2006).

PIN proteins cycle continuously between endosomal compartments and the PM, it means exocytotically to the PM after *de novo* synthesis and endocytotically from PM to the endosomal compartments (Vanneste and Friml, 2009). The exocytosis requires the activity of GNOM protein, an endosomal ADP-ribosylation factor GTPase guanine nucleotide exchange factor (ARF-GEF) (Steinmann et al., 1999; Geldner et al., 2001; Richter et al., 2007), whereas endocytosis occurs in a clathrin-dependent manner (Dhonukshe et al., 2007) and depends on the sterol composition of the PM (Willemsen et al., 2003; Men et al., 2008), which also influences AUX1 (Kleine-Vehn et al., 2006) or ABCB trafficking (Titapiwatanakun et al., 2009; Titapiwatanakun and Murphy, 2009). GNOM seems to be more crucial for basal polar targeting, because the apical PM localization of PINs and AUX1 is not strongly affected when GNOM function is inhibited by BFA (Kleine-Vehn et al., 2008). SORTING NEXIN1 (SNX1) is another component which is involved in regulation of PIN1 cycling (Jaillais et al., 2007).

4.6.3. Auxin influx and efflux carriers – ABCB family

4.6.3.1. The ABC proteins – their discovery, structure and transport function

As it was already mentioned, discovery of ABC proteins is historically connected with the cancer research and with the quest for mechanism of multidrug resistance noticed in various cellular models. The ATP-binding cassette (ABC) proteins are members of the largest protein

superfamily with representatives in all phyla from prokaryotes to eukaryotes (Ames et al., 1992; Higgins, 1992; Rea, 2007; Rees et al., 2009). ABC proteins use the binding and hydrolysis of ATP to power the translocation of diverse substrates ranging from ions to macromolecules across impermeable membranes.

ABC transporters function as either importers or exporters, but no example has been known yet of an ABC transporter that could function physiologically in both directions. ABC importers are found in prokaryotes, in which they mediate the uptake of nutrients, such as amino acids, oligopeptides, oligosaccharides and essential metals. ABC exporters are found in both prokaryotes and eukaryotes, in which they mediate efflux of toxins, drugs and lipids (Kos and Ford, 2009; Rees et al., 2009). Perhaps the most studied ABC transporter is human MDR1, which maintains cholesterol distribution across the PM but it also extrudes other lipophilic compounds, including chemotherapeutics agents, resulting in the multidrug resistance of tumor cells (Ambudkar et al., 2003; Higgins, 2007). Surprisingly, ABC proteins are involved not only in transport of substrate across membranes but also in non-transport-related processes such as translation of RNA and DNA repair (Davidson et al., 2008).

The common structure of ABC transporters consists of two transmembrane domains (TMDs) and two cytoplasmic nucleotide-binding domains (NBDs) which catalyze nucleotide hydrolysis. In eukaryotes these four domains are frequently fused creating single polypeptide but almost any configuration of these domains in membrane can be found. ABC proteins are localized to PM or in organelle membranes but always on the cytoplasmic side of the membrane (Rea, 2007; Kos and Ford, 2009; Locher et al., 2009; Rees et al., 2009) (for details see Fig. 4).

TMDs which provide substrate recognition and its translocation across the PM contain 12 hydrophobic α-helices (in eukaryotes typically 6 per domain). The membrane-spanning subunits are structurally heterogeneous and currently there are recognized three distinct sets of folds: type I ABC importer (ModABC transporter from *Archeoglobus fulgidus* (Hollenstein et al., 2007a, b), $MalFGK_2$ transporter from *Escherichia coli* (Oldham et al., 2007), ModB transporter from *Methanosarcina acetivorans* (Gerber et al., 2008), MetNI transporter from *Escherichia coli* (Kadaba et al., 2008)), type II ABC importer (BtuCD transporter from *Escherichia coli* (Locher et al., 2002), Hi1470 and Hi1471 transporters from *Haemophilus influenzae* (Pinket et al., 2007), BtuCDF transporter from *Escherichia coli* (Hvorup et al., 2007)) and ABC exporter folds (Sav1866 transporter from *Staphylococcus aureus* (Dawson and Locher, 2006, 2007), MsbA transporter from *Salmonella typhimurium, Escherichia coli, Vibrio cholerae* (Ward et al., 2007)).

The NBDs structures are strongly conserved and serve as energy source for substrate translocation using energy released upon ATP hydrolysis. The TMDs are coupled to NBDs via helices which dock into cavities on the interfacial surface of the NBDs (Hollenstein et al., 2007a,

b). The NBDs can be further divided into two constituent domains: a catalytic core domain, which contains the conserved P-loop or Walker A motif, Walker B motif, Q-loop and H-motif; and a more structurally diverse α-helical domain, which contains the ABC signature motif LSGGQ (Schmitt et al., 2003). The Q loop is presumed to be involved in the interaction of the NBD and TMD, particularly in the coupling of nucleotide hydrolysis to the conformational changes of the TMD during substrate translocation. The *H motif* or switch region contains a highly conserved histidine residue that is also important for the interaction of the ABC domain with ATP (Davidson and Chen, 2004; Davidson et al., 2008).

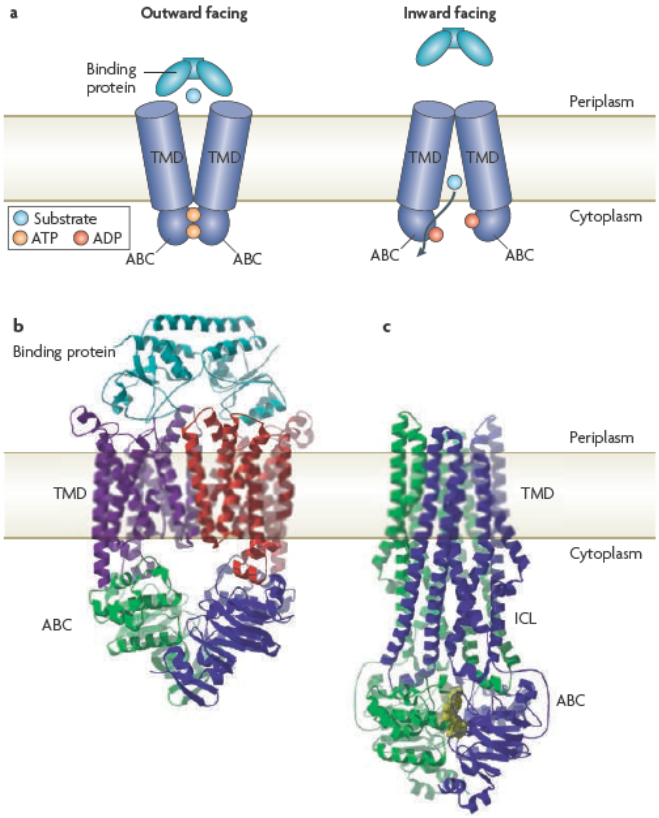

Figure 4. Molecular architecture of ABC transporters
a) Modular organization of ABC transporters, which are composed of two transmembrane domains (TMDs) and two ABC domains (or nucleotide-binding domains). The binding protein component that is required by importers is also shown. Two conformational states of the ABC transporter — outward facing and inward facing, with the substrate-binding site oriented towards the periplasmic (extracellular) and cytoplasmic (intracellular) regions, respectively — are depicted to show the alternating access mechanism of transport.
b) The *Escherichia coli* vitamin B12 importer BtuCDF22 consists of four subunits: the two TMD subunits (purple and red) and the two ABC subunits (green and blue). This complex also contains one copy the periplasmic binding protein (cyan).
c) The *Staphylococcus aureus* Sav1866 multidrug exporter consists of two subunits (green and dark blue), which contain a fused TMD and ABC domain. The nucleotides that are bound in this structure are shown by yellow space-filling models. ICL - intracellular loop, (adopted from Rees et al., 2009).

Export or import function seems to be determined by TMDs-NBDs interaction (Hollenstein et al., 2007a, b). Exporters have two intracellular loops from each TMD docked into NBDs in contrast to importers which are connected via one loop of each TMD.

The ABC dual transport activity, i.e. translocation of substrate in both directions in and out of the cell was not found out yet. However, Yang and Murphy (2009) indicated that ABCB4 expressed in *Schizosaccharomyces pombe* acts as an auxin importer under low substrate concentrations and as an auxin exporter under high substrate concentrations. Moreover, Yang and Murphy (2009) developed computational models of ABCB4 and ABCB19 based on the crystal structure of bacterial ABC transporter Sav1866 (Dawson and Locher, 2006). Structural comparisons indicate that ABCB4 and ABCB19 share a common architecture, but detailed sequence and structural analysis identified some differences. First, used COILS software program (http://www.ch.embnet.org/software/COILS_form.html) (Lupas et al., 1991) predicts

N-terminal coiled-coil structures in ABCB4 that are also found in the *Arabidopsis thaliana* ABCB14 guard cell malate importer (Lee et al., 2008), the *Coptis japonica* CjMDR1 putative berberine importer (Shitan et al., 2003), and ABCB21, a highly similar *Arabidopsis thaliana* ABCB protein (Verrier et al., 2008). No such N-terminal coiled-coil domain was found in the ABCB19 and ABCB1 exporters. Second, the hydrophobic region of TMH4 in ABCB4 is shifted below the membrane plane in the models and this fact could alter the TMD arrangement in ABCB4 and thus the direction of transport. Third, the linker domain of ABCB4, connecting NBD1 and TMD2, contains another coiled-coil structure, which is not found in the plant ABC importers CjMDR1, ABCB14 and ABCB21 or the ABCB1 and ABCB19 exporters, suggesting that this unique feature could also regulate ABCB4 activity. The switch between binding of the N-terminal coiled-coil domain to a binding protein or the linker coiled-coil domain could provide an explanation for the changeable directionality observed in ABCB4. Yang and Murphy (2009) also showed that IAA was primarily docked into two binding sites in the TMDs of ABCB19, while in ABCB4 the third unique binding site might function as a regulatory site, in which an interaction with IAA molecule activates export activity.

The high-resolution structures of eight intact ABC transporters (3 exporters and 5 importers) revealed different interactions between TMDs and NBDs and it seems that the substrate is probably one of the players responsible for conformational changes in the TMDs rather than passively transported molecule Kos and Ford (2009), and Rees et al. (2009).

At present time, three-dimensional structures of four complete ABC exporters are available including crystal structures of MsbA from *Escherichia coli* in an open conformation (Chang and Roth, 2001), as well as its homologs from *Vibrio cholerae* in a closed form (Chang, 2003) and from *Salmonella typhimurium* complexed with lipopolysaccharide and ADP-vanadate (Reyes and Chang, 2005); furthermore, the crystal structure of Sav1866 from *Staphylococcus aureus* is available (Dawson and Locher, 2006).

The structures of ABC proteins gave a view on their mode of action. Murakami et al. (2006) and Seeger et al. (2006) reported the structure of AcrB from *Escherichia coli* (for details see Fig. 5), transporter that uses the energy of the transmembrane proton gradient, while Dawson and Locher (2006) detailed the structure of Sav1866 from S*taphylococcus aureus*, transporter that derives its power from the breakdown of ATP molecules.

Schuldiner (2006) reviewed that the transport mechanisms of these two model proteins have a common feature: and inward-facing conformation with the substrate-binding site accessible from the cell interior, and an outward-facing conformation with an extrusion pocket exposed to the external medium. The transition between the two conformations is energy dependent. An important question for ABC transporters concerns the ratio of ATP hydrolysed

per translocated substrate, and whether or not there is a complete coupling of these processes under physiological conditions.

Figure 5. The structure of the AcrB–drug complex and proposed mechanism of drug transport

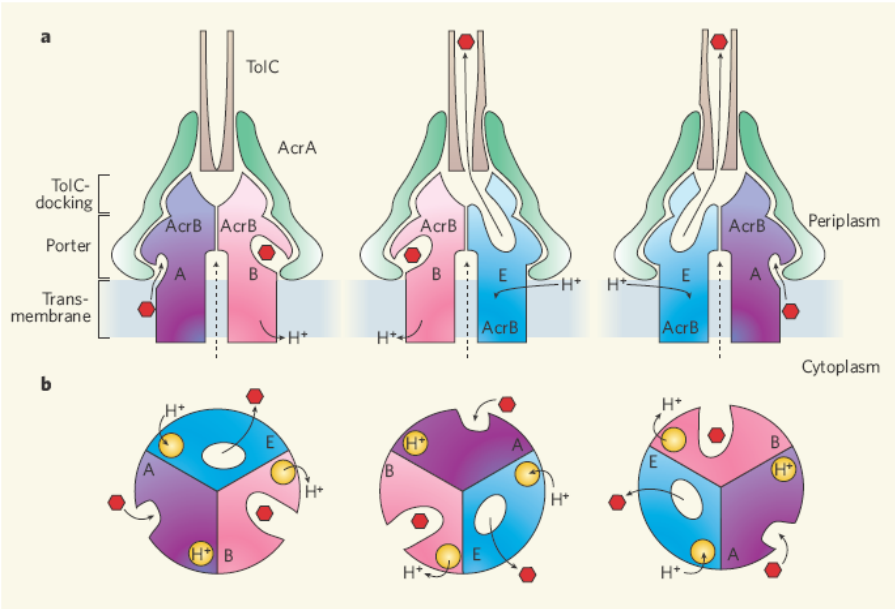

a) The complex is seen from the side, with the drug shown as a red hexagon. The dotted line indicates a possible pathway for substrates moving from the cytoplasm. The complex contains three molecules of AcrB, AcrA accessory proteins and the TolC channel to the exterior. The drug is proposed to enter AcrB when it is in the access (A) conformation, before binding more closely to the porter domain of AcrB in the binding (B) conformation. It is then transported to the opposite face and is released from the extrusion (E) conformation of AcrB. Transport of the xenobiotic is powered by the proton (H^+) gradient across the membrane. **b)** The proposed ordered multidrug binding change mechanism of the three-unit AcrB complex (adopted from Schuldiner, 2006).

The enzymatic hydrolysis of ATP requires the presence of two sets of properly positioned groups: for binding the phosphates and for catalysing the attack of water on the γ-phosphate. For a large family of nucleotide-binding proteins, including ABC transporters, the conserved Walker A and Walker B motifs participate by binding the nucleotide phosphates and the Mg^{2+} that is coordinated to the nucleotide, respectively (reviewed by Rees et al., 2009).

The mechanism that characterizes the conformational changes associated with binding of substrate is the "alternating-access model". In this model, the substrate binding site alternates between outward- and inward-facing conformations. The relative binding affinities of these two conformations for the substrate largely determines the net direction of transport. For importers the outward-facing conformation will have higher binding affinity for substrate whereas the substrate binding affinity in exporters will be greater in the inward-facing conformation (Rees et al., 2009).

A model that describes the conformational changes in the NBD as a result of ATP binding and hydrolysis is the "ATP-switch model". This model presents two principal conformations of the NBDs: formation of a closed dimer upon binding two ATP molecules and dissociation to an open dimer facilitated by ATP hydrolysis and release of inorganic phosphate (P_i) and adenosine diphosphate (ADP). Switching between the open and closed dimer conformations induces conformational changes in the TMD resulting in substrate translocation (Higgins and Linton, 2004) (for details see Fig. 6).

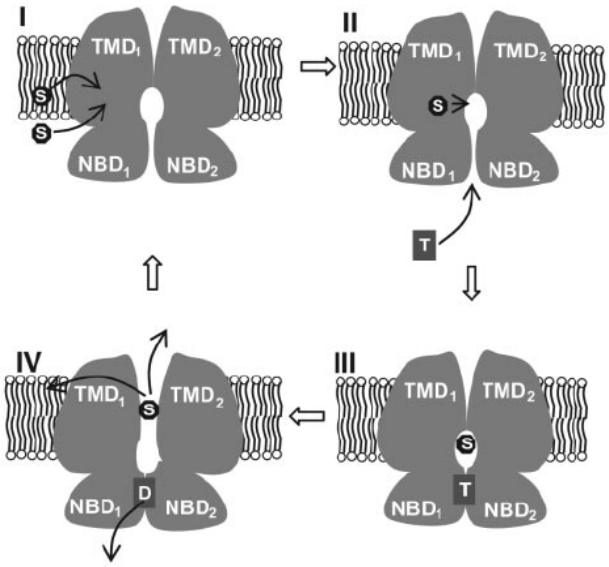

Figure 6. The figures schematize an ABC protein mediated transport
Substrate (S) coming from the cytosol or already within the membrane binds to a substrate binding site in one of the TMDs. This is followed by ATP (T) binding to the nucleotide-binding site localized at the interface between both NBDs. ATP binding and hydrolysis is accompanied by a structural rearrangement that allows the substrate to access to, and to be translocated through, a membrane path. Upon ADP (D) and phosphate dissociation, the protein returns to the initial state (adopted from Jasinsky et al., 2003).

However, general mechanism for the transport cycle of ABC transporters has not been fully elucidated but substantial structural and biochemical data has supported a model in which ATP binding and hydrolysis is coupled to transporter conformational changes.

4.6.3.2. Plant ABC proteins

The first complete inventory of the *Arabidopsis thaliana* ABC protein superfamily performed by Sánchez-Fernández et al. (2001b) revealed that the genome encodes 129 ABC proteins which were divided into 13 subfamilies (Fig. 7). Such a high number of plant ABC proteins is connected with their wide transport capacity together with exceptional metabolic versatility. More than 100 000 secondary metabolites have been identified in plants (*Arabidopsis* Genome Initiative, 2000), most of them would be toxic even in low concentrations, if they were not transported against steep concentration gradients across membranes out of the compartments in which they are synthesized (reviewed by Rea et al., 1998; Martinoia et al., 2000; Theodoulou, 2000; Yazaki, 2006). Later, Schulz and Kolukisaoglu (2006) brought new data from their phylogenomic analyses and Verrier et al. (2008) created new plant ABC proteins nomenclature.

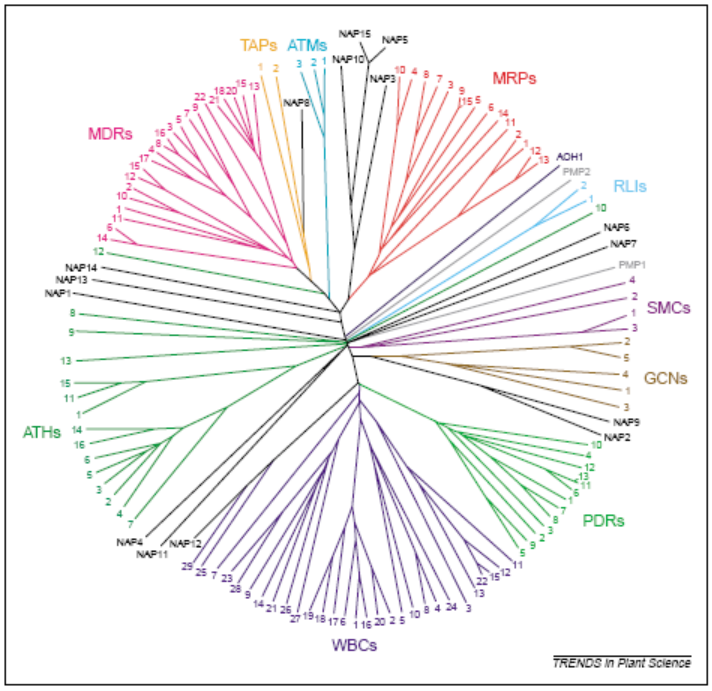

Figure 7. Phylogeny of *Arabidopsis* ABC proteins
The 13 subfamilies are shown in different colours. These are four subfamilies of full-molecule transporters (MDRs – multidrug resistance homologs, MRPs – multidrug resistance-associated protein homologs, PDRs – pleiotropic drug resistance homologs, AOH - ABC1 homolog), five subfamilies of half-molecule transporters (WBCs – white-brown complex homologs, ATHs – ABC2 homologs, ATMs – ABC transporter of the mitochondrion homologs, TAPs - transporter associated with antigen processing homologs and PMPs – peroxisomal membrane protein homologs) and four subfamilies of proteins lacking transmembrane spans (the RLIs – RNase L inhibitors homologs, GCNs – yeast GCN20, general control nonresponsible homologs, SMCs – structural maintenance of chromosomes homologs and NAPs – nonintrinsic ABC proteins) (adopted from Sánchez-Fernández R., 2001a).

Genome sequencing revealed 22 homologs to human and yeast MDR proteins in *Arabidopsis* (Sánchez-Fernández et al., 2001; Martinoia et al., 2002) and 17 homologs in rice (Jasinski et al., 2003), recently classified in ABCB protein subfamily (Verrier et al., 2008).

First plant homologue to mammalian *MDR* genes, the *ABCB1*, was cloned from *Arabidopsis thaliana* (Dudler and Hertig, 1992) with perspective to determine substrate specificity and find out its role in plant cells resistance to herbicides. The *ABCB1* homologue from barley (monocotyledonous plant) was isolated several years later (Davies, 1997). The first connection between ABCB1 and auxin transport was suggested by Sidler et al. (1998), when ABCB1 function in regulation of hypocotyl elongation has been proposed. Moreover, it was confirmed that the overexpression of ABCB1 protein causes resistance to herbicides (Windsor et al., 2003). Interestingly the compact stalk of agronomic important maize and sorghum mutants (*brachytic* (*br2*) and *dwarf* (*dw3*)) is caused by mutation in MDR-like gene (Multani et al., 2003). Later, Knöller et al. (2010) indicated that the function of ABCB1 in exporting auxin from meristematic regions is conserved in monocots and dicots, despite the pronounced differences observed in loss-of-function mutants (*br2* and *abcb1*).

Sidler et al. (1998) first demonstrated ABCB1 localization on PM. Later mainly apolar ABCBs cellular localization with partial apical localization in several tissues was proved (Geisler et al., 2005; Terasaka et al., 2005; Blakeslee et al., 2007; Cho et al., 2007).

Noh et al. (2001, 2003), Lin and Wang (2005) proved clear relation between auxin transport and ABCB1 or ABCB19 function, when they showed that *abcb1, abcb19* and double mutant as well exhibit pleiotropic growth phenotypes, like dwarf epinastic stature, curled leaves, and short stems and stamens. The *abcb19* and *abcb1abcb19* mutants also exhibit hypergravi- and hyperphototropic responses (Noh et al., 2003; Lin and Wang, 2005) and are defective in regulation of photomorphogenesis (Lin and Wang, 2005). Simultaneously high affinity binding of *Arabidopsis thaliana* ABCB1 and ABCB19 to the auxin efflux inhibitor NPA was confirmed (Noh et al., 2001; Murphy et al., 2002; Lin and Wang, 2005).

Polar auxin transport is reduced ~70% in *abcb1* and *abcb19*, while *pin1* exhibits a ~30% reduction (Blakeslee et al., 2007). However, *abcb* mutants show none of the defects in organogenesis that are seen in *pin1* (Noh et al., 2001). This suggests that ABCBs primarily regulate long-distance auxin transport and localized loading of auxin into the transport system and do not function in establishing the basal vectorial auxin flows that function in organogenesis (Bandyopadhyay et al., 2007; Blakeslee et al., 2007; Bailly et al., 2008).

The ability of ABCB1 and ABCB19 to mediate auxin efflux in a heterologous system (yeast, mammalian HeLa and tobacco BY-2 cells) was already confirmed (Geisler et al., 2005; Petrášek et al., 2006). In root hair growth and NAA transport assays in transformed BY-2

tobacco cells, ABCB4 seemed to function as an auxin exporter (Cho et al., 2007). While these studies showed ABCBs efflux activity, interestingly in ABCB4-transgenic and mutant plants auxin uptake activity was also observed. Similarly to *ABCB1* and *ABCB19, ABCB4* expression is upregulated by exogenous auxin. Furthermore, the *ABCB4* expression increases sensitivity of yeast for auxin and its analogues (Santelia et al., 2005). ABCB4 is strongly expressed in roots and regulates auxin distribution in lateral root cap thus affecting root gravitropism (Santelia et al., 2005, Terasaka et al., 2005). As it was already mentioned, ABCB4 exhibits structural similarity to the berberine uptake transporter CjMDR1/CjABCB1 from the medicinal plant *Coptis japonica* (Shitan et al., 2003) and, to a lesser extent, to the ABCB14 malate uptake transporter from *Arabidopsis thaliana* guard cells (Lee et al., 2008). The role of ABCB proteins (1, 4 and 19) in plant development and in cellular or long-distance auxin transport was reviewed by Geisler and Murphy (2006) and Rea (2007).

The enhancement of *ABCB19* expression in endodermal and pericycle cells which form the border of auxin streams suggested the inhibitory role of ABCB19 in auxin lateral movement. This was tested by measuring auxin "escape" from stellar stream by specially designed auxin transport assays (Bandyopadhyay et al., 2007; Blakeslee et al., 2007). Lewis et al. (2007) used *abcb1* and *abcb4* mutants to dissect the roles of two antiparallel auxin streams (acropetal and basipetal) in root growth and development and they confirmed importance of ABCB1 and ABCB4 transporters for root auxin transport, while they showed that mutations in *ABCB1* reduced acropetal auxin transport in roots by 80%, without affecting basipetal transport, and conversely, mutations in *ABCB4* blocked 50% of basipetal transport without affecting acropetal transport. (Wu et al., 2007) used the same mutants to investigate the role of the auxin transport streams in lateral root growth development.

A breakthrough into way of ABCBs action in auxin transport was revealing the role of ABCB1 and ABCB19 in PIN1 polar distribution in PM (Noh et al., 2003; Bandyopadhyay et al., 2007; Blakeslee et al., 2007; Titapiwatanakun et al., 2009; Titapiwatanakun and Murphy, 2009). When PINs and ABCBs are co-expressed in heterologous systems, their interaction enhances the rate of auxin efflux and increases the substrate specificity and efflux inhibitor sensitivity (Blakeslee et al., 2007). Moreover, the loss of auxin transport specificity was observed in *pin1* and *abcb19* mutants, which confirms the importance of coordinated ABCB-PIN action. On the other hand, the interaction between auxin influx carrier AUX1 and ABCB1 or ABCB19 was not observed. ABCBs and PINs exhibit overlapping expression patterns and co-localize in PIN polar domain (Blakeslee et al., 2007), but the mechanism of vesicular PIN1 trafficking is not involved in ABCB19 regulation (Titapiwatanakun et al., 2009; Titapiwatanakun and Murphy, 2009). Even if possible role of ABCB in PIN targeting was proposed (Noh et al., 2003), further analyses

showed that ABCB probably only stabilizes PINs in detergent resistant microdomains (Titapiwatanakun et al., 2009; Titapiwatanakun and Murphy, 2009) pointing at the composition of lipid membrane as an important factor in regulation of integral membrane proteins such as PINs and ABCBs. It was found that ABCB19 as well as PIN1 proteins are localized in sterol-rich detergent-resistant membrane fractions. In mutant *abcb19* PIN1 protein was not detected probably due to the loss of ABCB19-PIN1 interaction. The reason why PIN1 transport activity is not detected in *Saccharomyces cerevisiae* was probably a lack of such sterol-rich microdomains (Titapiwatanakun et al., 2009).

Relative to ABC proteins transport plasticity researchers were and are looking for specific ABC inhibitors to effectively block their function. NPA was initially used in affinity chromatography to isolate the ABCB1, 4, and 19 proteins (Murphy et al., 2002; Geisler et al., 2003; Terasaka et al., 2005). Murphy et al. (2002) also identified high and low affinity NPA binding sites in *Arabidopsis thaliana* membranes, consecutively FKBP immunophilin-like protein, TWD1/FKBP42 was co-purified with the ABCBs and it has been proposed to induce conformational changes in ABCB1 and ABCB19 (Geisler et al., 2003; Bouchard et al., 2006; Bailly et al., 2008) (for details about TWD1 see chapter 4.6.3.3.). Other inhibitor gravacin was originally identified as an inhibitor of gravitropic bending in hypocotyls (Surpin et al., 2005). Wild-type *Arabidopsis thaliana* seedlings treated with gravacin resulted in reductions of auxin transport that were similar to those seen in *abcb19*, while gravacin treatment of *abcb19* mutants resulted in further reductions in auxin transport (Rojas-Pierce et al., 2007). Treatment with gravacin did not alter the gravitropic response of *twd1*, and microsomes derived from *twd1* showed reduced binding to gravacin (Rojas-Pierce et al., 2007; Bailly et al., 2008). However, the immunolocalization of ABCB19 was unchanged in *twd1* mutants compared to wild type (Titapiwatanakun et al., 2009), suggesting that FKBP42 is more likely to function in activation, rather than localization of ABCB1/19 to the PM. Kim et al. (2010) identified BUM as another specific inhibitor of ABCB-related auxin transport.

Compared with the more dynamic processes regulating membrane localization of the AUX1 and PIN-family proteins, ABCB19 is more stably situated on the PM (Titapiwatanakun et al., 2009). Whereas the dynamic cycling of PIN1 is disrupted by short-term treatments with actin depolymerising compound latrunculin B (Geldner et al., 2001), the localization of ABCB19 is unaffected. Similarly ABCB19 subcellular localization is insensitive to short-term treatments with the microtubule depolymerizing compound oryzalin and is also insensitive to wortmannin (Titapiwatanakun et al., 2009). However, treatment with gravacin does interfere with the trafficking of ABCB19 to the PM resulting in aggregation of some ABCB19 protein in an unidentified compartment that does not co-localize with the endocytic marker FM4-64 (Rojas-

Pierce et al., 2007). As the trafficking of ABCB19 to the PM is not BFA-sensitive, it is not mediated by GNOM-dependent mechanisms (Titapiwatanakun et al., 2009). However, ABCB19 appears to be trafficked by GNOM-LIKE1 (GNL1), a BFA-insensitive ARF-GEF in the GNOM family that mediates vesicular ER-Golgi trafficking (Richter et al., 2007; Teh and Moore, 2007). In *Arabidopsis thaliana*, mutations in GNL1 exhibit a reduction in the abundance and PM localization of ABCB19, but not of PIN1 and PIN2. On the other hand, ABCB1 does aggregate in intracellular bodies with PIN2 after BFA treatment, suggesting that it is less stable and more readily endocytosed than ABCB19 (Blakeslee et al., 2007; Titapiwatanakun et al., 2009). This is even more likely, as ABCB1 exhibits stronger interactions with both FKBP42/TWD1 and the auxin transport inhibitor NPA (Murphy et al., 2002; Geisler et al., 2003; Bouchard et al., 2006; Bailly et al., 2008).

4.6.3.3. ABCB proteins are functionally regulated via immunophilin TWISTED DWARF 1

FK506-binding proteins (FKBPs), together with unrelated cyclophilins, belong to the immunophilins, an ancient and ubiquitous protein family (Schreiber, 1991; Harrar et al., 2001; He et al., 2004; Romano et al., 2004a, b). They were first described as receptors for immunosuppressive drugs in animal and human cells, FK506 and cyclosporine A, respectively (Schreiber, 1991). All FKBP-type immunophilins share a characteristic peptidyl-prolyl cis-trans isomerase domain (PPIase domain or FK506-binding domain (FKBD)) making protein folding a key feature among immunophilins (Schiene-Fischer and Yu, 2001; Bailly et al., 2006).

Immunophilins were shown to be distributed throughout the plant cell (Breiman et al., 1992; Luan et al., 1994), and it has been recently confirmed by detailed subcellular localization (e.g. Geisler et al., 2003; Bouchard et al., 2006). Twenty-three FKBP-type proteins have been identified in the *Arabidopsis thaliana* genome; however, their individual function is poorly understood. Anyway, the discovery of plant immunophilins has not only demonstrated conservation of these proteins in a full spectrum of biological systems but has also provided clues to their potential functions (Romano et al., 2004a, b). For example, some plant cyclophilin genes have been shown to be induced by a variety of biotic and abiotic stresses, suggesting that they may play a role in environmental response processes (Chou and Gasser, 1997; Kurek et al., 1999).

The FKBP domain of FKBP42 has been demonstrated to physically interact with the C-terminal NBDs of PM-localized transporters ABCB1 and ABCB19 (Geisler et al., 2003), whereas the TPR domain appears to be responsible for functional association with vacuolar transporters ABCC1 and ABCC2 (Geisler et al., 2004). The *Arabidopsis thaliana* mutant *twisted dwarf1* (*twd1)* Perez-Perez et al., 2004) lacks FKBP42 and displays a drastic pleiotropic auxin-

related phenotype that includes reduced development and cell elongation (dwarfism), and disoriented growth of all organs both on the epidermal and whole plant level (Geisler et al., 2003). Originally, Kamphausen et al. (2002) and Bouchard et al. (2006) predicted TWD1 to be membrane-localized (PM and tonoplast), but newly, Wu et al. (2010) showed TWD1 localization in ER, moreover they proved that mutations in *TWD1* caused mislocalization of ABCB1, ABCB4, and ABCB19 to the ER instead of PM comparing to unrelated PIN2 PM localization.

Earlier, ABCB1 and ABCB19 have been shown to directly mediate cellular auxin efflux (Geisler et al., 2005; Lin and Wang, 2005). Strikingly, the double mutant *abcb1/abcb19*, but not the corresponding single mutants, shares with *twd1* highly similar auxin-related phenotypes: dwarfism and agravitropic roots (Bailly et al., 2006; Bouchard et al., 2006). Bouchard et al. (2006) proved that cellular efflux of IAA from mutant cells is reduced compared with that from wild-type cells in the order wild type > *abcb1* > *abcb19* >> *abcb1/abcb19* ≥ *twd1*. Furthermore the overexpression of TWD1 has no effect on IAA export, whereas up-regulation of the ABC transporters ABCB1 and ABCB19 strongly enhances efflux. Expression and localization of PIN1 and PIN2 are not altered in *twd1*.

The simplest mechanistic model proposed TWD1-induced conformational changes in the C- termini of ABCB1 and ABCB19 increase ATP access to the second ATP-binding site of these proteins. In the absence of TWD1, the ATP-binding site would be blocked, leaving ABCB1/ABCB19 in an inactive state (Bouchard et al., 2006).

Recently, Bailly et al. (2008) reported specific disruption of ABCB-TWD1 interaction by NPA and flavonoids using BRET technique. This is in line with previous findings demonstrating NPA binding to plant ABCBs and inhibition of ABCB-mediated auxin transport by NPA (Santelia et al., 2005; Terasaka et al., 2005; Bouchard et al., 2006). In contrast to NPA, the auxin transport inhibitors (ATIs) 2,3,5-triiodobenzoic acid (TIBA) and 2-carboxylphenyl-3-phenylpropan-1,3-dione (CPD) had no significant effect on the ABCB1-TWD1 complex stability and auxin transport (Bailly et al., 2008). This is not unexpected, as TIBA is structurally unrelated and has been shown to displace NPA binding only partially and even to own weak auxin activity, suggesting a different locus and mode of action compared with NPA (Petrášek et al., 2003). Conversely, the flavonol quercetin was the most capable of disrupting ABCB1-TWD1 interaction (Bailly et al., 2008) probably due to the highest efficiency of quercetin in competing with NPA for auxin transporter binding sites (Jacobs and Rubery, 1988).

It seems reasonable to assume that impaired cell elongation and disoriented growth of *twd1* plants result from non-sufficient auxin transport and above all it supports the idea of TWD1 central position in ABCB-mediated auxin transport.

4.6.3.4. Regulation of ABCB proteins by flavonoids

Flavonoids are plant secondary polyphenolic metabolites and serve as important nutraceuticals. They have health-promoting effects, including antioxidant, anticarcinogenic, antiviral, and anti-inflammatory activities; however, the cellular targets of the *in vivo* protein remain largely unknown (Taylor and Grotewold, 2005; Morris and Zhang, 2006), apart from interactions of flavonoids with animal ABC transporters involved in drug absorption, distribution, excretion and resistance. Until now many studies have demonstrated inhibition of animal ABC transporters, mainly ABCB1, ABCC1, ABCC2 and ABCG2 by flavonoids (Morris and Zhang, 2006; Alvarez et al., 2010).

Flavonoids are widely distributed throughout the plant kingdom and are abundant in many flowers, fruits and leaves (reviewed by Winkel-Shirley, 2002; Taylor and Grotewold, 2005; Zhao and Dixon, 2009; Alvarez et al., 2010; Buer et al., 2010). In plants, besides playing a role in defence responses to environmental impacts (Treutter, 2005), allelopathy (Bais et al., 2006) or root nodule development (Subramanian et al., 2007; Mathesius, 2008) and modulating the levels of reactive oxygen species (ROS) (Taylor and Grotewold, 2005; Bais et al., 2006), they have been also shown to inhibit polar auxin transport (PAT) and consequently to enhance localized auxin accumulation (Stenlid, 1976; Marigo and Boudet, 1977; Jacobs and Rubery, 1988; Murphy et al., 2000; Brown et al., 2001; Peer et al., 2001, 2004, 2007). The regulatory impact of flavonoids on PAT was initially based on their ability to compete with NPA or herbicide for transporter binding sites. This concept is further supported by auxin-related phenotypes of *Arabidopsis thaliana* transparent testa mutants with altered flavonoids levels (Murphy et al., 2000; Brown et al., 2001; Peer et al., 2001, 2004; Taylor and Grotewold, 2005). At the present time flavonoids are considered to be transport regulators or modulators (Peer et al., 2007); nevertheless, the mechanisms by which flavonoids interfere with auxin efflux components are not yet clear.

It has been shown that treatment with flavonoids and mammalian MDR/PGP inhibitors reverse efflux of human MDR substrates to the point of net retention in mammalian cells (Zhang and Morris, 2003; Morris and Zhang, 2006). Consecutively it was confirmed that flavonoids are also functioning as inhibitors of plant ABCBs (Geisler et al., 2005; Terasaka et al., 2005; Bouchard et al., 2006), probably by mimicking ATP and competing for ABCB NBDs.

In addition to regulating ABCBs, a lack of flavonoids in *Arabidopsis thaliana* altered the expression and localisation of certain PIN proteins, and it was suggested that flavonoids could act by targeting PIN intracellular cycling, at least in the root tip. However, it is likely that PIN protein localisation is not regulated by flavonoids directly but by auxin localisation itself in a positive feedback loop (Peer et al., 2004). This could be regulated at the level of vesicle cycling

as auxin was shown to inhibit internalisation of PIN proteins mediated by BIG (calossin-like protein required for PAT), thus auxin could increase its own efflux from cells (Paciorek et al, 2005).

Studies in flavonoid-deficient *Arabidopsis thaliana* mutants confirmed that these plants had higher rates of auxin transport whereas mutants over accumulating flavonols show decreased auxin transport rates (Murphy et al., 2000; Brown et al, 2001; Peer et al., 2004). Flavonoids could be an ideal link between auxin transport and the environment because they are accumulated in response to a variety of environmental stimuli (Buer and Muday et al., 2004; Taylor and Grotewold, 2005). The co-localisation of flavonoids at sites of high auxin concentration supports their role in auxin transport control (Murphy et al., 2000; Peer et al., 2001; Buer and Muday, 2004; Buer et al., 2006).

Although we have lot of new information about flavonoids action in plants, there are still some questions connected with flavonoids activity e.g. what is their effect on AUX1 and LAX carriers or how much of free flavonoids remain in the cytoplasm to modulate the trafficking of the activity of auxin transporters?

Up to now, there is a lot of information about various auxin transporters and their role in plant development. However, there are also remaining open questions, many of them related to ABCB transporters and their mechanism of action in auxin transport.

5. Materials and Methods

5.1. Plant material

Cells of tobacco line BY-2 (*Nicotiana tabacum* L., cv. Bright-Yellow 2) (Nagata et al., 1992) were cultured in liquid medium (3% [w/v] sucrose, 4.3 $g.l^{-1}$ Murashige and Skoog salts, 100 $mg.l^{-1}$ inositol, 1 $mg.l^{-1}$ thiamin, 0.2 $mg.l^{-1}$ 2,4-D, and 200 $mg.l^{-1}$ KH_2PO_4 [pH 5.8]) in darkness at 26°C on an orbital incubator (Sanyo Gallenkamp, Schöeller Instruments Inc., Prague, Czech Republic; 150 rpm, 32 mm orbit) and subcultured weekly. Stock BY-2 calli were maintained on media solidified with 0.6% (w/v) agar and subcultured monthly. BY-2 cells were stably transformed by co-cultivation with *Agrobacterium tumefaciens* strain GV2260 carrying gene constructs with *Arabidopsis thaliana* genes under various promoters with various tags: pGVG::ABCB1-*myc* and pGVG::ABCB19-HA (Blakeslee et al., 2007), ABCB4::ABCB4:GFP (Cho et al., 2007), PIN1::PIN1:GFP (Benková et al., 2003) and pGVG::PIN7:GFP (Petrášek et al., 2006), as described in An et al. (1985) and Petrášek et al. (2003). The pGVG-ABCB1-*myc* and pGVG-ABCB19-HA plasmids were constructed by cloning the whole genomic coding region of *ABCB1* and *ABCB19* genes fused with the respective tag by primer extension PCR to pTA7002 (Aoyama and Chua, 1997), and transformed to the *UAS::GUS* (Weijers et al., 2003) line. Fifteen independent transgenic lines were analysed for each construct. Transgenic BY-2 cells and calli were maintained on the media supplemented with 40 $\mu g.ml^{-1}$ hygromycin or kanamycin and 100 µg.ml-1 cefotaxim. Expression of PIN and ABCB genes in tobacco cells was induced by the addition of dexamethasone or estradiol (DEX or EST, 1 µM, 24 hours, except for stated otherwise) at the beginning of the subcultivation period.

5.2. Expression and localization analysis

Tobacco RNA was isolated using the Plant RNA Qiagen Mini-Prep and RT-PCR performed using Qiagen® OneStep RT-PCR kits according to the manufacturer's protocols.

For Western Blots total protein fraction from GVG-ABCB19 and GVG-ABCB1 tobacco BY-2 cells was obtained after homogenization in liquid nitrogen. The frozen powder was then mixed with an equal volume of extraction buffer (50 mM Tris-HCl, pH 6.8; 2% (w/v) SDS; 36% (w/v) urea; 30% (w/v) glycerol; 5% (v/v) mercaptoethanol; 0.5 % (w/v) Bromphenol Blue), vortexed for 1 min, boiled for 3 min, and centrifuged at 13.000 rpm and 4°C for 5 min. The supernatant was transferred into a new tube and re-centrifuged at 13.000 rpm and 4°C for 5 min. The resulting supernatant was defined as total protein extract and stored at –20°C until use.

For immunolocalization GVG-ABCB19-HA and GVG-ABCB1-myc tobacco BY-2 cells were pre-fixed 30 min in 100 µM MBS and 30 min in 3.7% (w/v) PFA buffer consisting of 50

mM PIPES, 2 mM EGTA, 2 mM $MgSO_4$, (pH 6.9), at 25°C and subsequently in 3.7% (w/v) PFA and 1% Triton X-100 (w/v) in stabilizing buffer for 20 min. After treatment with an enzyme solution (1% (w/v) macerozyme and 0.2% (w/v) pectinase) for 7 min at 25°C and 20 min in ice cold methanol (at -20°C), the cells were attached to poly-L-lysine coated coverslips and treated with 1% (w/v) Triton X-100 in microtubule stabilizing buffer for 20 min. Then the cells were treated with 0.5% (w/v) bovine serum albumin in PBS and incubated with primary antibody for 45 min at 25°C. After washing with PBS, a secondary antibody in PBS was applied for 1 h at 25°C. Coverslips with cells were carefully washed in PBS, rinsed with water with Hoechst 33258 (0.1μg/ml) and embedded in Mowiol (Polysciences) solution. The following antibodies and dilutions were used: anti-HA (Sigma-Aldrich; 1:500), anti-*myc* (Sigma-Aldrich; 1:500), TRITC-(Sigma-Aldrich; 1:200), FITC-(Sigma-Aldrich; 1:200). Slides were observed using a microscope Nikon Eclipse E600 equipped with appropriate filter sets, DIC optics and color digital camera (DVC 1310C, USA).

5.3. Chemicals

Unless stated otherwise, all chemicals were supplied by Sigma-Aldrich, Inc. (St. Louis, USA). 1-naphthylphthalamic acid (NPA), was supplied by OlChemIm Ltd. (Olomouc, Czech Republic). ^{3}H-benzoic acid (BeA [4^{3H}]), ^{3}H-indole-3-acetic acid (IAA) and ^{3}H-2,4-dichlorophenoxyacetic acid (2,4-D) (all of specific radioactivity 20 Ci.mmol^{-1}) and ^{3}H-naphthalene-1-acetic acid (NAA) (specific radioactivity 25 Ci.mmol^{-1}) were supplied by American Radiolabeled Chemicals, Inc. (St. Louis, USA).

5.4. BY-2 cell microscopy

Cell densities were determined by counting cells in at least 8 aliquots of each sample using Fuchs-Rosenthal haemocytometer slide and inverted microscope Zeiss Axiovert 40C. Phenotype analyses (cell lengths and diameters) were observed with microscope Nicon Eclipse E600 (Japan) and images were grabbed with colour digital camera (DVC 1310C, USA) using LUCIA image analysis software (Laboratory Imaging, Prague, Czech Republic). For all in vivo observations Zeiss LSM510-DUO confocal microscope with a 40x C-Apochromat objective (NA=1.2W) was used.

5.5. Auxin accumulation assays in BY-2 cells

Auxin accumulation by two-day old cells was measured according to the Delbarre et al. (1996) as modified by Petrášek et al. (2006). Treatments were repeated at least two times and averaged values (± standard errors) were expressed as pmols of particular auxin accumulated per 10^6 cells. Depending on experiment, 10 μM 2-NOA or NPA (both from 50 mM DMSO stock) or

cold auxins 5 μM IAA and 2,4-D (50 mM ethanol stocks) were added at the beginning of the accumulation assay (together with the addition of radioactively labelled auxin) or 30 min before beginning of the accumulation assay (to increase inhibitor effect). The ^{3}H-2,4-D, ^{3}H-BeA, ^{3}H-IAA and ^{3}H-NAA were added to the cell suspension to give a final concentration of 2 nM. After a timed uptake period, 0.5-ml aliquots of cell suspension were collected and accumulation of label was terminated by rapid filtration under reduced pressure on 22-mm-diameter cellulose filters. The cell cakes and filters were transferred to scintillation vials, extracted in 0.5 ml of 96% ethanol for 30 min, and afterwards 4 ml of scintillation solution (EcoLite Liquid Scintilation Fluid, MP Biomedicals, Solon, USA) were added. Radioactivity was determined by liquid scintillation counter Packard Tri-Carb 2900TR (Packard-Canberra, Meridian, CT, USA) with automatic correction for quenching.

5.6. HPLC metabolic profiling

Two days old BY-2 cells were prepared for the experiment by equilibration in uptake buffer as for accumulation assays described (Petrášek et al., 2006). Experiments were done in uptake buffer and under standard cultivation conditions. Cells were incubated with addition of 20 nM ^{3}H-BeA, ^{3}H-IAA, ^{3}H-NAA and ^{3}H-2,4-D for a period of 0 and 10 min. Cells and media (uptake buffer) were collected and frozen (200 mg of fresh weight and 10 ml per sample). Extraction and purification of auxin metabolites in cells and media were performed as described (Dobrev and Kamínek, 2002, Dobrev et al., 2005). The radioactive metabolites were separated on HPLC. For this method column LunaC18 (2), 150 × 4.6 mm, 3 μm (Phenomenex, Torrance, CA, USA) was used, mobile phase A was 40 mM CH_3COONH_4, (pH 4.0) and mobile phase B was CH_3CN/CH_3OH, 1/1, (v/v). Flow rate was 0.6 ml min^{-1} with linear gradient 30–50 % B for 10 min, 50–100 % B for 1 min, 100 % B for 2 min, 10–30 % B for 1 min. The column eluate was monitored by a Ramona 2000 flow-through radioactivity detector (Raytest GmbH, Straubenhardt, Germany) after online mixing with three volumes (1.8 $ml.min^{-1}$) of liquid scintillation cocktail (Flo-Scint III, Perkin Elmer Life and Analytical Sciences, Shelton, CT, USA). The radioactive metabolites were identified on the basis of comparison of their retention times with authentic standards. For the results presentation the total integrated area of chromatogram plots was normalized based on the equalization of total accumulated radiolabel.

6. Results

6.1. Chapter 1 - PIN proteins perform a rate-limiting function in cellular auxin efflux

Jan Petrášek, Jozef Mravec, Rodoplhe Bouchard, Joshua J. Blakeslee, Melinda Abas, Daniela Seifertová, Justyna Wiśniewska, Zerihun Tadele, **Martin Kubeš**, Milada Čovanová, Pankaj Dhonukshe, Petr Skůpa, Eva Benková, Lucie Perry, Pavel Křeček, Ok Ran Lee, Gerald R. Fink, Markus Geisler, Angus S. Murphy, Christian Luschnig, Eva Zažímalová, Jiří Friml

Science 312, 914-918, 2006

This article is based on collaboration between Dr. Eva Zažímalová laboratory and several foreign laboratories. Here we have showed the specific and rate-limiting function of PIN proteins in cellular auxin efflux.

My contribution to this article was the transformation of BY-2 cells with GVG-ABCB19-HA construct, characterization of cell lines including expression analyses (RT-PCR, immunofluorescence localization and western blot) and auxin accumulation assays with radiolabeled auxins (see Fig. 4A, B, C below). My main finding is that the ABCB19-mediated NAA efflux was notably less sensitive to NPA compared to the PIN7-mediated auxin efflux.

Our part of this paper was supported by the Grant Agency of the Academy of Sciences of the Czech Republic, project A6038303 and the Ministry of Education of the Czech Republic, projectLC06034.

mobility and yield a charge of $12 \pm 2\ e^-$ per tubulin dimer under physiological conditions. This value may be important to elucidate the effect of in vivo electric forces on microtubules. Endogenous physiological electric fields, with a typical value up to 10^3 V/m, are shown to be involved in cell division, wound healing (*35*), and embryonic cell development (*36*), but their microscopic effect has so far not been understood. The application of biomotors in nanofabricated environments is an exciting development, offering novel possibilities for future developments in lab-on-chip sorting or purification applications.

References and Notes

1. R. K. Soong *et al.*, *Science* **290**, 1555 (2000).
2. F. Patolsky, Y. Weizmann, I. Willner, *Nat. Mater.* **3**, 692 (2004).
3. J. Xi, J. J. Schmidt, C. D. Montemagno, *Nat. Mater.* **4**, 180 (2005).
4. H. Hess, V. Vogel, *J. Biotechnol.* **82**, 67 (2001).
5. M. J. Schnitzer, S. M. Block, *Nature* **388**, 386 (1997).
6. K. J. Bohm, J. Beeg, G. M. zu Horste, R. Stracke, E. Unger, *IEEE Trans. Adv. Packag.* **28**, 571 (2005).
7. R. Yokokawa *et al.*, *Nano Lett.* **4**, 2265 (2004).
8. H. Hess, G. D. Bachand, V. Vogel, *Chemistry* **10**, 2110 (2004).
9. J. Clemmens *et al.*, *Langmuir* **19**, 10967 (2003).
10. S. G. Moorjani, L. Jia, T. N. Jackson, W. O. Hancock, *Nano Lett.* **3**, 633 (2003).
11. L. Jia, S. G. Moorjani, T. N. Jackson, W. O. Hancock, *Biomed. Microdevices* **6**, 67 (2004).
12. M. G. L. van den Heuvel, C. T. Butcher, S. G. Lemay, S. Diez, C. Dekker, *Nano Lett.* **5**, 235 (2005).
13. Y. Hiratsuka, T. Tada, K. Oiwa, T. Kanayama, T. Q. P. Uyeda, *Biophys. J.* **81**, 1555 (2001).
14. M. G. L. van den Heuvel, C. T. Butcher, R. M. M. Smeets, S. Diez, C. Dekker, *Nano Lett.* **5**, 1117 (2005).
15. S. Ramachandran, K. Ernst, G. D. Bachand, V. Vogel, H. Hess, *Small* **2**, 330 (2006).
16. R. Stracke, K. J. Bohm, L. Wollweber, J. A. Tuszynski, E. Unger, *Biochem. Biophys. Res. Commun.* **293**, 602 (2002).
17. Materials and methods are available as supporting information on *Science* Online.
18. At large fields, higher than ~110 kV/m, we observed an effect on the microtubule velocity along the electric field. Microtubules moving parallel to the electric field displayed higher and lower speeds depending on the direction of the field. For fields oriented perpendicular to the long axis, microtubules displayed sideward motion. We are investigating these effects.
19. T. Duke, T. E. Holy, S. Leibler, *Phys. Rev. Lett.* **74**, 330 (1995).
20. D. Stigter, *J. Phys. Chem.* **82**, 1417 (1978).
21. D. Stigter, C. Bustamante, *Biophys. J.* **75**, 1197 (1998).
22. The electrophoretic force on stationary microtubules in the absence of a bulk EOF consists of a direct force on the negative microtubule charge, $-|\sigma|\mathbf{E}$, and an opposing indirect friction, τ, exerted by the microtubule's counterions moving along the electric field. The velocity of the counterions increases from 0 at the microtubule surface to $|\mu_e|\mathbf{E}$. If $\lambda_D \ll R$, the magnitude of $\tau = +|\sigma|\mathbf{E} - c|\mu_e|\mathbf{E}$ and also equals the total force density exerted on the double layer, plus the drag force exerted on the moving counterions (*21*).
23. D. Stigter, *Biopolymers* **31**, 169 (1991).
24. The value of $g_\perp$ only depends on the ζ potential of a microtubule and the relative thickness of the double layer (λ_D) with respect to the cylinder radius a, i.e., $g_\perp = \Im(\zeta, a/\lambda_D)$, and numerical values have been tabulated (*20*). In the limit of infinitely small λ_D, $g_\perp$ reaches its maximum value of 1.5 and $\mu_{e,\perp} \rightarrow \mu_{e,\parallel}$. The experimentally determined value of $g_\perp$ is thus a measure of the ζ potential by $\zeta = \Im^{-1}(g_\perp, a/\lambda_D)$, using $a = 12.5$ nm and $\lambda_D = 0.8$ nm for the Debye length in our 160 mM buffer.
25. A. J. Hunt, F. Gittes, J. Howard, *Biophys. J.* **67**, 766 (1994).
26. We calculate $c_\perp$ using the analytical result from Hunt *et al*. (*25*) with the following numerical values: Microtubule radius $a = 12.5 \pm 1$ nm, viscosity $\eta = 0.89 \pm 0.09 \times 10^{-3}$ kg/ms, and $h = 30 \pm 10$ nm for the distance of the microtubule axis to the surface.
27. F. Gittes, B. Mickey, J. Nettleton, J. Howard, *J. Cell Biol.* **120**, 923 (1993).
28. H. Felgner, R. Frank, M. Schliwa, *J. Cell Sci.* **109**, 509 (1996).
29. For long microtubules and high kinesin density, the persistence length of the microtubule trajectory L_{tr} equals the persistence length of the tip L_p (*19*). This trajectory persistence length of microtubules in the absence of electric fields has been quantified to be 0.11 mm (*37*). Our value of the tip persistence length is close to this value. The suggestion of Kis *et al*. (*38*) that protofilament sliding reduces the stiffness of short lengths of microtubules could serve as a possible explanation of the low L_p, together with possible defects in the tip structure.
30. The use of the linear Grahame equation is strictly speaking only valid for $\zeta \ll k_BT/e = 26$ mV. However, at $\zeta = 50$ mV, the use of the linearized Grahame equation introduces an error in σ of only 14%. The use of the nonlinear version of the Grahame would invoke an unknown source of error, because we would then have to assume a value for the double-layer capacitance of the microtubule.
31. E. Nogales, S. G. Wolf, K. H. Downing, *Nature* **393**, 191 (1998).
32. P. S. Dittrich, P. Schwille, *Anal. Chem.* **75**, 5767 (2003).
33. A. Y. Fu, C. Spence, A. Scherer, F. H. Arnold, S. R. Quake, *Nat. Biotechnol.* **17**, 1109 (1999).
34. H. A. Stone, A. D. Stroock, A. Ajdari, *Annu. Rev. Fluid Mech.* **36**, 381 (2004).
35. B. Song, M. Zhao, J. V. Forrester, C. D. McCaig, *Proc. Natl. Acad. Sci. U.S.A.* **99**, 13577 (2002).
36. K. R. Robinson, L. F. Jaffe, *Science* **187**, 70 (1975).
37. T. Nitta, H. Hess, *Nano Lett.* **5**, 1337 (2005).
38. A. Kis *et al.*, *Phys. Rev. Lett.* **89**, 248101 (2002).

39. We thank J. Howard and S. Diez for kindly providing us with the kinesin expression vector and for advice with protocols; S. G. Lemay, I. Dujovne, and D. Stein for useful discussions; Y. Garini and Olympus Netherlands for lending optical equipment; and Hamamatsu Germany for kindly providing us a C7780 color camera. This work was funded by the Dutch Organization for Scientific Research (NWO) and the European Community Biomach program.

Supporting Online Material

www.sciencemag.org/cgi/content/full/312/5775/910/DC1
Materials and Methods
SOM Text
Figs. S1 and S2
References and Notes
Movie S1

23 December 2005; accepted 9 March 2006
10.1126/science.1124258

PIN Proteins Perform a Rate-Limiting Function in Cellular Auxin Efflux

Jan Petrášek,[1,2] Jozef Mravec,[3] Rodolphe Bouchard,[4] Joshua J. Blakeslee,[5] Melinda Abas,[6] Daniela Seifertová,[1,2,3] Justyna Wiśniewska,[3,7] Zerihun Tadele,[8] Martin Kubeš,[1,2] Milada Čovanová,[1,2] Pankaj Dhonukshe,[3] Petr Skůpa,[1,2] Eva Benková,[3] Lucie Perry,[1] Pavel Křeček,[1,2] Ok Ran Lee,[5] Gerald R. Fink,[9] Markus Geisler,[4] Angus S. Murphy,[5] Christian Luschnig,[6] Eva Zažímalová,[1]* Jiří Friml[3,10]

Intercellular flow of the phytohormone auxin underpins multiple developmental processes in plants. Plant-specific pin-formed (PIN) proteins and several phosphoglycoprotein (PGP) transporters are crucial factors in auxin transport–related development, yet the molecular function of PINs remains unknown. Here, we show that PINs mediate auxin efflux from mammalian and yeast cells without needing additional plant-specific factors. Conditional gain-of-function alleles and quantitative measurements of auxin accumulation in *Arabidopsis* and tobacco cultured cells revealed that the action of PINs in auxin efflux is distinct from PGP, rate-limiting, specific to auxins, and sensitive to auxin transport inhibitors. This suggests a direct involvement of PINs in catalyzing cellular auxin efflux.

Auxin, a regulatory compound, plays a major role in the spatial and temporal coordination of plant development (*1*–*3*). The directional active cell-to-cell transport controls asymmetric auxin distribution, which underlies multiple patterning and differential growth processes (*4*–*7*). Genetic approaches in *Arabidopsis thaliana* identified candidate genes coding for regulators of auxin transport, among them permease-like AUX1 (*8*), plant-specific PIN proteins (*9*) (fig. S1), and homologs of human multiple drug resistance transporters PGP1 and PGP19 (*10*, *11*). PGP1 has been shown to mediate the efflux of auxin from *Arabidopsis* protoplasts and heterologous systems such as yeast and HeLa cells (*12*). Similarly, PIN2 in yeast conferred decreased retention of structural auxin analogs (*13*, *14*). Plants defective in PIN function show altered auxin distribution and diverse developmental defects, all of which can be phenocopied by chemical inhibition of auxin efflux (*1*, *4*–*7*, *9*). All results demonstrate that PINs are essential components of the auxin transport machinery, but the exact mechanism of their action remains unclear.

Studies of the molecular function of PINs have been hampered mainly by the technical inability to quantitatively assess auxin flow across the plasma membrane (PM) in a multicellular system. We therefore established *Arabidopsis* cell suspension culture from the *XVE-PIN1* line, in which we placed the *PIN1* sequence under control of the estradiol-inducible promoter (*15*). Treatment with estradiol led to the activation of *PIN1* expression as shown by the coexpressed green fluorescent protein (GFP) reporter and reverse transcription polymerase chain reaction (RT-PCR) of *PIN1* in seedlings (Fig. 1A) and cultured cells (fig. S2). In estradiol-treated *XVE-PIN1* cells, the overexpressed PIN1 was localized at the PM (Fig. 1, B and C). The syn-

thetic auxin naphthalene-1-acetic acid (NAA) enters cells easily by diffusion and is a poor substrate for active uptake but an excellent substrate for active efflux (*16*). Therefore, change in accumulation of radioactively labeled NAA inside cells provides a measure of the rate of auxin efflux from cells. Untreated *XVE-PIN1* cells as well as nontransformed cells displayed [^{3}H]NAA accumulation kinetics indicative of saturable auxin efflux and sensitive to a well-established (*1*, *9*) noncompetitive inhibitor of auxin efflux: 1-naphthylphthalamic acid (NPA) (Fig. 1D). Estradiol did not influence control cells but led to substantial decrease of [^{3}H]NAA accumulation in *XVE-PIN1* cells (Fig. 1, D and E). This demonstrates that PIN1 overexpression leads to the stimulation of efflux of auxin from *Arabidopsis* cultured cells.

Arabidopsis cultured cells are not sufficiently friable to be useful in transport assays. Instead, we used tobacco BY-2 cells, a well-established model for quantitative studies of cellular auxin transport (*17*). PIN7, the most representative member of the subfamily including *PIN1*, *PIN2*, *PIN3*, *PIN4*, *PIN6*, and *PIN7* (fig. S1), was placed under the control of a dexamethasone (DEX)–inducible system (*18*) and stably transformed into BY-2 cells. The resulting line (*GVG-PIN7*) showed up-regulation of *PIN7* expression as early as 2 hours after DEX treatment and the up-regulated PIN7 protein was detected at the PM (Fig. 2A). Nontransformed cells displayed saturable, NPA-sensitive [^{3}H]NAA efflux, which was unaffected by DEX (Fig. 2B). Induction of expression of PIN7 or its close (PIN4) and the most distant (PIN6) homologs (fig. S1) resulted in a decrease in [^{3}H]NAA accumulation, to roughly half of the original level (Fig. 2C). The kinetics of NAA efflux after the initial loading of BY-2 cells (Fig. 2D), as well as displacement curves using competitive inhibition by nonlabeled NAA (fig. S3A), clearly confirm that PIN7 overexpression stimulates saturable efflux of auxin from cells. The efflux of other auxins—such as synthetic 2,4-dichlorophenoxyacetic acid (2,4-D) or naturally occurring indole-3-acetic acid (IAA), but not its precursor tryptophan—was also stimulated (Fig. 2, E and G). The PIN7-dependent efflux of all auxins was NPA sensitive (Fig. 2G), competitively inhibited by nonlabeled NAA, and unaffected by the structurally related but biologically inactive weak organic acid, benzoic acid (BeA) (fig. S3B). Furthermore, the increasing levels of induced PIN7, as achieved with the use of different concentrations of DEX for induction, and monitored by dot blot, clearly correlated with the gradual increase in [^{3}H]NAA efflux (Fig. 2F). These data imply that different PIN proteins are rate-limiting factors in NPA-sensitive, saturable efflux of auxins from BY-2 cells. This similarity in the molecular function of PINs, together with the diversity in their regulation, provides a basis for their complex functional redundancy observed in planta (*6*, *19*, *20*).

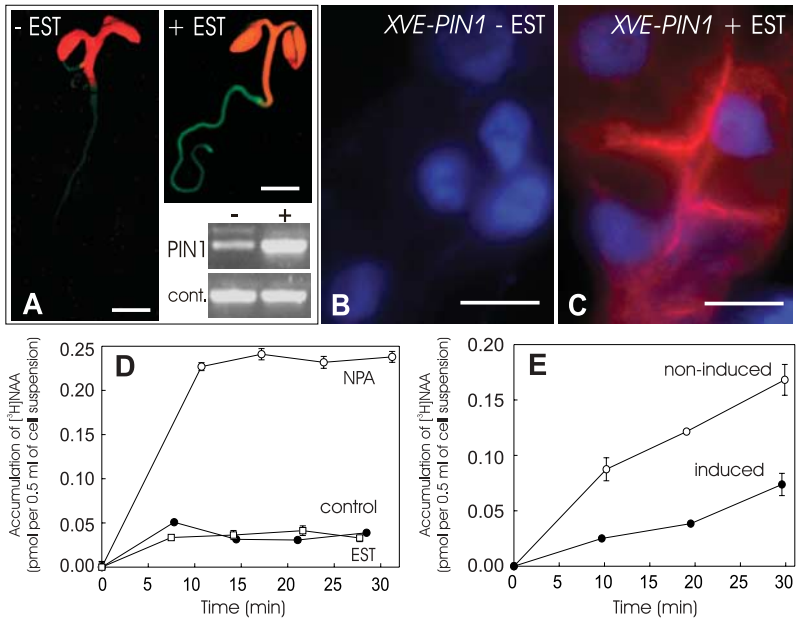

Fig. 1. PIN1-dependent auxin efflux in *Arabidopsis* cultured cells. (**A**) Up-regulation of PIN1 expression in *XVE-PIN1 Arabidopsis* seedlings after estradiol (EST) treatment (1 μM, 4 hours). The expression of coupled GFP reporter (green) and RT-PCR of *PIN1* [PGP19 expression was used as a control (cont.)] are shown. Scale bars, 3 mm. (**B** and **C**) Anti-PIN1 immunostaining (red) at the PM of *XVE-PIN1* cultured cells after EST treatment (1 μM, 24 hours) (C). There was no signal in the untreated control (B). Nuclear counterstain is shown in blue. Scale bars, 10 μm. (**D**) Auxin accumulation in *Arabidopsis* wild-type cells. NPA (10 μM) increased [^{3}H]NAA accumulation inside cells, demonstrating inhibition of auxin efflux. EST treatment (1 μM, 24 hours) had no effect on [^{3}H]NAA accumulation. (**E**) [^{3}H]NAA accumulation kinetics in *XVE-PIN1* cells, demonstrating PIN1-dependent stimulation of NAA efflux after PIN1 overexpression. Error bars show SEM (n = 4); where error bars are not shown, the error was smaller than the symbols.

The evidence from cultured cells shows that PIN proteins are key rate-limiting factors in cellular auxin efflux. This approach, however, cannot distinguish whether PINs play a catalytic role in auxin efflux or act as positive regulators of endogenous plant auxin efflux catalysts. To address this issue, we used a nonplant system: Human HeLa cells contain neither PIN-related genes nor auxin-related machinery and allow efficient heterologous expression of functional eukaryotic PM proteins (*21*). We transfected HeLa cells with *PIN7* and its more distant homolog *PIN2*. Transfected cells showed strong PIN expression (Fig. 3A), which resulted in a substantial stimulation of net efflux of natural auxin [^{3}H]IAA, compared with empty vector controls (Student's t test: $P < 0.001$) (Fig. 3B). Efflux of [^{3}H]BeA was also stimulated but to a lesser extent. These data show that PIN proteins are capable of stimulating cellular auxin efflux in the heterologous HeLa cell system, albeit with decreased substrate specificity.

To test the role of PIN proteins in another evolutionarily distant nonplant system, we used yeast (*Saccharomyces cerevisiae*). PIN2 and PIN7 were expressed in yeast and showed localization at the PM (Fig. 3A). Kinetics of relative [^{3}H]IAA retention demonstrated that expression of the PINs led to a substantial increase in IAA efflux (Fig. 3C). Efflux assays in conjunction with control experiments, including testing metabolically less active yeast in the stationary phase, or after glucose starvation (Fig. 3D), confirmed an active PIN-dependent export of IAA and, to a lesser extent, of BeA from yeast (Fig. 3C and fig. S4B). To test the requirements of the subcellular localization for PIN2 action in yeast, we performed a mutagenesis of the PIN2 sequence to isolate mistargeted mutants. One of the mutations, which changed serine-97 to glycine (pin2Gly97), led to the localization of pin2Gly97

[1]Institute of Experimental Botany, the Academy of Sciences of the Czech Republic, 165 02 Prague 6, Czech Republic. [2]Department of Plant Physiology, Faculty of Science, Charles University, 128 44 Prague 2, Czech Republic. [3]Center for Plant Molecular Biology (ZMBP), University Tübingen, D-72076 Tübingen, Germany. [4]Zurich-Basel Plant Science Center, University of Zurich, Institute of Plant Biology, CH 8007 Zurich, Switzerland. [5]Department of Horticulture, Purdue University, West Lafayette, IN 47907, USA. [6]Institute for Applied Genetics and Cell Biology, University of Natural Resources and Applied Life Sciences–Universität für Bodenkultur, A-1190 Wien, Austria. [7]Department of Biotechnology, Institute of General and Molecular Biology, 87-100 Toruń, Poland. [8]Institute of Plant Sciences, University of Bern, 3013 Bern, Switzerland. [9]Whitehead Institute for Biomedical Research, Nine Cambridge Center, Cambridge, MA 02142, USA. [10]Masaryk University, Department of Functional Genomics and Proteomics, Laboratory of Molecular Plant Physiology, Kamenice 5, 625 00 Brno, Czech Republic.

*To whom correspondence should be addressed. E-mail: eva.zazim@ueb.cas.cz

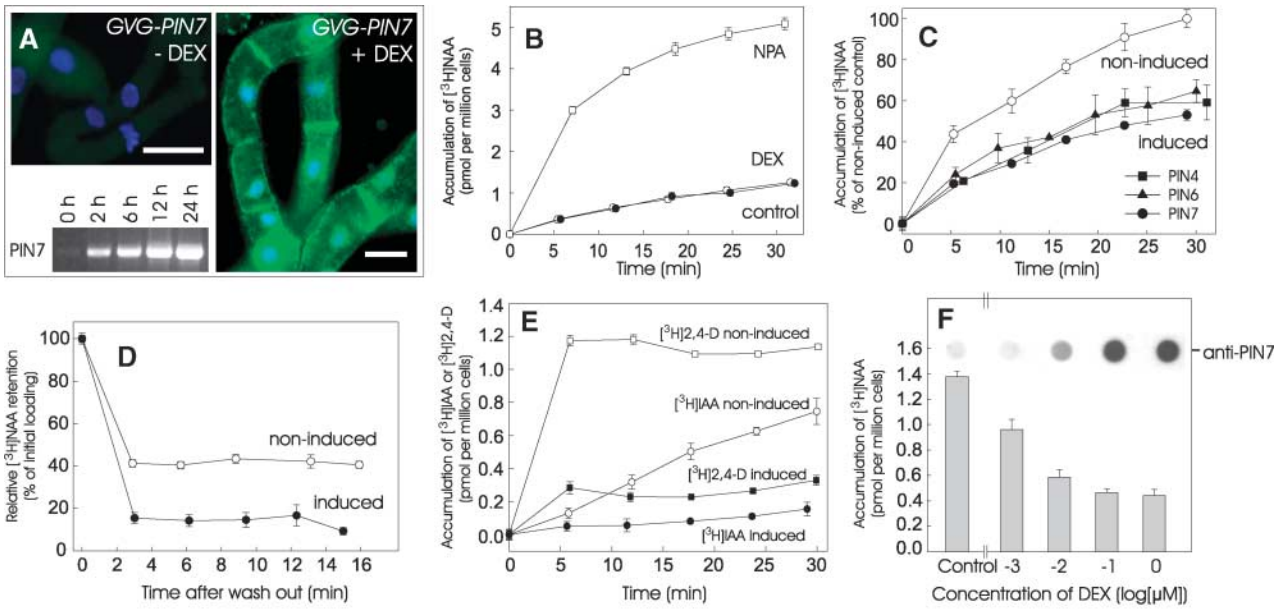

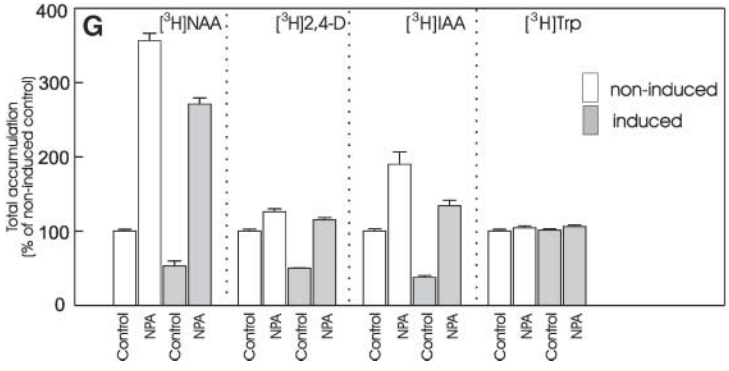

Fig. 2. PIN-dependent auxin efflux in BY-2 tobacco cultured cells. (**A**) Inducible PIN7 expression in *GVG-PIN7* tobacco cells. PIN7 immunostaining (green) is shown at the PM after DEX treatment (24 hours; 1 μM) but not in the untreated control; RT-PCR of *PIN7* was conducted within 24 hours of DEX treatment (1 μM). Nuclear counterstain is shown in blue. Scale bars, 40 μm. (**B**) Auxin accumulation in BY-2 control cells. NPA (10 μM) increased [^{3}H]NAA accumulation inside cells, demonstrating inhibition of auxin efflux. DEX treatment (1 μM, 24 hours) had no effect on [^{3}H]NAA accumulation. (**C**) [^{3}H]NAA accumulation kinetics in *GVG-PIN4*, *GVG-PIN6*, and *GVG-PIN7* cells demonstrating PIN4-, PIN6-, and PIN7-dependent stimulation of NAA efflux. Noninduced control is shown only for PIN7; those for PIN4 and PIN6 were within the range ±8% of the values for PIN7. Data are expressed as a percentage of noninduced control at 30 min after application of labeled [^{3}H]NAA. (**D**) Induced *GVG-PIN7* cells showed decreased retention of [^{3}H]NAA compared with noninduced control. (**E**) Accumulation kinetics in induced *GVG-PIN7* cells revealed PIN7-dependent stimulation of [^{3}H]IAA and [^{3}H]2,4-D efflux. (**F**) Treatments with increasing concentrations of DEX led to gradually higher levels of PIN7 in *GVG-PIN7* cells, as determined by dot blot (top) and to concomitant decrease of [^{3}H]NAA accumulation. (**G**) NPA inhibition of both endogenous and PIN7-dependent efflux of [^{3}H]NAA, [^{3}H]2,4-D, and [^{3}H]IAA. PIN7 overexpression or NPA treatment did not affect accumulation of related compound, [^{3}H]Trp. Open bars, noninduced cells; gray bars, induced cells. For all experiments, error bars show SEM (n = 4); where error bars are not shown, the error was smaller than the symbols.

in intracellular compartments (Fig. 3A). When tested in the [^{3}H]IAA efflux assay (fig. S4A), pin2Gly97 failed to mediate auxin efflux but rather increased [^{3}H]IAA accumulation inside cells (Fig. 3D). This shows that pin2Gly97 is still functional but fails to mediate auxin efflux, suggesting importance of PIN localization at PM. Overall, the results suggest that in yeast as well, PM-localized PIN proteins mediate, although with decreased specificity, a saturable efflux of auxin.

A role in auxin efflux has also been reported recently for PGP1 and, in particular, PGP19 proteins of *Arabidopsis* (*12*). PIN and PGP proteins seem to have a comparable effect on mediating auxin efflux in yeast and HeLa cells, but the genetic interference with their function in *Arabidopsis* has distinctive effects on development. All aspects of the *pin* mutant phenotypes can be mimicked by chemical interference with auxin transport (*4*–*7*, *9*). In contrast, *pgp1*/*pgp19* double mutants show strong but entirely different defects (*10*, *11*), which cannot be phenocopied by auxin transport inhibitors.

To compare the roles of PINs and PGPs in auxin efflux, we constructed the *GVG-PGP19:HA* (hemagglutinin) cell line of BY-2. DEX treatment led to the up-regulation of PGP19:HA protein, which was detected at the PM (Fig. 4A), and to a decrease in [^{3}H]NAA accumulation, similar to that observed in the *GVG-PIN4*, *GVG-PIN6*, and *GVG-PIN7* lines (Fig. 4B, compare with Fig. 2C). BeA did not interfere with [^{3}H]NAA accumulation and [^{3}H]Trp accumulation did not change after DEX treatment. However, compared with PIN-mediated auxin efflux, the PGP19-mediated NAA efflux was notably less sensitive to NPA. Whereas PIN-mediated transport was completely inhibited by NPA, about 20% of PGP19-dependent transport was NPA insensitive (Fig. 4C).

To address whether PIN action in planta requires PGP1 and PGP19 proteins, we analyzed effects of PIN1 overexpression on plant development in *pgp1*/*pgp19* double mutants. PIN1 overexpression in *XVE-PIN1* led to pronounced defects in root gravitropism, which could be detected within 4 hours after estradiol treatment. Quantitative evaluation of reorientation of root growth revealed that PIN1 overexpression in *pgp1*/*pgp19* had the same effects (Fig. 4D). These data show that PIN1 action on plant development does not strictly require function of PGP1 and PGP19 proteins, and they suggest that PINs and PGPs molecularly characterize distinct auxin transport systems. This is also supported by evidence that PIN2 mediates auxin efflux in yeast, which is known to lack homologs to *Arabidopsis* PGP proteins (*21*). It is still unclear whether these two auxin transport machineries act in planta entirely independently or in a coordinated fashion.

Rate-limiting, saturable, and specific action of PIN proteins in mediating auxin movement

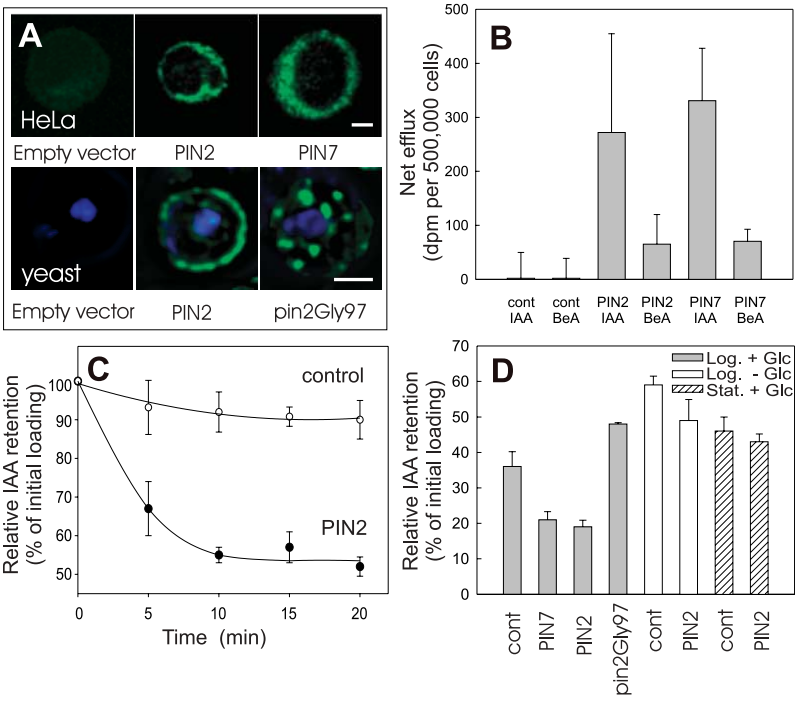

Fig. 3. PIN-dependent auxin efflux in mammalian and yeast cells. (**A**) PIN2:HA and PIN7:HA expression in HeLa and yeast. Anti-HA immunostaining detected PIN2:HA and PIN7:HA at the PM of transfected but not control (empty vector) HeLa cells (top). Anti-PIN2 immunostaining detected PIN2 at the PM and pin2Gly97 in intracellular compartments, compared with empty vector controls (bottom). Scale bars, 2 μm. (**B**) Transfected HeLa cells display PIN2- and PIN7-dependent net efflux of [^{3}H]IAA and to a smaller extent also of [^{3}H]BeA. dpm, disintegration per minute. (**C**) The kinetics of [^{3}H]IAA efflux. PIN2 stimulated saturable [^{3}H]IAA efflux in yeast JK93da strain. (**D**) [^{3}H]IAA retention measured 10 min after loading: PIN2 and PIN7 mediated [^{3}H]IAA efflux; pin2Gly97 failed to mediate efflux but increased [^{3}H]IAA retention. Yeast in stationary phase or without glucose showed much less [^{3}H]IAA efflux. Error bars show SEM (n = 4).

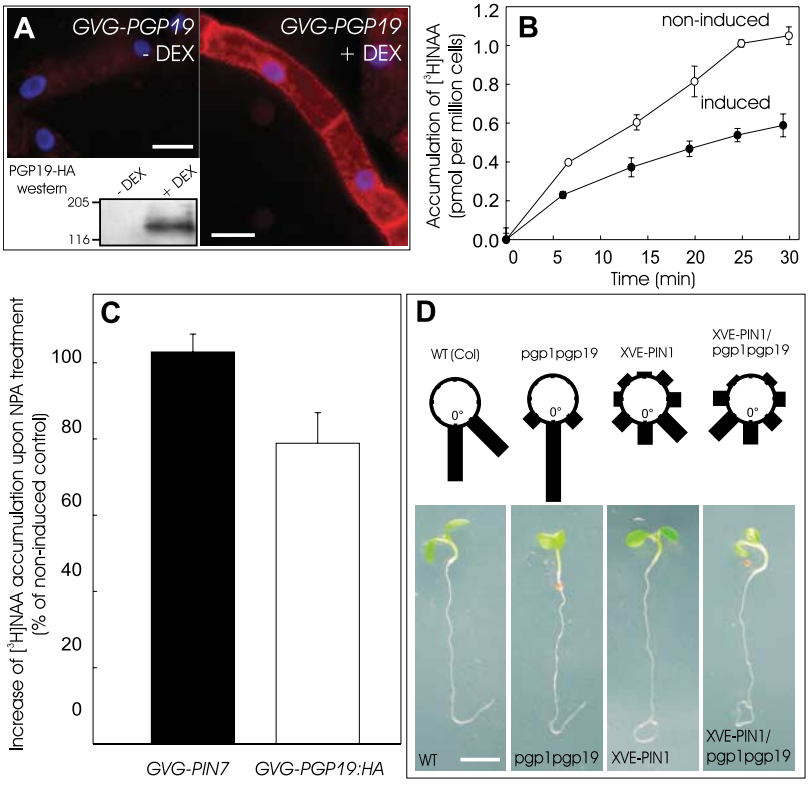

Fig. 4. Requirement of PGP function for PIN role in auxin efflux. (**A**) Inducible PGP19 expression in *GVG-PGP19:HA* tobacco cells. PGP19:HA immunostaining (red) at PM after DEX treatment (24 hours, 1 μM) is shown; no PGP19:HA immunostaining was present in the untreated control. An anti-HA immunoblot was conducted after 24 hours of DEX (1 μM) treatment. Nuclear counterstain is shown in blue. Scale bars, 40 μm. (**B**) [^{3}H]NAA accumulation decreased upon PGP19 expression, revealing function in auxin efflux in BY-2 cells. (**C**) Different sensitivities of PIN7- and PGP19-dependent [^{3}H]NAA efflux to NPA treatment (10 μM, 20 min) in *GVG-PIN7* and *GVG-PGP19:HA* cells (*23*). (**D**) Root gravitropism in *XVE-PIN1* seedlings. PIN1 overexpression (4 hours, 4 μM EST) led to gravitropic defects in *pgp1/pgp19* mutants in contrast to gravitropic growth of EST-treated nontransformed wild-type (WT) and *pgp1/pgp19* seedlings. Root gravitropism was scored 12 hours after gravity stimulation (n > 40). Scale bar, 3 mm. For (B) and (C), error bars show SEM (n = 4); where error bars are not shown, the error was smaller than the symbols.

across the PM out of plant cells largely clarifies a role of PIN proteins in intercellular auxin transport. Furthermore, the polar, subcellular PIN localization provides a vectorial component to the directional auxin flow (*22*). Therefore, transport function of PINs together with their asymmetric subcellular localization defines directional local auxin distribution underlying different developmental processes.

References and Notes

1. J. Friml, *Curr. Opin. Plant Biol.* **6**, 7 (2003).
2. A. W. Woodward, B. Bartel, *Ann. Bot. (Lond.)* **95**, 707 (2005).
3. S. Kepinski, O. Leyser, *Curr. Biol.* **15**, R208 (2005).
4. J. Friml, J. Wisniewska, E. Benková, K. Mendgen, K. Palme, *Nature* **415**, 806 (2002).
5. J. Friml *et al.*, *Cell* **108**, 661 (2002).
6. J. Friml *et al.*, *Nature* **426**, 147 (2003).
7. E. Benková *et al.*, *Cell* **115**, 591 (2003).
8. M. Bennett *et al.*, *Science* **273**, 948 (1996).
9. I. A. Paponov, W. D. Teale, M. Trebar, I. Blilou, K. Palme, *Trends Plant Sci.* **10**, 170 (2005).
10. B. Noh, A. S. Murphy, E. P. Spalding, *Plant Cell* **13**, 2441 (2001).
11. J. J. Blakeslee, W. A. Peer, A. S. Murphy, *Curr. Opin. Plant Biol.* **8**, 494 (2005).
12. M. Geisler *et al.*, *Plant J.* **44**, 179 (2005).
13. R. Chen, *Proc. Natl. Acad. Sci. U.S.A.* **95**, 15112 (1998).
14. C. Luschnig, R. A. Gaxiola, P. Grisafi, G. R. Fink, *Genes Dev.* **12**, 2175 (1998).

15. J. Zuo, Q. W. Niu, N. H. Chua, *Plant J.* **24**, 265 (2000).
16. A. Delbarre, P. Muller, V. Imhoff, J. Guern, *Planta* **198**, 532 (1996).
17. J. Petrášek *et al.*, *Plant Physiol.* **131**, 254 (2003).
18. T. Aoyama, N. H. Chua, *Plant J.* **11**, 605 (1997).
19. I. Blilou, *Nature* **433**, 39 (2005).
20. A. Vieten *et al.*, *Development* **132**, 4521 (2005).
21. M. Geisler, A. S. Murphy, *FEBS Lett.* **580**, 1094 (2006).
22. J. Wiśniewska, *Science* **312**, 883 (2006).
23. Materials and methods are available as supporting material on *Science* Online.
24. We thank N. H. Chua for providing material, V. Croy for help with HeLa studies, and P. Brewer and M. Sauer for critical reading of the manuscript. This work was supported by the European Molecular Biology Organization Young Investigator programme (J.F.), the Volkswagenstiftung (J.F., J.M., D.S., P.D.), the Grant Agency of the Academy of Sciences of the Czech Republic, project A6038303 (E.Z., M.Č., M.K., P.K., J.P., L.P., D.S., and P.S.), the Ministry of Education of the Czech Republic, projects MSM0021622415 and LC06034, the Alexander von Humboldt Foundation (Feodor Lynen fellowship to M.G.), the Foundation for Polish Science (J.W.), Margarete von Wrangell-Habilitationsprogramm (E.B.), NSF grant 0132803 (A.M., J.B., and O.L.), and Austrian Science Fund (FWF) grant 16311 (L.A. and C.L).

Supporting Online Material
www.sciencemag.org/cgi/content/full/1123542/DC1
Materials and Methods
Figs. S1 to S4
References

7 December 2005; accepted 14 March 2006
Published online 6 April 2006;
10.1126/science.1123542
Include this information when citing this paper.

Oceanographic Basis of the Global Surface Distribution of *Prochlorococcus* Ecotypes

Heather A. Bouman,[1]* Osvaldo Ulloa,[1] David J. Scanlan,[3] Katrin Zwirglmaier,[3] William K. W. Li,[4] Trevor Platt,[4] Venetia Stuart,[5] Ray Barlow,[6] Ole Leth,[2] Lesley Clementson,[7] Vivian Lutz,[8] Masao Fukasawa,[9] Shuichi Watanabe,[9] Shubha Sathyendranath[5]

By using data collected during a continuous circumnavigation of the Southern Hemisphere, we observed clear patterns in the population-genetic structure of *Prochlorococcus*, the most abundant photosynthetic organism on Earth, between and within the three Southern Subtropical Gyres. The same mechanisms that were previously invoked to account for the vertical distribution of ecotypes at local scales accounted for the global (horizontal) patterns we observed. Basin-scale and seasonal variations in the structure and strength of vertical stratification provide a basis for understanding large-scale horizontal distribution in genetic and physiological traits of *Prochlorococcus*, and perhaps of marine microbial communities in general.

Prochlorococcus is the smallest and most abundant phytoplankter in the global ocean and contributes significantly to the primary productivity of tropical and subtropical oceans (*1*). That the genus thrives throughout a wide range of photic zone conditions has been explained by the discovery of genetically and physiologically distinct populations, commonly referred to as high light (HL)– and low light (LL)–adapted ecotypes (*2*). *Prochlorococcus* ecotypes partition themselves according to depth in a stratified water column (*3*); however, the coexistence of multiple ecotypes (*2*) and phylotypes (*4*–*6*) has also been reported and attributed to vertical mixing in response to local physical forcing. But the effect of physical forcing on *Prochlorococcus* ecotypes at the global scale has not been explored. By using data collected during a circumnavigation of the Southern Hemisphere, we investigated whether the genetic structure of *Prochlorococcus* populations changes in response to vertical mixing within and between the major ocean basins of the world.

Samples were collected during the Blue Earth Global Expedition (BEAGLE) (Fig. 1A). The 7-month expedition spanned the southern Pacific (winter), Atlantic (late spring), and Indian (summer) Oceans (*7*); covered several biogeochemical provinces (*8*); and provided a rare opportunity to study physical forcing of phytoplankton at the global scale. We used the depth of the surface mixed layer (z_m) and the strength of the vertical density gradient (N) as indicators of the physical state of the water column (*9*). The three ocean basins differed markedly in these properties (Fig. 1B). The basin-scale variations in the vertical structure of the water column observed in the BEAGLE data are partly due to seasonal and latitudinal differences in the sampling of the three ocean basins. Mixed-layer–depth climatology reveals strong seasonality in z_m, with high values of z_m occurring during the Austral winter in all three ocean basins, and relatively uniform and shallow z_m values in the summer months (fig. S1). However, differences among basins are also found. Thus, spatial differences in vertical mixing as indexed by z_m observed during the BEAGLE have a seasonal as well as a geographical component.

Prochlorococcus cell abundance was determined by flow cytometry, and the concentration of divinyl chlorophyll a (DV Chla), a pigment marker for this genus, was measured by high performance liquid chromatography (HPLC). A clear difference between the geographic patterns of these two indices of abundance was found (Fig. 2A). *Prochlorococcus* abundance has a minimum in the well-mixed, mesotrophic waters of the Western Pacific Basin and a maximum in the strongly stratified oligotrophic waters of the Indian Ocean, a pattern that is consistent with our current understanding of the distribution of this genus (*1*, *10*, *11*). However, the concentration of divinyl chlorophyll a is high in the Pacific Basin (except near 140°W) and low in the Atlantic and Indian Basins. This is perhaps counterintuitive; it can be explained as follows. Because all samples were collected within the top 10 m of the water column, vertical mixing would be an important mechanism altering the growth conditions (light and nutrients) of the phytoplankton cells. Thus, the high divinyl chlorophyll a concentrations in the Pacific may arise from photoacclimatory (physiological) or photoadaptive (genetic) response of the cells to a decrease in mean light intensity. Basin-scale patterns in the intracellular concentration of divinyl chlorophyll a (C_i) for *Prochlorococcus* are evident (Fig. 2B), with low C_i values observed in the strongly stratified Indian Ocean during the summer (averaging 0.14 fg DV Chla per cell), consistent with those found in the surface waters of the subtropical North Atlantic (*12*), and high values observed in the well-mixed Archipelagic Deep Basins Province (*8*) during the winter (averaging 1.00 fg DV Chla per cell), similar to those typically found deeper in the water column in subtropical gyres (*12*).

Because light decreases exponentially with depth, phytoplankton cells mixed deeper in the water column would experience a lower mean daily irradiance than if they remained at the sea surface. Phytoplankton respond to this reduction in irradiance by increasing the concentration of pigment per cell. An inverse relation between C_i

[1]Laboratorio de Procesos Oceanográficos y Clima, Departamento de Oceanografía, and Centro de Investigación Oceanográfica en el Pacífico Sur-Oriental, [2]Departamento de Geofísica, Universidad de Concepción, Casilla 160-C, Concepción, Chile. [3]Department of Biological Sciences, University of Warwick, Coventry CV4 7AL, UK. [4]Bedford Institute of Oceanography, Dartmouth, Nova Scotia, B2Y 4A2, Canada. [5]Department of Oceanography, Dalhousie University, Halifax, Nova Scotia, B3H 4J1, Canada. [6]Marine and Coastal Management, Private Bag X2, Rogge Bay 8012, Cape Town, South Africa. [7]Commonwealth Scientific and Industrial Research Organization, Marine Research, Post Office Box 1538, Hobart, Tasmania, Australia, 7001. [8]Instituto Nacional de Investigación y Desarrollo Pesquero, Paseo Victoria Ocampo 1, 7600 Mar del Plata, Argentina. [9]Japan Agency for Marine-Earth Science and Technology, 2-15, Natsushima, Yokosuka, 237-0061, Japan.

*To whom correspondence should be addressed. E-mail: heather@profc.udec.cl

www.sciencemag.org/cgi/content/full/1123542/DC1

Supporting Online Material for

PIN Proteins Perform a Rate-Limiting Function in Cellular Auxin Efflux

Jan Petrášek, Jozef Mravec, Rodolphe Bouchard, Joshua J. Blakeslee, Melinda Abas, Daniela Seifertová, Justyna Wiśniewska, Zerihun Tadele, Martin Kubeš, Milada Čovanová, Pankaj Dhonukshe, Petr Skůpa, Eva Benková, Lucie Perry, Pavel Křeček, Ok Ran Lee, Gerald R. Fink, Markus Geisler, Angus S. Murphy, Christian Luschnig, Eva Zažímalová,* Jiří Friml

*To whom correspondence should be addressed. E-mail: eva.zazim@ueb.cas.cz

Published 6 April 2006 on *Science* Express
DOI: 10.1126/science.1123542

This PDF file includes:

Supporting online material

Materials and Methods

Plant material, gene constructs, transformation and inducible expression

Arabidopsis seedlings were grown at a 16 hours light/8 hours dark cycle at 18-25 °C on 0.5 x MS with sucrose as described (*1*). The *XVE-PIN1* (Col-0) transgenic plants were obtained by introducing the $p_{G10\text{-}90}$*::XVE* activator and the *LexA::PIN1*; *LexA::GFP* reporter constructs (*2, 3*) into *pin1-7* mutant line. This line was crossed with *pgp1pgp19* double mutant (*4*) to generate *XVE-PIN1/pgp1pgp19* line. The *XVE-PIN1* construct was generated using *PIN1* cDNA (GenBank accession number AF089084). *GVG-PIN4,6,7* constructs were generated by inserting the corresponding cDNAs (*PIN4*: AF087016, *PIN6*: AF087819, *PIN7*: AF087820) into the pTA7002 vector (*5*). *GVG-PGP19:HA* construct was generated by introducing the full length genomic fragment of *PGP19* (locus name At3g28860) with C-terminal hemaglutinin tag (HA) into pTA7002 vector (*5*).

Cell suspension from *XVE-PIN1 Arabidopsis* line was established from calli induced on young leaves (*6*) and grown in liquid MS medium containing 1 μM 2,4-D. BY-2 tobacco cells (*Nicotiana tabacum* L., cv. Bright Yellow 2, (*7*)) were grown as described (*8*) and stably transformed by co-cultivation with *Agrobacterium* (*8*). Transgenic tobacco cells and calli were maintained on the media supplemented with 40 μg ml^{-1} hygromycin and 100 μg ml^{-1} cefotaxim. Expression of *PIN* and *PGP* genes in tobacco cells was induced by the addition of dexamethasone (DEX, 1 μM, 24 hours, except for stated otherwise) at the

beginning of the subcultivation period. The same approach was used for *Arabidopsis* cell culture, where 1 μM β-Estradiol (EST) was added. Both DEX and EST were added from stock solutions in DMSO (200 μM), appropriate volume of DMSO was added in controls.

Expression and localization analysis

Tobacco and *Arabidopsis* RNA was isolated using the Plant RNA Qiagen Mini-Prep and RT-PCR performed using Qiagen® OneStep RT-PCR or Invitrogen SuperSriptII kits according to the manufacturer's protocols.

Total protein fraction from *GVG-PGP19* tobacco cells was obtained after homogenization in liquid nitrogen using mortar and pestle. The frozen powder was then mixed with an equal volume of extraction buffer (50 mM Tris-HCl, pH 6.8; 2 % SDS; 36 % w/v urea; 30 % v/v glycerol; 5 % v/v mercaptoethanol; 0,5 % w/v Bromphenol Blue), vortexed for 1 min, boiled for 3 min, and centrifuged at 13,000 rpm and 4°C for 5 min. The supernatant was transferred into a new tube and re-centrifuged at 13,000 rpm and 4°C for 5 min. The resulting supernatant was defined as total protein extract and stored at –20°C until use.

Microsomal protein fraction from *GVG-PIN7* tobacco cells was used for immunoblot analysis of PIN7 protein. Briefly, cells were homogenized by sonication in extraction buffer (50mM Tris pH 6.8; 5% (v/v) glycerol; 1.5% (w/v) insoluble polyvinylpolypyrrolidone; 150mM KCl; 5mM Na EDTA; 5mM Na EGTA; 50mM NaF; 20mM beta-glycerol phosphate; 0.5% (v/v) solubilized casein, 1mM benzamidine; 1mM PMSF; 1μg/ml pepstatin; 1μg/ml leupeptin; 1μg/ml aprotinin; 1 Roche Complete Mini Protease Inhibitor tablet per 10ml). After centrifugation at 3,800 x *g* for 20 minutes, the supernatant was filtered through nylon mesh and spun again at 3,800 x *g*. The supernatant was centrifuged

at 100,000 x *g* for 90 min. The resulting pellet was homogenized and re-suspended in buffer containing 50mM Tris pH 7.5; 20% glycerol; 2mM EGTA; 2mM EDTA; 50-500µM DTE; 10µg/ml solubilized casein and protease inhibitors as in the extraction buffer. Equal amounts of protein (about 10µg) were heated at 60°C for 40 min in sample buffer (3% (w/v) SDS; 40mM DTE; 180mM Tris pH 6.8; 8M urea), and transferred on PVDF membrane using dot-blot (SCIE-PLAS, U.K.) or semi-dry electro-blot. Primary rabbit polyclonal anti-PIN7 antibody (*10*) or mouse monoclonal anti-HA antibody (Sigma) followed by secondary HRP-conjugated anti-rabbit antibody and ECL detection kit (Amersham Biosciences, U.K.) were used for dot or western blot analysis.

Indirect immunofluorescence method was used for immunolocalizations in *Arabidopsis* cell suspension (11) and BY-2 cells (*8*). Briefly, *Arabidopsis* cells were fixed for 30 min at room temperature with 4% (w/v) paraformaldehyde in 0.1 M PIPES, pH 6.8, 5 mM EGTA, 2 mM $MgCl_2$, and 0.4% (w/v) Triton X-100. Cells were then treated with the solution of 0.8% (w/v) macerozyme R-10 and 0.2% (w/v) pectolyase Y-23 in 0.4 M mannitol, 5 mM EGTA, 15 mM MES, pH 5.0, 1 mM PMSF, 10 µg/ml of leupeptin, and 10 µg/ml of pepstatin A. Then the cells were washed in PBS buffer and attached to poly-L-lysine coated coverslips and incubated for 30 min in 1% (w/v) BSA in PBS and incubated for 1 h with primary antibody. The specimens were then washed three times for 10 min in PBS and incubated for 1 h with secondary antibody. Coverslips with cells were carefully washed in PBS, rinsed with water with Hoechst 33258 (0,1µg/ml) and embedded in Mowiol (Polysciences) solution.

Tobacco BY-2 cells were pre-fixed 30 min in 100 µM MBS and 30 min in 3.7% (w/v) PFA in buffer consisting of 50 mM PIPES, 2 mM EGTA, 2 mM $MgSO_4$, pH 6.9, at 25°C and

subsequently in 3.7% (w/v) PFA and 1% Triton X-100 (w/v) in stabilizing buffer for 20 minutes. After treatment with an enzyme solution (1% (w/v) macerozyme and 0.2% (w/v) pectinase) for 7 min at 25°C and 20 minutes in ice cold methanol (at -20°C), the cells were attached to poly-L-lysine coated coverslips and treated with 1% (w/v) Triton X-100 in microtubule stabilizing buffer for 20 minutes. Then the cells were treated with 0.5% (w/v) bovine serum albumin in PBS and incubated with primary antibody for 45 minutes at 25°C. After washing with PBS, a secondary antibody in PBS was applied for 1 h at 25°C. Coverslips with cells were carefully washed in PBS, rinsed with water with Hoechst 33258 (0,1μg/ml) and embedded in Mowiol (Polysciences) solution.

The following antibodies and dilutions were used: anti- PIN1 (*13*, 1: 500), anti-PIN7 (*10*, 1:500), anti-HA (Sigma-Aldrich; 1:500), TRITC- (Sigma-Aldrich; 1:200), FITC- (Sigma-Aldrich; 1:200) anti-rabbit secondary antibodies. PIN immunostaining in yeast and HeLa cells was performed as described (*13, 14*).

All preparations were observed using an epifluorescence microscope (Nikon Eclipse E600) equipped with appropriate filter sets, DIC optics, monochrome integrating CCD camera (COHU 4910, USA) or colour digital camera (DVC 1310C, USA).

Quantitative analysis of root gravitropism

5 days old seedlings of WT-Col, *pgp1pgp19*, *XVE-PIN1* and *XVE-PIN 1/pgp1pgp19* lines grown vertically were transferred on new MS plates containing 4 μM β-estradiol for 12 hours. Seedlings were then stretched and plates turned through 135° for additional 12 hour gravity stimulation in dark. The angle of root tips from the vertical plane was measured using ImageJ software (NIH, USA). All gravistimulated roots were assigned to one of the

eight 45° sectors on gravitropism diagram. The length of bars represents the percentage of seedlings showing respective direction of root growth.

Auxin accumulation assays in plant, HeLa and yeast cells

Auxin accumulation experiments in suspension-cultured tobacco BY-2 cells were performed and the integrity of labeled auxins during the assay was checked exactly as described (*15, 8, 12*). The same protocol was used for suspension-cultured *Arabidopsis* cells. Labeled [^{3}H]IAA, [^{3}H]2,4-D and [^{3}H]Trp (specific activities 20 Ci/mmol, American Radiolabeled Chemicals, St. Louis, MO), and [^{3}H]NAA (specific radioactivity 25 Ci/mmol, Institute of Experimental Botany, Prague, Czech Republic) were used. Briefly, the accumulation was measured in 0.5-mL aliquots of cell suspension. Each cell suspension was filtered, resuspended in uptake buffer (20 mM MES, 40 mM Suc, and 0.5 mM $CaSO_4$, pH adjusted to 5.7 with KOH), and equilibrated for 45 min with continuous orbital shaking. Equilibrated cells were collected by filtration, resuspended in fresh uptake buffer, and incubated on the orbital shaker for 1.5 h in darkness at 25°C. [^{3}H]NAA was added to the cell suspension to give a final concentration of 2 nM. After a timed uptake period, 0.5-mL aliquots of suspension were withdrawn and accumulation of label was terminated by rapid filtration under reduced pressure on 22-mm-diameter cellulose filters. The cell cakes and filters were transferred to scintillation vials, extracted in ethanol for 30 min, and radioactivity was determined by liquid scintillation counting (Packard Tri-Carb 2900TR scintillation counter, Packard Instrument Co., Meriden, CT). Counts were corrected for surface radioactivity by subtracting counts obtained for aliquots of cells collected immediately after the addition of [^{3}H]NAA. Counting efficiency was determined by

automatic external standardization, and counts were corrected automatically. NPA was added as required from ethanolic stock solutions to give the appropriate final concentration. The concentration dependence of auxin accumulation in response to NPA or BFA was determined after a 20-min uptake period. For wash out experiments cells were loaded with [^{3}H]NAA (2 nM) for 30 min. After quick wash out, cells were re-suspended in fresh loading buffer but without [^{3}H]NAA; cell density before and after wash out was maintained the same. Relative NAA retention was measured as a radioactivity retained inside cells at particular time points after wash out and expressed as % of total radioactivity retained inside the cells just before wash out. The accumulation of various auxins or structurally related inactive compound (Trp) after induction of PIN or PGP expression was expressed together with SEs as the percentage of the accumulation of non-induced cells at time 30 min after application of respective labelled compound. If not indicated otherwise, 24 hours treatments with dexamethasone (1 μM) or β-estradiol (1 μM) were performed. Different sensitivities of PIN7- and PGP19-dependent [^{3}H]NAA efflux to NPA treatment (10 μM, 20 min) in *GVG-PIN7* and *GVG-PGP19:HA* cells was determined as the average value from three independent experiments. In each, the accumulation of [^{3}H]NAA was measured in NPA-treated induced and non-induced cells and scored after 20 minutes of incubation. The increase in the accumulation of [^{3}H]NAA upon NPA treatment in non-induced cells was considered as 100% and all other values expressed as the percentage of this increase.

The transient vaccinia expression system was used to transfect HeLa cells with PIN1:HA, PIN2:HA, and PIN7:HA in 6-well plates. The expression was verified by RT-PCR and western blot analysis. Auxin transport assays were performed exactly as described (*16, 14*). 16-24h after transfection cells were washed and incubated 40 min at 37°C, 5% CO_2 with

[^{3}H]IAA (26 Ci/mmol, Amersham Biosciences, Piscataway, NJ), or [^{3}H]BeA (20 Ci/mmol, American Radiolabeled Chemicals, St. Louis, MO). After incubation, cells were harvested, and retained radiolabeled substrate was quantitated. Net efflux is expressed as dpm/500,000 cells divided by the amount of auxin retained by cells transformed with empty vector minus the amount of auxin retained by cells transformed with gene of interest. Thus, the PIN-dependent decrease in retention is presented as positive efflux value expressed as means (n=3) with standard deviations. Cell viability after treatment was confirmed visually and via cell counting.

For auxin accumulation and growth assays in yeast, PIN2, PIN7 or PIN2:HA were expressed in *S. cerevisiae* strains *gef1* (*13*) and JK93da or *yap1-1* (*17*). The expression was verified by western blot analysis or immunolocalization. Export of [^{3}H]IAA (specific activity 20 Ci/mmol, American Radiolabeled Chemicals, St. Louis, MO) and [^{14}C]BeA (53 mCi/mmol, Moravek Biochemicals, Brea, CA) and growth assays were performed exactly as described (*17, 14*). The effluent species was determined by thin-layer chromatography of aliquots of exported [^{3}H]IAA (Supplementary fig. S4a) and images were taken using a phosphoimager (Cyclone, Packard Instruments) and by UV detection using [^{3}H]IAA as standard. Yeast viability before and after transport experiments was ascertained by light microscopy.

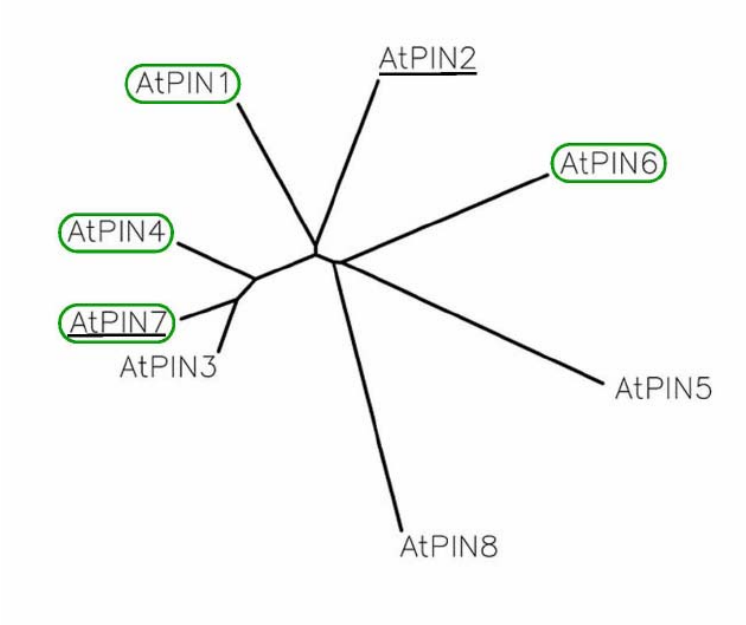

fig. S1 Arabidopsis *PIN* genes family.

Phylogenetic tree of 8 Arabidopsis *PIN* genes. Phenotypes of loss-of-function mutants in *PIN1*, *PIN2*, *PIN3*, *PIN4* and *PIN7* clearly suggest role in polar auxin transport and they all can be phenocopied by inhibitors of auxin transport (*18*). PIN6 remains functionally uncharacterized. PIN5 and PIN8 lack the middle hydrophilic domain and seem to by functionally distinct (*19*). Based on homology, *PIN7* is the most typical member of PIN family forming a distinct homologous subclade with *PIN3* and *PIN4*. *PIN6*, on the other hand, is the least homologous *PIN* from the *PIN1,2,3,4,6,7* subfamily. PIN1, PIN4, PIN6 and PIN7 (respective genes encircled in green) have been shown here to mediate auxin efflux *in planta*. PIN2 and PIN7 (genes underlined) show auxin efflux activity in heterologous systems. Notably, the confirmed expression of PIN1 in HeLa or yeast cells did not result in increased auxin efflux suggesting, in contrast to PIN2 and PIN7, that either PIN1 loses its functionality, when expressed in heterologous system, or distinctively PIN1 requires plant-specific factor(s) to mediate its function in auxin efflux.

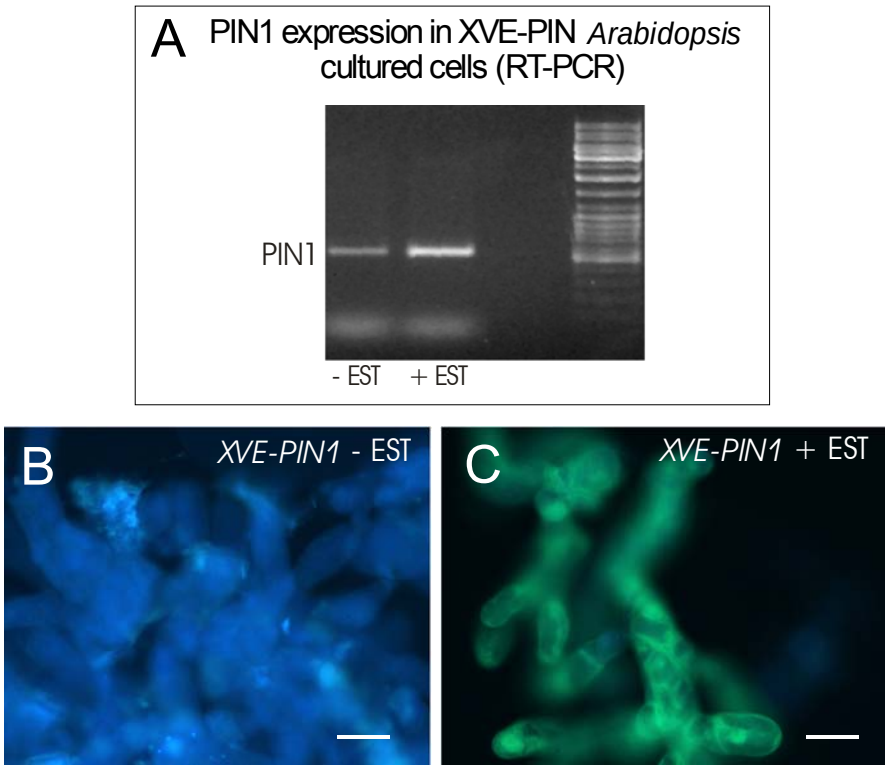

fig. S2 The expression of PIN1 in *XVE-PIN1 Arabidopsis* cultured cells

(A) RT-PCR of PIN1 in non-induced and β-estradiol-induced (1 μM, 24h) cells. (B, C) The activation of expression verified by the fluorescence of co-expressed GFP reporter. Compare the autofluorescence of cell walls in non-induced cells (B) with GFP fluorescence after 24 h incubation in 1 μM β-estradiol (C). Scale bars 30μm.

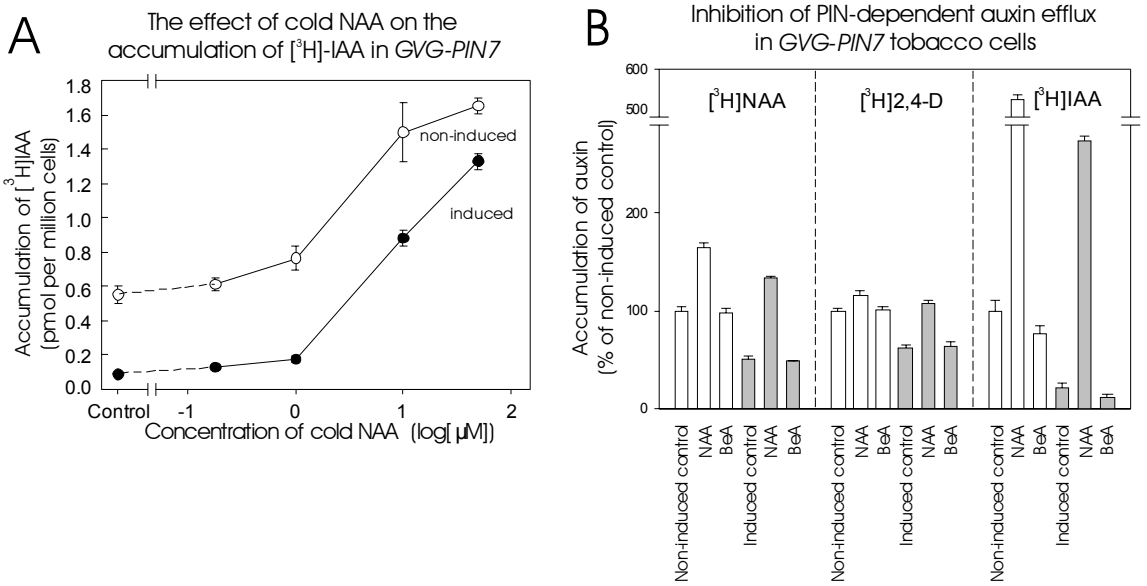

fig. S3 Auxin accumulation in *GVG-PIN7* BY-2 cells

(A) Displacement curve: The competitive inhibitory effect of cold (non-labeled) NAA on the accumulation of [^{3}H]IAA in non-induced and induced *GVG-PIN7* cells. (B) Effects of NAA and benzoic acid (BeA) on efflux of different auxins in DEX-treated (induced, full bars) and non-induced (open bars) *GVG-PIN7* cells. NAA (10 μM), a good substrate for auxin efflux machinery, interferes with both endogenous and PIN7-dependent efflux of [^{3}H]NAA, [^{3}H]2,4-D and [^{3}H]IAA in non-induced and induced *GVG-PIN7* cells, respectively. In contrast, structurally similar but inactive BeA (10 μM) does not have any detectable effect in the same experimental system.

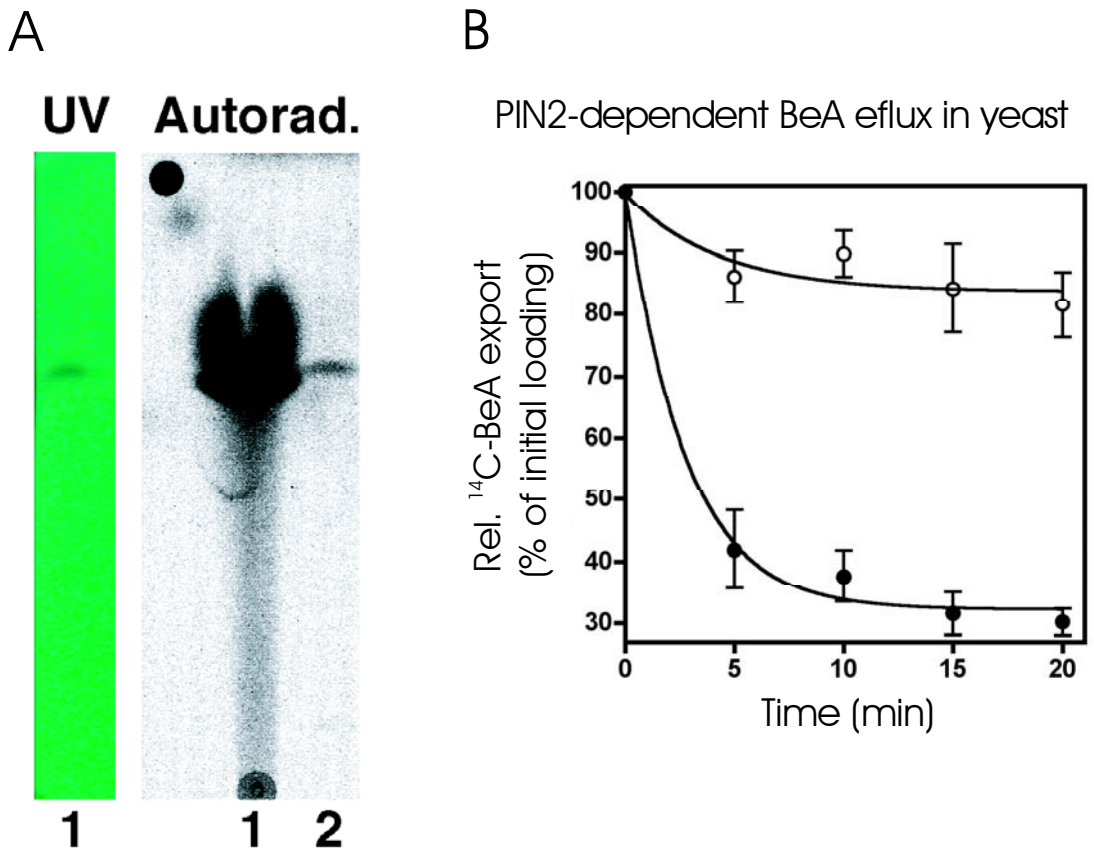

fig. S4 Control experiments for auxin efflux assays in yeast.

(A) The effluent species in yeast were determined to be [^{3}H]IAA by thin layer chromatography (lane 2). Non-exported [^{3}H]IAA was used as the standard which itself was verified by UV detection (lane 1). Images were taken using a phosphoimager (Cyclone, Packard Instruments) and by UV detection using [^{3}H]IAA as the standard. The integrity of exported [^{3}H]IAA in this assay was also proved by MS-MS, as described elsewhere (*14*).

(B) PIN2-expressing yeast show increased net efflux of [^{14}C]benzoic acid ([^{14}C]BeA)

compared to empty vector controls. [^{14}C]BeA (53 mCi/mmol, Moravek Biochemicals, Brea, CA) was used and transport experiments were performed exactly as described (*14*).

Supporting references and notes

1. E. Benková *et al.*, *Cell* **115**, 591 (2003).

2. P. J. Jensen, R. P. Hangarter, M. Estelle, *Plant. Physiol.* **116**, 455 (1998).

3. J. Zuo., Q.W. Niu, N.H. Chua, *Plant J.* **24**, 265 (2000).

4. B. Noh, A.S. Murphy, E.P. Spalding *Plant Cell* **13**, 2441 (2001).

5. T. Aoyama, N. H. Chua, *Plant J.* **11**, 605 (1997).

6. J. Mathur, C. Koncz, in *Methods in Molecular Biology: Arabidopsis Protocols*, J.M. Martinez-Zapater, J. Salinas, Eds. (Humana Press, Totowa, New Jersey, 1998), vol. 82, pp. 27-30.

7. T. Nagata, Y. Nemoto, S. Hasezawa, *Int. Rev. Cytol.* **132**, 1 (1992).

8. J. Petrášek *et al.*, *Plant Physiol.* **131**, 254 (2003).

9. A. Müller, *EMBO J.* **17**, 6903 (1998).

10. J. Friml *et al.*, *Nature* **426**, 147 (2003).

11. A. P. Smertenko *et al.*, *Plant Cell* **16**, 2035 (2004).

12. T. Paciorek *et al.*, *Nature* **435**, 1251 (2005).

13. C. Luschnig, R. A. Gaxiola, P. Grisafi, G. R. Fink *Genes Dev.* **12**, 2175 (1998).

14. M. Geisler *et al.*, *Plant J.* **44**, 179 (2005).

15. A. Delbarre, P. Muller, V. Imhoff, J. Guern *Planta* **198**, 532 (1996).

16. C. A. Hrycyna, *Biochemistry* **38**, 13887 (1999).

17. R. Prusty, P. Grisafi, G. R. Fink, *Proc. Natl. Acad. Sci. USA* **101**, 4153 (2004).

18. J. Friml, J. Wisniewska, in: *Annual Plant Reviews, Intercellular Communication in Plants,* A Fleming, Ed. (Blackwell Publishing, Oxford, UK, 2005), vol. 16, pp. 1-26.

19. I. A. Paponov, W. D. Teale, M. Trebar, I. Blilou, K. Palme, *Trends Plant Sci.* **10**, 170 (2005).

6.2. Chapter 2 - Interaction of PIN and PGP transport mechanisms in auxin distribution-dependent development

Jozef Mravec, **Martin Kubeš**, Agnieszka Bielach, Vassilena Gaykova, Jan Petrášek, Petr Skůpa, Suresh Chand, Eva Benková, Eva Zažímalová and Jiří Friml

Development 135, 3345-3354, 2008

This paper is based on collaboration between Dr. Jiří Friml and Dr. Eva Zažímalová laboratories. Here, we have analyzed the importance of the functional interaction between PIN- and ABCB/PGP-dependent auxin transport in plant development.

My contribution to this article was in the characterization of PIN- and ABCB/PGP-mediated auxin efflux at the cellular level. For this comparison I used DEX-inducible BY-2 cell lines GVG-ABCB19-HA and GVG-PIN7.

To find out how increased auxin efflux influences cellular behaviour of BY-2 cells, I examined the growth and morphology of DEX-treated and untreated cells in these two cell lines. After induction of PIN7 or ABCB19-HA expression, identical phenotypical changes occurred: cells ceased to divide, started to elongate, and formed and accumulated starch granules. Importantly, this cellular behaviour could be mimicked by cultivation of cells in medium with a decreased amount of auxin or no auxin (see Fig. S1E -G in the supplementary material). All phenotypic changes induced by overexpression of PIN7 in the GVG-PIN7 line were completely reversed by application of the auxin efflux inhibitor NPA (Fig. 1C, G; see Fig. S1J, K in the supplementary material). By contrast, after induction of ABCB19-HA expression in the GVG-ABCB19-HA line, NPA treatment was ineffective in rescuing auxin starvation phenotypes (Fig. 1F, G; see Fig. S1J, K in the supplementary material).

Our part of this paper was supported by the Ministry of Education, Youth and Sports of the Czech Republic, project LC06034 and by the Grant Agency of the Academy of Sciences of the Czech Republic (KJB600380604).

Development 135, 3345-3354 (2008) doi:10.1242/dev.021071

Interaction of PIN and PGP transport mechanisms in auxin distribution-dependent development

Jozef Mravec[1,2], Martin Kubeš[3,4], Agnieszka Bielach[1,2], Vassilena Gaykova[2], Jan Petrášek[3,4], Petr Skůpa[3,4], Suresh Chand[2], Eva Benková[1,2], Eva Zažímalová[3] and Jiří Friml[1,2,*]

The signalling molecule auxin controls plant morphogenesis via its activity gradients, which are produced by intercellular auxin transport. Cellular auxin efflux is the rate-limiting step in this process and depends on PIN and phosphoglycoprotein (PGP) auxin transporters. Mutual roles for these proteins in auxin transport are unclear, as is the significance of their interactions for plant development. Here, we have analysed the importance of the functional interaction between PIN- and PGP-dependent auxin transport in development. We show by analysis of inducible overexpression lines that PINs and PGPs define distinct auxin transport mechanisms: both mediate auxin efflux but they play diverse developmental roles. Components of both systems are expressed during embryogenesis, organogenesis and tropisms, and they interact genetically in both synergistic and antagonistic fashions. A concerted action of PIN- and PGP-dependent efflux systems is required for asymmetric auxin distribution during these processes. We propose a model in which PGP-mediated efflux controls auxin levels in auxin channel-forming cells and, thus, auxin availability for PIN-dependent vectorial auxin movement.

KEY WORDS: PGP, PIN, Auxin transport, Embryogenesis, Organogenesis, Tropisms

INTRODUCTION

Directional (polar) transport of the signalling molecule auxin between cells is a plant-specific form of developmental regulation. Transport-based asymmetric auxin distribution within tissues (auxin gradients) plays an important role in many developmental processes, including patterning and tropisms (reviewed by Tanaka et al., 2006). Because the auxin molecule is charged inside cells and, thus, membrane impermeable, its intercellular transport relies on carrier-mediated cellular influx and efflux (reviewed by Kerr and Bennett, 2007; Vieten et al., 2007). Genetic approaches in *Arabidopsis thaliana* have identified two groups of proteins that are involved in auxin export from cells: PIN-FORMED (PIN) proteins and several ABC transporter-like phosphoglycoproteins (PGPs) (reviewed by Bandyopadhyay et al., 2007; Vieten et al., 2007).

The PIN protein family consists of plant-specific integral plasma membrane proteins that have been identified based on mutants defective in organogenesis (*pin-formed1* or *pin1*) (Okada et al., 1991; Gälweiler et al., 1998) and tropism (*pin2/agr1/eir1*) (Luschnig et al., 1998). The *Arabidopsis* genome encodes eight PIN-related sequences, most of which have been already characterized at cellular and developmental levels (reviewed by Vieten et al., 2007; Zažímalová et al., 2007). PIN proteins are expressed in different parts of the plant and are almost universally required for all aspects of auxin-related plant development, including embryogenesis (Friml et al., 2003), organogenesis (Benková et al., 2003; Reinhardt et al., 2003), root meristem patterning and activity (Friml et al., 2002a; Blilou et al., 2005), tissue differentiation and regeneration (Scarpella et al., 2006; Xu et al., 2006; Sauer et al., 2006a), and tropisms (Luschnig et al., 1998; Friml et al., 2002b). Most phenotypic aberrations in *pin* loss-of-function alleles can be phenocopied by external application of auxin efflux inhibitors, such as 1-naphthylphthalamic acid (NPA) (Tanaka et al., 2006). When expressed in plant and non-plant cultured cells, PIN proteins perform a rate-limiting function in cellular auxin efflux (Petrášek et al., 2006). Importantly, PIN proteins show distinct polar subcellular localization that determines auxin flux direction, as predicted by classical models of directional auxin transport (Wiśniewska et al., 2006). The dynamic regulation of the intracellular movement of PINs, their polar targeting and their protein stability provides a means to regulate directional throughput of auxin flow (Friml et al., 2004; Paciorek et al., 2005; Abas et al., 2006; Michniewicz et al., 2007). Moreover, the PIN-dependent auxin distribution network involves redundancy and auxin-mediated crossregulation of PIN expression and PIN targeting (Sauer et al., 2006a; Blilou et al., 2005; Vieten et al., 2005). A crucial role for PIN-dependent auxin efflux in generation of morphogenetic asymmetric auxin distribution has recently been suggested by mathematical modelling (Grieneisen et al., 2007).

Plant orthologues of the mammalian multidrug-resistance proteins (Martinoia et al., 2002; Verrier et al., 2008) PGP1 (ABCB1) and PGP19 (MDR1/ABCB19), similarly to PIN proteins, have been shown to perform cellular auxin efflux in both plant and heterologous systems; accordingly, basipetal auxin transport is decreased in *pgp1* and *pgp19* mutants (Noh et al., 2001; Geisler et al., 2005; Petrášek et al., 2006). In addition, these proteins bind auxin efflux inhibitors, such as NPA (Murphy et al., 2002). Phenotypic defects caused by loss of PGP function are most pronounced in vegetative organs and include dwarfism, curly wrinkled leaves, twisted stems and reduced apical dominance, supporting their role in auxin-based development (reviewed by Bandyopadhyay et al., 2007). However, expression, localization and roles of PGPs in patterning processes are less characterized compared with PINs. The cellular localization of PGPs is mainly apolar, but instances of asymmetric cellular distribution have been reported (Geisler et al., 2005; Blakeslee et al., 2007; Wu et al., 2007).

[1]Department of Plant Systems Biology, VIB, and Department of Molecular Genetics, Ghent University, 9052 Gent, Belgium. [2]Center for Plant Molecular Biology (ZMBP), University of Tübingen, D-72076 Tübingen, Germany. [3]Institute for Experimental Botany, Academy of Sciences of the Czech Republic, Rozvojová 263, 165 02 Praha 6, Czech Republic. [4]Department of Plant Physiology, Faculty of Science, Charles University, Viničná 5, 128 44 Praha 2, Czech Republic.

*Author for correspondence (e-mail: jiri.friml@psb.ugent.be)

Accepted 20 August 2008

Important questions in auxin research relate to the roles of these two types of auxin efflux proteins in auxin transport. Do they represent independent mechanisms? What would be the functional requirements for two distinct transport systems? Do they cooperate and how? The only partial colocalization of PINs and PGPs at the plasma membrane and the difference in the corresponding mutant phenotypes favours a scenario in which PGPs and PINs have independent functions. Nevertheless, recent biochemical studies have demonstrated an interaction between PIN and PGP proteins that is functionally relevant in heterologous systems, because it influences the rate of efflux, its substrate specificity and its sensitivity to inhibitors (Blakeslee et al., 2007; Bandyopadhyay et al., 2007). However, the relevance of the interaction between PINs and PGPs in planta and, eventually, in asymmetric auxin distribution, remains unclear.

Here, we present evidence that PINs and PGPs define independent auxin transport mechanisms that cooperate to mediate auxin distribution-mediated development during embryogenesis, organogenesis and root gravitropism. Our data suggest a model for how non-polar auxin efflux mediated by PGPs is linked with vectorial transport driven predominantly by PINs.

MATERIALS AND METHODS

Plant material and DNA constructs

We used wild-type *Arabidopsis thaliana* plants of ecotypes Wassilewskija (Ws) and Columbia (Col-0); mutants *pgp1*, *pgp19*, *pgp1pgp19* (Noh et al., 2001), *pin1pgp1pgp19* (Blakeslee et al., 2007), *pin1-1* (Okada et al., 1991), *pin1-3×DR5rev::GFP* (R ži ka et al., 2007), *rcn1-1* (Garbers et al., 1996), *eir1-3* (Luschnig et al., 1998), *eir1pgp1pgp19* (Blakeslee et al., 2007); and transgenic lines *DR5::GUS* (Sabatini et al., 1999), *DR5rev::GFP* (Friml et al., 2003), *XVE-PIN1* (Petrášek et al., 2006), *pPGP1::PGP1-myc* and *pPGP19::PGP19-HA* (Blakeslee et al., 2007). *pPGP1::PGP1-myc* was generated as previously described for *pPGP19::PGP19-HA* (Blakeslee et al., 2007). For *pPGP19::PGP19-GFP* and *pPGP1::PGP1-GFP*, tag sequences in *pPGP19::PGP19-HA* and *pPGP1::PGP1-myc*, respectively (Blakeslee et al., 2007), were replaced by an enhanced green fluorescent protein (GFP) sequence to create C-terminal fusion constructs and was transformed to *pgp19* or *pgp1* mutants. The pGVG-PGP1-*myc* and pGVG-PGP19-HA plasmids were constructed by cloning the whole genomic coding region of *PGP1* and *PGP19* genes fused with the respective tag by primer extension PCR to pTA7002 (Aoyama and Chua, 1997), and transformed to the *UAS::GUS* (Weijers et al., 2003) line. Fifteen independent transgenic lines were analysed for each construct.

Growth conditions

Arabidopsis plants were grown in a growth chamber under long-day conditions (16 hours light/8 hours dark) at 18-23°C. Seeds were sterilized with chlorine gas or ethanol, and stratified for 2 days at 4°C. Seedlings were grown vertically on half Murashige and Skoog medium with 1% sucrose and supplemented with 5 μmol/l NPA, 4 μmol/l β-estradiol (EST) or 5 μmol/l dexamethasone (DEX). Drugs were purchased from Sigma-Aldrich (St Louis, MO, USA).

BY-2 cell lines

The transgenic lines *GVG-PIN4*, *GVG-PIN6*, *GVG-PIN7*, *GVG-PGP19-HA* and *pPIN1::PIN1-GFP* (Petrášek et al., 2006; Benková et al., 2003) of *Nicotiana tabacum* Bright Yellow-2 (BY-2) cells (Nagata et al., 1992) were grown as described (Petrášek et al., 2006). Expression of PIN7 and PGP19 was induced by the addition of 1 μM DEX at the beginning of subcultivation. For the NPA effect, 10 μM NPA was added together with DEX. For microscopy, an Eclipse E600 microscope (Nikon, Tokyo, Japan) and a colour digital camera 1310C (DVC, Austin, TX, USA) were used. Reciprocal plots of cell size distribution represent individual cell lengths and diameters measured by LUCIA image analysis software (Laboratory Imaging, Prague, Czech Republic). At least 170 cells in total were measured on five optical fields for each variant.

Immunotechniques and microscopy

Arabidopsis embryos and roots were stained immunologically as described (Sauer et al., 2006b). The antibodies used were anti-PIN1 (Paciorek et al., 2005) (1:1000), anti-c-*myc* (1:500) from rabbit and anti-GFP (1:500) from mouse (Roche Diagnostics, Brussels, Belgium) (1:500). Fluorescein isothiocyanate isomer I (FITC) or Cy3-conjugated anti-rabbit or anti-mouse secondary antibodies were purchased from Dianova (Hamburg, Germany) and diluted 1:600. The microscopic analyses were carried out on a SP2 confocal microscope (Leica-Microsystems, Wetzlar, Germany). GFP samples were scanned without fixation.

Phenotype analyses

Plates with grown seedlings (5 or 10 days old) were scanned on a flatbed scanner and measured with ImageJ software (http://rsb.info.nih.gov/ij/). The vertical growth index (VGI) was calculated as described (Grabov et al., 2005). The hypocotyl twisting index was determined as the relation between hypocotyl length and the distance from the root base to the apical hook. For embryo and root tip morphology analyses, we used chloral hydrate clearing (Friml et al., 2003) and microscopy was carried out on an Axiophot microscope (Zeiss, Jena, Germany) equipped with a digital camera. Lateral roots were analysed and GUS staining was performed as described (Benková et al., 2003).

RESULTS

Effects of PIN- and PGP-inducible overexpression in cultured BY-2 cells

For the characterization of PIN- and PGP-mediated auxin efflux at the cellular level, we used BY-2 cells that harbour DEX-inducible PGP19-HA (*GVG-PGP19-HA*) or PIN7 (*GVG-PIN7*) constructs that had already been used to study the ability of corresponding proteins to mediate efflux from plant cells (Petrášek et al., 2006). After induction of *GVG-PGP19-HA* or *GVG-PIN7* constructs, cells accumulated less auxin because of the increased auxin efflux (Petrášek et al., 2006). To study how increased auxin efflux influences cellular behaviour in BY-2 cells, we examined the growth and morphology of DEX-treated and untreated cells in these lines. After induction of PIN7 or PGP19-HA expression, identical phenotypical changes occurred: cells ceased to divide, started to elongate, and formed and accumulated starch granules (Fig. 1A,B,D,E). A similar set of morphological changes was observed in induced *GVG-PIN4* and *GVG-PIN6* lines, and in a line constitutively expressing PIN1-GFP that also showed increased auxin efflux (see Fig. S1A-D,H,I in the supplementary material). Importantly, this cellular behaviour could be mimicked by cultivation of cells in medium with a decreased amount of or no auxin (see Fig. S1E-G in the supplementary material). These experiments imply that the enhanced efflux after induction of either PIN7 or PGP19-HA expression leads to depletion of auxin from cells, resulting in a change in the developmental program reflected by the switch from cell division to cell elongation.

All phenotypic changes induced by overexpression of PIN7 in the *GVG-PIN7* line were completely reversed by application of the auxin efflux inhibitor NPA (Fig. 1C,G; see Fig. S1J,K in the supplementary material). By contrast, after induction of PGP19-HA expression in the *GVG-PGP19-HA* line, NPA treatment was ineffective in rescuing auxin starvation phenotypes (Fig. 1F,G; see Fig. S1J,K in the supplementary material). These observations are in line with previously reported differences in sensitivities of PGP19- and PIN7-mediated auxin efflux to NPA (Petrášek et al., 2006). These data collectively suggest that, although PGP and PIN proteins play similar cellular roles in mediating auxin efflux and inducing the switch from cell division to cell elongation, they define two distinct auxin efflux mechanisms that differ in sensitivity to auxin efflux inhibitors.

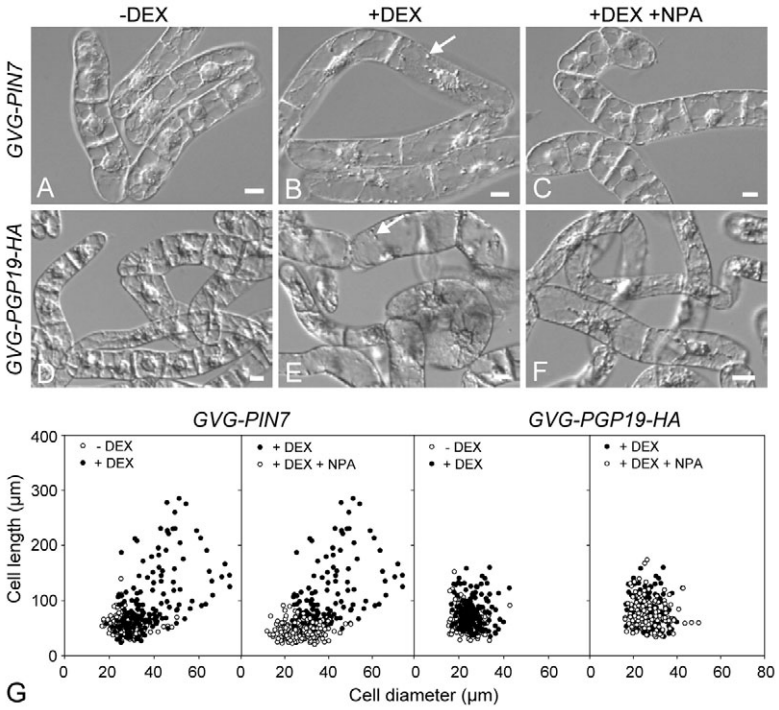

Fig. 1. Identical phenotypes indicative of auxin starvation in DEX-induced expression of *PIN7* or *PGP19* in BY-2 cells. (**A**,**B**,**D**,**E**) Effect of DEX induction in *GVG-PIN7* and *GVG-PGP19-HA* tobacco cell lines. Non-induced *GVG-PIN7* (A) and *GVG-PGP19-HA* line (D). *GVG-PIN7* (B) and *GVG-PGP19-HA* (E) cells after 3 days of cultivation with DEX, showing decrease in cell division, increase in cell elongation and formation of starch-containing amyloplasts (arrows in B,E). (**C**,**F**) Chemical inhibition of auxin transport (10 μM NPA) reversing these defects in DEX-induced *GVG-PIN7* cells (C) but not in DEX-induced *GVG-PGP19-HA* cells (F). Scale bars: 20 μm. (**G**) Depiction (reciprocal plots) of the cell size distribution (cell length and cell diameter) after NPA treatment (10 μM, 3 days) in DEX-induced *GVG-PIN7* and *GVG-PGP19-HA* cells scored at day 3 after inoculation. Non-induced *GVG-PIN7* and *GVG-PGP19-HA* cells were used as a control.

Effect of PIN- and PGP-inducible overexpression in *Arabidopsis* seedlings

To study what effects overexpression of PINs and PGPs may have at the multicellular level, we analysed transgenic lines overexpressing PIN1, PGP1 or PGP19. After induction of PIN1 expression in the estradiol-inducible *XVE-PIN1* line (Petrášek et al., 2006) (Fig. 2A,B), seedlings lost the gravitropic response and had retarded root growth (Fig. 2F,R). This effect was stronger at increased concentrations of oestradiol, supporting the rate-limiting function of PIN proteins (Fig. 2R). Immunolocalization confirmed that ectopically expressed PIN1 was localized predominantly on the basal side of root epidermal cells (Fig. 2A,B), consistent with previous reports (Wiśniewska et al., 2006). In hypocotyls of dark-grown seedlings, we observed a previously uncharacterized phenotype. Unlike the straight-growing hypocotyls of non-induced plants, induced *XVE-PIN1* plants had a twisted growth along the vertical axis. Twisting was usually more pronounced close to the hypocotyl base (Fig. 2I,J). To test for possible changes in auxin distribution after induction of PIN1 expression, we crossed the *XVE-PIN1* line with the *DR5::GUS* reporter line, a widely used auxin response reporter (Hagen and Guilfoyle, 2002). *DR5::GUS* staining of the *XVE-PIN1* line after estradiol treatment suggested a stronger auxin accumulation in the root tip, which rationalizes the root agravitropic phenotype (Fig. 2N,O). In dark-grown seedlings, weak uniform GUS staining along the hypocotyl axis was seen in non-induced controls. This pattern changed after induction of PIN1 expression, and DR5 signal became stronger, with random maxima along the hypocotyl (Fig. 2L,M) reflecting differential cell elongation and hypocotyl twisting. Similar to the situation in BY-2 cells, PIN1-inducible overexpression phenotypes (root elongation and hypocotyl twisting) could be partially rescued by exogenous application of NPA (Fig. 2K,S). Notably, similar phenotypic aberrations and NPA treatment-based rescue were also detected at different levels of induced PIN expression (data not shown) and in other PIN1-overexpressing lines, such as DEX-inducible *GVG-PIN1* and constitutive *35S::PIN1* (data not shown). This confirmed that the phenotypic changes and changes in patterns of DR5 activity observed are due to the overexpression of PIN1 protein.

For comparison, we analysed *GVG-PGP1-myc* and *GVG-PGP19-HA* lines, which conditionally overexpress functional PGP1-*myc* and PG19-HA versions. As confirmed by the activity of the co-regulated GUS reporter construct (see Fig. S2A,B in the supplementary material), RT-PCR (see Fig. S2C,D in the supplementary material) and immunolocalization (Fig. 2C,D), both PGP1-*myc* and PGP19-HA were overexpressed after DEX treatment and localized mostly symmetrically at the plasma membrane (Fig. 2C,D). This confirmed induction of PGP1-*myc* and PGP19-HA expression, however, did not lead to gravitropic defects (data not shown), reduced root growth (Fig. 2G,H,T) or twisting of the dark-grown hypocotyls (data not shown). Instead, *GVG-PGP19-HA* seedling showed reduced outgrowth of cotyledons (Fig. 2G) and slightly shorter dark-grown hypocotyls (Fig. 2T). The *DR5rev::GFP* construct (Friml et al., 2003) introduced into *GVG-PGP19-HA* plants revealed a reduced *DR5* activity in the root tip, contrasting with the increased *DR5* signal after PIN1 overexpression (Fig. 2P,Q). Furthermore the sensitivity to NPA was not visibly altered in these lines (Fig. 2T).

Although other post-transcriptional events may influence the outcome of these overexpression experiments, observations that overexpression of PIN1 when compared with that of PGP1 and PGP19 leads to qualitatively different phenotypes suggest that, unlike in cultured cells, overexpression of PINs and PGPs in planta have different effects on auxin distribution and seedling development. This hypothesis is consistent with a scenario in which PIN and PGP efflux machineries are distinct and might have both overlapping and distinct functions in auxin transport-dependent development.

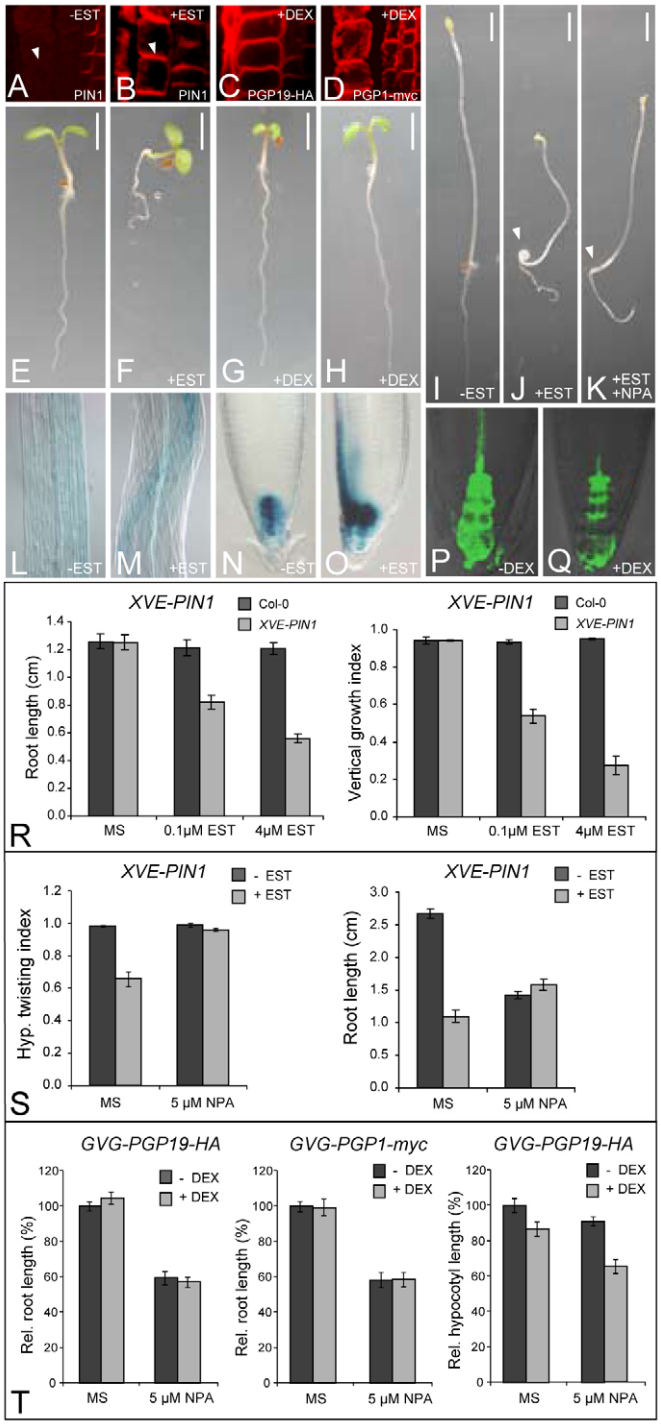

Fig. 2. Differential effect of PIN1 and PGP19 overexpression in *Arabidopsis* seedlings. (**A**,**B**) Immunolocalization of PIN1 in the *XVE-PIN1* line without (A) and with estradiol (B) induction. Ectopically expressed PIN1 localizes to the basal (lower) side of epidermal cells (arrowheads). (**C**,**D**) Immunolocalization of DEX-induced PGP19-HA in *GVG-PGP19-HA* (C) and PGP1-*myc in GVG-PGP1-myc* (D) lines show non-polar localization in epidermal cells. (**E-H**) Differential effects of PIN1, PGP19-HA and PGP1-*myc* overexpression on seedling development. Non-induced control (E); reduced root length and gravitropic response by induced PIN1 expression (F); no dramatic phenotypes caused by induced PGP19-HA (G) and PGP1-*myc* (H) expression, apart from a reduction in cotyledon outgrowth in the DEX-treated *GVG-PGP19-HA* line (G). (**I-K**) PIN1 overexpression phenotypes in dark-grown seedlings: straight hypocotyls in untreated controls (I); hypocotyl twists in estradiol-treated seedlings (J); this phenotype is almost completely reversed by the auxin transport inhibitor NPA (K). (**L-O**) Changes in the *DR5::GUS* auxin response reporter expression after PIN1 overexpression: *DR5::GUS* is weakly and equally expressed in hypocotyls of dark-grown seedlings (L), but shows randomly distributed local maxima that correlate with unequal cell elongation after PIN1 induction (M); GUS signal in the root tip is confined to the columella in the non-induced control (N), but increases and extends to the lateral root cup after PIN1 induction (O). (**P**,**Q**) Reduction of *DR5rev::GFP* signal in the columella after PGP19-HA expression (Q) when compared with untreated controls (P). (**R**) Concentration-dependent effect of estradiol-induced PIN1 overexpression on root elongation and gravitropism (calculated as vertical growth index (VGI) (Grabov et al., 2005). (**S**) Hypocotyl twisting and inhibition of root length following PIN overexpression can be reversed by NPA. (**T**) PGP1-*myc* and PGP19-HA overexpression have no pronounced effects on root growth, hypocotyl growth in the dark or sensitivity to NPA. Scale bars: 3 mm. Error bars represent s.e.m., *n*=20.

PGP proteins are expressed and synergistically interact with PIN1 protein during embryogenesis

To study whether distinct PIN- and PGP-dependent transport mechanisms have common developmental roles, we studied role of PIN- and PGP-dependent transport during different auxin transport-mediated processes. Many data on the developmental roles of various members of the PIN family are available (Tanaka et al., 2006), but comparable information for PGP1 and PGP19 is still largely lacking.

First, we studied the involvement of PIN- and PGP-dependent transport during *Arabidopsis* embryogenesis, which is known to be regulated by PIN-dependent asymmetric auxin distribution (Friml et al., 2003; Weijers et al., 2005). Various PIN proteins are expressed at different stages of embryogenesis in distinct cells, and *PIN* gene mutants (single and double), as well as mutants with defective PIN localization, are defective in embryo patterning (Steinmann et al., 1999; Friml et al., 2003; Friml et al., 2004; Weijers et al., 2005; Michniewicz et al., 2007). However, in *pgp* mutants, no embryo patterning defects have been reported and the function of PGPs in embryogenesis has not been studied so far. To investigate expression and cellular localization of PGP1 and PGP19 during embryogenesis, we used the functional tagged constructs *pPGP1::PGP1-myc* (Blakeslee et al., 2007) and *pPGP19::PGP19-GFP* (see Fig. S3 in the supplementary material). PGP1-*myc* was expressed from the earliest embryo stages onwards in all pro-embryo and suspensor cells. Cellular localization was mainly apolar, but more intense signals were observed between freshly divided cells (Fig. 3A,B). PGP19-GFP was also expressed at early stages, predominantly in the basal cell lineage that forms the suspensor until approximately the octant stage (Fig. 3C). At dermatogen (16-cell) stage, PGP19-GFP expression extended from suspensor to the lower tier cells of the pro-embryo (Fig. 3D). At mid-globular and later stages, PGP19-GFP expression was gradually confined to the outer layers, including protoderm and cells surrounding vascular precursor cells with no expression between initiating cotyledon primordia (Fig. 3E). At later stages, PGP19-GFP expression persisted in cells surrounding the forming vasculature (pericycle, endodermis and protoderm) (Fig. 3H). As for PGP1, no apparent polar localization

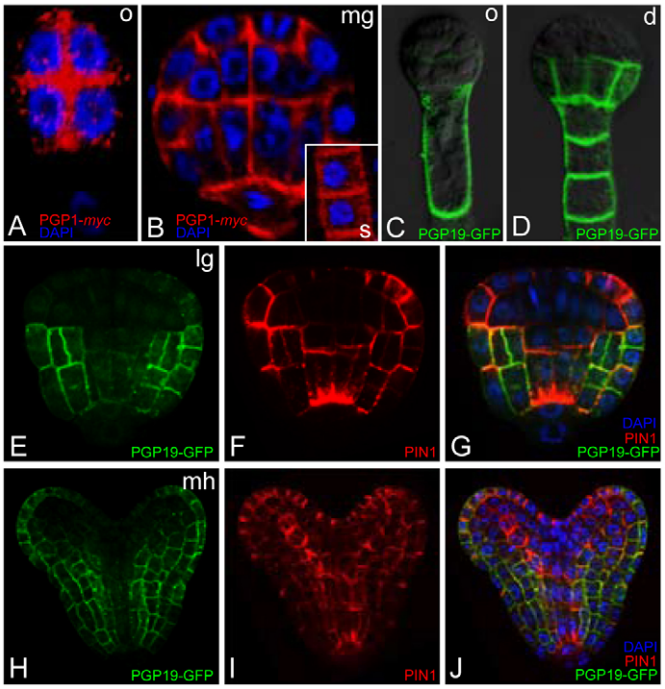

Fig. 3. Expression and localization of PGP1 and PGP19 during *Arabidopsis* embryogenesis. (**A**,**B**) Immunolocalization of PGP1-*myc* in *Arabidopsis* embryos (PGP1 in red, DAPI in blue). Expression of PGP1-*myc* in all cells and non-polar localization to the plasma membrane at octant (o) (A) and mid-globular (mg) (B) stages. Inset shows staining in the suspensor (s). (**C**,**D**) PGP19-GFP localization during early embryogenesis. PGP19-GFP localizes apolarly to the plasma membrane in derivatives of the basal cells at the octant stage (C) and in the suspensor and lower tier cells at the dermatogens (d) stage (D). (**E-J**) Restriction of the expression of PGP19-GFP at later stages of embryogenesis to protoderm and cells surrounding the vascular primordium, which is mainly complementary to PIN1 expression. Immunolocalization at late-globular (lg) (E-G) and mid-heart (mh) stages (H-J) of PGP19-GFP (green) (E,H), PIN1 (red) (F,I). (G,J) Overlay of PIN1, PGP19 and DAPI (blue).

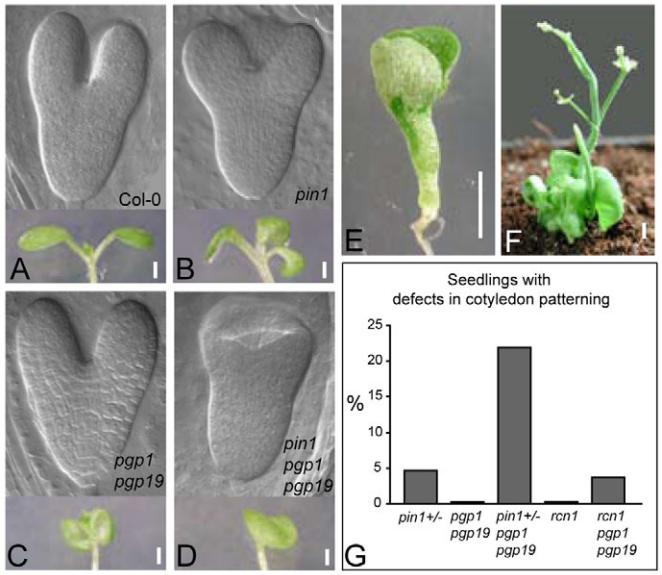

Fig. 4. Genetic interaction of PGPs with PIN1 during embryonic leaf formation. (**A-D**) Synergistic interaction of *pgp1pgp19* and *pin1* during cotyledon formation. Typical defects in cotyledon formation during embryogenesis and their postgermination appearance are shown: wild type (A), *pin1* (B), *pgp1pgp19* (C) and *pin1pgp1pgp19* (D). (**E**) Cup-shaped cotyledons of the *pin1pgp1pgp19* seedling that are rarely seen in the *pin1* mutant. (**F**) Strong enhancement of the *pin1* phenotype in post-embryonal development by the *pgp1pgp19* mutation. An adult, 5-week-old, plant with extremely dwarf appearance, reduced leaf number and apical dominance is shown. (**G**) Quantification of frequencies of cotyledon defects in different mutants and their combinations (*n*=200). Scale bars: 1 mm in A-D; 5 mm E,F.

was observed. Interestingly, the PGP19-GFP expression pattern at globular and later stages was roughly complementary to that of PIN1 (Fig. 3E-J). PGP19-expressing cells appeared to separate the inner basipetal and outer acropetal auxin streams, which are defined by PIN1 expression and localization (Friml et al., 2003; Vieten et al., 2005) (Fig. 3F,I).

To investigate the function of PGPs and eventually PGP-PIN interactions for embryonic development, we analysed young seedlings of *pin1*, *pgp1pgp19* and *pin1pgp1pgp19* genotypes. No patterning defects were observed in *pgp1pgp19* double mutant seedlings (Fig. 4C,G). In the progeny of *pin1*+/– plants, ~5% of seedlings had a defective cotyledon formation, including tricots and fused cotyledons (Fig. 4B,G), as reported previously (Okada et al., 1991). In the progeny of *pgp1pgp19pin1*+/– plants, almost 25% of seedlings had fused cotyledons and some were cup-shaped, a feature that is extremely rarely seen in *pin1* seedlings (Fig. 4D,E,G). Corresponding mutant phenotypes were also seen during embryogenesis at heart and later stages (Fig. 4A-D). As reported (Blakeslee et al., 2007), later post-embryonic development in *pin1pgp1pgp19* mutants was also very strongly affected (Fig. 4F).

These results reveal a previously unknown role of PGPs during embryogenesis. PGP1 and PGP19 are not strictly required for embryo development, but they act synergistically with PIN1 protein, mainly during cotyledon formation.

PGP genetically interacts with RCN1 in embryogenesis and root development

To test further the functional interaction between PGP- and PIN-dependent auxin transport systems in embryogenesis and patterning, we generated *rcn1pgp1pgp19* mutant that, besides lacking PGP-mediated efflux, is defective in *RCN1* (*Root Curling on NPA*). This gene encodes a subunit of protein phosphatase 2A (PP2A) that has been shown to be involved in various developmental and signalling processes (Garbers et al., 1996; Kwak et al., 2002; Larsen and Cancel, 2003). Importantly, PP2A phosphatase, together with PINOID kinase, regulates PIN polar targeting and, thus, directionality of PIN-dependent auxin transport (Friml et al., 2004; Michniewicz et al., 2007). Some features of the *rcn1* mutant are similar to those of the *pgp1pgp19* mutant, such as wavy root growth, but they do not include embryonic patterning defects (Garbers et al., 1996) (Fig. 4G). Strikingly, *rcn1pgp1pgp19* triple mutants exhibited strong embryonic and post-embryonic auxin-related phenotypes. Some seedlings of the *rcn1pgp1pgp19* mutant were defective in apical-basal patterning (11/97) or cotyledon formation (3/97) (Fig. 5E,F). During embryogenesis, *rcn1pgp1pgp1* exhibited aberrant hypophysis divisions (16/20) at the globular stage (Fig. 5A-D). This spectrum of developmental aberrations is typical for mutants with

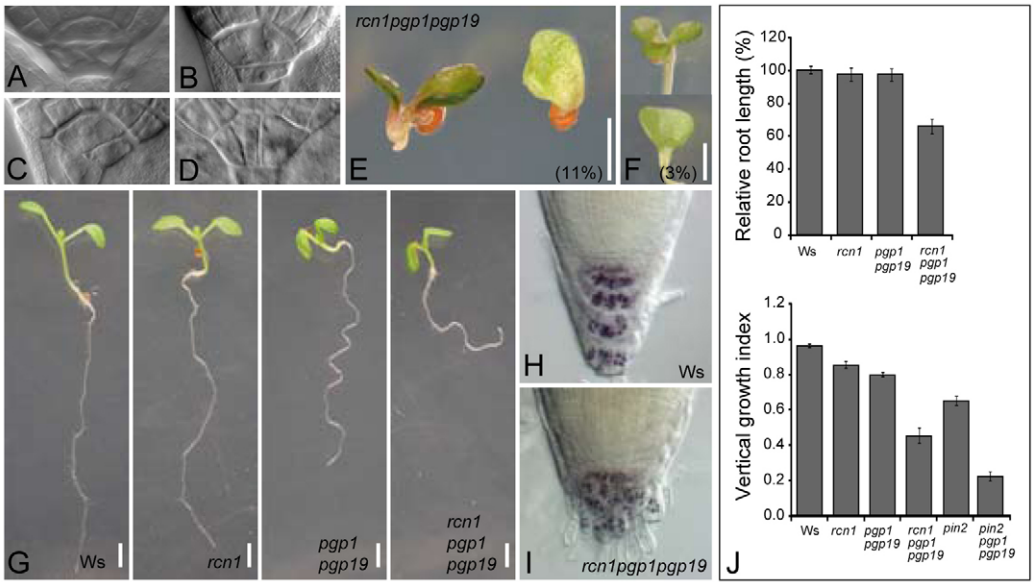

Fig. 5. Genetic interaction of PGPs with RCN1. (**A-D**) Aberrant cell divisions of the hypophysis at the globular stage in *rcn1pgp1pgp19* mutant embryos. The wild-type hypophysis divides into two derivatives: the smaller lens-shaped cells and bigger basal cells (A). Different aberrations in the cell division of the *rcn1pgp1pgp19* mutant (B-D). (**E**,**F**) Rootless (E) and cotyledon patterning (F) defects in *rcn1pgp1pgp19* seedlings (*n*=97). (**G**) Enhanced defects in root elongation and gravitropism in 10-day-old seedlings of *rcn1pgp1pgp19* as compared with controls. (**H**,**I**) Defects in root tip organization, visualized by a lugol staining in *rcn1pgp1pgp19* (I) when compared with wild type (H). (**J**) Quantification of root length and gravitropism phenotypes of the *rcn1pgp1pgp19* mutant. For comparison, *pin2* and *pin2pgp1pgp19* data are also included (*n*=25). Scale bars: 2 mm. Error bars represent s.e.m.

strong defects in auxin transport (for example, *pin1pin3pin4pin7*) (Friml et al., 2003) or auxin signalling (*monopteros* and *bodenlos*) (Hardtke and Berleth, 1998; Hamann et al., 2002). In post-embryonic development, roots of *rcn1pgp1pgp19* seedlings were reduced in length and showed enhanced defects in the gravitropic response and differentiation of columella cells when compared with *rcn1* single or *pgp1pgp19* double mutants (Fig. 5H-J).

This observation further confirms that PGP function significantly contributes to auxin-mediated patterning processes and supports a scenario in which PGP- and PIN-dependent transport systems functionally interact during embryogenesis at the level of the whole transport systems rather than directly through protein interactions.

Diverse functions of PGP1 and PGP19 in lateral root organogenesis

Next, we studied the role of PGP-dependent auxin efflux and its possible interaction with PIN-dependent mechanisms in lateral root initiation and emergence, other processes that involve PIN-dependent auxin transport. Pharmacological or genetic modulation of local transport-dependent auxin distribution inhibits lateral root initiation and its morphogenesis (Benková et al., 2003; Casimiro et al., 2003). The role of PGP1 and PGP19 in lateral root development has already been proposed (Lin and Wang, 2005; Wu et al., 2007), but their precise function and interaction with PINs in initiation and emergence remains unknown.

We determined expression and localization patterns of PGP1 and PGP19 during early post-embryonic development by using *pPGP1::PGP1-GFP* and *pPGP19::PGP19-GFP* constructs. *pPGP1::PGP1-GFP* and *pPGP19::PGP19-GFP* complemented most aspects of the corresponding *pgp1* and *pgp19* mutant phenotypes, such as hypocotyl elongation defect (see Fig. S3A-E in the supplementary material). Similarly to expression during embryogenesis, PGP1-GFP did not exhibit tissue-specific expression pattern and was detected in all cells of hypocotyls and roots (Fig. 6A,C,D), except root-tip columella cells. The expression of PGP19-GFP was also found in hypocotyls and main roots, but, in contrast to PGP1-GFP, exhibited a more tissue-specific pattern, with strongest expression in endodermal and pericycle tissues (Fig. 6B,E,F), in agreement with published data on PGP19-HA (Blakeslee et al., 2007) and MDR1(PGP19)-GFP (Wu et al., 2007). In addition, PGP19-GFP expression was detected also in root tip epidermal cells, which is not supported by the published pattern of MDR1(PGP19)-GFP (Wu et al., 2007). Both proteins are also expressed during all stages of lateral root development and persisted after lateral root emergence as shown previously (Geisler et al., 2005; Wu et al., 2007). PGP1-GFP expression was observed from the first stage of lateral root primordium organogenesis on (Fig. 6G). During developmental stage I, PGP1-GFP was localized to anticlinal membranes of short initials, and, later, when lateral root primordia are formed, apolar membrane localization was detected in all cells of primordia. Expression and membrane localization of PGP19-GFP at developmental stage I fully overlapped with PGP1, but at later developmental stages PGP19-GFP expression was more restricted to endodermis and pericycle. In emerged lateral roots, PGP19-GFP was detected also in cortical and epidermal cells, similar to its expression in primary root tips (Fig. 6H).

Next, we investigated the consequence of PGP1 and PGP19 loss in lateral root initiation and emergence, and their functional interaction with PIN1 in this process. Both *pgp* single mutants initiated fewer lateral roots (Fig. 6I), whereas, interestingly, the combination of *pgp1* and *pgp19* mutations almost completely rescued the effect of single mutations (Fig. 6I). This genetic complementation of *pgp1* and *pgp19* mutations was also observed during lateral root emergence (Fig. 6J). Both single mutants had a reduced progression rate through consecutive stages of lateral root development, but this defect was largely recovered in *pgp1pgp19*

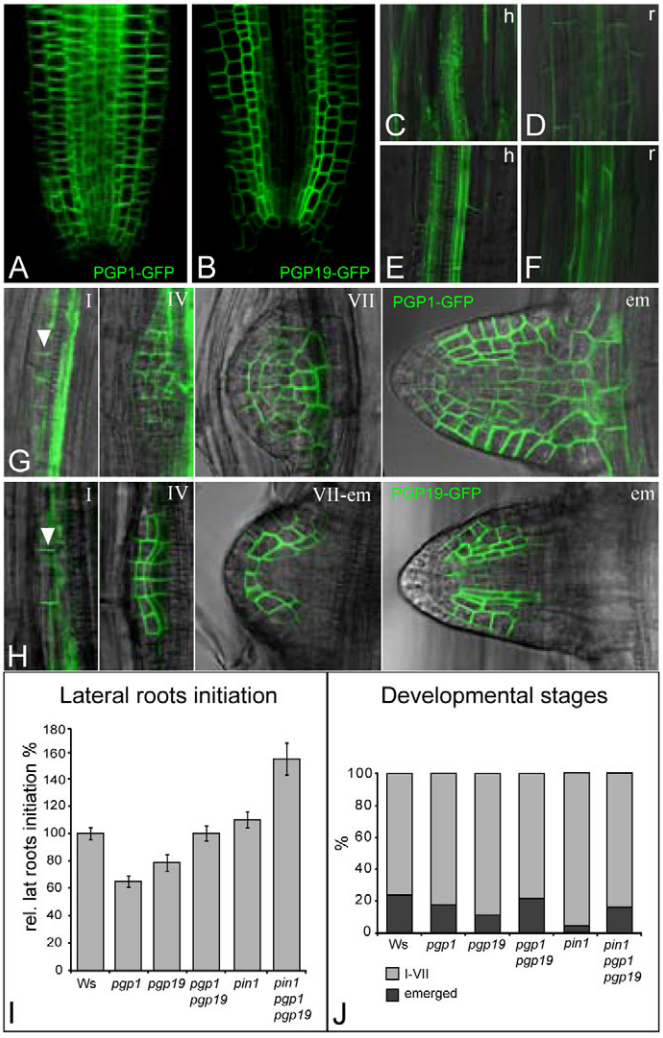

Fig. 6. Post-embryonic expression and the role of PGP1/PGP19 in lateral root development. (**A**,**B**) Expression and localization of PGP1-GFP and PGP19-GFP in root tips of 5-day-old seedlings. PGP1-GFP is expressed in all cells, except the columella (A); PGP19-GFP expression is more restricted to endodermal and pericycle cells (B). (**C-F**) Expression of PGP1-GFP and PGP19-GFP in hypocotyls and main root. PGP1-GFP is expressed in all cells of hypocotyls (C) and main root (D), whereas PGP19-GFP expression is more restricted to cells surrounding vascular tissues in hypocotyls (E) and main root (F). h, hypocotyl; r, root. (**G**,**H**) Expression of PGP1-GFP and PGP19-GFP during lateral root development. PGP1-GFP expression is detected in all cells during all stages (G) (indicated) and that of PGP19-GFP is more confined at later stages (indicated) to the new forming endodermal and pericycle cells (H). Arrowheads indicate the localization of PGP1/PGP19-GFP on anticlinal membranes at stage I. (**I**) Initiation and (**J**) emergence phenotypes of *pgp1*, *pgp19*, *pin1*, *pgp1pgp19* and *pin1pgp1pgp19* mutants (*n*=40).

double mutants (Fig. 6J). Addition of *pin1* to the *pgp1pgp19* mutant surprisingly led to rescue of *pin1* phenotype, which is characterized by delayed lateral root primordium development (Benková et al., 2003), and even slightly increased lateral root initiation above wild-type level (Fig. 6I,J).

These analyses show that functions of PGP1, PGP19 and PIN1 are required for lateral root formation and suggest a complex interaction of these proteins at multiple stages of the process.

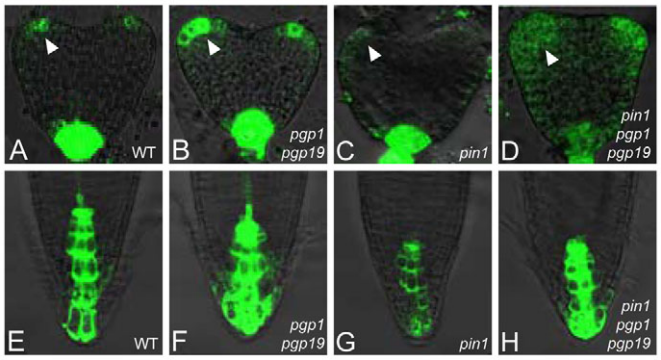

Fig. 7. Role of PGPs and PINs in the regulation of the spatial distribution of the auxin response. (**A-H**) Roles of PGP1/PGP19 and PIN1 in auxin response distribution (as visualized by *DR5rev::GFP*) in heart-stage embryos (A-D) and root tips (E-H). Wild type (A,E). Increased signal in *pgp1pgp19* (B,F), decreased signal in *pin1* (C,G) and pronounced defects in the distribution of the DR5 signal in the *pin1pgp1pgp19* embryos (D) are seen, but restoration occurs in roots (H). At least five roots or embryos from all mutant combination were simultaneously analysed in two independent experiments (for *pin1* and *pin1pgp1pgp19* mutants, only embryos with visible phenotypes were analysed). Arrowheads in A-D indicate auxin maxima in cotyledon primordia.

Antagonistic and synergistic effects of PIN- and PGP-dependent transport on the spatial pattern of auxin responses

To gain further insights into how PGP- and PIN-mediated transport mechanisms together regulate auxin-dependent plant development, we analysed changes in auxin distribution, as visualized indirectly by the *DR5rev::GFP* auxin response reporter (Friml et al., 2003). During embryogenesis, spatial distribution of *DR5rev::GFP* signal did not dramatically change in *pgp1pgp19* mutants, but auxin response maxima in cotyledon primordia and at the root pole were enhanced (Fig. 7A,B). Conversely, *pin1* mutant embryos had a reduced *DR5* signal at the root pole and cotyledon primordia (Fig. 7A,C). When *pin1* and *pgp1pgp19* mutations were combined, the spatial pattern of *DR5* activity distribution in embryos was strongly distorted. The *DR5* activity maxima were less well defined and *DR5* signal was more diffuse (Fig. 7D). These results clearly show that both PGP- and PIN1-mediated transport systems are required together for the spatial pattern of auxin distribution and formation of well-defined auxin maxima during embryogenesis. This observation also fully explains the observed synergistic genetic interaction between *pin1* and *pgp1pgp19* mutations (Fig. 4A-E,G).

In post-embryonic roots, the situation is somewhat different: maintenance of auxin maxima in the quiescent centre/columella region is crucial for controlling root meristem activity (Sabatini et al., 1999; Friml et al., 2002a; Grieneisen et al., 2007). We detected quantitative changes in *DR5* activity similar to those during embryogenesis, including and increase in *DR5* activity in *pgp1pgp19* mutants, but a reduction in *pin1* mutant roots (Fig. 7E-G). However, when *pgp1pgp19* and *pin1* mutations were combined, the spatial pattern of *DR5* activity was not impaired and the level of activity was roughly restored to that of the wild type (Fig. 7H). This apparent difference between the requirements of PGP and PIN transport systems for spatial patterning of the auxin response in embryos and seedling roots is probably due to pronounced

functional redundancy of PIN proteins for auxin delivery to the central root meristem during post-embryonic development (Blilou et al., 2005; Vieten et al., 2005).

Opposite roles of PIN and PGP transport mechanisms were also observed during auxin redistribution after gravitropic stimulation (Lin and Wang 2005), where auxin redistribution to the lower side of gravistimulated root is more pronounced in *pgp1pgp19* (see Fig. S4A,B in the supplementary material), but inhibited in *pin2* mutants (Luschnig et al., 1998). Contrasting functions of PIN and PGP are also supported by the synergistic effects of PIN1 gain-of-function and PGP loss-of-function alleles. For example, defects in root elongation and hypocotyl twisting were more pronounced after *XVE-PIN1* induction in *pgp1pgp19* mutant than they were after PIN1 induction in wild type (Fig. 8A).

In summary, these data show that even when PGP- and PIN-dependent auxin transport mechanisms have opposite or even antagonistic effects on auxin distribution and development during several developmental processes, both systems are complementary and are required together to maintain a dynamic spatial pattern of auxin distribution and subsequent development.

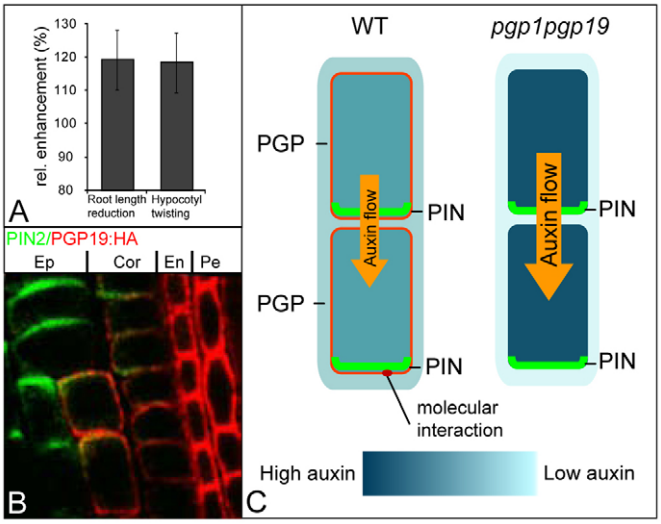

Fig. 8. Model for interaction of PGPs and PINs in the local auxin distribution in meristematic tissues. (**A**) Enhanced effects (~20%) of estradiol-induced *PIN1* overexpression on root length and hypocotyl twisting in the *pgp1pgp19* mutant when compared with wild type, confirming the antagonistic roles of PIN1 and PGP1/PGP19 in seedling development. Error bars represent s.e.m., *n*=20. (**B**) Immunolocalization of PIN2 and PGP19-HA. Polar and non-polar localization of PIN2 and PGP19-HA in the root epidermis, respectively. Expression of PGP19 is higher in the endodermis and the pericycle that form the border between acropetal and basipetal auxin streams. (**C**) Model of PIN and PGP interaction. PGPs and PINs interact intermoleculary at the PIN-containing polar domain, possibly regulating the PIN stability in the plasma membrane. The PGPs remaining in these cells control the cellular auxin pool available for the PIN transport. In *pgp1pgp19*, the cellular auxin concentration is increased and, therefore, the PIN transport is enhanced but less focused.

DISCUSSION

Carrier-mediated auxin efflux is considered to be the crucial step in the intercellular auxin transport and is required for multitude of auxin distribution-dependent developmental processes (Tanaka et al., 2006; Vieten et al., 2007). PGP and PIN proteins from *Arabidopsis* are both involved in auxin efflux (Geisler et al., 2005; Petrášek et al., 2006) and can physically and functionally interact in mediating this process (Blakeslee et al., 2007). However, the developmental relevance of the PGP and PIN interactions is unclear. Here, we have systematically studied the distinct and common roles of both auxin efflux systems in auxin distribution-dependent development and provide new insights into understanding the purpose of these two independent auxin efflux mechanisms for regulating plant development.

PGPs and PINs define two distinct auxin efflux systems

Since the identification of both PINs and PGPs as being involved in the same process of cellular auxin efflux (Geisler et al., 2005; Petrášek et al., 2006), an important issue is whether they represent independent transport systems or act together as necessary parts of one transport system. Our results strongly support the scenario in which PGPs and PINs characterise two distinct auxin efflux mechanisms. The earlier observations of the largely non-overlapping phenotypes observed in *pin* and *pgp* loss-of-function mutants (Vieten et al., 2007) indicated a different role for these protein families that could be explained by the distinct expression patterns of the family members. More significantly, when both proteins are overexpressed under comparable general promoters in the present study, the resulting phenotypes, although similar in cultured cells, appear to be distinct in planta, and show different sensitivities to the auxin efflux inhibitor NPA. Phenotypes resulting from PIN overexpression can be reversed by NPA, but similar sensitivities to NPA are not possible to demonstrate in PGP overexpression lines. The different effects of PIN and PGP overexpression, together with the different responses of these transporters to inhibitors, clearly favours the scenario that PIN and PGP protein families define two distinct auxin efflux machineries.

However, the identity of the molecular mechanism that underlies the effect of auxin efflux inhibitors such as NPA still has to be clarified. Previous reports have clearly shown that NPA binds PGP proteins (Noh et al., 2001; Murphy et al., 2002; Rojas-Pierce et al., 2007), that PGP-mediated auxin efflux activity is inhibited by NPA in heterologous systems (Petrášek et al., 2006; Blakeslee et al., 2007) and that NPA inhibits PGP19 action in phototropism (Nagashima et al., 2008). It is possible that NPA and other auxin efflux inhibitors have multiple binding and regulatory sites with different affinities. Moreover, auxin efflux inhibitors might have multiple effects, including modification of actin-based subcellular dynamics (Dhonukshe et al., 2008) or of the PGP-PIN interaction (Blakeslee et al., 2007).

PGP- and PIN-mediated transport are required together for embryogenesis and organogenesis

Another important argument for distinct roles of the PGP- and PIN-dependent transport systems are the divergent phenotypes in *pin* loss-of-function mutants when compared with *pgp1* and *pgp19* mutants. PGP proteins play an important role in determining the plant architecture during vegetative growth (Noh et al., 2001; Lin and Wang, 2005; Wu et al., 2007). For example, agriculturally interesting dwarf mutations in maize and sorghum results from loss of PGP activity and from a reduction in auxin transport (Multani et al., 2003). However, *pgp* mutants do not show clear patterning defects, whereas *pin* single and multiple mutants show defects in embryogenesis, organogenesis, tissue differentiation and meristem activity (Tanaka et al., 2006; Vieten et al., 2007). We found that an important role of PGP1 and PGP19 in patterning processes can be unmasked if the PIN-

dependent transport is compromised. During embryogenesis, the *pgp1pgp19* mutation enhances greatly the effect of the *pin1* mutation on the formation of embryonic leaves. Furthermore, analysis of mutant combinations of *pgp1pgp19* and *rcn1* [a gene encoding a regulatory subunit of PP2A phosphatase that does not influence the PIN function directly, but through the phosphorylation-dependent the PIN polar subcellular targeting (Michniewicz et al., 2007)] revealed very strong embryo and seedling patterning phenotypes that are not observed in any of the single combinations. The phenotypes are reminiscent of those found in mutants that are strongly defective in auxin transport, such as *gnom*/*emb30* (Steinman et al., 1999) and *pin1pin3pin4pin7* (Friml et al., 2003) mutants. These results, together with expression and localization patterns of PGP1 and PGP19 during embryogenesis, reveal a previously unknown role of the PGP-dependent auxin transport in development and support the notion that the common functions of these two transport mechanisms contribute to patterning processes.

Concerted action of PGP- and PIN-mediated transports is required for auxin distribution

Auxin transport executes its effect on plant development largely by generating asymmetric auxin distribution, which is often indirectly monitored using the auxin response. The effects of gain- and loss-of-function mutations in PGPs and PIN proteins on the quantity of local auxin response and resulting development are, at times, seemingly opposite. For example, in root tip, PIN1 overexpression, but not *pgp1pgp19* loss of function, enhances auxin accumulation in central root meristem. Conversely, *pin1* loss of function and PGP19 overexpression both produce the opposite effect: a decrease in auxin response in the root-tip region. Similarly, during embryogenesis, the *pin1* mutation decreases auxin response maxima, but *pgp1pgp19* increases them. These results show that PGP- and PIN-dependent transport systems play, in some instances, opposing roles in mediating auxin accumulation in specific cells.

The opposite actions of PGP and PIN proteins can also be observed at the developmental level. Some features of PIN1 overexpression, such as twisting hypocotyls, can also be seen in the *pgp1pgp19* mutant (Noh et al., 2001) or in the mutant of the apparent activator of the PGP function – immunophilin-like protein TWISTED/DWARF (TWD) (Geisler et al., 2003). Furthermore, hypergravitropic root growth in *pgp1pgp19* seedlings (Lin and Wang, 2005) (see Fig. S4 in the supplementary material) contrasts with agravitropic growth of *pin2* or *pin3* seedlings. Significant also are the additive effects of *pgp1pgp19* mutations on the PIN1 overexpression-induced phenotypes. Interestingly, despite these opposite roles for PGPs and PINs in mediating the quantitative distribution of the auxin response, both transport systems are required together for generating proper spatial patterns of auxin distribution. This effect was observed for auxin distribution in *pin1pgp1pgp19* mutant embryos (Fig. 7H) or in *pin2pgp1pgp19* seedlings during the gravitropic response (Blakeslee et al., 2007) (Fig. 5J). Thus, both the PGP- and PIN-dependent auxin transport mechanisms play distinct, sometimes opposite, roles in auxin distribution, but both transport systems cooperate to generate and maintain the spatial pattern of auxin distribution that is necessary for patterning and tropisms.

Model of the PGP and PIN interaction in local auxin distribution in meristematic tissues

Based on previous and novel findings, we propose a model for the functional interaction between PGP- and PIN-dependent auxin transport mechanisms in embryos and root meristems (Fig. 8C). We take into account the prevalent non-polar cellular localization of PGP1 and PGP19 (Fig. 3, Fig. 6A-H, Fig. 8B) as well as the related loss-of function and overexpression phenotypes. In cells where PINs and PGPs are co-expressed, two types of interactions might take place. A direct interaction between PIN and PGP, which takes place at PIN polar membrane domains, contributes to the specificity and modulation of auxin efflux rate (Blakeslee et al., 2007). The proportion of PGPs that do not colocalize with PINs act multilaterally in auxin efflux and, thus, regulate the effective cellular auxin concentration available for PIN-mediated transport. This combined action of PIN and PGP action determines how much auxin flows through auxin channels. Observation of a higher cellular auxin concentration in *pgp* mutants (Bouchard et al., 2006) that might enhance PIN-mediated transport directly supports this scenario. However, establishment of such a specific auxin concentration by enhanced PGP19 expression in cells, where there is no direct PIN1-PGP19 colocalization (such as basal protoderm and endodermal initials in embryos), additionally focuses auxin flow. It is likely that for long-distance transport, e.g. in stems, another mode of PGP and PIN interaction applies, as suggested by strong auxin transport defects in *pgp* mutant stems (Noh et al., 2001; Geisler et al., 2005).

It is important to note that different internal or external cues, such as light, can influence the extent and mode of PIN-PGP interactions, for instance at the level of functional pairing of PINs and PGPs (Blakeslee et al., 2007) or by producing distinct effects on either PIN or PGP functions. Moreover, the activity of previously uncharacterized PGPs may also significantly contribute to auxin transport. In summary, our model could provide an explanation of the existence of two auxin transport mechanisms that ensure precise and proper formation of spatial and temporal auxin distribution in plants.

We are grateful to Angus Murphy and Markus Geisler for providing published material and helpful comments to the manuscript. This research was supported by the Volkswagenstiftung (J.F., J.M., V.G. and A.B.), by the Odysseus program of FWO (J.M.), by the EMBO Young Investigator Programme (J.F.), by the Deutsche Forschung Gemeinschaft (DFG) (S.C.), by the DAAD (J.M.), by the Margarete von Wrangell-Habilitationsprogramm (E.B.), by the Ministry of Education, Youth and Sports of the Czech Republic (LC06034), and by the Grant Agency of the Academy of Sciences of the Czech Republic (KJB600380604) (M.K., J.P., P.S. and E.Z.).

Supplementary material

Supplementary material for this article is available at
http://dev.biologists.org/cgi/content/full/135/20/3345/DC1

References

Abas, L., Benjamins, R., Malenica, N., Paciorek, T., Wiśniewska, J., Moulinier-Anzola, J. C., Sieberer, T., Friml, J. and Luschnig, C. (2006). Intracellular trafficking and proteolysis of the *Arabidopsis* auxin-efflux facilitator PIN2 are involved in root gravitropism. *Nat. Cell Biol.* **8**, 249-256.

Aoyama, T. and Chua, N.-H. (1997). A glucocorticoid-mediated transcriptional induction system in transgenic plants. *Plant J.* **11**, 605-612.

Bandyopadhyay, A., Blakeslee, J. J., Lee, O. R., Mravec, J., Sauer, M., Titapiwatanakun, B., Makam, S. N., Bouchard, R., Geisler, M., Martinoia, E. et al. (2007). Interactions of PIN and PGP auxin transport mechanisms. *Biochem. Soc. Trans.* **35**, 137-141.

Benková, E., Michniewicz, M., Sauer, M., Teichmann, T., Seifertová, D., Jürgens, G. and Friml, J. (2003). Local, efflux-dependent auxin gradients as a common module for plant organ formation. *Cell* **115**, 591-602.

Blakeslee, J. J., Bandyopadhyay, A., Lee, O. R., Mravec, J., Tipapiwatanakun, B., Sauer, M., Makam, S. N., Cheng, Y., Bouchard, R., Adamec, J. et al. (2007). Interactions among PIN-FORMED and P-glycoprotein auxin transporters in *Arabidopsis*. *Plant Cell* **19**, 131-147.

Blilou, I., Xu, J., Wildwater, M., Willemsen, V., Paponov, I., Friml, J., Heidstra, R., Aida, M., Palme, K. and Scheres, B. (2005). The PIN auxin efflux facilitator network controls growth and patterning in *Arabidopsis* roots. *Nature* **433**, 39-44.

Bouchard, R., Bailly, A., Blakeslee, J. J., Oehring, S. C., Vincenzetti, V., Lee, O. R., Paponov, I., Palme, K., Mancuso, S., Murphy, A. S. et al. (2006).

Immunophilin-like TWISTED DWARF1 modulates auxin efflux activities of *Arabidopsis* P-glycoproteins. *J. Biol. Chem*. **281**, 30603-30612.
Casimiro, I., Beeckman, T., Graham, N., Bhalerao, R., Zhang, H., Casero, P., Sandberg, G. and Bennett, M. J. (2003). Dissecting *Arabidopsis* lateral root development. *Trends Plant Sci*. **8**, 165-171.
Dhonukshe, P., Grigoriev, I., Fischer, R., Tominaga, M., Robinson, D. G., Hašek, J., Paciorek, T., Petrášek, J., Seifertová, D., Tejos, R. et al. (2008). Auxin transport inhibitors impair vesicle motility and actin cytoskeleton dynamics in diverse eukaryotes. *Proc. Natl. Acad. Sci. USA* **105**, 4489-4494.
Friml, J., Benková, E., Blilou, I., Wiśniewska, J., Hamann, T., Ljung, K., Woody, S., Sandberg, G., Scheres, B., Jürgens, G. et al. (2002a). AtPIN4 mediates sink driven auxin gradients and root patterning in *Arabidopsis*. *Cell* **108**, 661-673.
Friml, J., Wiśniewska, J., Benková, E., Mendgen, K. and Palme, K. (2002b). Lateral relocation of auxin efflux regulator PIN3 mediates tropism in *Arabidopsis*. *Nature* **415**, 806-809.
Friml, J., Vieten, A., Sauer, M., Weijers, D., Schwarz, H., Hamann, T., Offringa, R. and Jürgens, G. (2003). Efflux-dependent auxin gradients establish the apical-basal axis of *Arabidopsis*. *Nature* **426**, 147-153.
Friml, J., Yang, X., Michniewicz, M., Weijers, D., Quint, A., Tietz, O., Benjamins, R., Ouwerkerk, P. B. F., Ljung, K., Sandberg, G. et al. (2004). A PINOID-dependent binary switch in apical-basal PIN polar targeting directs auxin efflux. *Science* **306**, 862-865.
Gälweiler, L., Guan, C., Müller, A., Wisman, E., Mendgen, K., Yephremov, A. and Palme, K. (1998). Regulation of polar auxin transport by AtPIN1 in *Arabidopsis* vascular tissue. *Science* **282**, 2226-2230.
Garbers, C., DeLong, A., Deruére, J., Bernasconi, P. and Söll, D. (1996). A mutation in protein phosphatase 2A regulatory subunit A affects auxin transport in *Arabidopsis*. *EMBO J*. **15**, 2115-2124.
Geisler, M., Kolukisaoglu, H. U., Bouchard, R., Billion, K., Berger, J., Saal, B., Frangne, N., Koncz-Kalman, Z., Koncz, C., Dudler, R. et al. (2003). TWISTED DWARF1, a unique plasma membrane-anchored immunophilin-like protein, interacts with Arabidopsis multidrug resistance-like transporters AtPGP1 and AtPGP19. *Mol. Biol. Cell* **14**, 4238-4249.
Geisler, M., Blakeslee, J. J., Bouchard, R., Lee, O. R., Vincenzetti, V., Bandyopadhyay, A., Titapiwatanakun, B., Peer, W. A., Bailly, A., Richards, E. L. et al. (2005). Cellular efflux of auxin catalyzed by the Arabidopsis MDR/PGP transporter AtPGP1. *Plant J*. **44**, 179-194.
Grabov, A., Ashley, M. K., Rigas, S., Hatzopoulos, P., Dolan, L. and Vicente-Agullo, F. (2005). Morphometric analysis of root shape. *New Phytol*. **165**, 641-652.
Grieneisen, V. A., Xu, J., Marée, A. F. M., Hogeweg, P. and Scheres, B. (2007). Auxin transport is sufficient to generate a maximum and gradient guiding root growth. *Nature* **449**, 1008-1013.
Hagen, G. and Guilfoyle, T. (2002). Auxin-responsive gene expression: genes, promoters and regulatory factors. *Plant Mol. Biol*. **49**, 373-385.
Hamann, T., Benkova, E., Bäurle, I., Kientz, M. and Jürgens, G. (2002). The *Arabidopsis BODENLOS* gene encodes an auxin response protein inhibiting MONOPTEROS-mediated embryo patterning. *Genes Dev*. **16**, 1610-1615.
Hardtke, C. S. and Berleth, T. (1998). The *Arabidopsis* gene *MONOPTEROS* encodes a transcription factor mediating embryo axis formation and vascular development. *EMBO J*. **17**, 1405-1411.
Kerr, I. D. and Bennett, M. J. (2007). New insight into the biochemical mechanisms regulating auxin transport in plants. *Biochem. J*. **401**, 613-622.
Kwak, J. M., Moon, J. H., Murata, Y., Kuchitsu, K., Leonhardt, N., DeLong, A. and Schroeder, J. I. (2002). Disruption of a guard cell-expressed protein phosphatase 2A regulatory subunit, RCN1, confers abscisic acid insensitivity in *Arabidopsis*. *Plant Cell* **14**, 2849-2861.
Larsen, P. B. and Cancel, J. D. (2003). Enhanced ethylene responsiveness in the *Arabidopsis eer1* mutant results from a loss-of-function mutation in the protein phosphatase 2A A regulatory subunit, RCN1. *Plant J*. **34**, 709-718.
Lin, R. and Wang, H. (2005). Two homologous ATP-binding cassette transporter proteins, AtMDR1 and AtPGP1, regulate Arabidopsis photomorphogenesis and root development by mediating polar auxin transport. *Plant Physiol*. **138**, 949-964.
Luschnig, C., Gaxiola, R. A., Grisafi, P. and Fink, G. R. (1998). EIR1, a root-specific protein involved in auxin transport, is required for gravitropism in *Arabidopsis thaliana*. *Genes Dev*. **12**, 2175-2187.
Martinoia, E., Klein, M., Geisler, M., Bovet, L., Forestier, C., Kolukisaoglu, Ü., Müller-Röber, B. and Schulz, B. (2002). Multifunctionality of plant ABC transporters-more than just detoxifiers. *Planta* **214**, 345-355.
Michniewicz, M., Zago, M. K., Abas, L., Weijers, D., Schweighofer, A., Meskiene, I., Heisler, M. G., Ohno, C., Zhang, J., Huang, F. et al. (2007). Antagonistic regulation of PIN phosphorylation by PP2A and PINOID directs auxin flux. *Cell* **130**, 1044-1056.
Multani, D. S., Briggs, S. P., Chamberlin, M. A., Blakeslee, J. J., Murphy, A. S. and Johal, G. S. (2003). Loss of an MDR transporter in compact stalks of maize br2 and sorghum dw3 mutants. *Science* **302**, 81-84.
Murphy, A. S., Hoogner, K. R., Peer, W. A. and Taiz, L. (2002). Identification, purification, and molecular cloning of N-1-naphthylphthalmic acid-binding plasma membrane-associated aminopeptidases from Arabidopsis. *Plant Physiol*. **128**, 935-950.
Nagashima, A., Suzuki, G., Uehara, Y., Saji, K., Furukawa, T., Koshiba, T., Sekimoto, M., Fujioka, S., Kuroha, T., Kojima, M. et al. (2008). Phytochromes and cryptochromes regulate the differential growth of *Arabidopsis* hypocotyls in both a PGP19-dependent and a PGP19-independent manner. *Plant J*. **53**, 516-529.
Nagata, T., Nemoto, Y. and Hasezawa, S. (1992). Tobacco BY-2 cell line as the 'HeLa' cell in the cell biology of higher plants. *Int. Rev. Cytol*. **132**, 1-30.
Noh, B., Murphy, A. S. and Spalding, E. P. (2001). *Multidrug resistance*-like genes of Arabidopsis required for auxin transport and auxin-mediated development. *Plant Cell* **13**, 2441-2454.
Okada, K., Ueda, J., Komaki, M. K., Bell, C. J. and Shimura, Y. (1991). Requirement of the auxin polar transport system in early stages of *Arabidopsis* floral bud formation. *Plant Cell* **3**, 677-684.
Paciorek, T., Zažímalová, E., Ruthardt, N., Petrášek, J., Stierhof, Y.-D., Kleine-Vehn, J., Morris, D. A., Emans, N., Jürgens, G., Geldner, N. et al. (2005). Auxin inhibits endocytosis and promotes its own efflux from cells. *Nature* **435**, 1251-1256.
Petrášek, J., Mravec, J., Bouchard, R., Blakeslee, J. J., Abas, M., Seifertová, D., Wiśniewska, J., Tadele, Z., Kubeš, M., Čovanová, M. et al. (2006). PIN proteins perform a rate-limiting function in cellular auxin efflux. *Science* **312**, 914-918.
Reinhardt, D., Pesce, E.-R., Stieger, P., Mandel, T., Baltensperger, K., Bennett, M., Traas, J., Friml, J. and Kuhlemeier, C. (2003). Regulation of phyllotaxis by polar auxin transport. *Nature* **426**, 255-260.
Rojas-Pierce, M., Titapiwatanakun, B., Sohn, E. J., Fang, F., Larive, C. K., Blakeslee, J., Cheng, Y., Cuttler, S., Peer, W. A., Murphy, A. S. et al. (2007). *Arabidopsis* P-glycoprotein19 participates in the inhibition of gravitropism by gravacin. *Chem. Biol*. **14**, 1366-1376.
Růžička, K., Ljung, K., Vanneste, S., Podhorská, R., Beeckman, T., Friml, J. and Benková, E. (2007). Ethylene regulates root growth through effect on auxin biosynthesis and transport-dependent auxin distribution. *Plant Cell* **19**, 2197-2212.
Sabatini, S., Beis, D., Wolkenfelt, H., Murfett, J., Guilfoyle, T., Malamy, J., Benfey, P., Leyser, O., Bechtold, N., Weisbeek, P. et al. (1999). An auxin-dependent distal organizer of pattern and polarity in the *Arabidopsis* root. *Cell* **99**, 463-472.
Sauer, M., Balla, J., Luschnig, C., Wiśniewska, J., Reinöhl, V., Friml, J. and Benková, E. (2006a). Canalization of auxin flow by Aux/IAA-ARF-dependent feed-back regulation of PIN polarity. *Genes Dev.* **20**, 2902-2911.
Sauer, M., Paciorek, T., Benková, E. and Friml, J. (2006b). Immnocytochemical techniques for whole mount *in situ* protein localization in plants. *Nat. Protocols* **1**, 98-103.
Scarpella, E., Marcos, D., Friml, J. and Berleth, T. (2006). Control of leaf vascular patterning by polar auxin transport. *Genes Dev*. **20**, 1015-1027.
Steinmann, T., Geldner, N., Grebe, M., Mangold, S., Jackson, C. L., Paris, S., Gälweiler, L., Palme, K. and Jürgens, G. (1999). Coordinated polar localization of auxin efflux carrier PIN1 by GNOM ARF GEF. *Science* **286**, 316-318.
Tanaka, H., Dhonukshe, P., Brewer, P. B. and Friml, J. (2006). Spatiotemporal asymmetric auxin distribution: a means to coordinate plant development. *Cell. Mol. Life Sci*. **63**, 2738-2754.
Verrier, P. J., Bird, D., Burla, B., Dassa, E., Forestier, C., Geisler, M., Klein, M., Kolukisaoglu, U., Lee, Y., Martinoia, E. et al. (2008). Plant ABC proteins- a unified nomenclature and updated inventory. *Trends Plant Sci*. **13**, 151-159.
Vieten, A., Vanneste, S., Wiśniewska, J., Benková, E., Benjamins, R., Beeckman, T., Luschnig, C. and Friml, J. (2005). Functional redundancy of PIN proteins is accompanied by auxin-dependent cross-regulation of PIN expression. *Development* **132**, 4521-4531.
Vieten, A., Sauer, M., Brewer, P. B. and Friml, J. (2007). Molecular and cellular aspects of auxin-transport-mediated development. *Trends Plant Sci*. **12**, 160-168.
Weijers, D., Van Hamburg, J. P., Van Rijn, E., Hooykaas, P. J. and Offringa, R. (2003). Diphtheria toxin-mediated cell ablation reveals interregional communication during *Arabidopsis* seed development. *Plant Physiol*. **133**, 1882-1892.
Weijers, D., Sauer, M., Meurette, O., Friml, J., Ljung, K., Sandberg, G., Hooykaas, P. and Offringa, R. (2005). Maintenance of embryonic auxin distribution for apical-basal patterning by PIN-FORMED-dependent auxin transport in *Arabidopsis*. *Plant Cell* **17**, 2517-2526.
Wiśniewska, J., Xu, J., Seifertová, D., Brewer, P. B., Růžička, K., Blilou, I., Rouquié, D., Benková, E., Scheres, B. and Friml, J. (2006). Polar PIN localization directs auxin flow in plants. *Science* **312**, 883.
Wu, G., Lewis, D. R. and Spalding, E. P. (2007). Mutations in *Arabidopsis multidrug resistance-like* ABC transporters separate the roles of acropetal and basipetal auxin transport in lateral root development. *Plant Cell* **19**, 1826-1837.
Xu, J., Hofhuis, H., Heidstra, R., Sauer, M., Friml, J. and Scheres, B. (2006). A molecular framework for plant regeneration. *Science* **311**, 385-388.
Zažímalová, E., Křeček, P., Skůpa, P., Hoyerová, K. and Petrášek, J. (2007). Polar transport of the plant hormone auxin - the role of PIN-FORMED (PIN) proteins. *Cell. Mol. Life Sci*. **64**, 1621-1637.

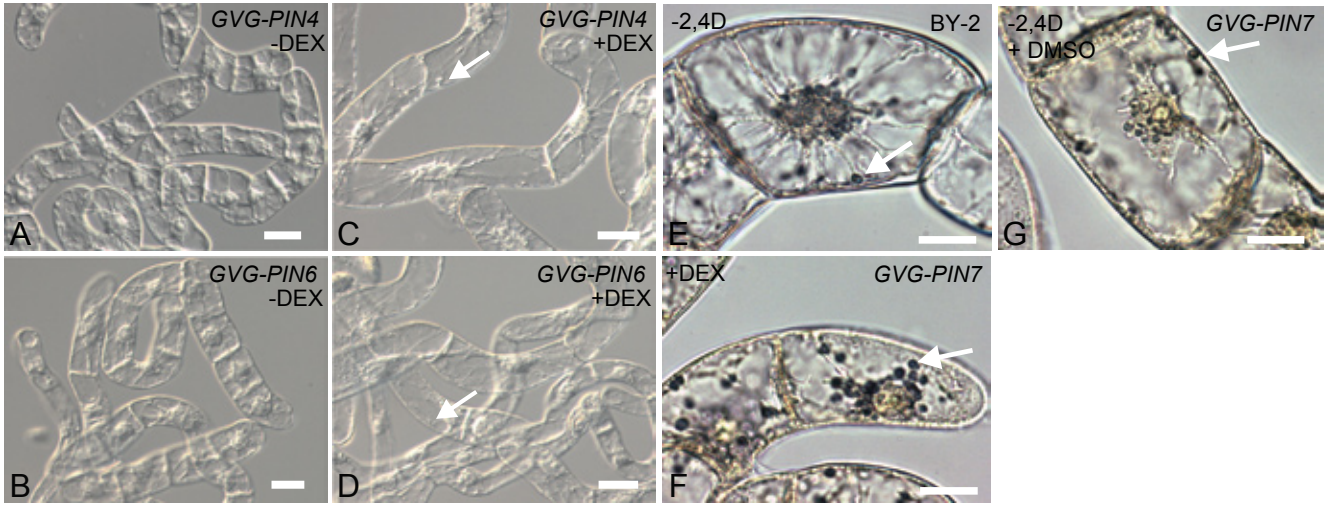

PIN-dependent increase in cell length in inducible (*GVG-PIN4*, *GVG-PIN6* and *GVG-PIN7*) and constitutive (*PIN1::PIN1:GFP*) BY-2 cell lines

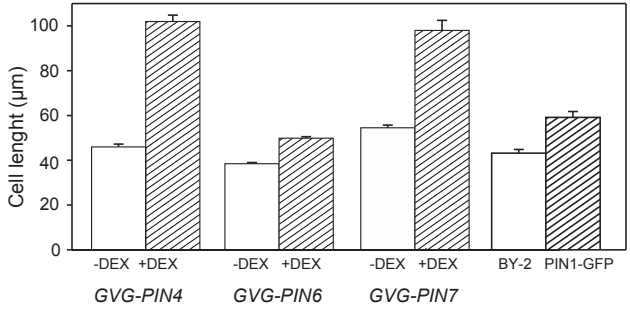

H

Accumulation assay in PIN1::PIN1-GFP BY-2 cell lines

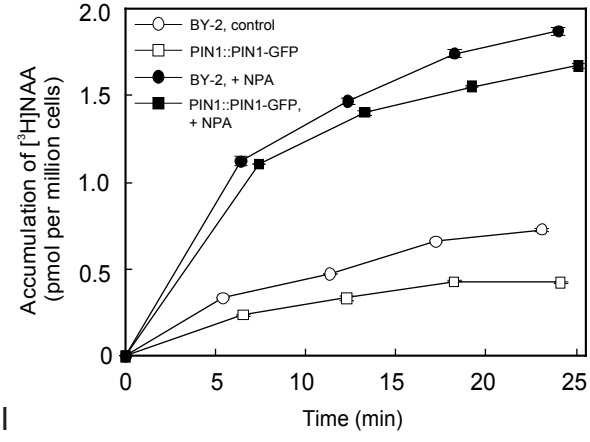

I

GVG-PIN7 and *GVG-PGP19-HA* cells- quantification of length

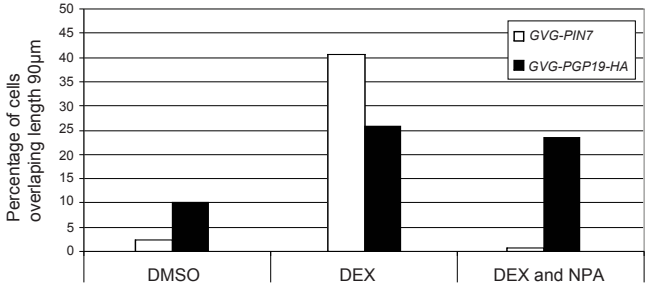

J

GVG-PIN7 and *GVG-PGP19-HA* cells
Arithmetic means of lengths and diameters

GVG-PIN7	DMSO		DEX		DEX and NPA	
	length	diameter	length	diameter	length	diameter
aritmetic mean± standard error	54.6 ±1.2	27.6 ±0.41	98.0 ±4.5	38.0 ±1.0	44.3 ±1.1	26.9 ±0.6

GVG-PGP19-HA	DMSO		DEX		DEX and NPA	
	length	diameter	length	diameter	length	diameter
aritmetic mean± standard error	63.8 ±1.6	23.3 ±0.3	78.0 ± 2.0	25.9 ± 0.4	75.8 ± 1.9	26.8 ± 0.5

K

GVG-PGP19-HA

light dark

A

GVG-PGP1-myc

light dark

B

PGP19

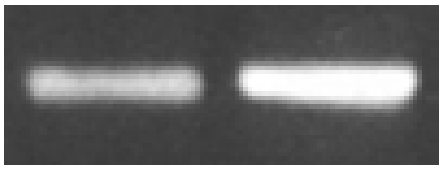

Act.

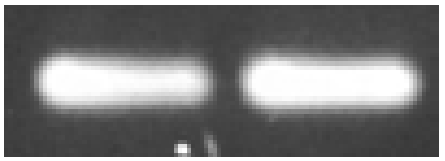

-DEX +DEX

C

PGP1

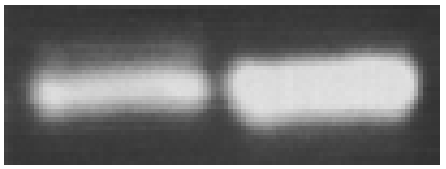

Act.

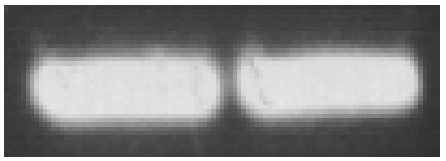

-DEX +DEX

D

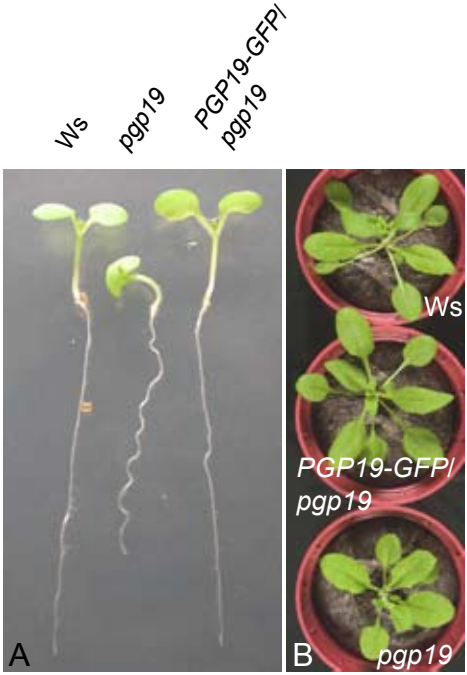
Ws
pgp19
PGP19-GFP/
pgp19
A
Ws
PGP19-GFP/
pgp19
B
pgp19

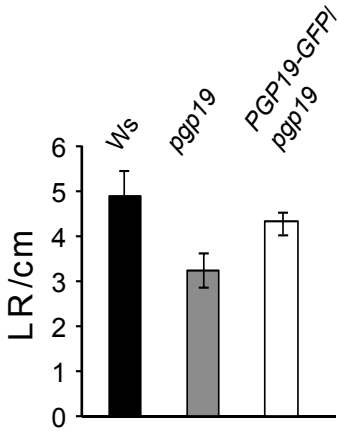
Ws
pgp19
PGP19-GFP/
pgp19
LR/cm
0
1
2
3
4
5
6
C

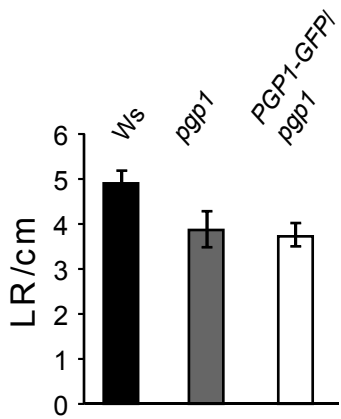
Ws
pgp1
PGP1-GFP/
pgp1
LR/cm
0
1
2
3
4
5
6
D

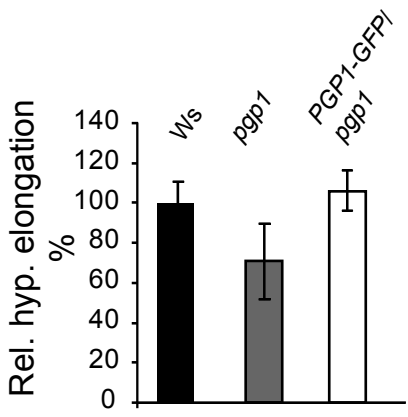
Ws
pgp1
PGP1-GFP/
pgp1
Rel. hyp. elongation
%
0
20
40
60
80
100
120
140
E

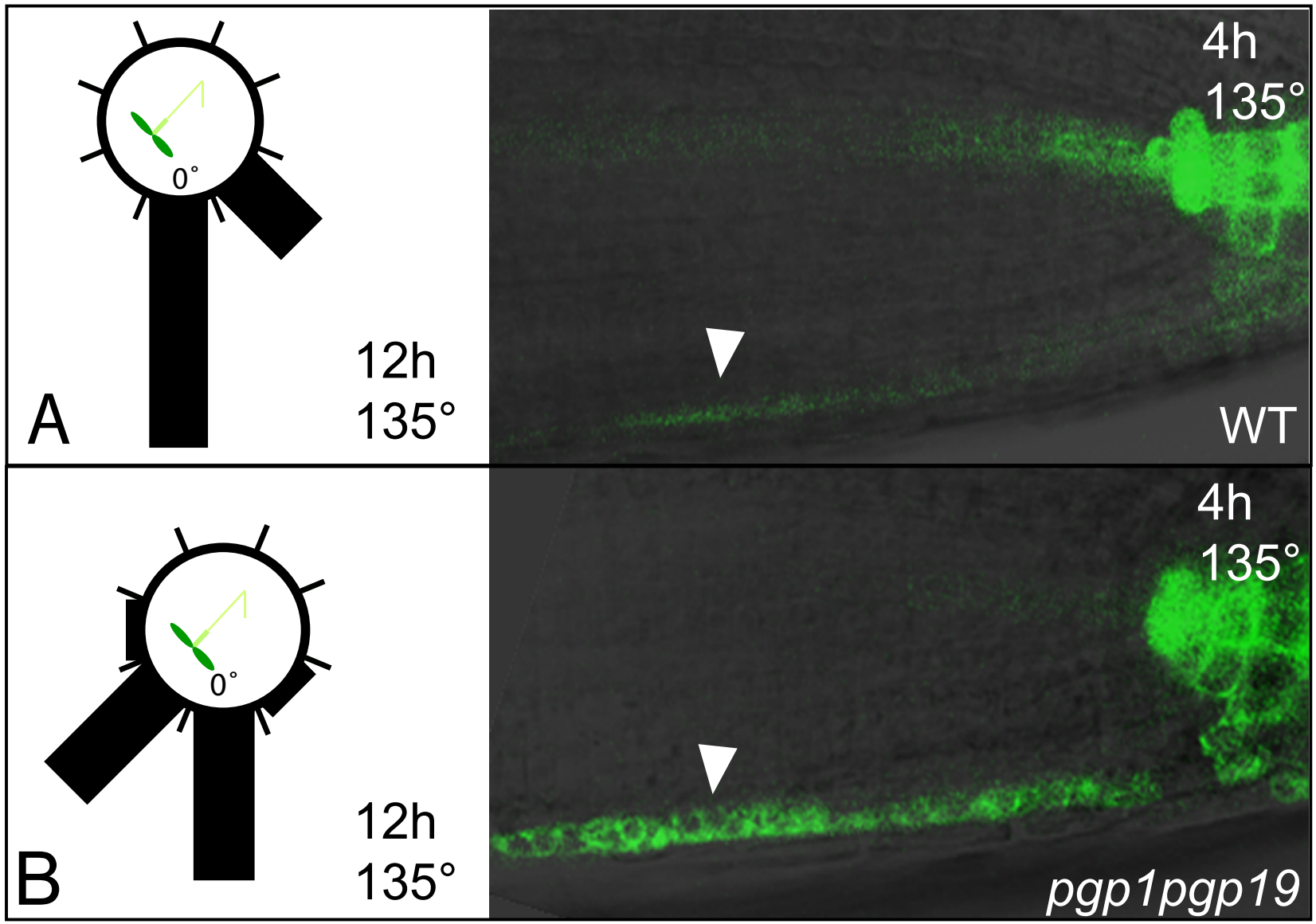
A
0°
12h
135°
4h
135°
WT
B
0°
12h
135°
4h
135°
pgp1pgp19

Fig. S1. Effects of PIN and PGP overexpression in BY-2 cells. (**A-D**) DEX-induced expression of PIN4 and PIN6, resulting in similar phenotypes in *GVG-PIN4* and *GVG-PIN6* BY-2 cells. The phenotype of non-induced *GVG-PIN4* (A) and *GVG-PIN6* cells (B) after 3-day-long cultivation. DEX induction (1 μM) resulted in the stimulated cell elongation and amyloplasts formation (arrows) in both *GVG-PIN4* (C) and *GVG-PIN6* (D) cells. Scale bars: 40 μm. (**E-G**) Induction of BY-2 cell elongation and starch accumulation by auxin starvation. BY-2 cells cultivated in the medium without 2,4-D (E) show defects similar to those after induction of PIN7 or PGP19 expression in *GVG-PIN7* and *GVG-PGP19-HA* lines, namely inhibition of cell division, enhanced elongation and accumulation of starch granules. Non-induced (F) and DEX-induced (G) *GVG-PIN7* cells. Identity of the starch granules (marked by arrows) was confirmed by lugol staining. Scale bars: 20 μm. (**H**) Quantification of increased cell lengths in DEX-induced (+) and non-induced (−) *GVG-PIN4*, *GVG-PIN6* and *GVG-PIN7* cell lines (1 μM DEX, 3 days). Similar increase in cell length was observed in cells constitutively overexpressing PIN-GFP in *PIN1::PIN1-GFP* line at day 3 of the subculture interval. Constitutive expression of PIN1 under natural promoter results in overall prolongation of subculture interval accompanied with decrease in cell division activity (data not shown). Error bars represent standard errors of the mean (n=400). (**I**) Decreased accumulation of ^{3}HNAA in *PIN1::PIN1:GFP* cells (Benková et al., 2003; Zazímalová et al., 2007) reflects increased auxin efflux in comparison with control BY-2 cells. Interestingly, decrease in the ^{3}HNAA accumulation by ~35% corresponds well with the already reported decrease following inducible expression of *Arabidopsis* PIN 4, 6 and 7 in BY-2 cells (Petrasek et al., 2006). Error bars represent s.e.m. (n=4); where invisible, they are covered by the symbols. (**J**,**K**) Quantification of the effect of DEX and DEX/NPA treatment in *GVG-PIN7* and *GVG-PGP19-HA* lines. (J) For better comprehensibility of our results (Fig. 1G), upper limit (90 μm) for the length of all variants were determined. After DEX induction, the percentage of oversized cells increased in both *GVG-PIN7* and *GVG-PGP19-HA* lines. However, the effect of the NPA treatment was clearly different between *GVG-PIN7* and *GVG-PGP19-HA* lines. Although in the *GVG-PIN7* line, the number of cells exceeding the determined limits was restored to levels nearly the same as in the non-induced variant, increased length and diameter of *GVG-PGP19-HA* was not restored with NPA. (K) The table shows the arithmetic means of all measured cell lengths and diameters expressed with standard error (170 cells in each sample).

Fig. S2. Analysis of inducible expression of PGP1-*myc* and PGP19-HA in *GVG-PGP lines.* (**A-D**) Inducibility of PGP1 and PGP19 in *GVG-PGP19-HA* (A,C) and *GVG-PGP1-myc* (B,D) lines confirmed by GUS staining of co-regulated *UAS::GUS* reporter construct (A,B) and by RT-PCR (C,D). Strong GUS staining was observed in seedlings germinated on DEX plates either in the light or in darkness.

Fig. S3. Complementation of the *pgp19* and *pgp1* mutant phenotypes by the *pPGP19::PGP19-GFP* and *pPGP1::PGP1-GFP* constructs. (**A-C**) Morphological phenotype of *pgp19* mutant (epinastic cotyledons and wavy root growth) in seedlings (A); leaf phenotype in adult plants (B) and partially lateral root formation phenotype (C) could be complemented by the *pPGP19::PGP19-GFP* construct (PGP19-GFP). (**D**,**E**) Lateral root initiation phenotype of *pgp1* mutant could not be complemented by the *pPGP1::PGP1-GFP* (*PGP1-GFP*) construct (D), whereas the hypocotyl elongation phenotype of *pgp1* could be complemented by the *pPGP1::PGP1-GFP* construct (E).

Fig. S4. Opposite effect of *pgp1pgp19* and *pin2* mutations on root gravitropism. (**A**) Normal bending and relocation of the *DR5::GFP* signal in root tip epidermis after 5 hours of gravistimulation in wild type. (**B**) Enhanced relocation of *DR5::GFP* signal in *pgp1pgp19* reflects the enhanced gravitropic bending. The gravitropism diagram was created as described (Petrásek et al., 2006) (12 hours of gravity stimulation, n=40).

6.3. Chapter 3 - Probing plant membranes with FM dyes: tracking, dragging or blocking?

Adriana Jelínková, Kateřina Malínská, Sibu Simon, Jürgen Kleine-Vehn, Markéta Pařezová, Přemysl Pejchar, **Martin Kubeš**, Jan Martinec, Jiří Friml, Eva Zažímalová, Jan Petrášek

The Plant Journal 61, 883-892, 2010

This article is based on collaboration between Dr. Eva Zažímalová, Dr. Jiří Friml and Dr. Jan Martinec laboratories. The goal of this manuscript is to describe side-effects of the FM (Fei Mao) styryl dyes, which are widely used probes that label processes of endocytosis and vesicle trafficking in eukaryotic cells.

My contribution to this article was the transformation of BY-2 cells with ABCB4::ABCB4:GFP construct, characterization of cell line including expression analyses (immunofluorescence localization) and analysis of cell phenotype. I was involved in microscopy analysis of FM 4-64 effect on ABCB4-GFP plasma membrane localization in BY-2 cells expressing ABCB4-GFP.

FM styryl dyes were used for characterization of endosomal trafficking of proteins involved in the auxin efflux machinery in BY-2 cell lines. Direct application of 2 μM FM 4-64 to BY-2 cells constitutively expressing either PIN1–GFP or ABCB4–GFP resulted in transient internalization of these proteins from the PM. Control cells showed localization of PIN1–GFP and ABCB4–GFP in the PM and the cortical cytoplasm (Figure 2a, b, 0 min, and Figure S1a). Prolonged incubation with FM 4-64 (up to 30 min) resulted in remarkable endocytosis of FM 4-64, but PIN1–GFP as well as ABCB4–GFP vesicles disappeared from the cortical cytoplasm, restoring a control-like situation (i.e. localization on the PM; Figure 2a, b, 30 min).

This work was supported by the Grant Agency of the Academy of Sciences of the Czech Republic (KJB600380604), by the Grant Agency of Charles University (43-252455) and by the Ministry of Education, Youth and Sports of the Czech Republic, project LC06034.

the plant journal

SEB SOCIETY FOR EXPERIMENTAL BIOLOGY

The Plant Journal (2010) **61**, 883–892 doi: 10.1111/j.1365-313X.2009.04102.x

TECHNICAL ADVANCE

Probing plant membranes with FM dyes: tracking, dragging or blocking?

Adriana Jelínková[1,2,†], Kateřina Malínská[1,†,*], Sibu Simon[1], Jürgen Kleine-Vehn[3], Markéta Pařezová[1], Přemysl Pejchar[1], Martin Kubeš[1], Jan Martinec[1], Jiří Friml[3], Eva Zažímalová[1] and Jan Petrášek[1,2]

[1]*Institute of Experimental Botany, Academy of Sciences of the Czech Republic, Rozvojová 263, 165 02 Prague 6, Czech Republic,*
[2]*Department of Plant Physiology, Faculty of Science, Charles University, Viničná 5, 128 44 Prague 2, Czech Republic, and*
[3]*Department of Plant Systems Biology, Flanders Institute for Biotechnology, and Department of Plant Biotechnology and Genetics, Ghent University, 9052 Ghent, Belgium*

Received 12 August 2009; revised 23 November 2009; accepted 2 December 2009; published online 22 January 2010.
*For correspondence (fax +420 225 106 446; e-mail malinska@ueb.cas.cz).
†These authors contributed to this paper equally.

SUMMARY

Remarkable progress in various techniques of *in vivo* fluorescence microscopy has brought an urgent need for reliable markers for tracking cellular structures and processes. The goal of this manuscript is to describe unexplored effects of the FM (Fei Mao) styryl dyes, which are widely used probes that label processes of endocytosis and vesicle trafficking in eukaryotic cells. Although there are few reports on the effect of styryl dyes on membrane fluidity and the activity of mammalian receptors, FM dyes have been considered as reliable tools for tracking of plant endocytosis. Using plasma membrane-localized transporters for the plant hormone auxin in tobacco BY-2 and *Arabidopsis thaliana* cell suspensions, we show that routinely used concentrations of FM 4-64 and FM 5-95 trigger transient re-localization of these proteins, and FM 1-43 affects their activity. The active process of re-localization is blocked neither by inhibitors of endocytosis nor by cytoskeletal drugs. It does not occur in *A. thaliana* roots and depends on the degree of hydrophobicity (lipophilicity) of a particular FM dye. Our results emphasize the need for circumspection during *in vivo* studies of membrane proteins performed using simultaneous labelling with FM dyes.

Keywords: FM 4-64, FM 1-43, plasma membrane, tobacco BY-2 cells, endocytosis.

INTRODUCTION

FM dyes are fluorescent markers that were originally developed as membrane potential sensors (Grinvald *et al.*, 1988) and later optimized to stain synaptic vesicles *in vivo* (Betz and Bewick, 1992; Betz *et al.*, 1992, 1996; Gaffield and Betz, 2006). They are widely used in tracking processes of membrane trafficking in eukaryotic organisms (Gaffield and Betz, 2006), including plants (Bolte *et al.*, 2004; Aniento and Robinson, 2005). The amphiphilic character of FM molecules (Figure 1) allows their penetration through the cell wall followed by insertion into the plasma membrane (PM) and subsequent tracking of intracellular membrane dynamics. The tail region of the FM molecule is responsible for its lipophilicity. A higher number of carbons in the tail increases the lipophilicity of the molecule, but PM staining becomes irreversible (Betz *et al.*, 1996). The composition of the bridge region determines the fluorescence wavelength of the molecule. More double bonds in this region shift emission to the red part of the spectrum. In contrast to the hydrophobic environments of the PM, fluorescence of FM dyes is strongly reduced in a polar solvent (water). This makes FM dyes optimal for selective tracking of membrane dynamics. Moreover, positively charged head regions prevent the movement of the dye across the membrane via phospholipid flip-flopping. These chemical properties make FM dyes useful tools in tracking endocytosis and vesicle trafficking in living cells.

The most commonly used FM dyes in plant biology are FM 4-64 (*N*-(3-triethylammoniumpropyl)-4-(6-(4-(diethylamino)phenyl)hexatrienyl)pyridinium dibromide) and FM 1-43 (*N*-(3-triethylammoniumpropyl)-4-(4-(dibutylamino)styryl) pyridinium dibromide). In addition to tracking endocytosis (Emans *et al.*, 2002), these dyes are often used in tracking

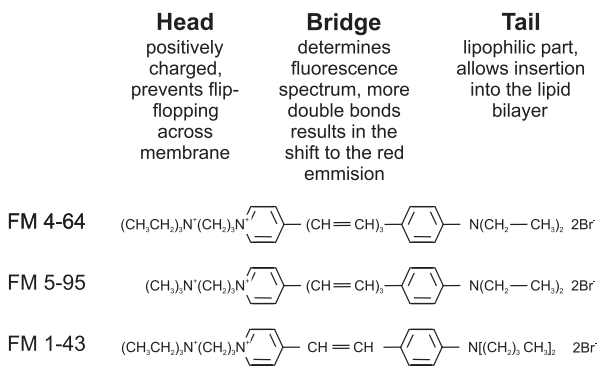

Figure 1. Structure of the FM dyes (Betz *et al.*, 1996) used in this study.

secretory pathways (Dettmer *et al.*, 2006), as after some time they end up in the vacuolar membrane, and thus can also be exploited for studies of vacuolar dynamics (Kutsuna and Hasezawa, 2002). There are also several other organelles stained by FM dyes (for review see Bolte *et al.*, 2004). Because of differences in the speed of incorporation into endomembranes, FM 1-43 and FM 4-64 can be used as selective dyes for exo- and endocytosis in pollen tubes (Zonia and Munnik, 2008). Moreover, a slightly less lipophilic variant of the FM 4-64 molecule, red-fluorescing FM 5-95 (*N*-(3-trimethylammoniumpropyl)-4-(6-(4-(diethylamino)phenyl)hexatrienyl) pyridinium dibromide), can be used as an alternative. The hydrophobicity of the above mentioned FM dyes gradually decreases from FM 4-64 through FM 5-95 to FM 1-43 (information provided in Molecular Probes The Handbook).

Recent progress in plant molecular biology has provided evidence for the existence of plant clathrin-dependent endocytosis of PINFORMED (PIN) auxin efflux carriers (Dhonukshe *et al.*, 2007). It appears that, after fluid phase endocytosis (Oparka, 1990), clathrin-dependent endocytosis is the major endocytic route in plants (Perez-Gomez and Moore, 2007). Thus, FM dyes are now considered as preferential markers for this type of endocytosis, being blocked largely at the PM of the cells where the clathrin molecule is not functional (Dhonukshe *et al.*, 2007). The suitability of FM dyes as markers for endocytic pathways has recently been supported by experiments involving micro-injection of FM 4-64 directly into the cytosol of *Nicotiana tabacum* BY-2 cells and *Tradescantia virginiana* stamen hair cells (van Gisbergen *et al.*, 2008). Moreover, a set of Förster Resonance Energy Transfer (FRET) data measured between FM 4-64 and cytoplasmic GFP (Griffing, 2008) also showed that this dye is taken up into cells preferentially by endocytosis.

However, even though FM dyes are undoubtedly valuable tools for several applications, few reports on their side effects have been published. Styryl-based dyes have been shown to influence membrane fluidity (Rodes *et al.*, 1995). In addition, they block mechanotransduction channels (Gale *et al.*, 2001) as well as the activity of muscarinic and nicotinic acetylcholine receptors (for review, see Gaffield and Betz, 2006). Therefore, careful investigation of their effects on cellular structures and their activities would help in understanding the mechanism of FM dye action and validate their exploitation as endocytotic markers.

Here we show that some concentrations of FM dyes, even much lower than those widely used, have the potential to disturb the localization and activity of integral PM proteins, such as auxin carriers, in cell suspension cultures. To characterize this phenomenon, we used tobacco BY-2 or Arabidopsis cell cultures expressing translational fusions with GFP using either the auxin efflux carrier PIN1 (*PIN1::PIN1:GFP*; Benkova *et al.*, 2003; Petrášek *et al.*, 2006) or the multi-drug resistance (MDR) type conditional auxin efflux carrier PGP4/ABCB4 (*PGP4::PGP4:GFP*; Cho *et al.*, 2007; Terasaka *et al.*, 2005; Yang and Murphy, 2009) from *A. thaliana*. In both cases, transient internalization of GFP-tagged proteins from PM was observed upon treatment with FM 4-64 and FM 5-95, but not with FM 1-43. The internalization was not blocked by inhibitors of endocytosis or cytoskeletal drugs, but was sensitive to the metabolic drug sodium azide. Moreover, all three dyes interfered to various degrees with the activity of endogenous tobacco auxin carrier proteins and phospholipid metabolism.

RESULTS

FM 4-64 induces transient re-localization of plasma membrane proteins in BY-2 cells

We used FM styryl dyes for characterization of endosomal trafficking of proteins involved in the auxin efflux machinery in a tobacco BY-2 cell line. It was very easy to reproduce already published data describing the use of FM dyes (Bolte *et al.*, 2004). However, in addition to this, other previously uncharacterized effects of FM 4-64 treatment were repeatedly observed. Direct application of 2 μM FM 4-64 to BY-2 cells stably expressing either PIN1–GFP or PGP4–GFP resulted in transient internalization of these proteins from the PM. Control cells showed localization of PIN1–GFP and PGP4–GFP in the PM and the cortical cytoplasm (Figure 2a,b, 0 min, and Figure S1a). After 2 min of treatment with FM 4-64, a remarkable increase in the internal pool of both fusion proteins was observed as punctate GFP signal (Figure S1). This phenomenon clearly preceded the endocytosis of FM 4-64, because the dye was still localized mainly on the PM 2 min after its application (Figure S1). As FM 4-64 internalization proceeded (Figure 2a,b, 10 min), FM-labelled endosomes did not co-localize with FM-induced PIN1–GFP patches (Figure 2c,d). Similarly, no co-localization between PGP4–GFP patches and FM-decorated endosomes was observed (data not shown). Prolonged incubation with FM 4-64 (up to 30 min) resulted in remarkable endocytosis of FM 4-64, but PIN1–GFP as well as PGP4–GFP vesicles disappeared from the cortical cytoplasm, restoring a

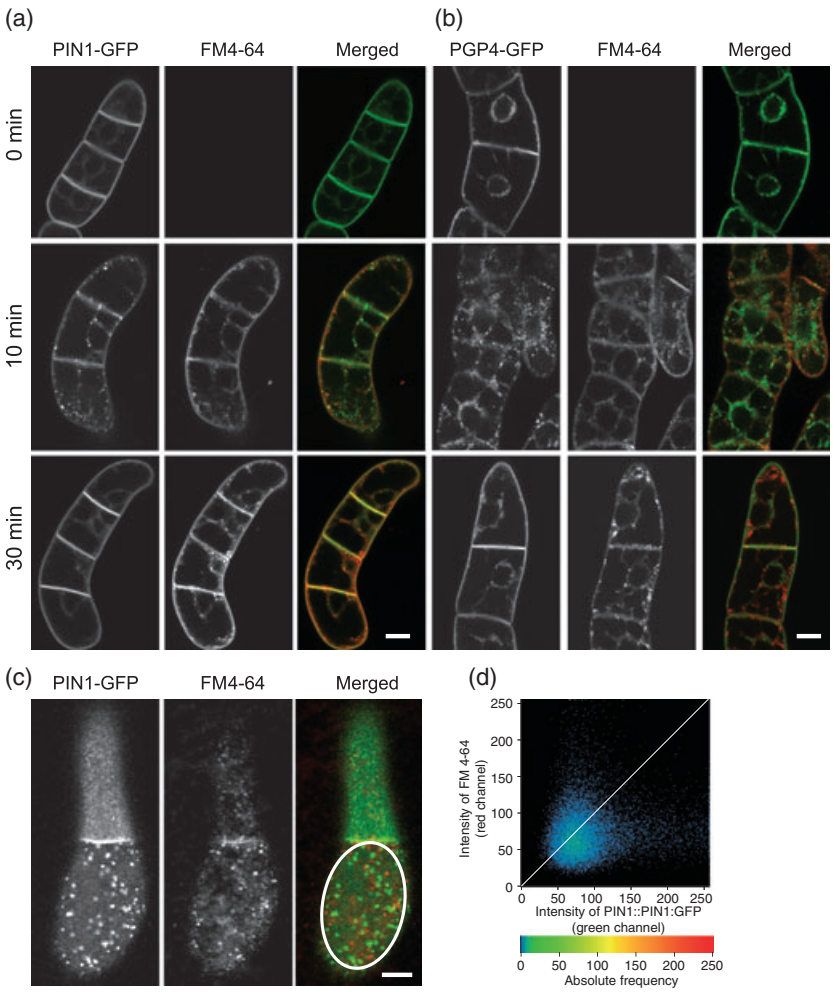

Figure 2. FM 4-64-stimulated transient internalization of plasma membrane-located auxin carriers.
(a, b) *In vivo* confocal microscopy of PIN1–GFP (a) and PGP4–GFP (b) in 3-day-old tobacco BY-2 cells; treatment with 2 μM FM 4-64 for the indicated times. PIN1–GFP and PGP4–GFP localized at transversal plasma membranes of control cells (upper row) and were internalized after 10 min of incubation with FM 4-64 (middle row). Notice the patchy pattern in the green channel. Restored plasma membrane localization of PIN1–GFP and PGP4–GFP after 30 min of treatment with FM 4-64 was accompanied by endocytosis of FM 4-64 (bottom row).
(c) Longitudinal sections through the cortical layer of the cytoplasm showing internalized PIN1–GFP and FM 4-64 after 10 min incubation with 2 μM FM 4-64.
(d) Scattergram created from the oval region indicated in (c), demonstrating no co-localization of PIN1–GFP and FM 4-64 fluorescence.
Scale bars = 20 μm.

control-like situation (i.e. localization on the PM; Figure 2a,b, 30 min). Movie S1 shows PIN1–GFP-containing vesicles 3 min after FM 4-64 application in comparison with the control (Movie S2).

Altogether, the results show that application of FM 4-64 dye, at a concentration even lower than that routinely used for tracking of endocytosis, results in transient re-localization of at least two integral PM proteins in exponentially growing BY-2 cells.

FM dye-induced transient internalization of plasma membrane proteins is cell suspension culture-specific, and may be tissue- and/or species-specific

To address the question of whether the above described effect of FM 4-64 on PM proteins is common in plant cell suspensions, we studied this effect in a cell suspension derived from *A. thaliana* PIN1::PIN1:GFP plants (Benkova *et al.*, 2003). PIN1–GFP localization in the Arabidopsis PM differs from that in BY-2 cells; the fluorescence intensity is less homogeneous and some intracellular accumulation is seen (Figure 3a, 0 min). Nevertheless, 10 min after addition of FM 4-64, similar transient re-localization of PIN1–GFP to that reported for BY-2 cells was observed (Figure 3a, 10 min). FM-labelled endosomes did not co-localize with FM-induced PIN1–GFP patches. In comparison with BY-2, the recovery of PIN1–GFP PM localization appeared to be slower (Figure 3a, 40 min).

The FM 4-64 effect was also examined in *A. thaliana* seedlings expressing another auxin efflux carrier, PIN2–GFP (Xu and Scheres, 2005) or aquaporin water channel PIP2–GFP (Cutler *et al.*, 2000). PIN2–GFP (Figure 3b) or PIP2–GFP (Figure 3c) seedlings were treated with FM 4-64. The dye was washed out and images of root epidermis and cortex at various time points up to 1 h after addition of FM dye were collected. Neither of these two proteins showed enhanced FM-induced internalization compared to mock treatment.

Although a tissue and even species specificity cannot be excluded, FM dye-induced transient internalization of PM proteins appears to be cell suspension culture-specific.

FM dye-induced transient internalization of plasma membrane proteins correlates with dye hydrophobicity

To establish whether the above-mentioned effects of FM 4-64 are specific for this particular dye or whether they are

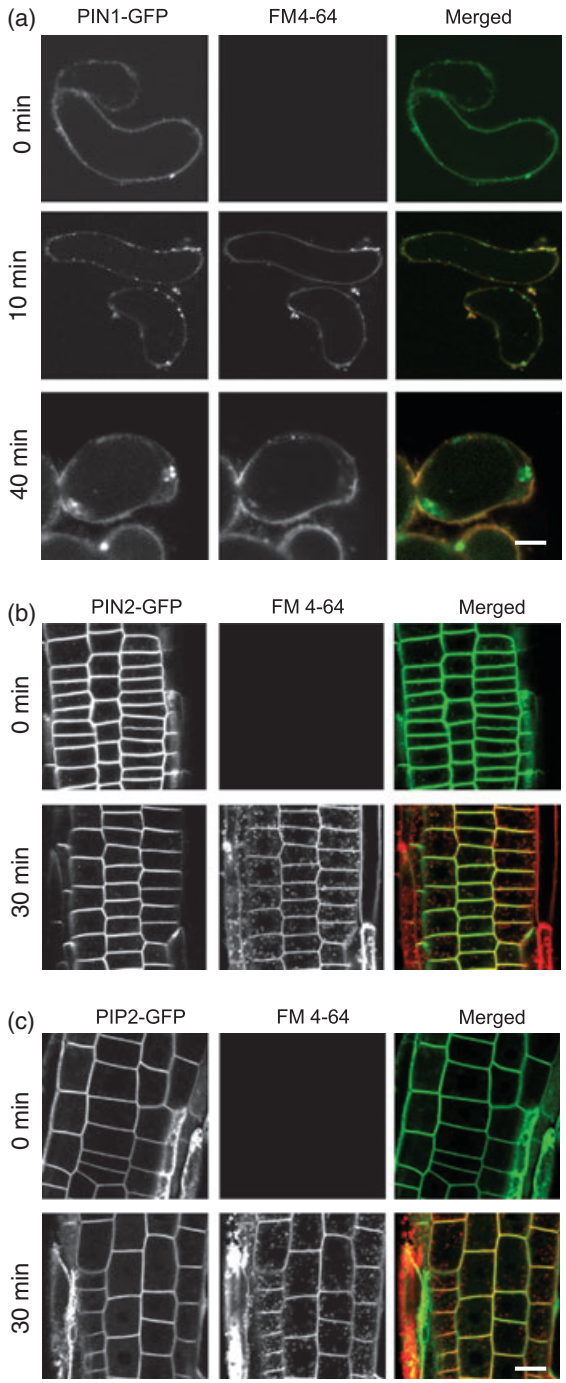

Figure 3. FM dye-induced transient internalization of plasma membrane proteins is cell suspension culture-specific.
(a) *In vivo* confocal microscopy of PIN1–GFP in 3-day-old Arabidopsis cell suspension culture; treatment with 2 μM FM 4-64 for the indicated times. PIN1–GFP localized at plasma membranes of control cells (0 min) and was internalized after 10 min of incubation with FM 4-64. Notice the patchy pattern in the green channel. Plasma membrane localization of PIN1–GFP was restored after 40 min of treatment with FM 4-64.
(b, c) Five-day-old Arabidopsis seedlings expressing *PIN2–GFP* (b) or *PIP2–GFP* (c) were incubated for 30 min in the presence or absence of FM4-64 dye. No apparent PIN2 or PIP2 internalization (in green) was observed within 30 min.
Scale bars = 20 μm.

more general, we compared them with similar FM dyes: the less hydrophobic FM 5-95 and FM 1-43. To secure full saturation of the PM with FM dyes (2 μM), providing a comparable situation at the beginning of the experiment, a protocol of FM staining on ice and subsequent observation at room temperature was used (Emans *et al.*, 2002). This approach is often used because, at the beginning of the experiment, when the PM is saturated with FM dye on ice, endocytosis does not occur; later on, it can be easily restored upon transfer of cells to room temperature. For all these experiments, a PIN1–GFP-transformed BY-2 cell line was used. After loading the cells with FM 4-64 on ice and subsequent transfer to room temperature, the PIN1–GFP re-localization resembled that observed using a protocol without pre-incubation on ice (Figure 4a). It was also transient. Although with slower kinetics, FM 5-95 also induced internalization of PIN1–GFP (Figure 4b) and PGP4–GFP (data not shown). In contrast, the least hydrophobic dye among those tested (FM 1-43) never induced any observable re-localization of PIN1–GFP (Figure 4c) or PGP4–GFP (data not shown), even after prolonged incubation. The effect of all three FM dyes was compared as the relative decrease of the PIN1–GFP fluorescence intensity at the plasma membrane after 15 min incubation (Figure S1e).

These results suggest a positive correlation between the FM dye hydrophobicity and the ability to re-localize integral PM proteins.

Active metabolism, but neither endocytosis nor cytoskeleton dynamics, are necessary for FM-induced internalization of plasma membrane proteins

To assess possible mechanisms triggered by the addition of FM dyes, the metabolic inhibitor sodium azide (NaN_3) was used to block ATP-dependent processes in BY-2 cells. Both FM 4-64 endocytosis and PIN1–GFP internalization were totally prevented by 15 mM NaN_3 (Figure 5a). This indicates an active, energy-dependent process involved in PIN1–GFP re-localization. On the other hand, treatments that effectively block FM dye endocytosis, including prolonged incubation on ice (Figure 5b) as well as application of the phosphatidylinositol 3-kinase inhibitor wortmannin (Figure 5c), were not effective in blocking the transient internalization of PIN1–GFP caused by FM 4-64. Interestingly, FM dye-induced formation of PIN1–GFP patches was even more pronounced on ice, was not transient (over short time periods) and persisted for at least 1 h. Figure S2 shows that de-polymerization of neither actin filaments (treated with 500 nM latrunculin B) nor microtubules (treated with 20 μM oryzalin) is able to abolish the FM dye effect on PIN1–GFP localization completely. Interestingly, de-polymerization of actin filaments (in contrast to the de-polymerization of microtubules) slightly decreased the amount of re-localized PIN1–GFP, suggesting partial dependence of this process on the actin cytoskeleton.

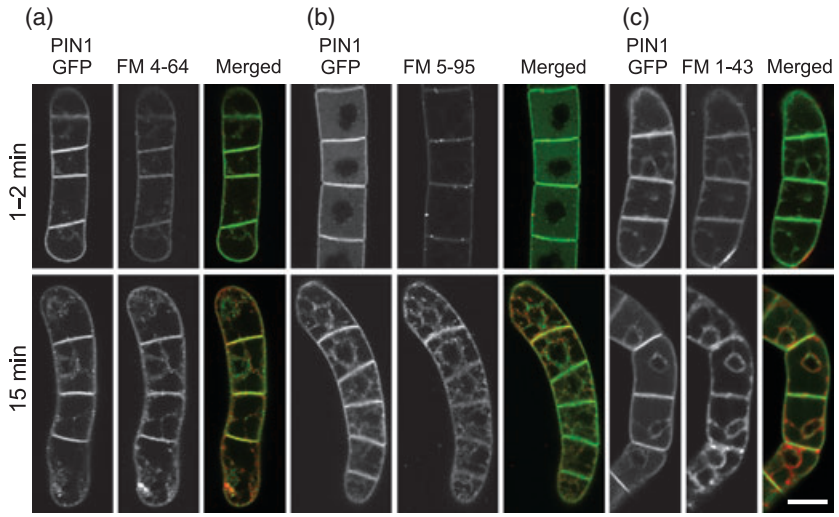

Figure 4. FM-induced transient internalization of plasma membrane proteins correlates with the dye hydrophobicity.
In vivo confocal microscopy of PIN1–GFP in 3-day-old tobacco BY-2 cells after 15 min pre-incubation on ice followed by 15 min treatment with FM 4-64 (a), FM 5-95 (b) or FM 1-43 (c) at 26°C. Notice no internalization of PIN1–GFP after FM 1-43 treatment, in contrast to FM 4-64 and FM 5-95. Scale bars = 20 μm.

To address the question of whether FM-induced PIN1–GFP patches are formed from the PM or from the endosomal pool of PIN1–GFP, brefeldin A (BFA), an inhibitor of anterograde vesicle trafficking in plant cells, was used. BFA compartments were formed close to the nucleus after 1 h incubation in 20 μM BFA for FM-treated as well as control cells (data not shown). Treatment with BFA did not prevent the extensive formation of PIN1–GFP-containing patches after FM 4-64 application (Figure 5d). In cells treated with BFA but without FM 4-64, no similar PIN1–GFP patches close to the PM were observed even after 30 min (data not shown). BFA compartments containing PIN proteins usually started to form after 40 min of BFA treatment, mostly in the vicinity of the nucleus. Their formation in all cells was completed after 1 h of incubation with BFA. Therefore, the BFA compartment is not yet developed in Figure 5(d).

Altogether, FM 4-64-induced patches are not formed from vesicles that possibly have not fused with the PM, but are rather derivatives of the PM itself. FM-induced dragging of PM proteins into cells is an active process that does not require phosphatidylinositol 3-kinase-dependent pathways.

FM dyes interfere with the activity of integral plasma membrane auxin carriers

To test how FM dyes interfere with the activity of integral PM auxin carriers, the radioactively labelled synthetic auxins 2,4-dichlorophenoxyacetic acid ([^{3}H]2,4-D) and naphthalene-1-acetic acid ([^{3}H]NAA) were used as markers for active auxin influx and efflux, respectively (Petrášek *et al.*, 2006). The active auxin influx decreased immediately after the addition of 2 μM FM 1-43 and to lesser extent after addition of 2 μM FM 4-64 or FM 5-95, as indicated by significantly decreased auxin accumulation in 2-day-old wild-type BY-2 cells (Figure 6a). The active auxin efflux was also partly influenced by FM 1-43 (i.e. the accumulation of [^{3}H]NAA increased); however, FM 4-64 and FM 5-95 had no significant effect (Figure 6b). It appears that the transient re-localization of auxin carriers caused by FM 4-64 and FM 5-95 is not sufficient to change the overall balance of auxin transport across membranes, and so changes in accumulation of labelled auxin are hardly detectable in living cells. Nevertheless, the most hydrophilic FM dye FM 1-43, which did not cause internalization of auxin carriers from the PM, had a significant effect on the auxin accumulation in cells, suggesting another mode of direct interference with auxin carrier activity.

FM dyes interfere with phospholipid metabolism

To test the influence of FM dyes on the PM, we investigated the dynamics of phosphatidylcholine (PC) hydrolysis. PC is a major component of the PM and a substrate of phospholipases; it plays a crucial role in many signal transduction processes in plants (Meijer and Munnik, 2003; Wang, 2004). Level of fluorescently labelled diacylglycerol (BOPIPY-DAG), a direct product of BODIPY-PC hydrolysis by the action of non-specific phospholipase C (NPC) or a non-direct product of BODIPY-PC hydrolysis by the action of phospholipase D (PLD), was used as a marker of these enzyme activities. The level of BOPIPY-DAG significantly decreased after treatment of the BY-2 cells by virtually all tested FM dyes. In 2 μM FM 1-43-treated cells, the level of BODIPY-DAG decreased to approximately 60% within 15 min compared to non-treated cells. The effect of FM 5-95 was less obvious, and the decrease in BOPIPY-DAG caused by FM 4-64 was almost non-significant (Figure 6c). When cells were treated for 30 min, there was no further decrease in BODIPY-DAG (data not shown).

Thus, FM 4-64 does not alter the levels of DAG significantly. However, as in the case of auxin carrier activity, the most hydrophilic FM dye FM 1-43 strongly inhibits enzyme(s) of phospholipid metabolism in cells.

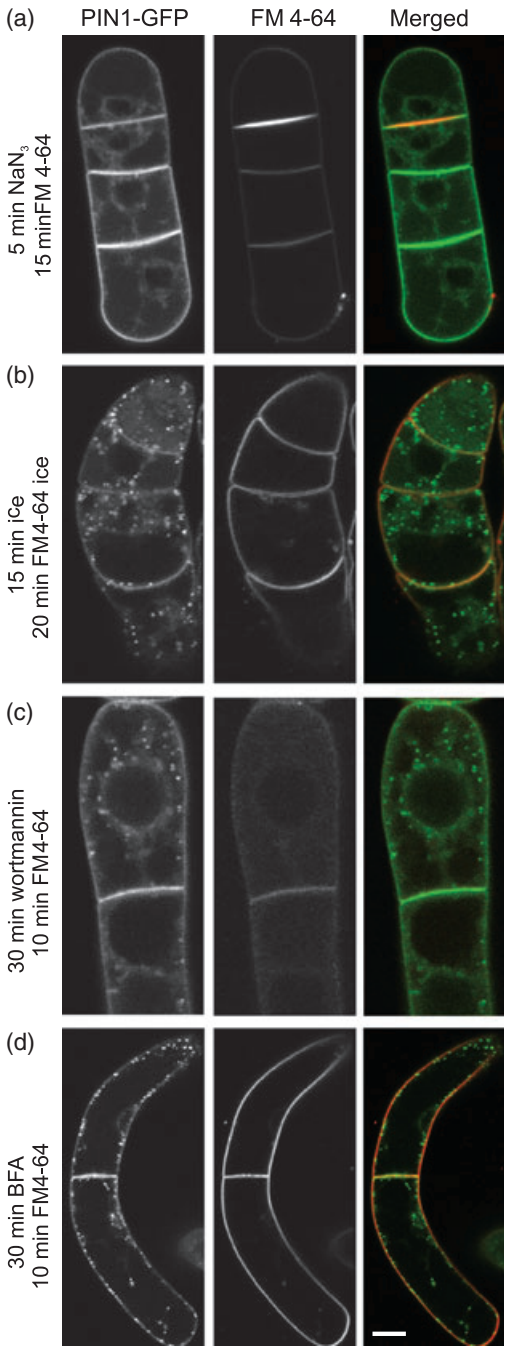

Figure 5. Testing the mechanism of FM-induced internalization of plasma membrane proteins.
In vivo confocal microscopy of PIN1–GFP in 3-day-old tobacco BY-2 cells; treatment with 2 μM FM 4-64 for the indicated times. Transversal confocal sections.
(a) Total inhibition of both FM 4-64 endocytosis and internalization of PIN1–GFP after 5 min pre-incubation with 15 mM sodium azide (NaN_3) followed by 15 min incubation with 2 μM FM 4-64.
(b) Pre-incubation on ice for 15 min followed by addition of 2 μM FM 4-64 and subsequent 20 min incubation on ice. Notice patches of PIN1–GFP and blocked endocytosis of FM 4-64.
(c, d) Pre-incubation with 50 μM wortmannin (c) or 20 μM brefeldin A (d) for 30 min followed by 10 min incubation with 2 μM FM 4-64. Notice patches of PIN1–GFP after both treatments.
Scale bars = 20 μm.

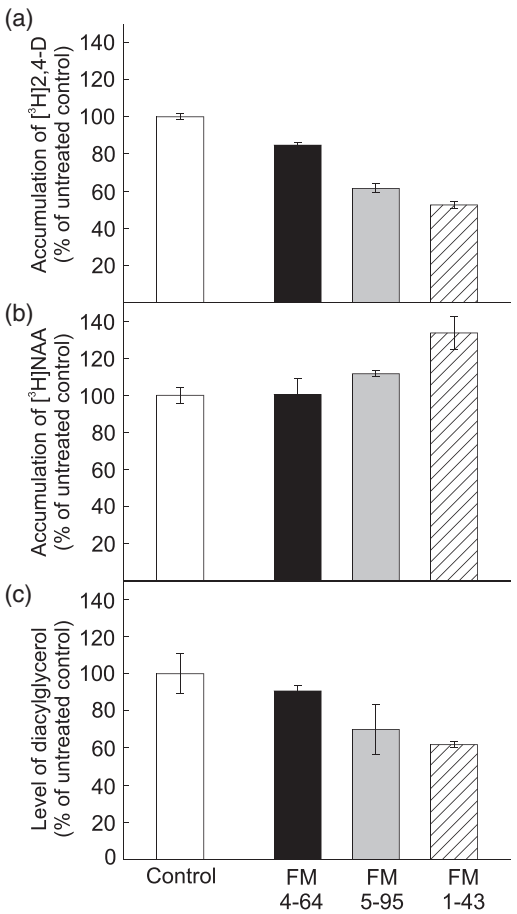

Figure 6. The activity of endogenous auxin influx and efflux carriers after treatment with 2 μM FM 4-64, FM 5-95 or FM 1-43.
(a) Accumulation of radioactively labelled synthetic auxin [^{3}H]2,4-D reflecting the activity of auxin influx carriers.
(b) Accumulation of radioactively labelled synthetic auxin [^{3}H]NAA reflecting the activity of auxin efflux carriers.
(c) Production of fluorescently labelled BODIPY-DAG reflecting enzyme activities of phospholipases.
Error bars represent SEs of the means (n = 4).

DISCUSSION

The results presented here show a phenomenon that has not been described before, i.e. that treatment with styryl dyes of the FM family can change the localization as well as the activity of at least some integral PM proteins in plant cells. FM4-64 and FM5-95 influenced the localization of integral PM proteins. This effect was transient and related to the early phases of the interaction between FM dyes and the PM. In addition, application of FM 1-43 did not interfere with the trafficking of PM proteins, but it significantly decreased the activity of auxin transporters and phospholipid metabolism. These findings are important, especially given the fact that FM dyes are widely used for tracking the dynamics of the PM. The properties of FM molecules (Betz *et al.*, 1996) imply

that they cannot penetrate the PM, and so enter the cell interior only by PM internalization. This has been verified recently by testing the FRET between FM 4-64 and cytoplasmic GFP (Griffing, 2008) and by micro-injection of FM 4-64 into the cell interior (van Gisbergen *et al.*, 2008). In addition to clathrin-mediated endocytosis (Dhonukshe *et al.*, 2007) and sterol endocytosis (Kleine-Vehn *et al.*, 2006; Klima and Foissner, 2008), FM 4-64 also appears to be a good marker for all other PM internalization processes in plants (Bolte *et al.*, 2004). No toxicity or similar unwanted side effects were reported after application of optimized concentrations of FM dyes (usually between 1 and 30 μM; for review, see Bolte *et al.*, 2004). In BY-2 tobacco cells, saturation of the PM was achieved using 17 μM FM 4-64 (Bolte *et al.*, 2004), and this concentration did not inhibit cell division or cell-cycle progression (Kutsuna and Hasezawa, 2002). In our study, 2 μM of FM dye was enough to induce transient re-localization of PM proteins. Thus, the effective concentrations of FM dyes used in our experiments are almost 10 times lower than that reported as optimal (Bolte *et al.*, 2004).

Interestingly, FM-induced changes in the localization of integral PM proteins were not observed in *A. thaliana* root epidermis and cortex cells. However, tissue and even species specificity cannot be excluded. Among other possible explanations, the composition of PM in various cell types and extracellular space conditions may play critical roles here. The dye must be hydrophilic enough to pass through the cell wall and hydrophobic enough to be incorporated preferentially into the PM. In agreement with this, Meckel *et al.* (2004) showed that, in the highly turgescent guard cells of *Vicia faba*, only the most hydrophobic dye FM 4-64 can be used for tracking endocytosis, while FM 1-43 non-specifically labelled various cytoplasmic structures and mitochondria.

With the current knowledge of the mechanism by which FM dyes incorporate into the PM, it is not easy to explain their effect on re-localization of integral PM proteins unambiguously. While it is not clear whether there is a preferential target for FM dyes among the spectrum of plant PM phospholipids, it is obvious that all FM dyes are positively charged and prefer specific lipids in prokaryotes. In the PM of *Bacillus subtilis* or *Escherichia coli*, FM 4-64, FM 1-43 and FM 5-95 were incorporated into the same lipid spiral-like structure enriched with anionic phospholipid phosphatidyl glycerol (Barak *et al.*, 2008). Thus binding to specific lipids could result in lipid phase segregation, preferentially destabilizing proteins with specific requirements for lipid environment. As the degree of mis-localization of the PM auxin carriers correlated with the hydrophobicity of FM dyes, we can assume that FM 4-64, as the most hydrophobic (lipophilic) form of FM dye tested in our experiments, is incorporated into the lipid bilayer very effectively. The rapid change in the composition of the PM could trigger transient processes until a new steady state of the PM with FM dye incorporated is reached. These processes could include steric competition between FM dyes and some PM proteins, temporary changes in PM fluidity, lipid phase segregation, or a combination of any of these processes. Consequently, changes in the physical properties of the phospholipid bilayer could result in the release of some material from the PM – as in the case described here, where the formation of particles that lack FM dye but contain some PM proteins was observed. At present, we are not able to conclude whether these particles are in the form of vesicles, lipid droplets or other structures.

A further aspect worth mentioning is that FM dyes differ significantly in their ability to associate with a lipid bilayer. It was shown that neuronal membranes were half-saturated with FM 4-64 at a concentration approximately 10 times lower than required for half saturation with FM 1-43 (Zhu and Stevens, 2008). Therefore, a membrane can hold 10 times more molecules of FM 1-43 than of FM 4-64. Thus, it can be speculated that membrane fluidity, which is known to be altered by styryl-based dyes (Rodes *et al.*, 1995), is influenced more by FM 1-43 than by FM 4-64. It is also known that alternations of membrane fluidity affect phospholipase activities (Villaverde and Verstraeten, 2003); this would explain the significant reduction of DAG levels in FM 1-43-treated cells.

Various treatments of BY-2 cells were performed to examine the character of FM dye-induced PIN1–GFP or PGP4–GFP patches and the mechanism of their internalization. Treatment with BFA, which in plants act as an inhibitor of anterograde vesicle trafficking, showed that FM 4-64-induced patches were derivatives of PM and are not formed from secretory vesicles that had not been able to fuse with the PM. To check the involvement of endocytosis, low temperature and the phosphatidylinositol-3-kinase inhibitor wortmannin, which have all been successfully shown to block endocytosis in plants (Emans *et al.*, 2002; Dettmer *et al.*, 2006), were tested. As none of the treatments prevented the formation of FM-induced patches, we concluded that it was not this type of endocytosis, but some other process, that was stimulated by the addition of FM dyes. This was further supported by distinct localizations of FM-induced PIN1–GFP or PGP4–GFP patches and FM-stained vesicles, and also by the overall different timing of endocytosis labeled with FM and appearance of patches. Prolonged incubation on ice prevented formation of FM-labelled endosomes but increased and prolonged the FM-induced re-localization effect. This suggests the mechanism requiring lower amounts of energy than the clathrin-dependent one. The formation of FM-induced PIN1 or PGP4 patches was blocked only after sodium azide treatment. This suggests that the process of FM-induced PM protein re-localization is energy-dependent, possibly via an ATP-driven step. Alternatively, FM-induced internalization could also be indirectly dependent on the cell energy

pool, as reported in yeast for the transmembrane potential-induced re-distribution of specific transporter proteins (Grossmann *et al.*, 2007).

A well-established auxin accumulation assay (Delbarre *et al.*, 1996; Petrášek *et al.*, 2006) was used to test the effect(s) of FM dyes on the function of proteins of interest, i.e. to monitor the activity of tobacco BY-2 endogenous auxin carriers *in vivo*. In contrast to the formation of FM-induced patches, FM 1-43 was the most active in inhibiting cellular auxin influx and efflux, followed by FM 5-95 and FM 4-64. The timing of the FM 1-43 inhibitory action on the auxin influx and efflux activities was fully comparable to the effects of widely used specific inhibitors of active auxin influx (1-naphthoxyacetic acid) and efflux (1-naphthylphthalamic acid) (Petrášek *et al.*, 2003; Hoyerová *et al.*, 2008). This means that both the specific inhibitors of auxin influx and efflux, as well as FM 1-43, modify auxin accumulation immediately after their application, without any lag phase. This suggests direct action on carrier proteins residing in the PM. As FM 1-43 did not induce any re-localization of PM auxin carriers, its action on auxin transporters might be related to an inhibitory effect on phospholipase(s) reflected in changed levels of DAG. DAG is a PM-located second messenger directly involved in the phosphoinositide-dependent signalling system, which plays an important role in plant signalling processes. Alternatively, FM 1-43 could also interfere with the function of auxin carrier molecules by steric blockage, etc. Similar effects were observed with FM 1-43 for mechanotransduction channels of murine hair cells, neuronal cells (Gale *et al.*, 2001; Drew and Wood, 2007) and muscarinic acetylcholine receptors (Mazzone *et al.*, 2006). Interestingly, the inhibitory action of FM dyes on both active auxin influx and efflux was inversely proportional to their hydrophobicity. The action of FM 4-64 and 5-95 might have been attributed to the fact that after their use there are fewer auxin carriers at the PM. However, this does not apply to FM 1-43, which did not induce any internalization of these proteins. Generally, after application of these dyes to living cells, all carriers and other proteins are affected in parallel. In the case of inhibition of influx, intracellular auxin accumulation is decreased, and, in contrast, in the case of inhibition of efflux, auxin accumulation is increased. Thus the sum of these auxin transport processes across the PM, resulting in the net capacity for auxin accumulation in living cells, does not directly reflect the individual activity of auxin carriers. Only the use of auxins that are preferential 'substrates' for either influx or efflux carriers gives an indication of the effect(s) of FM dyes on auxin transporter activity. Such treatments showed that FM dyes, particularly FM 1-43, do influence the activity of auxin transport processes across the PM, and that they do so immediately after application.

Altogether, even though the FM dyes are very useful tools for tracking endocytosis *in vivo*, they also can induce transient internalization of at least some PM proteins and alter their activity, mainly in suspension-cultured cell lines. Therefore, a very careful characterization of action of these dyes should be performed under specific experimental conditions before they are used as endocytotic markers. The data also indicate that FM dyes do not label all endocytic pathways in plants.

EXPERIMENTAL PROCEDURES

Plant material and gene constructs

The tobacco BY-2 cell line (*N. tabacum* L. cv. Bright Yellow 2; Nagata *et al.*, 1992) and BY-2 cells transformed with *A. thaliana* PIN1::PIN1:GFP (Benkova *et al.*, 2003; Zažímalová *et al.*, 2007) were cultivated in darkness at 25°C on an orbital incubator (IKA KS501, IKA Labortechnik, http://www.ika.net) at 120 rpm (orbital diameter 30 mm) in liquid medium (3% sucrose, 4.3 g L^{-1} Murashige and Skoog salts, 100 mg L^{-1} inositol, 1 mg L^{-1} thiamin, 0.2 mg L^{-1} 2,4-dichlorophenoxyacetic acid and 200 mg L^{-1} KH_2PO_4, pH 5.8) supplemented (transformed cells only) with 100 mg L^{-1} kanamycin and 100 mg L^{-1} cefotaxim, and sub-cultured weekly. Calli were maintained on the same medium solidified with 0.6% w/v agar. A gene construct containing *A. thaliana PGP4::PGP4:GFP* in pGPTV–GFP (Cho *et al.*, 2007) was introduced into *Agrobacterium tumefaciens* strain GV2260 and then into tobacco cells by co-cultivation as described previously (An, 1985; Petrášek *et al.*, 2003). The PGP4-transformed lines were cultivated in liquid medium supplemented with 100 mg L^{-1} kanamycin, 300 mg L^{-1} claforan and 50 mg L^{-1} hygromycin B.

Plants were grown on Murashige and Skoog (MS) plates (with sucrose) under a 16 h light/8 h dark photoperiod at 21/18°C. Experiments were performed during the light period. Uptake experiments using 2 μM FM4-64 were performed on 5-day-old seedlings expressing *PIN2::PIN2–GFP* (Xu and Scheres, 2005) or *35S::PIP2:GFP* (Cutler *et al.*, 2000) in liquid MS medium.

The *A. thaliana* cell suspension culture was derived from *PIN1::PIN1:GFP*-expressing plants (Benkova *et al.*, 2003) as described by Petrášek *et al.* (2006).

Chemicals

Boron-dipyrromethane-phosphatidylcholine [2-decanoyl–1-(*O*-(11-(4,4-difluoro-5,7-dimethyl-4-bora-3a,4a-diaza-*s*-indacene-3-propionyl)amino)undecyl)*sn*-glycero-3-phosphocholine] (BODIPY-PC) was obtained from Invitrogen (http://www.invitrogen.com/). Phospholipase A_2 (PLA_2) from bee venom, PC-PLC from *Bacillus cereus* and PLD from cabbage were obtained from Sigma-Aldrich Co. (http://www.sigmaaldrich.com/). HPLC-grade chloroform, ethanol, methanol and high-performance thin layer chromatography (HP-TLC) plates were obtained from Merck (http://www.merck.com). All other chemicals were of analytical grade.

FM dyes 4-64, 5-95 and 1-43 (Molecular Probes, catalogue numbers T13320, T23360, T3163), brefeldin A, wortmannin, latrunculin B and oryzalin (all Sigma-Aldrich, http://www.invitrogen.com) were kept as 20, 50, 10, 2.5 and 57 mM stock solutions, respectively, in DMSO at −20°C. Sodium azide was added from a 1.5 M stock solution in water to a final concentration of 15 mM.

Application of FM dyes and inhibitors

FM dyes were added to 1 ml of 2–3-day-old BY-2 cell suspension under continuous shaking in multi-well plates, and samples were observed at the time indicated. Alternatively, the protocol described by Emans *et al.* (2002) was used. 1 ml of a 2–3-day-old BY-2 cell

suspension was placed on ice for 15 min and then supplemented with 2 μM FM dye. After another 15 min of incubation on ice, cells were transferred to an orbital shaker at 26°C and observed at the time indicated. Brefeldin A, sodium azide and wortmannin were added directly to the cultivation medium to final concentrations of 20 μM, 15 mM and 50 μM, respectively. The same amount of solvent was added to controls.

Seedlings were primed for 5 min on ice with MS medium containing 2 μM FM4-64, subsequently rinsed three times in liquid MS medium, and analysed by confocal microscopy.

Microscopy

For *in vivo* microscopy, a Zeiss LSM 5 DUO confocal microscope with a 40× C-Apochromat objective (NA = 1.2 W) was used (http://www.zeiss.com/). Fluorescence signals for GFP (excitation 488 nm, emission 505–550 nm), FM 4-64 and FM 5-59 (both excitation 561 nm, emission >575 nm) were detected. Sequential scanning was used to avoid any cross-talk between fluorescence channels. To separate FM1-43 and GFP fluorescence, spectral fluorescence detection and subsequent linear unmixing were used. Lambda series (excitation 488 and 561 nm) were collected using the Zeiss META system. Nineteen channels (10.7 nm wide) of the META detector were used to span an emission range of 497–700 nm. Linear unmixing was performed using Zeiss LSM IMAGE EXAMINER software. Reference spectra of GFP and FM1-43 were acquired from single labelled specimens. The scattergram of fluorescence intensities in the red and green channels was constructed using Zeiss IMAGE EXAMINER software. Independent experiments were performed in triplicate with the same results, and representative images are shown.

Auxin accumulation assay

Auxin accumulation by BY-2 cells was measured according to the method described by Delbarre *et al.* (1996), as modified by Petrášek *et al.* (2003). Accumulation by the cells of [^{3}H]NAA (specific radioactivity 935 GBq mmol^{-1}, synthesized at the Isotope Laboratory, Institute of Experimental Botany, Prague, Czech Republic) or [^{3}H]2,4-D (specific radioactivity 20 Ci mmol^{-1}, American Radiolabeled Chemicals Inc., http://www.arcincusa.com) was measured in 0.5 ml aliquots of cell suspension (cell density approximately 7×10^5 cells ml^{-1}, as determined by counting cells in a Fuchs–Rosenthal haemocytometer). FM dyes were added at the beginning of the accumulation assay. The values for the net accumulation of auxin (with the value at time 0 subtracted) after 20 min of incubation with radioactive auxin and FM dye were plotted relative to the control accumulation without FM dyes.

Determination of non-specific phospholipase C activity

Fluorescent substrate (0.66 μg ml^{-1} BODIPY-PC) was added to a 3-day-old BY-2 cell suspension. The suspension was diluted to 0.056 g FW ml^{-1}. After 10 min of incubation, FM dye was added to the final concentration of 10 μM. After incubation on an orbital shaker at 26°C in darkness for 15 min, the cells were harvested for the extraction of lipids and HP-TLC analysis of reaction products. Lipids were extracted by a modification of the method described by Bligh and Dyer (1959). Briefly, 4 ml of methanol/chloroform (2/1 v/v) was added to harvested cells. After 30 min of extraction, 2 ml 0.1 M KCl was added, and the mixture was left at 4°C for at least 30 min. Then samples were centrifuged for 15 min at 420 ***g***. The lower phase was evaporated to dryness using a vacuum evaporator and re-dissolved in ethanol. Samples were applied to HP-TLC silica gel-60 plates using a Linomat IV sampler (Camag, http://www.camag.com). After 10 min of saturation, plates were developed in a horizontal developing chamber (Camag) in a mobile phase of chloroform/methanol/water (65/25/4 v/v/v) (Scherer *et al.*, 2002). Plates were dried and scanned using a video camera (Kodak DC 120, http://www.kodak.com) under UV light for computer-assisted quantification (Kodak ds 1D). Identification of individual spots was based on comparison with fluorescently labelled lipid standards.

ACKNOWLEDGEMENTS

We thank Jan Malínský (Institute of Experimental Medicine, Prague, the Czech Republic) for helpful discussion, Hyung-Taeg Cho (Chungnam National University, Daejeon, Korea) and Angus Murphy (Purdue University, West Lafayette, IN, USA) for *PGP4:: PGP4:GFP* gene constructs, and Ben Scheres (Utrecht University, Utrecht, the Netherlands) and Chris Somerville (University of California, Berkeley, CA, USA) for *A. thaliana* seeds expressing PIN2–GFP and PIP2–GFP proteins, respectively. This work was supported by the Grant Agency of the Academy of Sciences of the Czech Republic (grant number KJB600380604 to J.P.), by the Grant Agency of Charles University (grant number 43-252455 to A.J. and S.S.) and by a grant from the Ministry of Education, Youth and Sports of the Czech Republic to E.Z. (LC06034).

SUPPORTING INFORMATION

Additional Supporting Information may be found in the online version of this article:

Figure S1. FM 4-64-stimulated transient internalization of plasma membrane-located auxin carriers.

Figure S2. De-polymerization of the actin or microtubule cytoskeleton does not abolish FM 4-64-induced internalization of plasma membrane-located auxin carriers.

Movie S1. Re-localization of PIN1–GFP into patches in the cytoplasm after 3 min treatment with 2 μM FM 4-64.

Movie S2. PIN1–GFP localization after 3 min mock treatment with the appropriate amount of solvent (DMSO).

Please note: As a service to our authors and readers, this journal provides supporting information supplied by the authors. Such materials are peer-reviewed and may be re-organized for online delivery, but are not copy-edited or typeset. Technical support issues arising from supporting information (other than missing files) should be addressed to the authors.

REFERENCES

An, G. (1985) High-efficiency transformation of cultured tobacco cells. *Plant Physiol.* **79**, 568–570.

Aniento, F. and Robinson, D.G. (2005) Testing for endocytosis in plants. *Protoplasma*, **226**, 3–11.

Barak, I., Muchova, K., Wilkinson, A.J., O'Toole, P.J. and Pavlendova, N. (2008) Lipid spirals in *Bacillus subtilis* and their role in cell division. *Mol. Microbiol.* **68**, 1315–1327.

Benkova, E., Michniewicz, M., Sauer, M., Teichmann, T., Seifertova, D., Jurgens, G. and Friml, J. (2003) Local, efflux-dependent auxin gradients as a common module for plant organ formation. *Cell*, **115**, 591–602.

Betz, W.J. and Bewick, G.S. (1992) Optical analysis of synaptic vesicle recycling at the frog neuromuscular-junction. *Science*, **255**, 200–203.

Betz, W.J., Mao, F. and Bewick, G.S. (1992) Activity-dependent fluorescent staining and destaining of living vertebrate motor-nerve terminals. *J. Neurosci.* **12**, 363–375.

Betz, W.J., Mao, F. and Smith, C.B. (1996) Imaging exocytosis and endocytosis. *Curr. Opin. Neurobiol.* **6**, 365–371.

Bligh, E.G. and Dyer, W.J. (1959) A rapid method of total lipid extraction and purification. *Can. J. Biochem. Physiol.* **37**, 911–917.

Bolte, S., Talbot, C., Boutté, Y., Catrice, O., Read, N.D. and Satiat-Jeunemaitre, B. (2004) FM-dyes as experimental probes for dissecting vesicle trafficking in living plant cells. *J. Microsc.* **214**, 159–173.

Cho, M., Lee, S. and Cho, H. (2007) P-glycoprotein 4 displays auxin efflux transporter-like action in Arabidopsis root hair cells and tobacco cells. *Plant Cell*, **19**, 3930–3943.

Cutler, S.R., Ehrhardt, D.W., Griffitts, J.S. and Somerville, C.R. (2000) Random GFP :: cDNA fusions enable visualization of subcellular structures in cells of *Arabidopsis* at a high frequency. *Proc. Natl Acad. Sci. USA*, **97**, 3718–3723.

Delbarre, A., Muller, P., Imhoff, V. and Guern, J. (1996) Comparison of mechanisms controlling uptake and accumulation of 2,4-dichlorophenoxy acetic acid, naphthalene-1-acetic acid, and indole-3-acetic acid in suspension-cultured tobacco cells. *Planta*, **198**, 532–541.

Dettmer, J., Hong-Hermesdorf, A., Stierhof, Y.D. and Schumacher, K. (2006) Vacuolar H^+-ATPase activity is required for endocytic and secretory trafficking in *Arabidopsis*. *Plant Cell*, **18**, 715–730.

Dhonukshe, P., Aniento, F., Hwang, I., Robinson, D., Mravec, J., Stierhof, Y. and Friml, J. (2007) Clathrin-mediated constitutive endocytosis of PIN auxin efflux carriers in Arabidopsis. *Curr. Biol.* **17**, 520–527.

Drew, L.J. and Wood, J.N. (2007) FM1-43 is a permeant blocker of mechanosensitive ion channels in sensory neurons and inhibits behavioural responses to mechanical stimuli. *Mol. Pain*, **3**, 1.

Emans, N., Zimmermann, S. and Fischer, R. (2002) Uptake of a fluorescent marker in plant cells is sensitive to brefeldin A and wortmannin. *Plant Cell*, **14**, 71–86.

Gaffield, M.A. and Betz, W.J. (2006) Imaging synaptic vesicle exocytosis and endocytosis with FM dyes. *Nat. Protoc.* **1**, 2916–2921.

Gale, J.E., Marcotti, W., Kennedy, H.J., Kros, C.J. and Richardson, G.P. (2001) FM1-43 dye behaves as a permeant blocker of the hair-cell mechanotransducer channel. *J. Neurosci.* **21**, 7013–7025.

van Gisbergen, P., Esseling-Ozdoba, A. and Vos, J. (2008) Microinjecting FM4-64 validates it as a marker of the endocytic pathway in plants. *J. Microsc.* **231**, 284–290.

Griffing, L. (2008) FRET analysis of transmembrane flipping of FM4-64 in plant cells: is FM4-64 a robust marker for endocytosis? *J. Microsc.* **231**, 291–298.

Grinvald, A., Frostig, R.D., Lieke, E. and Hildesheim, R. (1988) Optical imaging of neuronal activity. *Physiol. Rev.* **68**, 1285–1366.

Grossmann, G., Opekarová, M., Malinsky, J., Weig-Meckl, I. and Tanner, W. (2007) Membrane potential governs lateral segregation of plasma membrane proteins and lipids in yeast. *EMBO J.* **26**, 1–8.

Hoyerová, K., Perry, L., Hand, P., Laňková, M., Kocábek, T., May, S., Kottová, J., Pačes, J., Napier, R. and Zažímalová, E. (2008) Functional characterization of PaLAX1, a putative auxin permease, in heterologous plant systems. *Plant Physiol.* **146**, 1128–1141.

Kleine-Vehn, J., Dhonukshe, P., Swarup, R., Bennett, M. and Friml, J. (2006) Subcellular trafficking of the Arabidopsis auxin influx carrier AUX1 uses a novel pathway distinct from PIN1. *Plant Cell*, **18**, 3171–3181.

Klima, A. and Foissner, I. (2008) FM dyes label sterol-rich plasma membrane domains and are internalized independently of the cytoskeleton in characean internodal cells. *Plant Cell Physiol.* **49**, 1508–1521.

Kutsuna, N. and Hasezawa, S. (2002) Dynamic organization of vacuolar and microtubule structures during cell cycle progression in synchronized tobacco BY-2 cells. *Plant Cell Physiol.* **43**, 965–973.

Mazzone, S.B., Mori, N., Burman, M., Palovich, M., Belmonte, K.E. and Canning, B.J. (2006) Fluorescent styryl dyes FM1-43 and FM2-10 are muscarinic receptor antagonists: intravital visualization of receptor occupancy. *J. Physiol.* **575**, 23–35.

Meckel, T., Hurst, A.C., Thiel, G. and Homann, U. (2004) Endocytosis against high turgor: intact guard cells of *Vicia faba* constitutively endocytose fluorescently labelled plasma membrane and GFP-tagged K^+-channel KAT1. *Plant J.* **39**, 182–193.

Meijer, H.J.G. and Munnik, T. (2003) Phospholipid-based signaling inplants. *Annu. Rev. Plant Biol.* **54**, 265–306.

Nagata, T., Nemoto, Y. and Hasezawa, S. (1992) Tobacco BY-2 cell-line as the HeLa cell in the cell biology of higher plants. *Int. Rev. Cytol.* **132**, 1–30.

Oparka, K.J. (1990) What is phloem unloading? *Plant Physiol.* **94**, 393–396.

Perez-Gomez, J. and Moore, I. (2007) Plant endocytosis: it is clathrin after all. *Curr. Biol.* **17**, R217–R219.

Petrášek, J., Černá, A., Schwarzerová, K., Elčkner, M., Morris, D.A. and Zažímalová, E. (2003) Do phytotropins inhibit auxin efflux by impairing vesicle traffic? *Plant Physiol.* **131**, 254–263.

Petrášek, J., Mravec, J., Bouchard, R. *et al.* (2006) PIN proteins perform a rate-limiting function in cellular auxin efflux. *Science*, **312**, 914–918.

Rodes, J.F., Berreurbonnenfant, J., Tremolieres, A. and Brown, S.C. (1995) Modulation of membrane fluidity and lipidic metabolism in transformed rat fibroblasts induced by the sesquiterpenic hormone farnesylacetone. *Cytometry*, **19**, 217–225.

Scherer, G.F.E., Paul, R.U., Holk, A. and Martinec, J. (2002) Down-regulation by elicitors of phosphatidylcholine-hydrolyzing phospholipase C and up-regulation of phospholipase A in plant cells. *Biochem. Biophys. Res. Commun.* **293**, 766–770.

Terasaka, K., Blakeslee, J.J., Titapiwatanakun, B. *et al.* (2005) PGP4, an ATP binding cassette P-glycoprotein, catalyzes auxin transport in *Arabidopsis thaliana* roots. *Plant Cell*, **17**, 2922–2939.

Villaverde, M.S. and Verstraeten, S.V. (2003) Effects of thallium(I) and thallium(III) on liposome membrane physical properties. *Arch. Biochem. Biophys.* **417**, 235–243.

Wang, X. (2004) Lipid signaling. *Curr. Opin. Plant Biol.* **7**, 329–336.

Xu, J. and Scheres, B. (2005) Dissection of Arabidopsis ADP-RIBOSYLATION FACTOR 1 function in epidermal cell polarity. *Plant Cell*, **17**, 525–536.

Yang, H.B. and Murphy, A.S. (2009) Functional expression and characterization of Arabidopsis ABCB, AUX 1 and PIN auxin transporters in *Schizosaccharomyces pombe*. *Plant J.* **59**, 179–191.

Zažímalová, E., Křeček, P., Skůpa, P., Hoyerová, K. and Petrášek, J. (2007) Polar transport of the plant hormone auxin – the role of PIN-FORMED (PIN) proteins. *Cell. Mol. Life Sci.* **64**, 1621–1637.

Zhu, Y. and Stevens, C.F. (2008) Probing synaptic vesicle fusion by altering mechanical properties of the neuronal surface membrane. *Proc. Natl Acad. Sci. USA*, **105**, 18018–18022.

Zonia, L. and Munnik, T. (2008) Vesicle trafficking dynamics and visualization of zones of exocytosis and endocytosis in tobacco pollen tubes. *J. Exp. Bot.* **59**, 861–873.

Figure S1

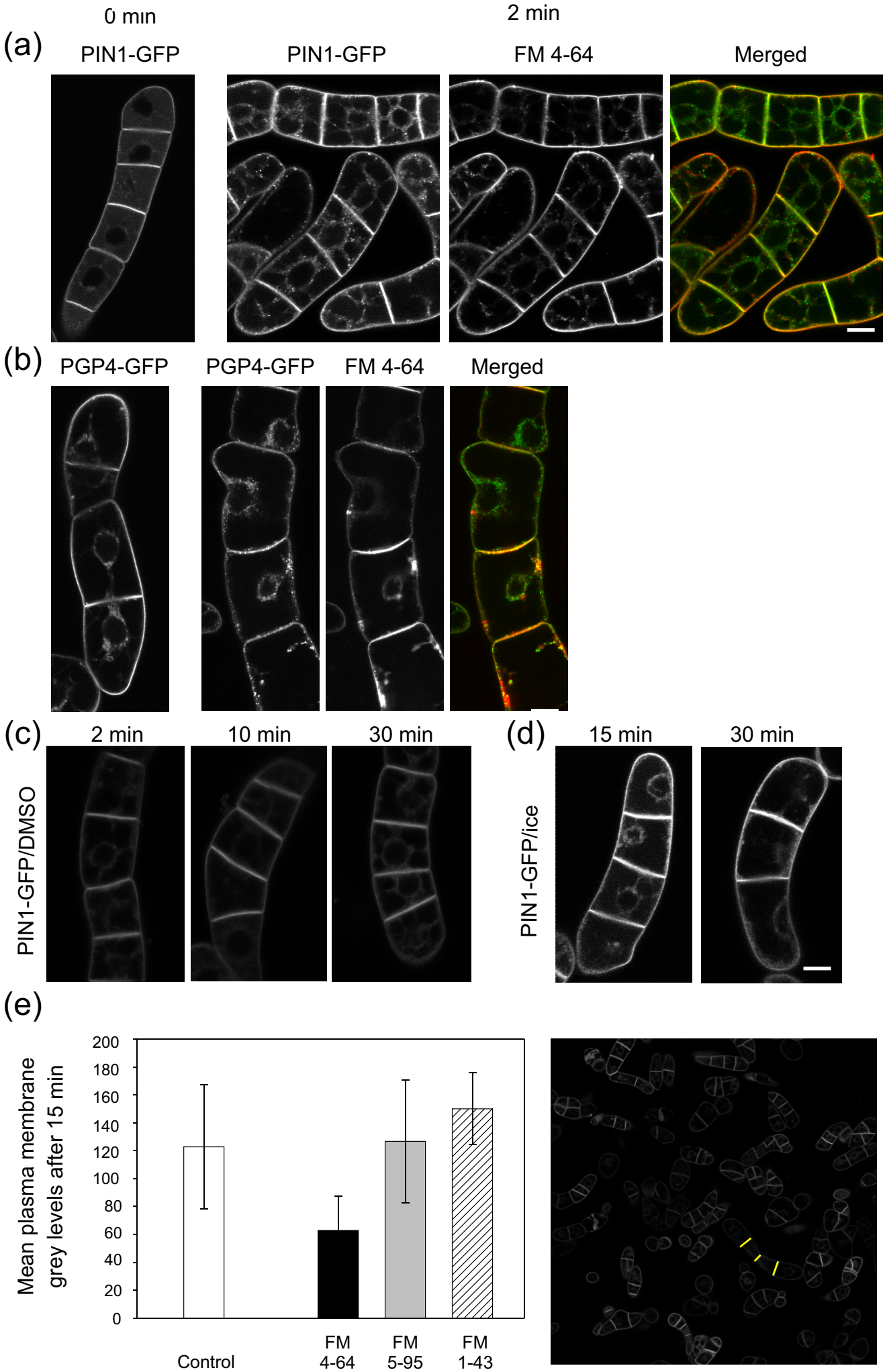
0 min
2 min
(a)
PIN1-GFP
PIN1-GFP
FM 4-64
Merged
(b)
PGP4-GFP
PGP4-GFP
FM 4-64
Merged
(c)
2 min
10 min
30 min
PIN1-GFP/DMSO
(d)
15 min
30 min
PIN1-GFP/ice
(e)
Mean plasma membrane grey levels after 15 min
200
180
160
140
120
100
80
60
40
20
0
Control
FM 4-64
FM 5-95
FM 1-43

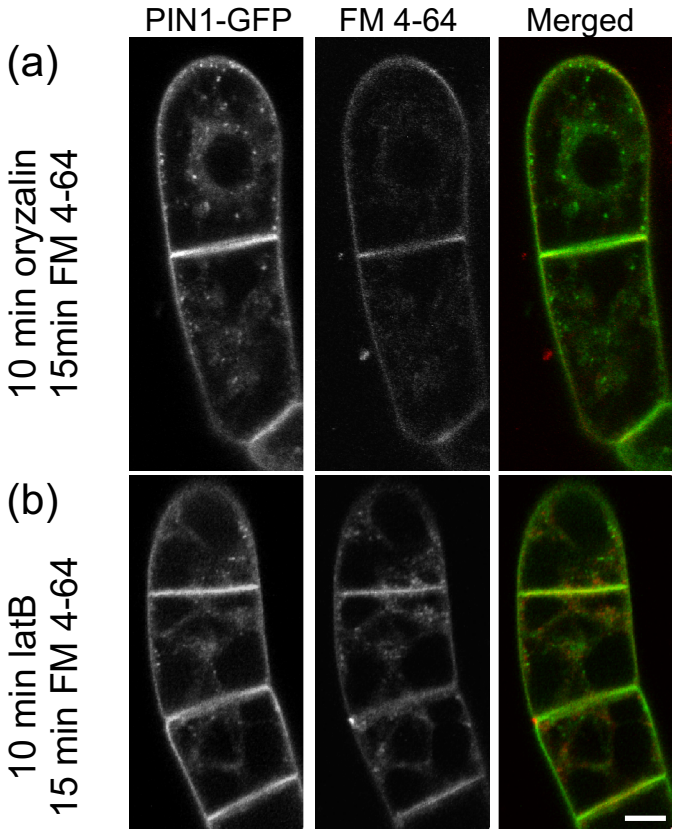
PIN1-GFP
FM 4-64
Merged
(a)
10 min oryzalin
15min FM 4-64
(b)
10 min latB
15 min FM 4-64

Supporting Information

Figure S1. FM 4-64-stimulated transient internalization of plasma membrane-located auxin carriers, fast effects, mock treatments and the quantification. *In vivo* confocal microscopy of PIN1-GFP (a) and PGP4-GFP (b) in 3-day-old tobacco BY-2 cells; treatment with 2 µM FM 4-64 for indicated times. (c) Mock treatment for figure 2a. DMSO 1:10 000 (v/v) was added to PIN1-GFP expressing cells and images were taken at 2 minutes, 10 minutes and 30 minutes after the addition of DMSO. No changes in the localization of PIN1-GFP were observed compared to the non-treated cells and no increase in the formation of PIN1-GFP patches was observed. (d) Mock treatment for figure 4b. Cells were pre-incubated on ice for 15 minutes, than DMSO 1:10000 (v/v) was added and cells further incubated on ice. Images were captured at 15 and 30 minutes after the addition of DMSO. DMSO did not induce the formation of PIN1-GFP vesicles as observed after FM4-64 treatment. (e) Mean plasma membrane grey levels after 15 min treatment with FM dyes reflecting the relocalization of the PIN1-GFP into the endosomal space. Note that FM 4-64 has the most remarkable effect. After the interactive thresholding of the plasma membranes (indicated by yellow bars in the image on the right) the mean value of fluorescence intensity was recorded for both time points: just after the application of the respective dye and after 15 min incubation. Cells treated for 15 minutes with DMSO (1:10000 v/v) or 2µM FM dyes were compared to the non-treated cells, mean grey levels (8 bit resolution) reflect the intensity of the fluorescence in the plasma membrane. All cell chains containing three and more cells from 9 optical fields were analyzed. Error bars represent SD.

The test of equality of variances indicated that the variances of the grey levels of the plasma membrane after 15 min of treatment were significantly different from control cells both for FM 4-64-treated cells ($F=3.2$, $p=0.004$) and FM 1-43-treated cells ($F=2.98$, $p=0.002$) and significantly equal for FM 5-59-treated cells ($F=1.01$, $p=0.486$). Therefore, a two sample t-tests that do not assume equal variances were performed for the comparison of mean grey levels reflecting the plasma membrane fluorescence of control and FM 4-64 and FM 1-43-treated cells. For FM 5-59, a two sample t-test assuming equal variances was performed. The mean grey levels for FM 4-64-treated cells ($M=62.77$; $SD=24.85$; $n=22$) were significantly smaller than in control cells ($M=122.78$; $SD=44.48$; $n=28$) as tested by the two-sample t-test for unequal variances, $t(44)=6.04$, $p<=0.001$. Differences in grey values for FM1-43 and FM 5-59 were statistically insignificant using the t test for unequal and equal variances, respectively ($p>=0.005$).

Figure S2. Depolymerization of actin or microtubule cytoskeleton does not abolish FM 4-64-induced internalization of plasma membrane-located auxin carriers. *In vivo* confocal microscopy of PIN1-GFP in 3-day-old tobacco BY-2 cells treated with latrunculin B (a) or oryzalin (b). Cells were stained with 2 µM FM 4-64 for 15 minutes. In cells with depolymerized actin is PIN1GFP localization less affected by FM4-64 dye, whereas depolarization of microtubules results in increased relocalization of PIN1GFP. To depolymerize actin cytoskeleton, BY2 cells were incubated with 500nM Latrunculin B for 10 minutes. Subsequently 2µM FM 4-64 was added and images were taken at times indicated. For depolymerization of microtubules 20µM oryzalin was used.

6.4. Chapter 4 - Auxin influx inhibitors 1-NOA, 2-NOA, and CHPAA interfere with membrane dynamics in tobacco cells

Martina Laňková, Richard Smith, Bedřich Pešek, **Martin Kubeš**, Eva Zažímalová, Jan Petrášek, Klára Hoyerová

Journal of Experimental Botany 61, 3589-3598

This paper is the result of Dr. Eva Zažímalová laboratory with a small contribution from the Univ. Bern, Switzerland. In this report, we reveal the mechanism of action of the auxin influx inhibitors 1-NOA, 2-NOA, and CHPAA by direct measurements of auxin accumulation, cellular phenotypic analysis, as well as by localization studies of *Arabidopsis* auxin carriers heterologously expressed in BY-2 cells.

My contribution to this article was in the transformation of BY-2 cells with ABCB4::ABCB4:GFP construct, characterization of cell line including expression analyses (immunofluorescence localization) and analysis of cell phenotype. I was involved in microscopy analysis of the effects of the auxin influx inhibitors (1-NOA, 2-NOA and CHPAA) on subcellular distribution of ABCB4-GFP fusion proteins in tobacco BY-2 cells.

To determine whether the auxin influx inhibitors (1-NOA, 2-NOA and CHPAA) can influence AUX1, PIN1, ABCB4 proteins distribution, *XVE::EYFP:AUX1*, *XVE::PIN1:GFP, ABCB4::ABCB4:GFP* BY-2 cell lines were used. In control situation the PM fluorescence of all fusion proteins was observed without visible vesicles in the cortical cytoplasm (Fig. 4A, E, I). After 3 h treatment with 20 μM 1-NOA, both PIN1:GFP and EYFP:AUX1 (Fig. 4B, F) were observed in vesicles reminiscent of endosomes and located in the cortical cytoplasm. Similar treatment with 2-NOA induced these patches as well, but the effect was weaker (Fig. 4C, G). A 3 h exposure to 20 μM CHPAA did not induce any protein redistributions (Fig. 4D, H). Interestingly, only after 24 h treatment with 1-NOA ABCB4:GFP fusion protein appeared in a form of few membrane aggregates (Fig. 4J, K, L).

The work was supported by the Grant Agency of the Czech Republic (KJB600380702), by the Ministry of Education, Youth and Sports of the Czech Republic, project LC06034, and by the European Fund for Regional Development, the Operational Programme Prague-Competitiveness, project 504 CZ.2.16/3.1.00/21159.

Journal of Experimental Botany, Page 1 of 10
doi:10.1093/jxb/erq172
This paper is available online free of all access charges (see http://jxb.oxfordjournals.org/open_access.html for further details)

Journal of Experimental Botany
www.jxb.oxfordjournals.org

RESEARCH PAPER

Auxin influx inhibitors 1-NOA, 2-NOA, and CHPAA interfere with membrane dynamics in tobacco cells

Martina Laňková[1], Richard S. Smith[2], Bedřich Pešek[1], Martin Kubeš[1], Eva Zažímalová[1], Jan Petrášek[1] and Klára Hoyerová[1,*]

[1] Institute of Experimental Botany, the Academy of Sciences of the Czech Republic, Rozvojová 263, CZ-165 02 Prague 6, Czech Republic
[2] Institute of Plant Sciences, University of Bern, Altenbergrain 21, CH-3013 Bern, Switzerland

* To whom correspondence should be addressed: E-mail: hoyerova@ueb.cas.cz

Received 26 February 2010; Revised 26 April 2010; Accepted 25 May 2010

Abstract

The phytohormone auxin is transported through the plant body either via vascular pathways or from cell to cell by specialized polar transport machinery. This machinery consists of a balanced system of passive diffusion combined with the activities of auxin influx and efflux carriers. Synthetic auxins that differ in the mechanisms of their transport across the plasma membrane together with polar auxin transport inhibitors have been used in many studies on particular auxin carriers and their role in plant development. However, the exact mechanism of action of auxin efflux and influx inhibitors has not been fully elucidated. In this report, the mechanism of action of the auxin influx inhibitors (1-naphthoxyacetic acid (1-NOA), 2-naphthoxyacetic acid (2-NOA), and 3-chloro-4-hydroxyphenylacetic acid (CHPAA)) is examined by direct measurements of auxin accumulation, cellular phenotypic analysis, as well as by localization studies of *Arabidopsis thaliana* L. auxin carriers heterologously expressed in *Nicotiana tabacum* L., cv. Bright Yellow cell suspensions. The mode of action of 1-NOA, 2-NOA, and CHPAA has been shown to be linked with the dynamics of the plasma membrane. The most potent inhibitor, 1-NOA, blocked the activities of both auxin influx and efflux carriers, whereas 2-NOA and CHPAA at the same concentration preferentially inhibited auxin influx. The results suggest that these, previously unknown, activities of putative auxin influx inhibitors regulate overall auxin transport across the plasma membrane depending on the dynamics of particular membrane vesicles.

Key words: Auxin efflux carrier, auxin influx carrier, auxin transport, auxin transport inhibitor, membrane dynamics, tobacco BY-2 cells.

Introduction

Differential distribution of the plant growth regulatory substance auxin is known to mediate many fundamental processes in plant development, such as the formation of the embryogenic apical–basal axis, pattern formation, tropisms, and organogenesis (reviewed in Vanneste and Friml, 2009). The distribution of auxin and the formation of auxin gradients in the tissues is directed by the activity of the plasma membrane-localized auxin influx carriers AUXIN RESISTANT 1/LIKE AUXIN RESISTANT (AUX1/LAX) and auxin efflux carriers PIN-FORMED (PIN) as well as the ATP-Binding Cassette subfamily B (ABCB)/multidrug resistance (MDR)/phosphoglycoprotein (PGP)-type transporters (Noh *et al.*, 2001; Swarup *et al.*, 2001; Friml *et al.*, 2002*a*, *b*, 2003; Benková *et al.*, 2003; Blilou *et al.*, 2005; Vieten *et al.*, 2007; Pernisová *et al.*, 2009). Auxin influx carriers (AUX1/LAX), belonging to the family of plasma membrane amino acid permeases (AAP family), mediate the uptake of auxin into the cell (auxin influx). AUX1 was characterized at the molecular level in *Arabidopsis* by Bennett *et al.* (1996) and its transport function was shown by Yang *et al.* (2006). In addition, the function of LAX3 was characterized in *Arabidopsis* as well (Swarup *et al.*, 2008).

Although most of the native auxin indole-3-acetic acid (IAA) is transported into cells by diffusion, the importance

of AUX1/LAX carriers could be clearly demonstrated in many developmental processes. They are involved in embryogenesis (Ugartechea-Chirino *et al.*, 2010), hypocotyl apical hook development (Vandenbussche *et al.*, 2010), root gravitropism (Bennett *et al.*, 1996), lateral root development (Swarup *et al.*, 2001), root hair development (Jones *et al.*, 2009), phloem loading and unloading (Marchant *et al.*, 2002), and phyllotaxis (Bainbridge *et al.*, 2008). Generally, the importance of auxin uptake carriers lies mainly in their role in the pumping of auxin against its concentration gradient. Mathematical modelling further supports the role of AUX1/LAX proteins in the creation of local auxin maxima as demonstrated for phyllotaxis (Smith *et al.*, 2006).

Over the last two decades, auxin efflux inhibitors such as 2,3,5-triiodobenzoic acid (TIBA) or 1-naphthylphthalamic acid (NPA) (see a review by Rubery, 1990; Lomax *et al.*, 1995; Morris *et al.*, 2004) have significantly contributed to the present knowledge about auxin efflux transporters and their involvement in the control of physiological and developmental processes in plants. Compounds that inhibit auxin efflux include synthetic phytotropins (NPA and 2-(1-pyrenoyl)benzoic acid (PBA) being the most prominent representatives), cyclopropyl propane dione (CPD) and TIBA, and also natural flavonoids (e.g. quercetin). Moreover, inhibitors of intracellular protein trafficking, such as monensin and brefeldin A (BFA), also affect auxin efflux (Wilkinson and Morris, 1994; Morris and Robinson, 1998). BFA operates through plasma membrane localization of PINs and ABCBs but not AUX1/LAXes (Titapiwatanakun and Murphy, 2009).

The synthetic compounds 1-naphthoxyacetic acid (1-NOA), 2-naphthoxyacetic acid (2-NOA), and 3-chloro-4-hydroxyphenylacetic acid (CHPAA) have been used to disrupt auxin influx (uptake). The inhibitors were originally selected on the basis of their structural similarities with 2,4-dichlorophenoxyacetic acid (2,4-D), an auxin influx carrier substrate, or with naphthalene-2-acetic acid (2-NAA), a substance that inhibits auxin influx carriers (Imhoff *et al.*, 2000). The synthetic inhibitors share some structural features with auxins in containing an aromatic moiety substituted with an acidic side-chain with a carboxyl group, which is, among other things, believed to bind specifically a particular region of the putative auxin receptor (Edgerton *et al.*, 1994). Importantly, the naturally occurring substance chromosaponin (Rahman *et al.*, 2001) was found to be a possible endogenous analogue to synthetic inhibitors such as 1-NOA (Parry *et al.*, 2001).

Although the mechanism of action of auxin transport inhibitors is still far from being fully understood, recent data (Dhonukshe *et al.*, 2008) suggest that some of these compounds (e.g. PBA, TIBA, but not NPA) can act through actin-mediated vesicle trafficking processes in eukaryotic cells. As shown in tobacco BY-2 cells, actin dynamics seems to be at both the genomic and the non-genomic levels under the control of auxin itself and NPA interferes with this process (Maisch and Nick, 2007; Nick *et al.*, 2009). The modulation of intracellular trafficking of both AUX1 and PIN auxin transporters (Kleine-Vehn *et al.*, 2006) by auxin transport inhibitors is thus critical for their overall abundance at the plasma membrane. Obviously, besides the action of (native) auxin transport inhibitors, many other processes regulate the overall performance of auxin transporters as well (for a review see Titapiwatanakun and Murphy, 2009).

In this paper, the function and mechanism of action of the synthetic auxin influx inhibitors 1-NOA, 2-NOA, and CHPAA were investigated. Assays of auxin transport in tobacco BY-2 cells showed that, in contrast to 2-NOA and CHPAA, the mode of action of 1-NOA is not entirely specific for auxin influx. Changes in the subcellular distribution of both *At*EYFP:AUX1 and *At*PIN1:GFP fusion proteins expressed heterologously in tobacco BY-2 cells, and the resulting defects in the polarity of cell division, indicate that 1-NOA acts largely through changes in membrane dynamics. 2-NOA was less effective and CHPAA was almost ineffective in this respect. On the basis of these findings the mechanism of action of these inhibitors was proposed related to the dynamics of membrane vesicles transporting particular auxin carriers.

Materials and methods

Chemicals

Unless stated otherwise, all chemicals were supplied by Sigma Aldrich (St Louis, MO, USA).

Construction of transformation vectors

The estradiol-inducible *XVE::PIN1:GFP* construct was prepared using DNA sequence *PIN1:GFP* which was PCR amplified from plasmid DNA (Benková *et al.*, 2003). The primers containing the attB1 and attB2 Gateway recombination sites were used. The purified PCR product was placed into the Gateway pDONR 221 donor vector (BP reaction). Recombination (LR reaction) was then made with the pMDC7 binary destination vector (Curtis and Grossniklaus, 2003) containing the estradiol-inducible transactivator XVE. The resulting plasmid was verified by sequencing from the left to the right borders.

The estradiol-inducible *XVE::EYFP:AUX1* construct was prepared using *AUX1* and *EYFP* DNA sequences which were PCR amplified separately from plasmid DNA (Yang *et al.*, 2006). The primers contained attB multisite Gateway recombination sites. For *EYFP* and *AUX1* amplification, attB1, attB5r sites, and attB5, attB2 sites were used in this respect. The purified PCR products were then placed into Gateway pDONR 221 P1-P5r and pDONR 221 P5-P2 donor vectors (BP reactions). Multisite recombination (LR reaction) was then made with the pMDC7 binary destination vector (Curtis and Grossniklaus, 2003) containing the estradiol-inducible transactivator XVE. The resulting plasmid was verified by sequencing from the left to the right borders.

Primers used: *PIN1:GFP* forward (attB1), GGGGACAAGTTTGTACAAAAAAGCAGGCTCAACAATGATTACGGCGGCGGACTTCTAC, *PIN1:GFP* reverse (attB2), GGGGACCACTTTGTACAAGAAAGCTGGGTGTGTTTTGGTAATATCTCTTCA; *AUX1* forward (attB5), GGGGACAACTTTGTATACAAAAGTTGGCTCCGCGGCCGCCCCCTTCACC, *AUX1* reverse (attB2), GGGGACCACTTTGTACAAGAAAGCTGGGTATCAAAGACGGTGGTGTAAAG; *EYFP* forward (attB1), GGGGACAAGTTTGTACAAAAAAGCAGGCTCAACAATGGGCAAGGGCGAGGAGCTG, *EYFP* reverse (attB5r), GGGGACAACTTTTGTATACAAAGTTGTTGATGATCCCGGGCCCGCGG.

Plant material

Cells of tobacco line BY-2 (*Nicotiana tabacum* L., cv. Bright-Yellow 2) (Nagata *et al.*, 1992) were cultured in liquid medium [3% (w/v) sucrose, 4.3 g l^{-1} Murashige and Skoog salts, 100 mg l^{-1} inositol, 1 mg l^{-1} thiamine, 0.2 mg l^{-1} 2,4-D, and 200 mg l^{-1} KH_2PO_4 (pH 5.8)] in darkness at 27 °C on an orbital incubator (Sanyo Gallenkamp, Schoeller Instruments Inc., Prague, Czech Republic; 150 rpm, 32 mm orbit) and subcultured weekly. Stock tobacco BY-2 calli were maintained on the same media solidified with 0.6% (w/v) agar and subcultured monthly. BY-2 cell lines expressing GFP fusion with ABCB4 (PGP4:GFP) were described in Jelínková *et al.* (2010).

Stock solutions of 1-NOA (5 mM), 2-NOA (5 mM), CHPAA (10 mM), and NPA (10 mM) in ethanol were added to the BY-2 cell suspension to a final concentration of 10 μM at each subculturing. Samples of cells were taken regularly for microscopy and determination of cell density.

Expression of *EYFP:AUX1* and *PIN1:GFP* genes was induced by the addition of estradiol (β-estradiol, 1 μM, 24 h) at the beginning of the subculture interval. Stock solutions of 1-NOA (20 mM), 2-NOA (20 mM), CHPAA (20 mM), and NPA (20 mM) in DMSO were added to reach a final concentration of 20 μM for the 3 h and 24 h treatments, and of 50 μM for the 48 h treatments. The same amount of the solvent was added to controls. FM 4-64 (4 μM) (Molecular Probes) was applied to 1 ml of 3-d-old BY-2 cells that had been pretreated with 20 μM or 50 μM 1-NOA for 4 h, and incubated for 1 min under continuous shaking.

Transformation of BY-2 cells

The basic transformation protocol of An (1985) was used. Three-day-old BY-2 cells were co-incubated with *Agrobacterium tumefaciens* (Petrášek *et al.*, 2003) strain GV2260 carrying *XVE::EYFP:AUX1* or *XVE::PIN1:GFP* constructs and transformed BY-2 cells were maintained in culture media containing 100 μg ml^{-1} hygromycin and 100 μg ml^{-1} cefotaxim.

Microscopy and image analysis

Nomarski DIC microscopy was performed using Nikon Eclipse E600 (Nikon, Japan) and images were recorded with colour digital camera (DVC 1310C, USA) using LUCIA image analysis software (Laboratory Imaging, Prague, Czech Republic). To determine cell length, a population of 400 cells was meausured using LUCIA image analysis software and the average values were expressed in μm. Confocal microscopy was performed using Zeiss LSM 5 DUO confocal microscope equipped with a ×40 C-Apochromat objective (NA=1.2 W). Fluorescence signals were obtained for GFP or YFP (excitation 488 nm, emission 505–550 nm) and FM 4-64 (excitation 561 nm, emission >575 nm).

Cell densities were determined by counting cells in at least 10 aliquots of each sample using Fuchs–Rosenthal haemocytometer slide.

Auxin accumulation measurements

Auxin accumulation in 2-d-old cells was measured using radioactively labelled auxins according to Delbarre *et al.* (1996), as modified by Petrášek *et al.* (2006). Treatments were replicated at least three times and the average values (± standard errors) were expressed as pmols of the particular auxin accumulated per million cells. 1-NOA, 2-NOA, CHPAA, NPA, or BFA were added as required from ethanolic stock solutions to give a final concentration of 10 μM at the beginning of the accumulation assay (together with the addition of radioactively labelled auxin). In the combined experiments, BFA was added to a final concentration of 10 μM at the beginning of the accumulation assay together with the addition of [^{3}H]NAA (25 Ci $mmol^{-1}$; Isotope Laboratory of the Institute of Experimental Botany, Prague, Czech Republic). Individual inhibitors 1-NOA, 2-NOA, or NPA were added after 10 min to a final concentration 10 μM.

For time-course experiments, aliquots of cell suspension were removed at specified intervals from 0–30 min after the addition of radioactively labelled auxin. Accumulation of [^{3}H]2,4-D (20 Ci $mmol^{-1}$; American Radiolabeled Chemicals, Inc., St Louis, MO, USA) in response to particular concentrations of 1-NOA or 2-NOA was determined after 20 min uptake period.

Results

Phenotypic changes in tobacco BY-2 cells after treatments with various auxin transport inhibitors

To evaluate possible differential effects of auxin influx and efflux inhibitors on the overall course of the BY-2 cell line subculture interval, the culture media were supplemented with 10 μM concentrations of 1-NOA, 2-NOA, CHPAA, or NPA. Treatments with 1-NOA resulted in phenotypic changes different from those caused by 2-NOA or CHPAA. Thus, in the presence of 1-NOA the cells divided less frequently than controls, contained amyloplasts with starch, and cell elongation was significantly enhanced (Fig. 1A, B, F), in contrast to 2-NOA or CHPAA which even stimulated cell division slightly (Fig. 1C, D, G). Treatments with NPA under the same conditions had no significant effect on cell phenotype or cell division (Fig. 1E, G).

Altogether, the action of 1-NOA, a putative inhibitor of auxin influx, resulted in a distinct phenotype in comparison with the phenotype caused by 2-NOA, CHPAA, which likewise block mainly auxin influx, and NPA, which blocks mainly auxin efflux.

Auxin influx inhibitors 1-NOA, 2-NOA, and CHPAA have distinct impact on the accumulation of different types of auxin

The accumulation kinetics of radioactively labelled NAA and 2,4-D has been shown to reflect the activity of auxin efflux and influx carriers, respectively, and therefore both these synthetic auxins can be used as markers for measuring the activity of these carriers, namely in tobacco cells (Delbarre *et al.*, 1996; Petrášek and Zažímalová, 2006). The effects of the synthetic inhibitors of auxin influx on the accumulation of 2,4-D and NAA using 2-d-old tobacco BY-2 cells were investigated (Fig. 2A, B). At 10 μM concentration, 1-NOA, 2-NOA, and CHPAA all reduced the accumulation of [^{3}H]2,4-D, CHPAA being the most effective. The amount of [^{3}H]2,4-D that accumulated after 20 min in the presence of CHPAA was reduced by 3.5-times relative to the controls, by 2.5-times in the presence of 2-NOA, and by 1.4-times in the presence of 1-NOA (Fig. 2A). A comparison of the concentration dependence of the positional analogues 1-NOA and 2-NOA revealed that 1-NOA reduced the accumulation of [^{3}H]-2,4-D with a 10-times lower efficiency than 2-NOA (Fig. 2C).

Surprisingly, after the application of 1-NOA the accumulation of [^{3}H]NAA significantly increased, whereas application of 2-NOA or CHPAA raised the accumulation of this labelled auxin only slightly (Fig. 2A, B). Since NAA is taken

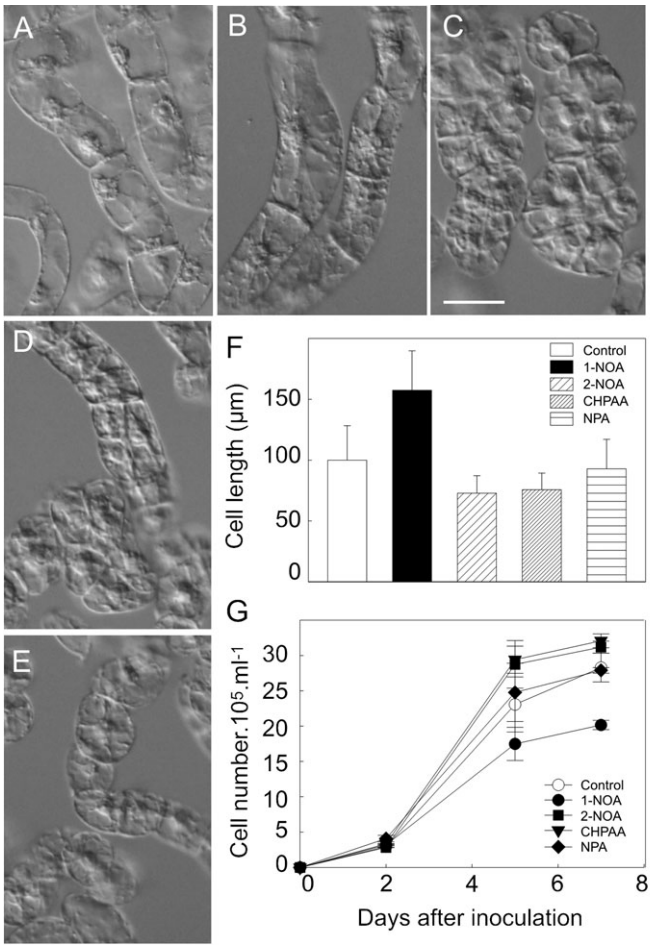

Fig. 1. Effects of auxin influx and efflux inhibitors on cell division activity and phenotype of tobacco BY-2 cells. The cells were grown (A) in a standard medium for 2 d, in the presence of auxin influx inhibitors (B) 1-NOA, (C) 2-NOA, (D) CHPAA, or (E) auxin efflux inhibitor NPA (10 μM each). Measurements of cell length (F) and cell density (G) showed that cells treated with 1-NOA were more elongated (F) and that cell division was reduced in contrast to cells treated with 2-NOA or CHPAA (G). Values in (F) and (G) represent means ±SE (n=10). (A–E) Scale bar, 50 μm.

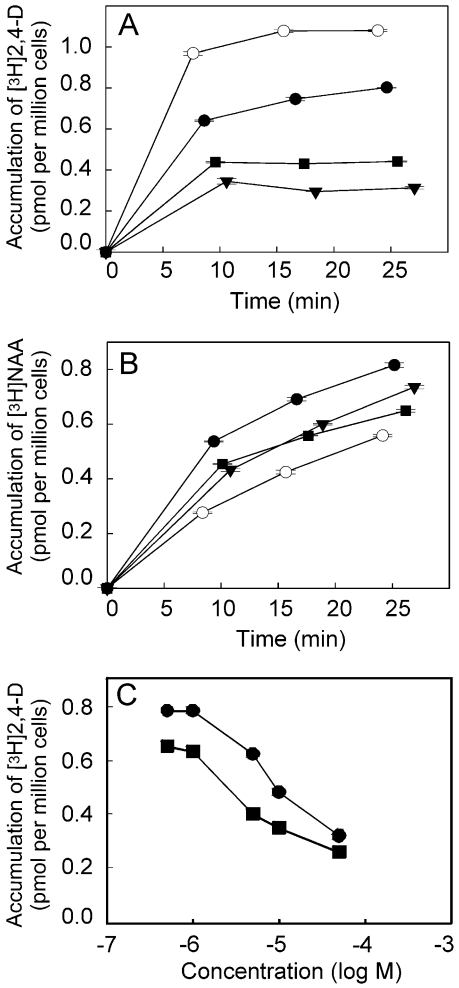

Fig. 2. The effect of the putative auxin influx inhibitors on intracellular accumulation of [^{3}H]2,4-D and [^{3}H]NAA in tobacco BY-2 cells. The kinetics of accumulation of 2 nM [^{3}H]2,4-D (A) and [^{3}H]NAA (B) in the presence of 10 μM 1-NOA (filled circles), 2-NOA (filled squares) or CHPAA (filled inverted triangles). Note the difference between the efficiency of 2-NOA, CHPAA, and 1-NOA in the inhibition of auxin influx as shown by reduced accumulation of [^{3}H]2,4-D (A) compared with control cells. Increased accumulation of [^{3}H]NAA (reflecting preferentially the activity of auxin efflux carriers) in the presence of 1-NOA is significantly higher than that in the presence of 2-NOA and CHPAA (10 μM each). (C) Concentration dependence of [^{3}H]2,4-D (2 nM) in response to specified concentrations of 1-NOA (filled circles) or 2-NOA (filled squares) was determined after 20 min uptake period. Accumulation of [^{3}H]2,4-D is suppressed more effectively with 2-NOA compared with 1-NOA. Error bars represent SE (n=4).

up only passively (and is a good substrate for the active auxin efflux) in tobacco cells, these results suggest that 1-NOA markedly inhibits the auxin efflux carrier(s) activity.

Taken together, the putative auxin influx inhibitor 1-NOA is much less effective in blocking the active auxin influx compared with 2-NOA or CHPAA and it also modifies the activity of auxin efflux carriers.

Effect of NPA on [^{3}H]NAA accumulation in tobacco BY-2 cells treated with 1-NOA or 2-NOA

To check whether 1-NOA or 2-NOA are able to inhibit auxin efflux activity, accumulation assays were performed with BY-2 cells using [^{3}H]NAA in the presence of 1-NOA (10 μM) or 2-NOA (10 μM). The established auxin efflux inhibitor NPA was applied at 10 μM concentration (Petrášek *et al.*, 2003, 2006) in-flight 10 min after the addition of [^{3}H]NAA together with 1-NOA or 2-NOA. In the presence of 1-NOA the NPA had almost no effect on the accumulation of [^{3}H]NAA (Fig. 3A), indicating that auxin efflux carriers were already blocked by the preceding application of 1-NOA. By contrast, in the presence of 2-NOA, the in-flight addition of NPA during the accumulation of [^{3}H]NAA caused elevation of auxin accumulation in the cells (Fig. 3B), suggesting that auxin efflux carriers were still active before the NPA treatment.

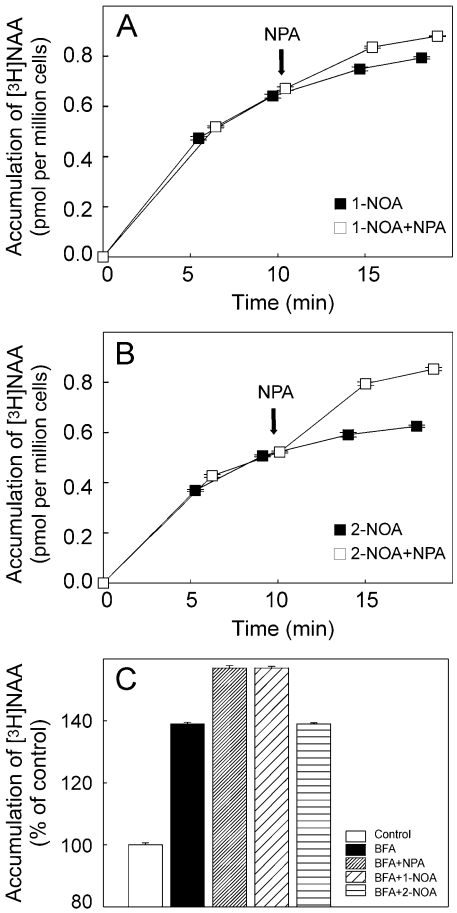

Fig. 3. The effect of NPA on the intracellular accumulation of [^{3}H]NAA in tobacco BY-2 cells treated with 1-NOA or 2-NOA. In-flight application of NPA (10 μM) to cells treated with 1-NOA (10 μM) (A) had very low impact on the accumulation of [^{3}H]NAA (2 nM). In-flight application of NPA to cells treated with 2-NOA (10 μM) (B) increased auxin accumulation, suggesting that auxin efflux carriers were still active before NPA treatment (note also the higher absolute values of auxin accumulation in the case of 1-NOA in contrast to 2-NOA even before NPA treatment). Error bars represent SE (n=4). (C) Effects of the auxin influx and efflux inhibitors 1-NOA, 2-NOA, and NPA on intracellular accumulation of [^{3}H]NAA in cells treated with the inhibitor of vesicle trafficking BFA. 2-NOA did not change the accumulation of [^{3}H]NAA in cells treated with BFA, while both NPA and 1-NOA increased it. Values are percentages of control at 20 min after application of [^{3}H]NAA and inhibitors. Error bars represent SE (n=4).

These results, therefore, indicate that 1-NOA, in contrast to 2-NOA, is effective in blocking auxin efflux in a way similar to NPA.

1-NOA, but not 2-NOA, increases the accumulation of [^{3}H]NAA in tobacco BY-2 cells treated with BFA

BFA, an inhibitor of Golgi-mediated vesicle trafficking, has been shown to reduce the plasma membrane pool of PIN auxin efflux carriers within 30 min (Geldner *et al.*, 2001). To obtain further insight into the mode of action of 1-NOA, the effect of 1-NOA, 2-NOA, and NPA on the accumulation of [^{3}H]NAA was investigated in BY-2 cells treated with BFA. The inhibitors were added to the cells after pre-treatment with 10 μM BFA. Similarly to the previous experiments with in-flight additions of NPA, both 1-NOA and NPA increased the accumulation of [^{3}H]NAA in cells pretreated with BFA; in contrast, 2-NOA had no additional effect (Fig. 3C).

These results provide further evidence for the role of the putative auxin influx inhibitor 1-NOA in modulating the auxin efflux carrier(s) activity. Moreover, they indicate that this inhibition is independent of anterograde membrane trafficking, suggesting either a direct influence on efflux carrier activity and/or their enhanced endocytosis.

NOAs affect subcellular distribution of AUX1, PIN1, and ABCB4

To determine whether the putative auxin influx inhibitors can influence the distribution of AUX1 or PIN1 proteins, *XVE::EYFP:AUX1* or *XVE::PIN1:GFP* constructs were expressed in tobacco BY-2 cells. After 24 h induction with β-estradiol (1 μM), the plasma membrane fluorescence of PIN1:GFP or EYFP:AUX1 fusion proteins was observed and no vesicles in the cortical cytoplasm were seen (Fig. 4A, E). After a subsequent 3 h in the presence of 20 μM 1-NOA, both PIN1:GFP (Fig. 4B) and EYFP:AUX1 (Fig. 4F) were observed in vesicles reminiscent of endosomes and located in the cortical cytoplasm. Similar treatment with 2-NOA induced these patches as well, but the effect was weaker (Fig. 4C, G). A 3 h exposure to 20 μM CHPAA did not induce any redistribution (Fig. 4D, H), although patches were occasionally observed in a few cells (data not shown). NOA-induced vesicles of EYFP:AUX1 and PIN1:GFP did not show any movement, and partially colocalized with the membrane-selective endocytic tracer FM 4-64 as shown for EYFP:AUX1 in Supplementary Fig. S1 at *JXB* online. Furthermore, the localization of another plasma membrane auxin transporter ABCB4, reported to be more stable in the plasma membrane (Titapiwatanakun and Murphy, 2009), after NOA treatment was different. ABCB4 proteins (PGP4:GFP) appeared only after 24 h in a form of few membrane aggregates (Fig. 4I–L).

These results show that both NOAs (1-NOA being more effective) can induce the formation of endosomes containing auxin carriers. At least partly this may be the reason for the decrease in auxin influx or efflux after the 1-NOA or 2-NOA treatments.

Long-term treatment with NOAs affect processes of membrane trafficking, leading to disruption of the polarity of cell division

To address the consequences of the effects of NOA, BY-2 cells transformed with *XVE::EYFP:AUX1* or *XVE::PIN1:GFP* constructs were incubated for 24 h with 1-NOA, 2-NOA, or CHPAA at 20 μM concentration, two times higher than that used for the cell phenotypic study. The most remarkable effect was disruption of cell plate formation (Fig. 5; see Supplementary Fig. S2 at *JXB* online). The

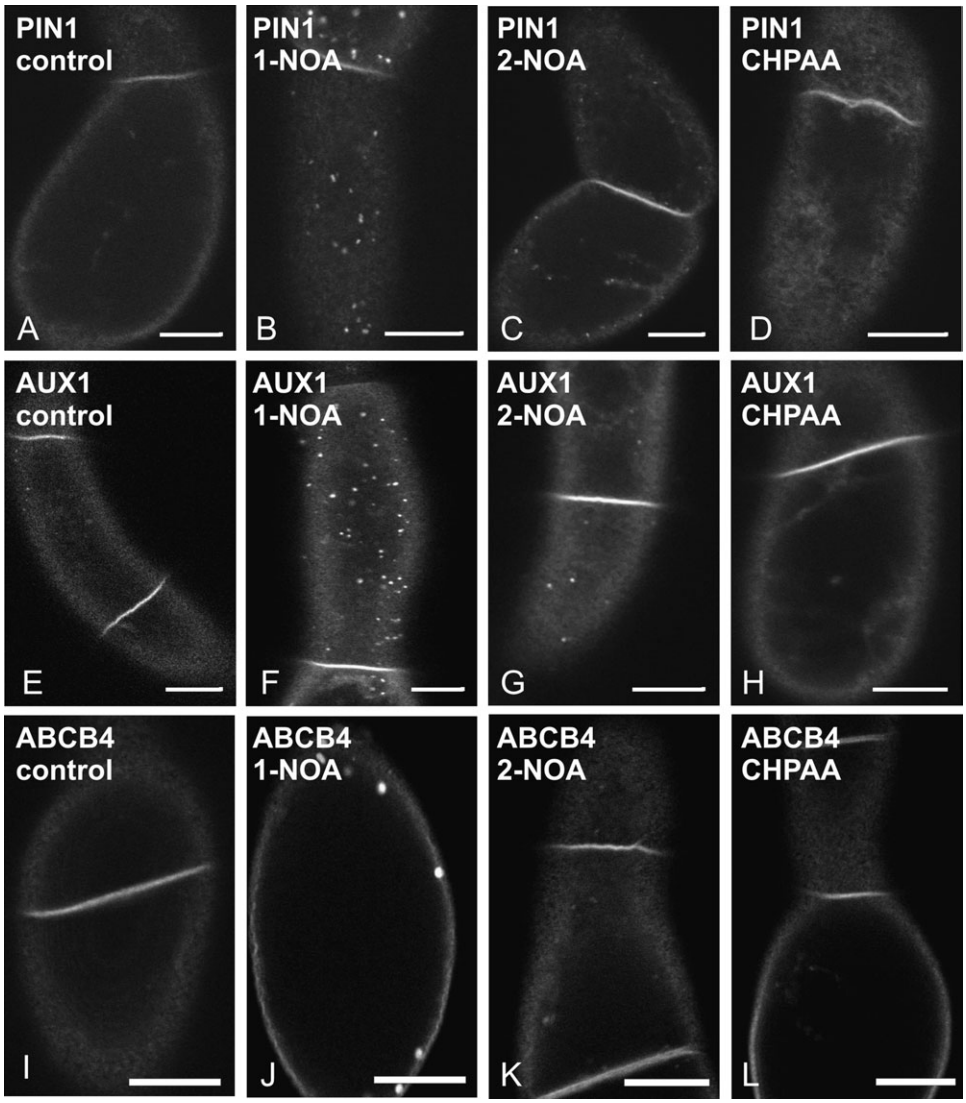

Fig. 4. The effects of the putative auxin influx inhibitors on subcellular distribution of PIN1:GFP, EYFP:AUX1, and ABCB4:GFP fusion proteins in tobacco BY-2 cells. (A, E, I) non-treated controls. The effects of 1-NOA (20 μM, 3 h) (B), 2-NOA (20 μM, 3 h) (C), and CHPAA (20 μM, 3 h) (D) on the subcellular distribution of PIN1:GFP. The effects of 1-NOA (20 μM, 3 h) (F), 2-NOA (20 μM, 3 h) (G), and CHPAA (20 μM, 3 h) (H) on the subcellular distribution of EYFP:AUX1. The effects of 1-NOA (20 μM, 24 h) (J), 2-NOA (20 μM, 24 h) (K), and CHPAA (20 μM, 24 h) (L) on the subcellular distribution of ABCB4:GFP. Single confocal sections through the cortical cytoplasm (C, Apochromat ×40 1.2 W water immersion objective with a 1 Airy Unit pinhole). Scale bars, 10 μm.

cell plate did not expand in the normal centrifugal manner, but often had a problem with the correct anchorage in the parental plasma membrane, leading to apolar cell division (Fig. 5B, C for AUX1 and F, G for PIN1) or even incomplete cell plates. Treatments with CHPAA did not affect the polarity of cell division at all (Fig. 5D, H). Interestingly, when the concentration of the inhibitors was further increased to 50 μM, the changes in the dynamics of the membrane appeared to be too extensive and after 48 h in 1-NOA and 2-NOA the overall fluorescence of EYFP:AUX1 and PIN1:GFP decreased substantially (see Supplementary Fig. S3B, C, F, G at *JXB* online). These cells were not dividing (data not shown). In contrast to 1-NOA or 2-NOA, a 48 h exposure to 50 μM CHPAA had only a weak effect on the AUX1 or PIN1 signals (see Supplementary Fig. S3D, H at *JXB* online).

These experiments indicate that treatments with increased concentrations of 1-NOA and 2-NOA completely block the dynamics of membranes, with subsequent detrimental effects on cell division. By contrast, similar treatments with CHPAA had no such dramatic effects, suggesting either shifted efficiency of this inhibitor or different mode of its action.

Discussion

Previously, Delbarre *et al.* (1996) described the specificity of cellular auxin uptake and efflux towards the auxins IAA, NAA, and 2,4-D using suspension-cultured cells of tobacco cv. Xanthi XHFD8. Using the same system to screen for compounds structurally similar to IAA and competing for the auxin influx carrier, 1-NOA and CHPAA were

characterized as inhibitors of active auxin influx (Imhoff *et al.*, 2000). It was further shown that 2-NAA inhibits auxin influx carriers, but that it might also affect the auxin efflux activity (Delbarre *et al.*, 1996; Imhoff *et al.*, 2000). Frequent use of these compounds for physiological and developmental studies postulated the need to understand modes of action of particular auxin transport inhibitors. Our study was aimed at the mode of action of inhibitors of carrier-mediated auxin influx using the well-established model for the auxin transport studies on cellular level, tobacco BY-2 cells (Petrášek *et al.*, 2006).

The effect of all three inhibitors, similarly to Xanthi tobacco cells (Imhoff *et al.*, 2000), reduced the activity of auxin influx carriers in the tobacco BY-2 cells. This was demonstrated firstly by decreased accumulation of [^{3}H]2,4-D, which is a preferential substrate for auxin influx carriers in tobacco cells. However, in contrast to 2-NOA and CHPAA, it was found that 1-NOA was less effective in reducing [^{3}H]2,4-D accumulation. Secondly, significant differences were also found in the effects of 1-NOA, 2-NOA, and CHPAA on the accumulation of [^{3}H]NAA, a preferential substrate for active auxin efflux which is, however, taken up into cells only passively (Delbarre *et al.*,1996; Petrášek *et al.*, 2003). As expected, neither 2-NOA nor CHPAA had any significant effect on the accumulation of this auxin in BY-2 cells in contrast to the application of 1-NOA, which significantly increased its accumulation. This unexpected finding suggests that 1-NOA also influences auxin efflux. Thirdly, the contrasting effects of 1-NOA compared with 2-NOA or CHPAA also appeared in the accumulation of [^{3}H]IAA (data not shown), which as a natural auxin is a good substrate for both auxin influx and efflux carriers. In this case 1-NOA had only a relatively minor impact on the accumulation of [^{3}H]IAA, again suggesting its action on both auxin influx and efflux carriers. The fourth piece of evidence for the action of 1-NOA on auxin efflux came from our experiments with NPA, an established inhibitor of auxin efflux. NPA was able to increase accumulation of [^{3}H]NAA in the presence of 2-NOA. Conversely, in the presence of 1-NOA the accumulation of [^{3}H]NAA did not change significantly after in-flight application of NPA. In this case, the auxin efflux carriers may have already been blocked by 1-NOA before the application of NPA, again supporting the idea that 1-NOA has a significant impact on the auxin efflux activity.

Collectively, these four pieces of evidence point to the conclusion that 1-NOA, in contrast to 2-NOA and CHPAA, also influences auxin efflux (besides the auxin influx). Interestingly, there are differences in the molecular structure of 1-NOA and the other two inhibitors (Fig. 6).

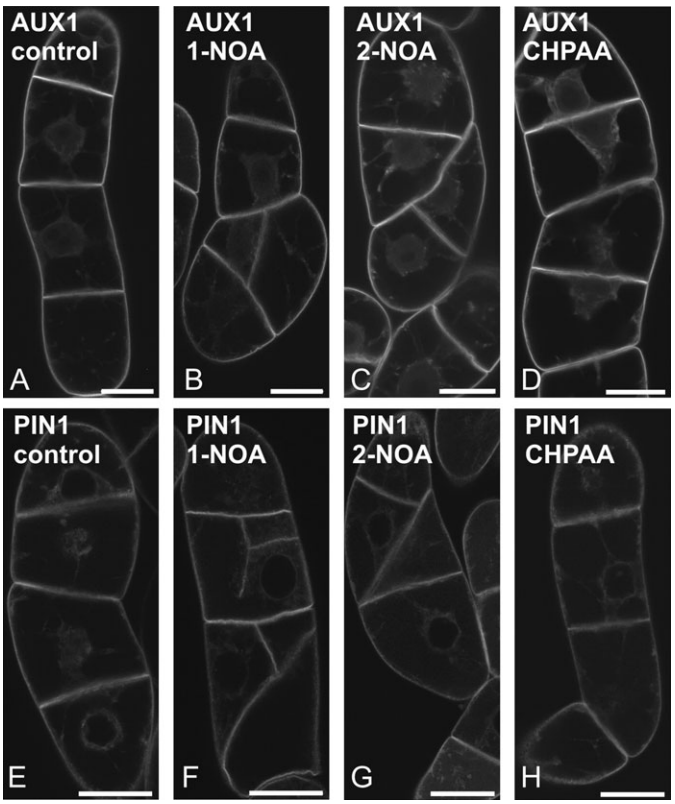

Fig. 5. Long-term treatments of EYFP:AUX1 or PIN1:GFP tobacco BY-2 cells with the putative auxin influx inhibitors. (A, E) non-treated controls. The effects of 1-NOA (20 μM, 24 h) (B), 2-NOA (20 μM, 24 h) (C), and CHPAA (20 μM, 24 h) (D) on cell division in BY-2 cells transformed with the *EYFP:AUX1* construct. The effects of 1-NOA (20 μM, 24 h) (F), 2-NOA (20 μM, 24 h) (G), and CHPAA (20 μM, 24 h) (H) on cell division in BY-2 cells transformed with the *PIN1:GFP* construct. Single confocal sections through the perinuclear region (C, Apochromat ×40 /1.2 W water immersion objective with a 1 Airy Unit pinhole). Scale bars, 20 μm.

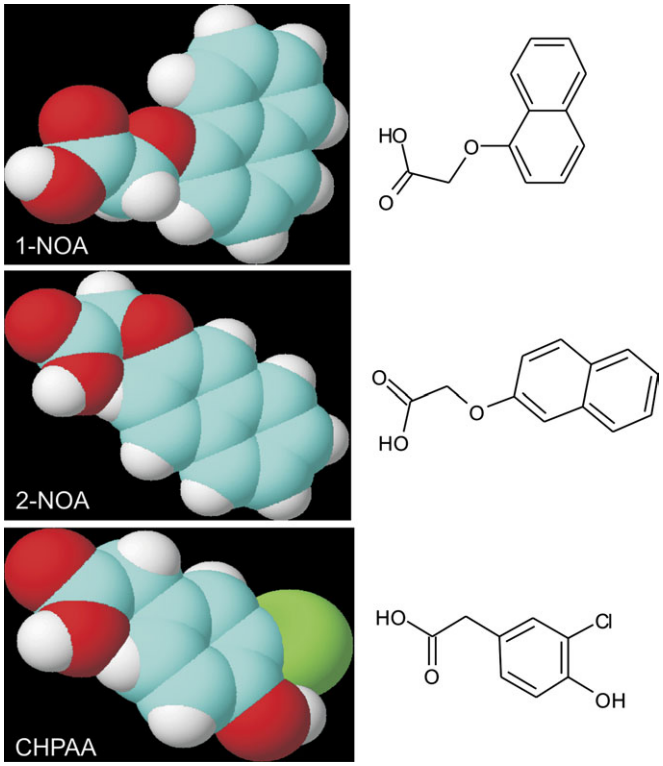

Fig. 6. Molecular structure of synthetic auxin influx inhibitors 1-NOA, 2-NOA, and CHPAA. Blue, carbon; red, oxygen; white, hydrogen; green, chlorine.

All three molecules share typical features of auxin influx inhibitors. However, in contrast to 2-NOA and CHPAA, the shape of the 1-NOA molecule is not linear because of the position of the side-chain in relation to the fused aromatics rings. It is speculated that this unique structural feature of the 1-NOA molecule may be responsible for the observed physiological effects, suggesting a distinct interaction with the plasma membrane or other membranes.

To elucidate the mechanism of how 1-NOA may affect the activity of auxin efflux carriers, experiments were performed with BFA. Generally, BFA application leads to inhibition of anterograde protein trafficking so that the plasma membrane pool of auxin efflux carriers of the PIN family (and some other proteins) is reduced (Geldner *et al.*, 2001). Major auxin influx carriers of the AUX1/LAX family were shown to be much less sensitive or almost insensitive to BFA (Kleine-Vehn *et al.*, 2006). In BFA-treated BY-2 cells, 2-NOA had no effect on NAA accumulation, whereas both 1-NOA and NPA increased auxin accumulation. It seems that 1-NOA and NPA act independently of BFA-dependent vesicle trafficking processes and so their effect(s) are additive to the effect of BFA alone. It could be concluded that 1-NOA either directly affects the auxin efflux carrier activity and/or somehow stimulates endocytosis; this would result in the depletion of the carriers from the plasma membrane and, consequently, in the reduction of auxin efflux. To test this hypothesis, it was necessary to follow the dynamics of membrane vesicles containing either the auxin influx carrier (AUX1) or the auxin efflux carrier (PIN1) directly.

Advantage was taken of the system of β-estradiol-inducible expression of fluorescently tagged fusion proteins in tobacco BY-2 cells. Upon induction of gene expression in control cells, the EYFP:AUX1 and PIN1:GFP signals were localized at the plasma membrane. No changes have been observed after 30 min treatment with inhibitors (see Supplementary Fig. S4 at *JXB* online). Surprisingly, after 3 h and more with 1-NOA both PIN1 and AUX1 were gradually redistributed into vesicles in the cortical cytoplasm, whereas 2-NOA was much less effective and CHPAA almost ineffective. However, more patches were observed after increasing the concentration of 2-NOA, but the effect was not very homogenous. In the population, there were always cells with stronger and weaker response. In contrast, increasing concentrations of CHPAA did not increase the number of patches formed (data not shown) pointing to the fact that CHPAA is probably the most reliable auxin inhibitor already acting at low concentrations and having the effect on the auxin influx carrier as depicted in the scheme (see Supplementary Fig. S5 at *JXB* online).

The colocalization of EYFP:AUX1 with the endocytic tracer FM 4-64 confirmed that the observed vesicles are at least partly of plasma membrane origin. Although the subcellular trafficking of AUX1 and PIN1 follows distinct pathways (Kleine-Vehn *et al.*, 2006), 1-NOA could affect the subcellular distribution of both carriers by acting upstream of these pathways, probably by changing the composition of plasma membrane. It has been suggested that 1-NOA could influence sterol composition of the membrane, which could lead to aberrant AUX1 targeting and influence the polar localization of PIN1 in *Arabidopsis* roots (Kleine-Vehn *et al.*, 2006). It was also shown that 1-NOA was effective in reducing the responses to 2,4-D in wild-type *Arabidopsis* but had no effect in *hyd1* and *hyd2/fk* mutants, which are defective in genes encoding Δ8-Δ7 sterol isomerase and sterol C14 reductase, respectively (Souter *et al.*, 2002). Thus, there may be a link between potential effects of 1-NOA on sterol composition in the plasma membrane and consequent defects in AUX1 targeting that lead to aggregation of AUX1 (Kleine-Vehn *et al.*, 2006).

The fact that NOA was not able to induce fast re-distribution of ABCB4 (as observed for AUX1 and PIN1) and that this ABCB4 appeared in membrane aggregates after longer treatment suggests a membrane composition-dependent NOA effect. The most important in this respect seems to be sterol composition, namely the presence of sterols and sterol-associated proteins (Borner *et al.*, 2005); since ABCB4 was reported to be present in these compartments (Titapiwatanakun and Murphy, 2009), thus the ABCB4 could be more resistant to 1-NOA treatment.

The changes in the polarity of cell division, visible after long-term treatment with NOAs, point also to the general effect of both 1-NOA and 2-NOA on the plasma membrane dynamics. As shown by Dhonukshe *et al.* (2006) the cell plate is mainly derived from the cell surface material (cell wall components and plasma membrane proteins); therefore, disruption of cell plate formation seems to be caused by defects in the plasma membrane. Moreover, the effect of NOAs on the polarity of cell plate formation and cell polarity establishment point to the possible involvement of actin filament dynamics that has been reported to reflect the changed levels of auxin (Maisch and Nick, 2007; Nick *et al.*, 2009).

In contrast to our results, Kleine-Vehn *et al.* (2006) did not observe any effects of high concentration of 1-NOA on the trafficking of PIN1 and AUX1 in *Arabidopsis* roots. It is speculated that, in contrast to the complex tissue of the root, the effect in single tobacco BY-2 cells may be more robust and readily visible, and thus redistribution of the carrier was observed even with a much lower concentration of the inhibitor.

Increased concentrations of 1-NOA and 2-NOA completely blocked the dynamics of membranes, with subsequent detrimental effects on cell division. In contrast, no such dramatic effects were seen following treatment with CHPAA, which therefore appears to be the most reliable auxin influx inhibitor that already acts at low concentrations and has no obvious influence on membrane dynamics.

Nevertheless, the possibility that higher concentrations of the inhibitors tested could affect vesicles that are transported towards the plasma membrane by a mechanism dependent on actin dynamics (Dhonukshe *et al.*, 2008) cannot be excluded.

The analysis of the phenotype and growth of the tobacco BY-2 cells revealed distinct effects of 1-NOA compared with 2-NOA and CHPAA. The action of 1-NOA resulted in

decreased cell division activity and in increased cell elongation. These defects could also possibly be attributed to a decreased dynamics of the plasma membrane and an observed 'auxin starvation' phenotype might be of secondary character. Interestingly, auxin influx inhibitors 2-NOA and CHPAA decreased the accumulation of [^{3}H]2,4-D (see Fig. 2), a good substrate for auxin influx carriers and their application even slightly stimulated cell division. This is consistent with the finding that their action might stimulate the synthesis of endogenous auxin, as reported after auxin deprivation in another tobacco cell line VBI-0 (Zažímalová *et al.*, 1995). Although 10 μM NPA had no significant effect in the experiments performed under conditions used in this study, at higher concentrations it may produce defects in the polarity of cell division in tobacco BY-2 cells as well as in another auxin-dependent tobacco cell line VBI-0 (Dhonukshe *et al.*, 2005; Petrášek *et al.*, 2002; respectively).

The effects of auxin transport inhibitors are summarized in the scheme shown in Supplementary Fig. S5 at *JXB* online. It also highlights the importance of the rate of the particular vesicle trafficking process that may determine the extent of the action of 1-NOA, 2-NOA, and CHPAA on the membrane dynamics. The potential importance of the distinct sensitivity of the membrane domains containing particular transport proteins to the action of inhibitors cannot be excluded. Generally, our results point to the so far unknown effect on vesicle trafficking of the putative auxin influx inhibitors.

Acknowledgements

The authors thank Professor Cris Kuhlemeier (University od Bern) for support and Dr Jan Marc (University of Sydney) for critical reading of the manuscript. We also thank Markéta Pařezová for transformation of BY-2 cell cultures. The work was supported by the Grant Agency of the Czech Republic, project KJB600380702, by the Ministry of Education, Youth and Sports of the Czech Republic, project LC06034 and by the European Fund for Regional Development, the Operational Programme Prague – Competitiveness, project no.: CZ.2.16/3.1.00/21159.

References

An G. 1985. High efficiency transformation of cultured tobacco cells. *Plant Physiology* **79,** 568–570.

Bainbridge K, Guyomarc'h S, Bayer E, Swarup R, Bennett M, Mandel T, Kuhlemeier C. 2008. Auxin influx carriers stabilize phyllotactic patterning. *Genes and Development* **22,** 810–823.

Benková E, Michniewicz M, Sauer M, Teichmann T, Seifertová D, Jürgens G, Friml J. 2003. Local, efflux-dependent auxin gradients as a common module for plant organ formation. *Cell* **115,** 591–602.

Bennett MJ, Marchant A, Green HG, May ST, Ward SP, Millner PA, Walker AR, Schulz B, Feldmann KA. 1996. Arabidopsis *AUX1* gene: a permease-like regulator of root gravitropism. *Science* **273,** 948–950.

Blilou I, Xu J, Wildwater M, Willemsen V, Paponov I, Friml J, Heidstra R, Aida M, Palme K, Scheres B. 2005. The PIN auxin efflux facilitator network controls growth and patterning in Arabidopsis roots. *Nature* **433,** 39–44.

Borner GHH, Sherrier DJ, Weimar T, Michaelson LV, Hawkins ND, MacAskill A, Napier JA, Beale MH, Lilley KS, Dupree P. 2005. Analysis of detergent-resistant membranes in Arabidopsis. Evidence for plasma membrane lipid rafts. *Plant Physiology* **137,** 104–116.

Curtis MD, Grossniklaus U. 2003. A gateway cloning vector set for high-throughput functional analysis of genes *in planta*. *Plant Physiology* **133,** 462–469.

Delbarre A, Müller P, Imhoff V, Guern J. 1996. Comparison of mechanisms controlling uptake and accumulation of 2,4-dichlorophenoxy acetic acid, naphthalene-1-acetic acid, and indole-3-acetic acid in suspension-cultured tobacco cells. *Planta* **198,** 532–541.

Dhonukshe P, Baluška F, Schlicht M, Hlavacka A, Šamaj J, Friml J, Gadella T. 2006. Endocytosis of cell surface material mediates cell plate formation during plant cytokinesis. *Developmental Cell* **10,** 137–150.

Dhonukshe P, Grigoriev I, Fischer R, *et al*. 2008. Auxin transport inhibitors impair vesicle motility and actin cytoskeleton dynamics in diverse eukaryotes. *Proceedings of the National Academy of Sciences, USA* **105,** 4489–4494.

Dhonukshe P, Mathur J, Hülskamp M, Gadella TW. 2005. Microtubule plus-ends reveal essential links between intracellular polarization and localized modulation of endocytosis during division-plane establishment in plant cells. *BMC Biology* **3,** 11.

Edgerton MD, Tropsha A, Jones AM. 1994. Modelling the auxin-binding site of auxin-binding protein 1 of maize. *Phytochemistry* **35,** 1111–1123.

Friml J, Benkova E, Blilou I, *et al*. 2002*b*. AtPIN4 mediates sink-driven auxin gradients and root patterning in *Arabidopsis*. *Cell* **108,** 661–673.

Friml J, Wisniewska J, Benková E, Mendgen K, Palme K. 2002*a*. Lateral relocation of auxin efflux regulator PIN3 mediates tropism in *Arabidopsis*. *Nature* **415,** 806–809.

Friml J. 2003. Auxin transport: shaping the plant. *Current Opinion in Plant Biology* **6,** 7–12.

Geldner N, Friml J, Stierhof YD, Jürgens G, Palme K. 2001. Auxin transport inhibitors block PIN1 cycling and vesicle trafficking. *Nature* **413,** 425–428.

Imhoff V, Muller P, Guern J, Delbarre A. 2000. Inhibitors of the carrier-mediated influx of auxin in suspension-cultured tobacco cells. *Planta* **210,** 580–588.

Jelínková A, Malínská K, Simon S, *et al*. 2010. Probing plant membranes with FM dyes: tracking, dragging or blocking? *The Plant Journal* **61,** 883–892.

Jones AR, Kramer EM, Knox K, Swarup R, Bennett MJ, Lazarus CM, Leyser HMO, Grierson CS. 2009. Auxin transport through non-hair cells sustains root-hair development. *Nature Cell Biology* **11,** 78–84.

Kleine-Vehn J, Dhonukshe P, Swarup R, Bennett M, Friml J. 2006. Subcellular trafficking of the *Arabidopsis* auxin influx carrier AUX1 uses a novel pathway distinct from PIN1. *The Plant Cell* **18,** 3171–3181.

Lomax TL, Muday GK, Rubery PH. 1995. Auxin transport. In: Davies PJ, ed. *Plant hormones: physiology, biochemistry and molecular biology*. Dordrecht, Netherlands: Kluwer, 509–530.

Maisch J, Nick P. 2007. Actin is involved in auxin-dependent patterning. *Plant Physiology* **143,** 1695–1704.

Marchant A, Bhalerao R, Casimiro I, Eklöf J, Casero PJ, Bennett M, Sandberg G. 2002. AUX1 promotes lateral root formation by facilitating indole-3-acetic acid distribution between sink and source tissues in the Arabidopsis seedling. *The Plant Cell* **14,** 589–597.

Morris DA, Robinson JS. 1998. Targeting of auxin carriers to the plasma membrane: differential effects of brefeldin A on the traffic of auxin uptake and efflux carriers. *Planta* **205,** 606–612.

Morris DA, Friml J, Zažímalová E. 2004. The transport of auxins. In: Davies PJ, ed. *Plant hormones: biosynthesis, signal transduction, action!* Dordrecht, Boston, London: Kluwer Academic Publishers, 437–470.

Nagata T, Nemoto Y, Hasezava S. 1992. Tobacco BY-2 cell line as the 'Hela' cell in the cell biology of higher plants. *International Review of Cytology* **132,** 1–30.

Nick P, Han M, An G. 2009. Auxin stimulates its own transport by shaping actin filaments. *Plant Physiology* **151,** 155–167.

Noh B, Murphy AS, Spalding EP. 2001. Multidrug resistance-like genes of Arabidopsis required for auxin transport and auxin-mediated development. *The Plant Cell* **13,** 2441–2454.

Parry G, Delbarre A, Marchant A, Swarup R, Napier R, Perrot-Rechenmann C, Bennett MJ. 2001. Novel auxin transport inhibitors phenocopy the auxin influx carrier mutation *aux1*. *The Plant Journal* **25,** 399–406.

Pernisová M, Klíma P, Horák J, *et al*. 2009. Cytokinins modulate auxin-induced organogenesis in plants via regulation of the auxin efflux. *Proceedings of the National Academy of Sciences, USA* **106,** 3609–3614.

Petrášek J, Elčkner M, Morris DA, Zažímalová E. 2002. Auxin efflux carrier activity and auxin accumulation regulate cell division and polarity in tobacco cells. *Planta* **216,** 302–308.

Petrášek J, Černá A, Schwarzerová K, Elčkner M, Morris DA, Zažímalová E. 2003. Do phytotropins inhibit auxin efflux by impairing vesicle traffic? *Plant Physiology* **131,** 254–263.

Petrášek J, Mravec J, Bouchard R, *et al*. 2006. PIN proteins perform a rate-limiting function in cellular auxin efflux. *Science* **312,** 914–918.

Petrášek J, Zažímalová E. 2006. The BY-2 cell line as a tool to study auxin transport. In: Nagata T, Matsuoka K, Inzé D, eds. *Biotechnology in agriculture and forestry* **58**, *Tobacco BY-2 cells: from cellular dynamics to omics*. Berlin Heidelberg: Springer-Verlag, 107–117.

Rahman A, Ahamed A, Amakawa T, Goto N, Tsurumi S. 2001. Chromosaponin I specifically interacts with AUX1 protein in regulating the gravitropic response of arabidopsis roots. *Plant Physiology* **125,** 990–1000.

Rubery PH. 1990. Phytotropins: receptors and endogenous ligands. *Symposia of the Society for Experimental Biology* **44,** 119–146.

Smith RS, Guyomarc'h S, Mandel T, Reinhardt D, Kuhlemeier C, Prusinkiewicz P. 2006. A plausible model for phyllotaxis. *Proceedings of the National Academy of Sciences, USA* **103,** 1301–1306.

Souter M, Topping J, Pullen M, Friml J, Palme K, Hackett R, Grierson D, Lindsey K. 2002. *hydra* mutants of *Arabidopsis* are defective in sterol profiles and auxin and ethylene signaling. *The Plant Cell* **14,** 1017–1031.

Swarup R, Friml J, Marchant A, Ljung K, Sandberg G, Palme G, Bennett MJ. 2001. Localization of the auxin permease AUX1 suggests two functionally distinct hormone transport pathways operate in the *Arabidopsis* root apex. *Genes and Development* **15,** 2648–2653.

Swarup K, Benková E, Swarup R, *et al*. 2008. The auxin influx carrier LAX3 promotes lateral root emergence. *Nature Cell Biology* **10,** 946–954.

Titapiwatanakun B, Murphy AS. 2009. Post-transcriptional regulation of auxin transport proteins: cellular trafficking, protein phosphorylation, protein maturation, ubiquitination, and membrane composition. *Journal of Experimental Botany* **60,** 1093–1097.

Ugartechea-Chirino Y, Swarup R, Swarup K, Péret B, Whitworth M, Bennett M, Bougourd S. 2010. The AUX1 LAX family of auxin influx carriers is required for the establishment of embryonic root cell organization in *Arabidopsis thaliana*. *Annals of Botany* **105,** 277–289.

Vandenbussche F, Petrášek J, Žádníková P, *et al*. 2010. The auxin influx carriers AUX1 and LAX3 are involved in auxin-ethylene interactions during apical hook development in *Arabidopsis thaliana* seedlings. *Development* **137,** 597–606.

Vanneste S, Friml J. 2009. Auxin: a trigger for change in plant development. *Cell* **136,** 1005–1016.

Vieten A, Sauer M, Brewer PB, Friml J. 2007. Molecular and cellular aspects of auxin-transport-mediated development. *Trends in Plant Science* **12,** 160–168.

Wilkinson S, Morris DA. 1994. Targeting of auxin carriers to the plasma membrane: effects of monensin on transmembrane auxin transport in *Cucurbita pepo* L. tissue. *Planta* **193,** 194–202.

Yang Y, Hammes UZ, Taylor CG, Schachtman DP, Nielsen E. 2006. High-affinity auxin transport by the AUX1 influx carrier protein. *Current Biology* **16,** 1123–1127.

Zažímalová E, Opatrný Z, Březinová A, Eder J. 1995. The effect of auxin starvation on the growth of auxin-dependent tobacco cell culture: dynamics of auxin reception and endogenous free IAA content. *Journal of Experimental Botany* **46,** 1205–1213.

6.5. Chapter 5 - Arabidopsis ABCB4 is a substrate-activated homeostatic regulator of auxin levels in Arabidopsis roots

Martin Kubeš*, Haibing Yang*, Gregory L. Richter, Yan Cheng, Xia Wang, Ewa Młodzińska, Nicola Carraro, Jan Petrášek, Eva Zažímalová, Klára Hoyerová, Wendy Ann Peer, Angus S. Murphy

* These authors contributed equally to this work.

The Plant Journal, *resubmitted*

This article is based on collaboration between Dr. Eva Zažímalová and Dr. Angus S. Murphy/Wendy A. Peer laboratories. The main message of this paper is the suggestion of mechanism, where ABCB4 gradually changes its auxin uptake to auxin efflux activity with increasing auxin levels. Moreover, we confirm that 2,4-D is transported by ABCB4 not only into the cells but also partially out from the cells and non-competitively interacts with ABCB4 to block its auxin efflux activity. This inhibition might be responsible for the effectiveness of 2,4-D as a commercial herbicide.

My contribution to this article was in the transformation of BY-2 cells with ABCB4::ABCB4:GFP construct, characterization of this cell line including expression analyses (immunofluorescence localization), analysis of cell phenotype, determination of cell growth curve, accumulation assays using radiolabeled (^{3}H-2,4-D, ^{3}H-BeA, ^{3}H-IAA and ^{3}H-NAA) and cold (2,4-D, IAA, NAA) auxins, and auxin transport inhibitors (2-NOA, NPA).

Expression of ABCB4-GFP in BY-2 cells produces phenotypes consistent with auxin efflux (Fig. 4A), but no cell elongation like in ABCB19 or PIN1 cells was observed (Fig. 4B). PM localisation of ABCB4-GFP is mainly non-polar compared to PIN1-GFP (Fig. 4C). Decrease in transversal localisation may be a consequence of faster lateral diffusion or trafficking of ABCB4 compared to PIN1-GFP as indicated by FRAP analysis (Fig. 4D). ABCB4-overexpressing cells exhibit increased ^{3}H-NAA net uptake after NPA treatment (Fig. 5A), suggesting that ABCB4 has also NPA-sensitive efflux activity. Further, these cells showed only a slight decrease in net ^{3}H-BeA retention (Fig. 5B), but cold BeA did not compete with ^{3}H-NAA or ^{3}H-IAA transport (Fig. 5C). Cold oxIAA did not compete with ^{3}H-IAA in control or ABCB4-GFP cells (Fig 5E, F). 2-NOA decreased the net uptake of ^{3}H-2,4-D in control and PIN1-expressing cells, but had a lesser effect on the accumulation of 2,4-D in ABCB4-overexpressing cells (Fig. 7B). However, 2,4-D

uptake was enhanced in cells expressing ABCB4 after background auxin uptake was blocked with 2-NOA (Fig. 7C), suggesting a non-competitive interaction of 2,4-D with the ABCB4-based auxin efflux activity. This notion was further supported by the fact that pre-treatment of cells expressing ABCB4 with cold 2,4-D, but not cold IAA, resulted in an enhanced net uptake of ^{3}H-2,4-D (Fig. S5). An enhancement of auxin influx in BY-2 expressing ABCB4 was also observed following addition of NPA to 2-NOA-pretreated cells. This treatment resulted in increased 2,4-D accumulation, which is consistent with continued 2,4-D import by ABCB4 in combination with inhibition of the weak PIN and ABCB (including ABCB4) efflux activity (Fig. 7D). Hereafter, we observed gradual reversal activity of ABCB4 during ^{3}H-IAA accumulation (Fig. S6).

Our part of the work was supported by the Ministry of Education, Youth and Sports of the Czech Republic, project LC06034, and by the Grant Agency of the Czech Republic (project P305/11/0797).

Arabidopsis ABCB4 is a substrate-activated homeostatic regulator of auxin levels in Arabidopsis roots

Martin Kubeš[1†], Haibing Yang[2†], Gregory L. Richter[2], Yan Cheng[2], Xia Wang[2], Ewa Młodzińska[2], Nicola Carraro[2], Jan Petrášek[1], Eva Zažímalová[1], Klára Hoyerová[1*], Wendy Ann Peer[2*], Angus S. Murphy[2]

[1]*Institute of Experimental Botany, the Academy of Sciences of the Czech Republic, Rozvojová 263, CZ-165 02 Prague 6, Czech Republic*
[2]*Department of Horticulture, Purdue University, West Lafayette, IN 47907-2010, USA*

Authors e-mail addresses:
Martin Kubeš - kubes@ueb.cas.cz, Haibing Yang - yang37@purdue.edu, Gregory L. Richter- grichter@purdue.edu, Yan Cheng- cheng23@purdue.edu, Xia Wang - xwang@purdue.edu, Ewa Młodzińska- ewamloda@biol.uni.wroc.pl, Nicola Carraro- ncarraro@purdue.edu, Jan Petrášek – petrasek@ueb.cas.cz, Eva Zažímalová - zazimalova@ueb.cas.cz, Klára Hoyerová – hoyerova@ueb.cas.cz, Wendy A. Peer - peer@purdue.edu, Angus S. Murphy - murphy@purdue.edu
†These authors contributed equally to this work.

***Corresponding authors:** Wendy Ann Peer, Department of Horticulture, Purdue University, West Lafayette, IN 47907-2010, USA, Tel +1 765 496 7958, FAX +1 765 494 0391, email peerw@purdue.edu ; Klára Hoyerová, Institute of Experimental Botany, the Academy of Sciences of the Czech Republic, Rozvojová 263, CZ-165 02 Prague 6, Czech Republic, Tel +420 225106436, FAX +420 225106446, e-mail, hoyerova@ueb.cas.cz

Running title: ABCB4 is a substrate-activated auxin transporter

Key words: auxin, auxin transporters, ABCB4, 2,4-D, oxIAA, oxIAA-Gluc, auxin metabolites, *Arabidopsis*, *Schizosaccharomyces pombe*, BY-2 tobacco cells

Total word count: 6984

Summary: 198

Introduction: 989

Results: 3332

Discussion: 692

Experimental procedures: 1025

Acknowledgments: 85

References: 2194

Figure Legends: 748

Summary

Arabidopsis ATP-binding cassette B4 (ABCB4) is a root-localised auxin efflux transporter with reported auxin uptake activity in low auxin concentrations. Results reported here indicate that ABCB4 is a substrate-activated regulator of cellular auxin levels. ABCB4 function in shootward auxin movement from the root apex increases with auxin concentration, but is evident in regulating root hair elongation at lower concentrations. ABCB4 plasma membrane (PM) localisation at the root apex is relatively insensitive to changes in auxin concentration, but is decreased by treatment with 1-naphthylphthalamic acid (NPA). *ABCB4*$_{pro}$:ABCB4-GFP is partially internalised in all cell types by 0.05% DMSO, but not 0.1% ethanol. In trichoblasts, *ABCB4*$_{pro}$:ABCB4-GFP PM signals are reduced by >200 nM indole-3-acetic-acid (IAA) and 2,4-dichlorophenoxyacetic acid (2,4-D). In heterologous systems and *in planta*, ABCB4 transports benzoic acid with lower affinity, but not the oxidative catabolism products oxindole-3-acetic-acid and 2-oxindole-3-acetyl-β-D-glucose. ABCB4 mediates uptake, but not efflux, of the synthetic auxin 2,4-D in cells lacking AUX1 activity. Results presented here suggest that 2,4-D is a non-competitive inhibitor of ABCB4, and modelling of 2,4-D docking with ABCB4 supports the binding of 2,4-D to a unique binding site that would inhibit efflux and indicates that ABCB4 is a target of 2,4-D herbicidal activity.

Introduction

ATP-binding cassette class B (ABCB) transporters are found in all eukaryotic phyla and have diversified to mobilise a wide range of substrates. Three Arabidopsis members of the family, ABCB1, 4 and 19, transport the phytohormone auxin and function primarily in auxin export and exclusion from the plasma membrane (PM) (reviewed in Titapiwatanakun and Murphy, 2009). ABCB1 and 19 constitute an independent auxin transport system that functions primarily in the loading and maintenance of long distance rootward auxin transport streams that contribute to vegetative development and tropic responses, but not early development or organogenesis (reviewed in Zažímalová and Murphy *et al*., 2010).

ABCB4/PGP4 is a root-specific ABCB transporter that functions in shootward epidermal transport of auxin from the root apex, conditional regulation of primary and lateral root elongation, and regulation of auxin movement into root hair cells (Santelia *et al*., 2005; Terasaka *et al*., 2005; Cho *et al*., 2007; Lewis *et al*., 2007). In root hair elongation, ABCB4 appears to regulate export of auxin from trichoblasts, as *abcb4* root hairs are longer than wild-type, and overexpression of *ABCB4* under the control of a root hair-specific promoter results in shorter root hairs similar to those resulting from overexpression of PIN efflux transporters (Cho *et al*., 2007).

The increased rates of root hair elongation observed in *abcb4* are difficult to reconcile with reports of decreased rates (30-50%) of shootward auxin transport in *abcb4* roots (Terasaka *et al*., 2005; Santelia, *et al*., 2005; Lewis *et al*., 2007), as those results suggest that less auxin is available to elongating trichoblasts in *abcb4* than in wild-type. However, other evidence suggests that the *abcb4* root epidermis contains sufficient auxin to stimulate enhanced root hair elongation when ABCB4 auxin efflux activity is absent in those cells. Roots of *abcb4* exhibit a slight increase rather than the decrease in gravitropic bending rates associated with decreased shootward auxin flows (Lewis *et al*., 2007). Further, although *abcb4* root apices have higher free indole-3-acetic acid (IAA) levels than wild-type (Santelia *et al*., 2005; Terasaka *et al*., 2005), IAA levels in the *abcb4* differentiation zone and mature lower root are similar to wild-type (Terasaka *et al*., 2005; Peer and Murphy, 2007). As increases in *ABCB4* expression after auxin treatment are not evident during the timecourse of shootward auxin transport experiments in roots (Terasaka *et al*., 2005), ABCB4 appears to be regulated by post-transcriptional processes.

ABCB4 efflux activity is directly activated by auxin levels. There are several lines of evidence that support this hypothesis. 1) Free IAA levels are significantly increased in the *abcb4* root apex where auxin levels are normally the highest, while little or no difference is observed in tissues where auxin levels are normally lower (Terasaka *et al*., 2005). 2) Lateral and primary root elongation phenotypes in *abcb4* are highly dependent on growth conditions and generally

correlate with conditions that increase endogenous auxin levels (Terasaka *et al*., 2004; Santelia *et al*., 2005; Lewis *et al*., 2007). 3) Altered *DR5revpro*:GFP signals in *abcb4* are only observed in graviresponding roots where auxin levels are increased in the elongation zone (Lewis *et al*., 2007). 4) Reductions in auxin transport in *abcb4* roots reported in radioisotope tracer and ion selective electrode assays appear to increase proportionately to the amount of auxin applied (Terasaka *et al*., 2005; Santelia *et al*., 2005; Lewis *et al*., 2007; Peer and Murphy, 2007).

Experiments in heterologous systems also support direct induction of ABCB4 export by threshold concentrations of IAA. In mammalian and yeast cells, ABCB4 expression results in increased net influx of IAA at low concentrations (10-60 nM) over short periods of time, but produces net efflux when intracellular IAA levels increase (Terasaka *et al*., 2005; Yang and Murphy, 2009). Overexpression of ABCB4 in tobacco BY-2 cells was reported to enhance 1-naphthalene acetic acid (NAA) efflux (Cho *et al*., 2007). However, NAA is taken up more readily than IAA by plant cells as it bypasses carrier-mediated uptake mechanisms via passive diffusion (Petrášek *et al*., 2006), and BY-2 cells are routinely cultured in micromolar concentrations of the synthetic auxin 2,4-dichlorophenoxyacetic acid (2,4-D). As such, sub-threshold intracellular auxin levels may be difficult to achieve in this system.

ABCB4 may also transport compounds other than IAA in Arabidopsis roots. ABCB4 exhibits sequence homology with the alkaloid uptake transporter CjMDR1/ABCB1 from *Coptis japonica* (Shitan *et al*., 2003) and is associated with a clade that is phylogenetically distinct from the ABCB1 and 19 auxin transporters (Knöller *et al*., 2010). ABCB4 transport appears to be biochemically distinct from ABCB1 and 19 as well, since expression of ABCB4, but not ABCB1 or 19, in *Schizosaccharomyces pombe* resulted in benzoic acid export at levels even greater than IAA (Yang and Murphy, 2009). Further, metabolomic analyses of root exudates from *abcb4* detected decreases in a root exudate compound (M*r* 186) that does not correspond to IAA or known IAA catabolites (Badri *et al*., 2008). Other ABCBs outside the ABCB1/19 clade may also be mixed affinity transporters, as the malate/citrate transporter ABCB14 has recently been implicated in modulation of auxin transport (Kaneda *et al*., 2011).

ABCB models based on high resolution crystal structures from other species (Yang and Murphy, 2009; Dawson and Locher, 2006; Aller *et al*., 2009) predict that ABCB4 has a canonical ABCB protein organisation consisting of two transmembrane and two nucleotide-binding domains (TMDs, NBDs) in the "twisted" TMD-NBD structure associated with eukaryotic ABC exporters (Hollenstein *et al*., 2007; Kos and Ford 2009; Rees *et al*., 2009). Substrate docking simulations identified an additional high-probability TMD binding site for auxin molecules in ABCB4 that is not found in the ABCB1/19 auxin efflux transporters (Yang and Murphy, 2009). Without IAA bound to this site, the model predicted IAA transfer into the PM cytoplasmic leaflet and

subsequent anionic trapping in the cytosol, whereas IAA binding would enhance the efflux activity of the protein. In support of this mechanism, 2,4-D, which was predicted to occlude this site, was experimentally shown to non-competitively inhibit ABCB4 auxin efflux (Yang and Murphy, 2009).

Here we re-examine ABCB4-mediated auxin transport in Arabidopsis roots, BY-2 cells, and *S. pombe* and provide evidence that ABCB4 functions as a homeostatic switch on the plasma membrane for regulation of cellular auxin levels. We show that substrate regulation of ABCB4 is initially a direct effect on the protein that precedes subsequent alterations in membrane localisation. We show that ABCB4 is activated by the primary auxin catabolite oxindole-3-acetic acid (oxIAA), but does not export this compound. Finally, we confirm that ABCB4 enhances 2,4-D uptake, but not efflux, and that this activity is likely to contribute to the herbicidal effects of 2,4-D.

Results

ABCB4 expression

Primary root and root hair elongation phenotypes of *abcb4* mutants vary with growth conditions (Teresaka *et al*., 2005; Santelia *et al*., 2005; Cho *et al*., 2007). Quantitative real-time PCR (qRT-PCR) and microarray data indicate that *ABCB4* expression is regulated by light and, to a much lesser extent, sucrose (Fig. S1). Etiolated seedlings shifted to light showed >2-fold reduction in *ABCB4* expression, while transfer to darkness or dim light increased expression (Fig. S1). However, no change in localisation or intensity of $ABCB4_{pro}$: ABCB4-GFP signals was detected in the root tip up to the elongation zone with different light treatments (see below). Variation of mineral nutrients had no effect on *abcb4* phenotypes or $ABCB4_{pro}$:ABCB4-GFP signals, although < 2 μM Fe inhibited root hair extension in both wild-type and *abcb4*. Exogenous treatment with IAA only slightly increased *ABCB4* expression, although 2,4-D treatment increased *ABCB4* expression ~3-fold after 5h (Terasaka *et al*., 2005; Fig. S1). Based on these results, the experiments reported here utilised seedlings grown in 100 μE m^{-1} s^{-1} light on 1/4 MS salts, 0.5% sucrose and transferred to dim light unless noted.

IAA stimulation of ABCB4-mediated shootward auxin transport in the root apex

A combination of activities contributes to auxin transport at the root tip, and auxin transport mutant phenotypes are consistent with transporter distribution and function (reviewed in Petrášek and Friml 2009; Zažímalová and Murphy *et al*., 2010). Loss of AUX1 function abolishes root gravitropic growth and reduces root hair formation (Bennett *et al*., 1996, Yamamoto and Yamamoto, 1998), loss of PIN2 and, to a lesser extent, PIN3, inhibits gravitropic bending

(Vieten *et al*., 2005; Abas *et al*., 2006), loss of ABCB1 and ABCB19 results in highly variable root gravitropic growth (Noh *et al*., 2003), and loss of ABCB4 results in variable elongation growth (Terasaka *et al*., 2005), altered root hair elongation (Santelia *et al*., 2005; Cho *et al*., 2007), and slightly increased root gravitropism (Lewis *et al*., 2007).

In the nanoscale experimental system used in our lab to monitor shootward auxin transport from the root apex, a 10nL droplet of 1 μM ^{3}H-IAA (10 fmol) is placed on either the root cap/columella or over the quiescent centre (QC) of the root (Peer and Murphy, 2007). For the experiments described here, the 1 μM ^{3}H-IAA was diluted with an equal part of 0.1% ethanol or 10 μM (100 fmol) cold IAA and administered in a 20 nL droplet overlaying the columella and QC to assess the contribution of AUX1, PIN2, ABCB1, ABCB4, and ABCB19 to shootward flows from the root apex (Fig. 1A). Assays were conducted in a gas exchange chamber to eliminate effects of ethylene accumulation (columella placement and ethylene controls are shown in Fig. S2A, B).

Reductions in 3H-IAA transport were observed in *aux1, pin2, abcb1,* and *abcb4*, but not *abcb19* in the assays shown in Fig. 1A. Although the ^{3}H-IAA transport decrease in *aux1* and *abcb19* was less than expected ($P<0.05$; Fig. 1A), *aux1* and *abcb19* exhibited a greater decrease in shootward ^{3}H-IAA transport compared to wild-type when the droplet was limited to the columella region or when ethylene was added to the system ($P<0.05$; Fig. S2A, B). An *ABCB4* overexpression line with higher ABCB4 expression levels in the root (Terasaka *et al*., 2005; Cho *et al*., 2007) exhibited shootward ^{3}H-IAA transport non-different from wild-type ($P>0.05$).

Shootward ^{3}H-IAA transport was reduced in wild-type when the equal part of 0.1% ethanol in the 20 nL droplet was replaced with 10 μM cold IAA ($P<0.05$; Fig. 1A), suggesting that the cold IAA competed with transport of the radiotracer or suppressed its transport in some other manner. By far, the greatest competitive reduction in auxin transport was seen in the *abcb4* loss-of-function mutant, implying that increased auxin application inhibited ABCB4 transport less than AUX1, PIN2, and the other ABCBs. A lack of competitive inhibition of shootward auxin transport observed in an ABCB4 overexpressor (ABCB4OX) ($P<0.05$; Fig. 1A) suggests that ABCB4 is non-transcriptionally activated by increased auxin levels. In support of this interpretation, $ABCB4_{pro}$:ABCB4-GFP signals decreased very slightly after a 1X nanoscale IAA application (Fig. 1B), and no further signal change was observed with increasing IAA application.

Transport assays were repeated in wild-type, *pin2*, and *abcb4* utilising increasing amounts of ^{3}H-IAA in a 30nL droplet to maintain ethanol concentrations at 0.1% (Fig. 1C). Reductions in auxin transport observed in *pin2* were consistent across all ^{3}H-IAA amounts applied. However, significant reductions in ^{3}H-IAA transport compared to wild-type ($P<0.05$) were not observed in

abcb4 until >25 fmol was applied and only reached the 30-50% reductions previously reported at 50 fmol and above (R^2=0.96, 0.95, 0.85 for Col-0, *pin2*, *abcb4*, respectively; Fig. 1C).

Short-term (1h) root tip incubation with radiolabelled compounds has previously been used to assess the role of the ABCG36/37 transporters in uptake of ^{3}H-IAA, indole-3-butyric acid (IBA), and benzoic acid (BeA) (Růžička *et al*., 2010). This method was adapted to measure uptake of ^{3}H-IAA for 15 or 30 minutes with the addition of 100 nM cold IAA to the incubation mixture in wild-type and *abcb4*. After 15 minutes, net accumulation of ^{3}H-IAA was lower than wild-type in *abcb4* root tips and higher in ABCB4 overexpression lines ($P<0.05$; Fig. 1D). However, after 30 minutes, this trend was reversed with slightly increased net accumulation observed in *abcb4* and decreased net accumulation in the *ABCB4* overexpression line ($P<0.05$; Fig. 1D). These results support a model where ABCB4 mediates uptake of low concentrations of IAA, but exports IAA as intracellular levels increase.

ABCB4 regulation of root hair length

It is difficult to reconcile decreased shootward auxin delivery to the root differentiation/ maturation zone with evidence that ABCB4-mediated auxin efflux activity inversely correlates with root hair length (Cho *et al*., 2007). However, free IAA levels in a 2 mm segment containing the differentiation/ maturation zone where root hair elongation is particularly pronounced in *abcb4* (starting 1.5 mm above the root apex) were equal to or even slightly greater than those in equivalent segments from wild-type roots (Fig. 1E). This suggests that auxin supply to trichoblasts in *abcb4* is sufficient for root hair elongation and that ABCB4 limits auxin movement out of the elongation zone as previously proposed (Terasaka *et al*., 2005).

Consistent with ABCB4 regulation of auxin levels in root hairs, addition of 10 nM IAA to the media resulted in increased root hair elongation in both wild-type and *abcb4,* although root hairs were still significantly longer in *abcb4* ($P<0.05$, Fig. 2A). As reported previously (Santelia *et al*., 2005), treatment with a higher concentration (50 nM) of IAA completely eradicated the growth difference between wild-type and *abcb4*, and higher IAA concentrations (up to 1 µM) inhibited root hair elongation in both lines (Fig. 2A). Attempts to correlate growth with direct or indirect auxin quantitations in root hairs were unsuccessful, as free IAA levels in root hairs collected by vacuum could not be reliably normalised and *DR5*rev$_{pro}$:GFP signals could not be detected in wild-type or *abcb4* trichoblasts. Further analyses of root hair-specific growth responses utilising expression of *ABCB4* driven by the *Expansin A7* (*PE7)* promoter (Cho and Cosgrove, 2002; Cho *et al*., 2007) was not pursued, as, in our hands, weaker *PE7:*GUS and GFP fusion signals were observed in atrichoblasts.

ABCB4 expression in trichoblast-forming epidermal cells is initially low, increases as the root hair elongates, and then decreases after elongation ceases (Fig. S3). Under the growth conditions used in the assays described here (3d light-grown seedlings acclimated to 20 μmol m^{-2} s^{-1} light for 24h before and during assays), elongated root hairs were readily observed in *abcb4* in a region starting 1.5 mm above the root apex (Fig. 2B). Examination of an *ABCB4pro*:ABCB4-GFP line (Cho *et al*., 2007) confirmed that, unlike AUX1, which is not expressed in trichoblasts (Jones *et al*., 2009), PM-localised ABCB4 is observed in all epidermal cells (Fig. 2C). The PM-localised ABCB4-GFP signal intensified slightly as root hairs began to form and extended with the root hair during all subsequent stages. Attempts to discern whether intracellular signals observed in root hairs were a result of ABCB4-GFP secretion using cycloheximide were unsuccessful, as cycloheximide completely inhibited root hair tip growth. However, FRAP analysis detected rapid restoration of signal to the PM, suggesting that these signals represented anterograde trafficking.

Like ABCB19, ABCB4 has been shown to exhibit stable membrane localisation and resistance to BFA (Cho *et al*., 2007; Wu et al., 2007; Titapiwatanakun *et al*., 2009). In the proximal elongation and maturation zones, PM ABCB4-GFP signals decreased slightly after treatment with 20-100 nM IAA or 2,4-D (Fig. 2D) and decreased substantially after 6h of treatment with 1 μM IAA or 2,4-D (Fig 2G,H). Auxin treatment also produced an increased intracellular signal not associated with endomembrane compartments nor in the control (Fig. 2C,D). Presumably this signal represents free GFP, as post transcriptional inactivation of ectopically-overexpressed *ABCB4* and proteolytic truncation of the ABCB4 C-terminus have been reported previously (Terasaka *et al*., 2005; Geisler et al., 2003; Titapiwatanakun *et al*., 2009).

ABCB4-GFP seedlings grown in continuous elevated light (100 μmol m^{-2} s^{-1}) exhibited very weak signals in trichoblasts, but signals in the atrichoblast PM were greatly increased (Fig. 2E). These results suggest that studies of root hair elongation in response to low concentrations of auxins in dim light are likely to primarily reflect effects on ABCB4 transport activity, not protein localisation/abundance. However, they also underscore the sensitivity of these assays to light conditions and auxin levels.

Solvent control experiments also revealed a sensitivity of ABCB4 membrane localisation to low concentrations of dimethyl sulfoxide (DMSO). Substantial internalisation of both N- and C-terminal GFP fusions of ABCB4 were observed after treatment with 0.05% DMSO (Fig. 2F,I). Presumably this is a result of dissociation of ABCB4 from hydrophobic membrane domains (Borner *et al*., 2005; Titapiwatanakun *et al*., 2009) as a result of introduction of water molecules at points of lipid-protein interaction (Notman *et al*., 2006). As a result, all assays of ABCB4

activity in Arabidopsis, BY-2 cells and *S. pombe* described herein were conducted with low auxin concentrations and compounds solubilised in ethanol.

PM localisation of ABCB4 is sensitive to NPA and high auxin concentrations

A standard inhibitor used in analyses of auxin transport is the efflux inhibitor 1-naphthylphthalamic acid (NPA) (Rubery, 1990; Muday, 2001). However, functional secretion of ABCB19 and ABCB4 out of the ER requires the immunophilin-like chaperone FKBP42/TWD1, and ABCB secretion is inhibited by overnight treatment with NPA which interrupts TWD1-ABCB interactions (Geisler *et al*., 2003; Bouchard *et al*., 2006; Rojas-Pierce *et al*., 2007; Wu *et al*., 2007, 2010). Treatment of ABCB4-GFP transformants with 10 μM NPA (5h) resulted in ABCB4-GFP localisation to intracellular inclusions similar to those seen in the *twd1-3* background (Fig. 2J,K). These results suggest that it would be difficult to differentiate between direct and indirect NPA effects on ABCB4-mediated efflux, so NPA was not utilised in any of the Arabidopsis growth and transport studies described herein.

oxIAA is not an ABCB4 transport substrate

Previously, ABCB4 was shown to transport benzoic acid (BeA) when expressed in *S. pombe* (Yang and Murphy, 2009). In root tip net uptake assays, ^{3}H-BeA uptake in wild-type, *abcb4*, and the *ABCB4OX* was similar at 15 min, but was increased in *abcb4* and decreased in *ABCB4OX* after 30 min (Fig. 3A). This suggested that ABCB4 may mobilise other organic acid substrates or conjugates in addition to IAA *in planta*. In Arabidopsis, 2-oxindole-3-acetic acid (oxIAA) and 2-oxindole-3-acetyl-β-glucose (oxIAA-Gluc) are the initial oxidative products generated when IAA is present at excessive levels (Ernstsen *et al*., 1987; Ostin *et al*., 1998), and thus are possible substrates for a transporter that regulates physiologically-relevant cellular auxin levels. LC-MS analysis of extracts indicated that increased levels of oxIAA and oxIAA-Gluc were generated in the root when shoot-derived auxin streams are increased by application of increasing amounts of ^{3}H-IAA to the shoot tip in wild-type seedlings (Fig. 3B) and oxIAA is not polarly transported (Fig. 3C).

However, levels of oxIAA and oxIAA-Gluc in roots of *abcb4* were not significantly higher compared to wild-type ($P>0.05$; Fig. 3D). As would be expected, levels of oxIAA and oxIAA-Gluc were slightly higher in *abcb1* and lower in *abcb19* due to changes in auxin movement in these mutants (Fig. 3D). Competition of IAA transport with oxIAA was also analysed in assays of shootward transport of ^{3}H-IAA from the root apex. No competitive inhibition was detected (Fig. 3E), and oxIAA appeared to enhance ^{3}H-IAA transport as was previously described for ABCB1 (Geisler *et al*., 2005). A small amount of competitive inhibition of ^{3}H-IAA uptake was

observed in yeast expressing ABCB4 (Fig. S4A), but no inhibition of efflux was observed (Fig. S4B).

Expression of ABCB4 in BY-2 cells produces phenotypes consistent with auxin efflux

Overexpression of *ABCB4* under the control of a *35S* promoter has previously been shown to enhance ^{3}H-NAA efflux in BY-2 cells (Cho *et al*., 2007). Expression of Arabidopsis ABCB4-GFP in BY-2 resulted in abundance and localisation similar to that reported for *35S*-driven expression in BY-2 (Cho *et al*., 2007) as well as a partial inhibition of cell division compared to untransformed cells (measured by cell density during a 7-day subculture period). This inhibition was similar to that produced by $PIN1_{pro}$:PIN1-GFP expression (Fig. 4A), but was less severe than in auxin-starved BY-2 cells or in cells expressing Arabidopsis PIN4, PIN6, PIN7 and ABCB19 (Petrášek *et al*., 2006; Mravec *et al*., 2008). Further, cell elongation observed with expression of Arabidopsis ABCB19 or PIN1 (Mravec *et al*., 2008) was not observed in 3-day ABCB4-GFP cells (Fig. 4B), perhaps due to decreased transversal PM localisation of ABCB4-GFP (Fig. 4C and Cho *et al*., 2007) compared to PIN1-GFP (Fig. 4C). This decrease in transversal localisation may be a consequence of faster lateral diffusion or trafficking of ABCB4 compared to PIN1-GFP as indicated by FRAP analysis (Fig. 4D). PM abundance and localisation of ABCB4-GFP also exhibited decreased sensitivity to IAA, NPA, and DMSO in BY-2 cells compared to Arabidopsis (Fig. 2G,I,J, Fig. 4C), presumably due to differences in FKBP content, membrane lipid composition, and cultivation of BY-2 cells in 2,4-D.

Auxin transport in BY-2 cells expressing ABCB4

As reported previously (Petrášek *et al*., 2002; 2006), PIN1 expression in BY-2 resulted in increased ^{3}H-NAA efflux, and NPA treatment abolished both native and PIN1-mediated efflux (Fig. 5A). BY-2 cells expressing $ABCB4_{pro}$:ABCB4-GFP exhibited little or no significant change in ^{3}H-NAA (2 nM) uptake or efflux at 15 min, but did exhibit increased net uptake after NPA treatment (Fig. 5A), suggesting that ABCB4 also has NPA-sensitive efflux activity. The weak uptake activity could not be further analysed due to the residual lipophilic uptake of ^{3}H-NAA observed in BY-2 cells, even after effective inhibition of AUX1/LAX transporters by 2-naphthoxyacetic acid (2-NOA) (Laňková *et al*., 2010).

BY-2 cells expressing ABCB4 showed only a slight decrease in net ^{3}H-BeA retention (Fig. 5B), but cold BeA (10 μM) did not compete with ^{3}H-NAA or ^{3}H-IAA transport (Fig. 5C, for IAA, data not shown). ^{3}H-IAA was selected as a more informative substrate for oxIAA competition assays, and cold oxIAA did not compete with ^{3}H-IAA in control or ABCB4 cells (Fig 5E,F). However, some caution is required in comparing BY-2 competition assays to those in

Arabidopsis and *S. pombe* as IAA catabolism is more rapid in BY-2 (Delbarre *et al*., 1994), presumably a consequence of BY-2 culture in 2,4-D as well as the required use of selective auxin uptake and efflux inhibitors for differentiation of heterologous and endogenous auxin transport activities in this system (Petrášek *et al*., 2006; Titapiwatanakun *et al*., 2009; Laňková *et al*., 2010).

ABCB4 uptake kinetics

All of the Arabidopsis auxin transporters examined to date are at least partially functional when expressed in the yeast *S. pombe* (Yang and Murphy, 2009; Růžička *et al*., 2010; Tsuda *et al*., 2011). If ABCB4 functions as an uptake transporter at low (<50 nM) IAA concentrations, saturation kinetics should be evident with expression of ABCB4 in this system. For comparison, saturation kinetics for AUX1 were determined, and AUX1 exhibited uptake saturation at >2 µM ^{3}H-IAA with an apparent Km of ~ 340 nM based on initial rates of uptake (Fig. 6A, B). This observed Km was lower than that reported for AUX1 in *Xenopus* oocytes (Yang *et al*., 2006), and it is likely due to cell size differences and the presence of a cell wall in *S. pombe*. In short term assays, ABCB4 showed influx activity at lower IAA concentrations and ABCB4 transport activity switched to efflux at concentrations >250 nM or with exposure to IAA for a longer period of time (Fig. 6C, vector control in Fig. S4C). Conversion to efflux rather than conventional saturation suggests that IAA uptake mediated by ABCB4 is an indirect effect of transporter activity and suggests that ABCB4 could mobilise other substrates. This uptake effect may be specific to ABCB4 and related ABCB isoforms, as no IAA uptake could be observed in the ABCB19 auxin efflux transporter under any conditions. Western blot analysis of membrane fractions confirmed that ABCB4 and ABCB19 proteins were expressed (Fig. S4D).

Uptake of 2,4-D by ABCB4 inhibits efflux activity

2,4-D is often used as a substitute for IAA in growth assays, as it is highly stable (Delbarre *et al*., 1996) and is poorly distributed through the plant by auxin polar transport mechanisms (Pitts *et al*., 1998). This synthetic auxin is taken up via AUX1/LAX permeases (Bennett *et al*., 1996; Yang *et al*., 2006; Yang and Murphy, 2009), was shown to be an uptake substrate for ABCB4 expressed in *S. pombe,* and to noncompetitively inhibit ABCB4 ^{3}H-IAA efflux activity (Yang and Murphy, 2009).

2,4-D is a weak efflux substrate for all ABCB and PIN proteins expressed in non-plant heterologous systems, but is a preferred efflux substrate for the ABCG37/PDR9 pleiotropic substrate transporter (Titapiwatanakun *et al*., 2009; Růžička *et al*., 2010). Analysis of 2,4-D effects on root hair elongation confirm that this compound is an ABCB4 uptake substrate *in*

planta. Low concentrations of 2,4-D (10 nM) compensated for differences in *abcb4* root hair elongation in a manner similar to what is seen with IAA, and higher 2,4-D concentrations inhibited root hair elongation equally in both *abcb4* and wild-type (Fig. 7A). However, unlike IAA, an intermediate concentration of 2,4-D (50 nM) inhibited wild-type root hair elongation to a greater extent than in *abcb4*, suggesting a direct role of ABCB4 in 2,4-D uptake. This result cannot be attributed to enhanced AUX1 uptake in *abcb4* root hairs, as *AUX1* is not expressed in trichoblasts (Jones *et al*., 2009).

2,4-D is also the preferred substrate for native 2-NOA-sensitive auxin influx assays in BY-2, and ABCB4 is resistant to 2-NOA inhibition (Laňková *et al*., 2010). As expected, 2-NOA (10 μM) decreased the net uptake of ^{3}H-2,4-D (2 nM) in control and PIN1-expressing cells, but had a lesser effect on the accumulation of 2,4-D in ABCB4-overexpressing cells (Fig. 7B). However, 2,4-D uptake was enhanced in cells expressing *ABCB4* after background auxin uptake was blocked with 2-NOA (Fig. 7C), suggesting a non-competitive interaction of 2,4-D with the ABCB4-based auxin efflux activity. This notion was further supported by the fact that pre-treatment of cells expressing *ABCB4* with cold 2,4-D, but not cold IAA, resulted in an enhanced net uptake of ^{3}H-2,4-D (Fig. S5; Fig. S6). An enhancement of auxin influx in BY-2 expressing ABCB4 was also observed following addition of NPA to 2-NOA-pretreated cells. This treatment resulted in an increase in 2,4-D accumulation, consistent with continued 2,4-D import by ABCB4 in combination with inhibition of the weak PIN and ABCB (including ABCB4) efflux activity (Fig. 7D).

One explanation for the lack of ^{3}H-NAA efflux seen in BY-2 cells expressing ABCB4 might be that the cells are routinely maintained on medium containing the synthetic auxin 2,4-D (Nagata *et al*., 1992). Although routinely washed out with uptake buffer before auxin transport assays are conducted (Cho *et al*., 2007; Fig. S7), 2,4-D from the BY-2 cell culturing medium bound to ABCB4 may be difficult to completely eliminate, especially as 2,4-D is poorly metabolized in tobacco cells compared to IAA and NAA (Delbarre *et al*. 1994, 1996). No condition, time point, expression level (35S or native promoter), or regimen could be identified where net ^{3}H-NAA efflux greater than that shown in Fig. 5D was observed in BY-2 cells expressing *ABCB4*.

Assays of ^{3}H-2,4-D binding to ABCB4 and ABCB19 expressed in mammalian HeLa cells suggest that the affinity of ABCB4 for 2,4-D is higher than that of ABCB19 (Fig. 7E). Further, the increased ^{3}H-2,4-D specific binding observed in cells expressing ABCB4 was not displaced with excess IAA. Modeling of 2,4-D and IAA docking to ABCB4 is consistent with allosteric rather than competitive regulation by 2,4-D, and 2,4-D binding to ABCB4 predicts binding configuration that would enhance efflux (Fig. 7F).

Discussion

The experimental evidence presented here indicates that ABCB4 regulates cellular auxin levels in the Arabidopsis root epidermis by enhancing auxin uptake when cellular levels are low and catalyzing auxin efflux when internal levels rise. A role for ABCB4 in regulating auxin homeostasis at the plasma membrane in root epidermal cells is consistent with the necessity to balance auxin levels in cells that are essential to streams regulating tropic growth and would be expected to complement PIN5-mediated auxin homeostasis at the ER membrane (Mravec et al., 2009).

The low (nanomolar) auxin concentrations required to induce efflux activity in ABCB4 suggest that this protein functions primarily as an efflux transporter in the root apex and catalyzes uptake only in cells distal to the meristematic region (Petersson *et al*., 2009). However, as excess auxin levels destabilise or reduce the abundance of ABCB4 on membranes in cells in the elongation zone and above, it is unlikely that ABCB4 functions in removal of toxic auxin concentrations in root epidermal cells. Instead, it appears that excess IAA is oxidatively catabolised in these cells and the oxidative products are either internalised in the vacuole or exported by ABCG36 and 37. Results presented herein as well as experiments documenting IAA induction of reactive oxygen species generation (Peer and Murphy, 2007) suggest that the threshold for oxidative IAA catabolism in non-apical tissues (100-500 nM) is well above the induction threshold for ABCB4 efflux.

This report also underscores the point that radiotracer assays are highly dependent on the concentrations, amounts, and types of auxin applied. The contribution of ABCB4 to physiologically relevant shootward auxin streams from the root apex appears to be relevant only as auxin levels increase, and ABCB4 may play a more important role in controlling auxin movement out of the elongation zone as previously proposed (Peer and Murphy, 2007). However, the localisation of ABCB4 in epidermal cells also suggests that this transporter could modulate the accumulation of microbially-produced auxins at the root surface. It is less likely that this is the function of ABCG36 and 37, as these proteins exhibit very low affinity for IAA (Růžička *et al*., 2010), the primary auxin produced by rhizosphere bacteria (Glick, 1995; Khakipour *et al*., 2008). It is also possible that ABCB4 modulates interactions with rhizobial communities by eliminating breakdown products or biosynthetic intermediates of indolic glucosinolate defense compounds in plants that produce these compounds.

A mechanistic basis for auxin uptake associated with ABCB4 may be derived from characteristics of its association with the PM lipid bilayer. ABCB4 exhibits greater hydrophobicity and is associated with sterol/sphingolipid-enriched detergent-resistant membranes (Borner *et al*., 2005; Titapiwatanakun *et al*., 2009). The instability of ABCB4 in

relatively low concentrations of the polar solvent DMSO suggests that the introduction of water molecules into the lipid bilayer disturbs hydrophobic interactions of the protein. Conformational changes in ABCB4 brought about by ATP hydrolysis may result in more perturbation of the outer membrane leaflet and consequent mobilisation of resident amphipathic molecules such as IAA, NAA, and 2,4-D to promote cytosolic trapping of these molecules.

Alternatively, the combination of more hydrophobic anchoring and additional IAA binding sites in ABCB4 may provide a mechanism for substrate uptake that would not occur in ABCB1 or 19 during the conformational change associated with the first of two ATP hydrolysis steps required for ABC transport function (Knöller and Murphy, 2010). Substrate activation and conformational change has been shown for other ABC transporters (Loo *et al*., 2003; Terasaka *et al*., 2005; Sauna *et al*., 2008), and apparent drug-induced reversal of mammalian ABCB1 and ABCG22 activity has recently been reported (Shi *et al*., 2011).

Finally, ABCB4 appears to be a direct herbicidal target of 2,4-D. Binding of 2,4-D to ABCB4 results in increased accumulation of both 2,4-D and other auxins in root epidermal cells and is likely to amplify the herbicidal effects of the compound including swelling, separation of epidermal and cortical cell layers of the root, and decreased root surface area due to loss of root hairs (Johanson and Muzik, 1961; Calahan and Engel, 1965). As such, tissue-specific manipulation of *ABCB4* expression may be a useful tool for decreasing damage to crop plants caused by 2,4-D drift.

Experimental procedures

Materials

Mutant alleles utilised were *aux1-7* (Pickett *et al*., 1990), *pin2/eir1-1* (Luschnig *et al*., 1998), *abcb1/pgp1-1* (Geisler *et al*., 2005, *abcb19/mdr19/pgp19-1* (Noh *et al*., 2001; Geisler *et al*., 2003) introgressed into Col-0 with three backcrosses, *abcb4/pgp4-1* and Pro35S:PGP4 (Terasaka *et al*., 2005). Control, PGP4-GFP, and PIN1-GFP BY-2 cells (*Nicotiana tabacum* L., cv. Bright-Yellow-2) were as described (Nagata *et al*., 1992; Petrášek *et al*. 2002; Jelínková and Malínská *et al*., 2010). Transgenic BY-2 cells and calli were maintained on media supplemented with 40 $\mu g.ml^{-1}$ hygromycin or 100 $\mu g.ml^{-1}$ kanamycin, and 300 $\mu g.ml^{-1}$ cefotaxim.

IAA, 2,4-D, 2-NOA, DMSO, IAA-Gluc, IAA-Asp were from Sigma-Aldrich (St. Louis, MO, USA). 1-naphthylphthalamic acid (NPA) was from OlChemIm Ltd. (Olomouc, Czech Republic). ^{3}H-IAA (20 or 30Ci $mmol^{-1}$, ^{3}H-BeA (26 or 20 Ci $mmol^{-1}$), ^{3}H-2,4-D (20 Ci $mmol^{-1}$), and ^{3}H-NAA (specific radioactivity 25 Ci $mmol^{-1}$, respectively) were from American Radiolabeled Chemicals (St. Louis, MO, USA). oxIAA from OlChemIm, Ltd. ^{3}H-oxIAA and ^{3}H-oxIAA-Gluc were synthesized by incubating 1g of 5d Col-0 seedlings in 5 mL ½ MS media (pH 5.5)

containing 3μM ^{3}H-IAA for 3h in low light with mild shaking. The seedlings were collected, frozen and ground in liquid nitrogen and extracted as previously described for IAA determinations (Kim *et al*., 2007), except that C8 rather than C18 SPE was used. Fractions were separated as described (Osten *et al*. 1998). Three primary peak fractions oxIAA-Gluc, oxIAA, and IAA (in order of elution) were obtained, identities were confirmed by LC-MS analysis (LCT-Premier, Micromass, Manchester, UK) and ester hydrolysis, and were used in transport assays.

Root auxin transport assays and root hair length determination in Arabidopsis

Root transport and uptake assays were performed as described (Blakeslee *et al*., 2007; Peer and Murphy, 2007 and references therein, see http://www.hort.purdue.edu/hort/research/murphy/The%20more%20than%20complete%20hitchhiker%27s%20guide%20to%20auxin%20transport.pdf). Samples were incubated in chambers fitted with flowthrough gas controllers (ambient or ethylene) under continuous yellow light (40 μE s^{-1} m^{2}). Root hair growth assays were performed using 5-day seedlings grown on ¼ MS (pH 5.5), 0.5% sucrose on 1.3% gellan gum. Root hair lengths were measured using a Zeiss Stemi 2000C microscope, Luminera Infinity2 camera, and ImageJ software (NIH). Ten root hairs were measured in a 2mm zone starting 1.5mm above apex. Only root hairs extending parallel to the surface were measured. Values are means of ten root hairs per plant from ten plants. Experiments were repeated three times.

IAA, oxIAA, oxIAA-Gluc, and IBA determinations in Arabidopsis tissues

Extraction, SPE preparation, and analysis of prepared extracts were as described (Kim *et al*., 2007) using ^{13}C-IAA as an internal standard, except C8 SPE (Isolute, Alexandria VA, USA) replaced C18 SPE, sample sizes were reduced to 220μg, and underivatised samples were analysed directly by using either an QLCT Premier or Agilent HPLC-MSD/TOF (Agilent, Santa Clara CA, USA). Determination of oxIAA, oxIAA-Gluc, IAA-Asp, and IAA-Gluc generation in roots after application of 3H-IAA (30 nL, 10μM, 50 seedling apices) was as described (Ostin *et al*., 1998). oxIAA standard for LC-MS and HPLC was from OlChemIm, Ltd.

Yeast and BY-2 auxin transport assays and HeLa binding assays

^{3}H-IAA transport assays in Schizosaccharomyces pombe

Auxin transport assays in *S. pombe* were performed as described previously (Yang and Murphy, 2009) with the following modifications. *Schizosaccharomyces pombe* cells were grown to OD_{600} ~ 2.0 in EMM (Edinburgh minimal media) containing 15μM thiamine. Then thiamine was

removed by washing twice with EMM, and cells were transferred to fresh EMM and incubated for 19h (final OD_{600} = 2–3) to induce the expression of proteins. Cells were spun at 6000 g for 30 sec. Pellets were washed once and resuspended in EMM (pH 4.5 for ABCB4/19, and pH5.5 for AUX1) to OD_{600} = 2. Cells were kept at 4°C in all following steps except where noted. ^{3}H-IAA (specific activity 20 Ci per mmol, American Radiolabelled Chemicals) was added into 25 µl cells with final concentrations 0.1, 0.25, 0.5, 1, and 2 µM and incubated at 30°C for 5 min (ABCB4) or 8 min (AUX1). Cells were washed twice with EMM (pH 4.5) and resuspended in 250 ml EMM (pH 4.5). Five mL EcoLiteTM scintillation cocktail was added and retained radioactivity was quantified by scintillation counting. The net transport of ^{3}H-IAA was calculated by subtracting empty vector controls from ABCB4/19 and AUX1. All transport assays were performed with three or four repeats. Substrate binding to ABCB4 expressed in HeLa cells was as described (Rojas-Pierce *et al*., 2007), using 3H-2,4-D as a substrate. BY-2 (control, PIN1-GFP, ABCB4-GFP) auxin accumulation assays were as described (Delbarre *et al*. 1996; Petrášek *et al*. 2006) with ≥2 repeats and 10 µM 2-NOA or NPA (in DMSO), 10 µM cold BeA, IAA, 2,4-D, or oxIAA (in ethanol) added at 0 or 30 min as indicated with the radiolabelled assay substrate at 2 nM.

Molecular docking of ABCB4

The sequence alignment of ABCBs (accession: NP_182223) with Sav1866 (accession: Q99T13) were performed in Multalin http://bioinfo.genotoul.fr/multalin/multalin.html (Corpet et al., 1998) and NCBI bl2seq http://blast.ncbi.nlm.nih.gov/Blast.cgi as described in Yang and Murphy (2009). Based on the sequence alignment and the crystal structure of Sav1866, ABCB4 model were computed with Modeller structural modeling software http://salilab.org/modeller (Sali and Blundell, 1993; Eswar et al., 2000). Computational simulation of ligand binding to ABCB TMDs was performed using MEDock at http://medock.csbb.ntu.edu.tw (Chang et al., 2005).

Microscopy

Arabidopsis thaliana. Images were collected using a Zeiss LSM 710 confocal laser scanning microscope with a 40x water immersion objective (1.4 numerical aperture, C-Apochromatic) and argon laser (Carl Zeiss, Jena Germany) as in Christie et al. (2011). *BY-2 cells.* Cell densities were determined with ≥8 aliquots per sample using a Fuchs-Rosenthal haemocytometer on a Zeiss Axiovert 40C. Cell lengths and diameters were observed with a Nikon Eclipse E600, DVC1310C camera, and LUCIA image analysis software (Laboratory Imaging, Prague, Czech Republic). For each variant 150 cells were measured on five optical fields. Analysis of fluorescent protein fusions utilised a Zeiss LSM5 DUO (40x C-Apochromat water immersion,

NA=1.2). For bleaching, a 40x20 pixel rectangle centred on the transversal membrane was bleached or used as a control, then tracked for fluorescence recovery for 300s in 10s intervals. Values are means of ≥25 cells.

Acknowledgements

The work was supported by the Ministry of Education, Youth and Sports of the Czech Republic, LC06034 to MK, JP, KH, and EZ, the Grant Agency of the Czech Republic, P305/11/0797 to MK, JP, KH, and EZ, the Division of Energy Biosciences, US Department of Energy DE-FG02-06ER15804 to ASM. We thank Kateřina Malínská for help with confocal microscopy and Jana Žabová for technical assistance, Ambreen Ahmed for her assistance in setting up root hair measurement assays, and Joshua Blakeslee for helpful comments on the manuscript.

Supporting Figure Legends

Figure S1. *ABCB4* expression in response to stimuli.

Figure S2. Shootward ^{3}H-IAA transport from the root apex in wild-type and auxin transport mutants.

Figure S3. *ABCB4* expression in root cell types and ABCB4-GFP ethanol solvent controls.

Figure S4. oxIAA competition experiments and transport assays controls.

Figure S5. ^{3}H-2,4-D accumulation in BY-2 cells pretreated with cold IAA or 2,4-D.

Figure S6. Gradual reversal of ABCB4 activity in BY-2 cells.

Figure S7. ^{3}H-2,4-D accumulation after washout with uptake buffer.

References

Abas, L., Benjamins, R., Malenica, N., Paciorek, T., Wirniewska, J., Moulinier-Anzola, J.C., Sieberer, T., Friml, J. and Luschnig, C. (2006) Intracellular trafficking and proteolysis of the Arabidopsis auxin-efflux facilitator PIN2 are involved in root gravitropism. *Nat. Cell Biol.,* **8**, 249-256.

Aller, S.G., Yu, J., Ward, A., Weng, Y., Chittaboina, S., Zhuo, R., Harrell, P.M., Trinh Y.T., Zhang, Q., Urbatsch, I.L. and Chang G. (2009) Structure of P-glycoprotein Reveals a Molecular Basis for Poly-Specific Drug Binding. *Science* **323**, 1718-1722.

Badri, D.V., Loyola-Vargas, V.M., Broeckling, C.D., De-la-Peña, C., Jasinski, M., Santelia, D., Martinoia, E., Sumner, L.W., Banta, L.M., Stermitz, F., and Vivanco, J.M. (2008). Altered profile of secondary metabolites in the root exudates of Arabidopsis ATP-binding cassette transporter mutants. *Plant Physiol*. **146**, 762-771.

Bennett, M.J., Marchant, A., Green, H.G., May, S.T., Ward, S.P., Millner, P.A., Walker, A.R., Schulz, B. and Feldmann, K.A. (1996) Arabidopsis AUX1 gene: a permease-like regulator of root gravitropism. *Science* **273**, 948-950.

Blakeslee, J.J., Bandyopadhyay, A., Lee, O.R., Mravec, J., Titapiwatanakun, B., Sauer, M., Makam, S.N., Cheng, Y., Bouchard, R., Adamec, J., Geisler, M., Nagashima, A., Sakai, T., Martinoia, E., Friml, J., Peer, W.A. and Murphy, A.S. (2007) Interactions among PIN-FORMED and P-glycoprotein auxin transporters in *Arabidopsis* . *Plant Cell* **19**, 131-147.

Borner, G.H.H., Sherrier, D.J., Weimar, T., Michaelson, L.V., Hawkins, N.D., MacAskill, A., Naper, J.A., Beale, M.H., Lilley, K.S. and Dupree P. (2005) Analysis of Detergent-Resistant Membranes in *Arabidopsis*. Evidence for Plasma Membrane Lipid Rafts. *Plant Physiology* **137**, 104-116.

Bouchard, R., Bailly, A., Blakeslee, J.J., Oehring, S.C., Vincenzetti, V., Lee, O.R., Paponov, I., Palme, K., Mancuso, S., Murphy, A.S., Schulz, B., and Geisler, M. (2006) Immunophilin-like TWISTED DWARF1 modulates auxin efflux activities of Arabidopsis P-glycoproteins. *J Biol Chem*. **281**, 30603-30612.

Calahan, L.M. and Engel, R.E. (1965). Tissue abnormalities induced in roots of colonial bentgrass by phenoxyalkylcarboxylic acid herbicides. *Weeds* **13**, 336-338.

Chang, D.T.-H., Oyang, Y.-J. and Lin, J.-H. (2005) MEDock: a web server for efficient prediction of ligand binding sites based on a novel optimization algorithm. *Nucleic Acid Research* **33**, W233–W238.

Cho, M., Lee, S.H. and Cho, H.T. (2007) P-glycoprotein4 displays auxin efflux transporter-like action in Arabidopsis root hair cells and tobacco cells. *Plant Cell* **19**, 3930-3943.

Cho, H.T., and Cosgrove, D.J. (2002). Regulation of root hair initiation and expansin gene expression in Arabidopsis. *Plant Cell* **14**, 3237-3253.

Christie, J.M., Yang, H., Richter, G.L., Sullivan, S., Thomson, C.E., Lin, J., Titapiwatanakun, B., Ennis, M., Kaiserli, E., Lee, O.R., Adamec, J., Peer, W.A., and Murphy, A.S. (2011). phot1 inhibition of ABCB19 primes lateral auxin fluxes in the shoot apex required for phototropism. PLoS Biol. **9**, e1001076.

Corpet, F. (1988) Multiple sequence alignment with hierarchical clustering. *Nucleic Acids Res* **16**, 10881–10890.

Dawson, R.J.P. and Locher, K.P. (2006) Structure of a bacterial multidrug ABC transporter. *Nature* **443**, 180-185.

Delbarre, A., Muller, P., Imhoff, V. and Guern, J. (1996) Comparison of mechanisms controlling uptake and accumulation of 2,4-dichlorophenoxy acetic acid, naphthalene-1-acetic acid, and indole-3-acetic acid in suspension-cultured tobacco cells. *Planta* **198**, 532-541.

Delbarre, A., Muller, P., Imhoff, V., Morgat, J.L., and Barbier-Brygoo, H. (1994) Uptake, accumulation and metabolism of auxins in tobacco leaf protoplasts. *Planta* **195**,159-167.

Dudler, R. and Hertig, C. (1992) Structure of an MDR-like gene from Arabidopsis thaliana evolutionary implications. *J. Biol. Chem.* **267**, 5882-5888.

Ernstsen, A., Dandberg, G., and Lundstrom, K. (1987) Identification of oxindole-3-acetic acid, and metabolic conversion of indole-3-acetic acid to oxindole-3-acetic acid in Pinus sylvestris seeds. *Planta* **172**, 47-52.

Eswar, N., Marti-Renom, M.A., Webb, B., Madhusudhan, M.S., Eramian, D., Shen, M.-Y., Pieper, U. and Andrej, S. (2000) Comparative protein structure modeling with MODELLER. *Current Protocols in Bioinformatics* **15**, 5.6.1-5.6.30.

Geisler, M., Blakeslee, J.J., Bouchard, R., Lee, O.R., Vincenzetti, V., Bandyopadhyay, A., Titapiwatanakun, B., Peer, W.A., Bailly, A., Richards, E.L., Ejenda, K.F.K., Smith, A.P., Baroux, C., Grossniklaus, U., Muller, A., Hrycyna, C.A., Dudler, R., Murphy, A.S. and Martinoia, E. (2005) Cellular efflux of auxin catalysed by the *Arabidopsis* MDR/PGP transporter AtPGP1. *Plant Journal* **44**, 179-194.

Geisler, M., Kolukisaoglu, H.U., Bouchard, R., Billion, K., Berger, J., Saal, B., Frangne, N., Koncz-Kalman, Z., Koncz, C., Dudler, R., Blakeslee, J.J., Murphy, A.S., Martinoia, E., and Schulz, B. (2003) TWISTED DWARF1, a unique plasma membrane-anchored immunophilin-like protein, interacts with Arabidopsis multidrug resistance-like transporters AtPGP1 and AtPGP19. *Mol Biol Cell* **14**, 4238-4249.

Glick, B.R. (1995). The enhancement of plant growth by free-living bacteria. *Can. J. Microbiol.* **41**, 109-117.

Hollenstein, K., Dawson, R.J.P. and Locher, K.P. (2007) Structure and mechanism of ABC transporter proteins. *Curr. Opin. Struc.Biol.* **17**, 412-418.

Johanson, N.G, and Muzik, T.J. (1961). Some effects of 2,4-D on wheat yield and root growth. *Botanical Gazette* **122**, 188-194.

Jones, A.R., Kramer, E.M., Knox, K., Swarup, R., Bennett, M.J., Lazarus, C.M., Leyser, H.M. and Grierson, C.S. (2009) Auxin transport through non-hair cells sustains root-hair development. *Nat. Cell. Biol.* **11,** 78–84.

Kaneda, M., Schuetz, M., Lin, B.S., Chanis, C., Hamberger, B., Western, T.L., Ehlting, J., and Samuels, A.L. (2011) ABC transporters coordinately expressed during lignification of Arabidopsis stems include a set of ABCBs associated with auxin transport. *J. Exp. Bot.* doi: 10.1093/jxb/erq416

Khakipour, N., Khavazi, K., Mojallali, H., Pazira, E., and Asadirahmani H. (2008) Production of auxin hormone by fluorescent pseudomonads. *Am-Euras. J. Agric. & Environ. Sci.* **4**, 687-692.

Kim, J.I., Sharkhuu, A., Jin, J.B., Li, P., Jeong, J.C., Baek, D., Lee, S.Y., Blakeslee, J.J., Murphy, A.S., Bohnert, H.J., Hasegawa, P.M., Yun, D.J., and Bressan, R.A. (2007) *yucca6*, a dominant mutation in Arabidopsis, affects auxin accumulation and auxin-related phenotypes. *Plant Physiol* **145**, 722-735.

Knöller, A.S., Blakeslee, J.J., Richards, E.L., Peer, W.A., and Murphy, A.S. (2010) Brachytic2/ ZmABCB1 functions in IAA export from intercalary meristems. *J Exp Bot*. **61**, 3689-3696.

Knöller, A.S., and Murphy, A.S. (2011). "ABC transporters and their function at the plasma membrane." In *The Plant Plasma Membrane*. (2010) Murphy AS, Schulz B, and Peer WA, eds. Springer-Verlag, Berlin. pp. 353-377.

Kos, V., and Ford, R.C. (2009) The ATP-binding cassette family: a structural perspective. *Cel. Mol. Life Sci.* **66**, 3111-3126.

Laňková, M., Smith, R.S., Pešek, B., Kubeš, M., Zažímalová, E., Petrášek, J., and Hoyerová, K. Auxin influx inhibitors 1-NOA, 2-NOA, and CHPAA interfere with membrane dynamics in tobacco cells. *J. Exp. Bot*. **61**, 3589-3598.

Lewis, D.R., Miller, N.D., Splitt, B.L., Wu, G.S. and Spalding, E.P. (2007) Separating the roles of acropetal and basipetal auxin transport on gravitropism with mutations in two Arabidopsis Multidrug Resistance-Like ABC transporter genes. *Plant Cell* **19**, 1838-1850.

Loo, T.W., Bartlett, M.C., and Clarke, D.M. (2003) Methanethiosulfonate derivatives of rhodamine and verapamil activate human P-glycoprotein at different sites. *J Biol Chem*. **278**, 50136-50141.

Luschnig, C., Gaxiola, R.A., Grisafi, P., and Fink, G.R. (1998). EIR1, a root-specific protein involved in auxin transport, is required for gravitropism in *Arabidopsis thaliana*. *Genes Dev*. **12,** 2175–2187.

Mravec, J., Kubeš, M., Bielach, A., Gaykova, V., Petrášek, J., Skůpa, P., Chand, S., Benková, E., Zažímalová, E., and Friml, J. (2008) Interaction of PIN and PGP transport mechanisms in auxin distribution-dependent development. *Development* **135**, 3345-3354.

Muday, G.K. (2001) Maintenance of asymmetric cellular localization of an auxin transport protein through interaction with the actin cytoskeleton. *J. Plant Growth Regul.* **19**, 385-396.

Nagata, T., Nemoto, Y., and Hasezawa, S. (1992) Tobacco BY-2 cell line as the "HeLa" cell in the cell biology of higher plants. *International Review of Cytology* **132**, 1-30

Noh, B., Murphy, A.S. and Spalding, E.P. (2001) Multidrug resistance-like genes of Arabidopsis required for auxin transport and auxin-mediated development. *Plant Cell* **13**, 2441-2454.

Noh, B., Bandyopadhyay, A., Peer, W.A., Spalding, E.P. and Murphy, A.S. (2003) Enhanced gravi- and phototropism in plant mdr mutants mislocalizing the auxin efflux protein PIN1. *Nature* **423**, 999-1002.

Notman, R., Noro, M., O'Malley, B., and Anwar, J. (2006) Molecular basis for dimethylsulfoxide (DMSO) action on lipid membranes. *J. Am. Chem. Soc.* **128**, 13982-12983.

Ostin, A., Kowalyczk, M., Bhalerao, R.P. and Sandberg, G. (1998) Metabolism of indole-3-acetic acid in Arabidopsis. *Plant Physiol* **118**, 285-296.

Peer, W.A. and Murphy, A.S. (2007) Flavonoids and auxin transport: modulators or regulators? *Trends Plant Sci.* **12**, 556-563.

Petersson, S.V., Johansson, A.I., Kowalczyk, M., Makoveychuk, A., Wang, J.Y., Moritz, T., Grebe, M., Benfey, P.N., Sandberg, G., and Ljung, K. (2009). An auxin gradient and maximum in the Arabidopsis root apex shown by high-resolution cell-specific analysis of IAA distribution and synthesis. *Plant Cell* **21**, 1659-1668.

Petrášek, J., Mravec, J., Bouchard, R., Blakeslee, J.J., Abas, M., Seifertová, D., Wisniewska, J., Tadele, Z., Kubeš, M., Čovanová, M., Dhonukshe, P., Skůpa, P., Benková, E., Perry, L., Křeček, P., Lee, O.R., Fink, G.R., Geisler, M., Murphy, A.S., Luschnig, C., Zažímalová, E. and Friml, J. (2006) PIN proteins perform a rate-limiting function in cellular auxin efflux. *Science* **312**, 914-918.

Petrásek, J., and Friml, J. (2009) Auxin transport routes in plant development. *Development* **136**, 2675-2688.

Petrásek, J., Elckner, M., Morris, D.A., and Zazímalová, E. (2002). Auxin efflux carrier activity and auxin accumulation regulate cell division and polarity in tobacco cells. *Planta* **216**, 302-308.

Pickett, F.B., Wilson, A.K., and Estelle, M. (1990). The *aux1* mutation of arabidopsis confers both auxin and ethylene resistance. *Plant Physiol* 94, 1462-1466.

Pitts, J.R., Cernac, A. and Estelle M. (1998) Auxin and ethylene promote root hair elongation in *Arabidopsis*. *Plant Journal* **16**, 553–560.

Rees, D.C., Johnson, E. and Lewinson, O. (2009) ABC transporters: the power to change. *Nat. Rev. Mol. Cell Biol.* **10**, 218-227.

Rojas-Pierce, M., Titapiwatanakun, B., Sohn, E.J., Fang, F., Larive, C.K., Blakeslee, J., Cheng, Y., Cuttler, S., Peer, W.A., Murphy, A.S. and Raikhel, N.V. (2007) Arabidopsis P-glycoprotein19 participates in the inhibition of Gravitropism by gravacin. *Chemistry & Biology* **14**, 1366-1376.

Rubery, P.H. (1990). Phytotropins: receptors and endogenous ligands. *Symp. Soc. Exp. Biol.* **44**, 119-146.

Růžička, K., Strader, L., Bailly, A., Yang, H. Blakeslee, J., Langowski, L., Nejedlá, E., Fujita, H., Itoh, H., Syono, K., Hejátko, J., Gray, W., Martinoia, E., Geisler, M., Bartel, B., Murphy, A.S. and Friml, J. (2010) Arabidopsis PIS1 encodes the ABCG37 transporter of auxinic compounds including the auxin precursor indole-3-butyric acid. *PNAS* **107**, 10749-10753.

Sali, A. and Blundell, T.L. (1993) Comparative protein modelling by satisfaction of spatial restraints. *Journal of Molecular Biology* **234**, 779–815.

Santelia, D., Vincenzetti, V., Azzarello, E., Bovet, L., Fukao, Y., Duchtig, P., Mancuso, S., Martinoia, E. and Geisler, M. (2005) MDR-like ABC transporter AtPGP4 is involved in auxin-mediated lateral root and root hair development. *FEBS Letters* **579**, 5399-5406.

Sauna, Z.E., Bohn, S.S., Rutledge, R., Dougherty, M.P., Cronin, S., May, L., Xia, D., Ambudkar, S.V., and Golin, J. (2008) Mutations define cross-talk between the N-terminal nucleotide-binding domain and transmembrane helix-2 of the yeast multidrug transporter Pdr5: possible conservation of a signaling interface for coupling ATP hydrolysis to drug transport. *J Biol Chem*. **283**, 35010-35022.

Shi, Z., Tiwari, A.K., Shukla, S., Robey, R.W., Singh, S., Kim, I.W., Bates, S.E., Peng, X., Abraham, I., Ambudkar, S.V., Talele, T.T., Fu, L.W., and Chen, Z.S. (2011) Sildenafil Reverses ABCB1- and ABCG2-Mediated Chemotherapeutic Drug Resistance. *Cancer Res*. **71**, 3029-3041.

Shitan, N., Bazin, I., Dan, K., Obata, K., Kigawa, K., Ueda, K., Sato, F., Forestier, C. and Yazaki, K. (2003) Involvement of CjMDR1, a plant multidrug-resistance-type ATP-binding cassette protein, in alkaloid transport in *Coptis japonica*. *Proc. Natl Acad. Sci. USA* **100**, 751-756.

Terasaka, K., Blakeslee, J.J., Titapiwatanakun, B., Peer, W.A., Bandyopadhyay, A., Makam, S.N., Lee, O.R., Richards, E.L., Murphy, A.S., Sato, F. and Yazaki, K. (2005) PGP4, an ATP binding cassette P-glycoprotein, catalyzes auxin transport in *Arabidopsis thaliana* roots. *Plant Cell* **17**, 2922-2939.

Titapiwatanakun, B., Blakeslee, J.J., Bandyopadhyay, A., Titapiwatanakun, B., Blakeslee, J.J., Yang, H., Mravec, J., Sauer, M., Cheng, Y., Adamec, J., Nagashima, A., Geisler, M., Sakai, T., Friml, J., Peer, W.A. and Murphy, A.S. (2009) ABCB19/PGP19 stabilises PIN1 in membrane microdomains in Arabidopsis. *Plant Journal* **57**, 27-44.

Titapiwatanakun, B. and Murphy A.S. (2009) Post-transcriptional regulation of auxin transport proteins: cellular trafficking, protein phosphorylation, protein maturation, ubiquitination, and membrane composition. *Journal of Experimental Botany* **60**, 1093-1107.

Tsuda, E., Yang, H., Nishimura, T., Uehara, Y., Sakai, T., Furutani, M., Koshib,a T., Hirose, M., Nozaki, H., Murphy, A.S., and Hayashi ,K.I. (2011) Alkoxy-auxins are selective inhibitors of auxin transport mediated by PIN, ABCB and AUX1 transporters. *J. Biol. Chem*. **286**, 2354-2364.

Vieten, A., Vanneste, S., Wisniewska, J., Benková, E., Benjamins, R., Beeckman, T., Luschnig, C., and Friml, J. (2005) Functional redundancy of PIN proteins is accompanied by auxin-dependent cross-regulation of PIN expression. *Development* **132**, 4521-4531.

Wu, G., Lewis, D.R. and Spalding, E.P. (2007) Mutations in Arabidopsis multidrug resistance-like ABC transporters separate the roles of acropetal and basipetal auxin transport in lateral root development. *The Plant Cell* **19**, 1826–1837.

Wu, G., Otegui, M.S., and Spalding, E.P. (2010) The ER-Localized TWD1 immunophilin is necessary for localization of multidrug resistance-like proteins required for polar auxin transport in Arabidopsis roots. *Plant Cell* **22**, 3295-304.

Yamamoto, M. and Yamamoto, K.T. (1998) Differential effects of 1-naphthaleneacetic acid, indole-3-acetic acid and 2,4-dichlorophenoxyacetic acid on the gravitropic response of roots in an auxin-resistant mutant of Arabidopsis, aux1. *Plant Cell Physiology* **39**, 660-664.

Yang, Y.D., Hammes, U.Z., Taylor, C.G., Schachtman, D.P. and Nielsen, E. (2006) High-affinity auxin transport by the AUX1 influx carrier protein. *Current Biology* **16**, 1123-1127.

Yang, H.B. and Murphy A.S. (2009) Functional expression and characterisation of Arabidopsis ABCB, AUX 1 and PIN auxin transporters in *Schizosaccharomyces pombe*. *Plant Journal* **59**, 179-191.

Zažímalová, E., Murphy A.S., Yang, H., Hoyerová, K. and Hošek, P. (2010) Auxin Transporters-Why So Many? *Cold. Spring. Harb. Perspect. Biol.* **2**, a001552.

Figure legends

Figure 1. ABCB4-mediated auxin transport is activated by IAA

A. Shootward ^{3}H-IAA (20 nL [25 fmol] placed on root cap/S3 columella) transport from the quiescent centre in 5-day-old Arabidopsis roots. "a" ^{3}H-IAA, "b"+10X cold IAA, ANOVA, Dunnet's post-hoc, $P<0.05$. **B.** *ABCB4$_{pro}$:*ABCB4-GFP signals in control and 3h after 200 nL 10 nmol IAA placed on root cap/S3 columella. Bar: 15 µm. **C**. Application of increasing 3H-IAA concentrations result in greater reductions in shootward transport in *abcb4* compared to Col-0 and *pin2*. **D.** Root tip (0.5mm) net 3H-IAA accumulation assays decreased in *abcb4* and increased in ABCB4 overexpressor (ABCB4-OX) at 15 min. The pattern is reversed at 30 min. $^{a,b,c}P<0.05$. **E.** Free IAA levels in differentiation/maturation zone of root (2mm segment starting 1.5mm from apex). Error bars, SD (n=3 pools of 10 seedlings for assays, except D., n=50 seedlings).

Figure 2. ABCB4 localisation in Arabidopsis root hairs.

5-d Arabidopsis seedlings. **A.** Treatment with increasing IAA concentrations inhibits root hair elongation. Mean lengths and SD from the first ten root hairs measured starting 1.5mm from the root apex (10 seedling pools, n=3). $*P<0.05$. **B.** Root hairs in region 1.5mm above the *abcb4* root apex are consistently longer than in wild-type. Bar, 100 µm. **C.** Visualisation of *ABCB4$_{pro}$:*ABCB4-GFP shows a signal at the plasma membrane in atrichoblast (a) and trichoblast (t) cells in dim light-acclimated light-grown seedlings. **D.** ABCB4-GFP signals in roots hairs after 5h 20 nM IAA treatment in dim light-acclimated light-grown seedlings**. E.** ABCB4-GFP signals in root hairs in light-grown seedlings. Bar, 50 µm (C-E). **(F-K)** *ABCB4$_{pro}$:*ABCB4-GFP localisation in epidermal cells is sensitive to auxins, NPA, and DMSO. **F.** Ethanol (EtOH), 0.1%, 5h; **G.** IAA, 1 µM, 5h; **H.** 2,4-D, 1 µM, 5h; **I.** DMSO, 0.05%, 5h; **J.** NPA, 10 µM, 5h; **K.** In *twd1-3*. Bar, 10 µm.

Figure 3. ABCB4 transports benzoic acid, but not oxIAA out of the root.

A. Root tip uptake assays indicate that ABCB4 mediates ^{3}H-benzoic acid (BeA) efflux. **B.** Application of increasing amounts of ^{3}H-IAA to the shoot apex results in increased oxIAA and oxIAA-Gluc accumulation in the root. (50 seedling pools, n=3, error bars, SD). **C.** ^{3}H-oxIAA purified from extracts (see Methods) is not polarly transported in Arabidopsis seedlings. **D.** ox-IAA and oxIAA-Gluc levels are not increased in *abcb4.* oxIAA-Gluc levels are normalized against a ^{13}C-IAA standard so are relative values. **E.** oxIAA does not compete with shootward

transport of ^{3}H-IAA from the root apex and activates ABCB4-mediated ^{3}H-IAA transport *in planta.* (10 seedling pools, n=3). Error bars, SD. ^{*,a,b}P<0.05.

Figure 4. ABCB4 overexpression in BY-2 cells shows auxin related phenotypes.
A. Decreased cell multiplication/density during 7-day sub-cultivation interval in PIN1-GFP and ABCB4-GFP cell lines. Error bars, SE (n=8). **B.** Cell size distribution in control and ABCB4-GFP cells scored 3-day post-inoculation. **C.** ABCB4-GFP and PIN1-GFP fluorescence from single confocal scans and differential interference contrast, DMSO solvent control, 2-day cell cultures. Bars, 40μm. **D.** FRAP dynamics in ABCB4-GFP and PIN1-GFP expressing cells.

Figure 5. IAA transport by ABCB4 in BY-2 cells.
A. Accumulation of ^{3}H-NAA (2 nM) in control, PIN1-GFP and ABCB4-GFP BY-2 cell lines increased after NPA (10 μM) addition. Error bars, SE (n=3). **B.** ABCB4-GFP expression reduces 3H-BeA retention. **C.** Cold BeA (10μM) does not compete with ^{3}H-2,4-D and 3H-NAA transport in control or ABCB4-GFP cells. **D, E.** 10 μM IAA, but not oxIAA, competes with ^{3}H-IAA net retention in control and ABCB4-GFP cells. Error bars, SE (n=3).

Figure 6. ABCB4-mediated 3H-IAA uptake in *S. pombe*.
A. 3H-IAA uptake by AUX1 (8 min assay). **B.** 3H-IAA uptake by AUX1 saturates at 2 μM (8 min assay). **C.** ^{3}H-IAA efflux by ABCB4 and ABCB19. ^{3}H-IAA uptake by ABCB4 saturates at >250 nM and reverses to efflux after 5 min. Error bars=SD, n=4, 2 independent experiments. Values are subtracted from vector controls (see Fig. S2C for vector).

Figure 7. ABCB4 mediates uptake but not efflux of 2,4-D.
A. Root hair responses to increasing concentrations of 2,4-D. **B**. Addition of 2-NOA (10μM) decreased accumulation of ^{3}H-2,4-D in ABCB4-GFP BY-2 cells. Error bars, SE (n=3). **C**. 2-NOA (10μM, 30min pre-treatment) initially blocked ^{3}H-2,4-D accumulation in ABCB4-GFP BT-2 cells but accumulation gradually increased after 15min. Error bars, SE (n=3). **D.** Accumulation of ^{3}H-2,4-D in ABCB4-GFP cell lines pre-treated 30min with 2-NOA or NPA (10μM) was reduced. NPA (10μM, at 13min) applied to 2-NOA pretreated cells increased ^{3}H-2,4-D accumulation compared to 2-NOA only. Error bars, SE (n=3). **E.** In binding assays of ABCB4 or 19 expressed in HeLa cells, ^{3}H-2,4-D binds ABCB4 with greater affinity than ABCB19 and is not competed away by IAA. Error bars, SD (n=3).*P<0.05. **F.** Modelling of IAA and 2,4-D binding sites to ABCB4.

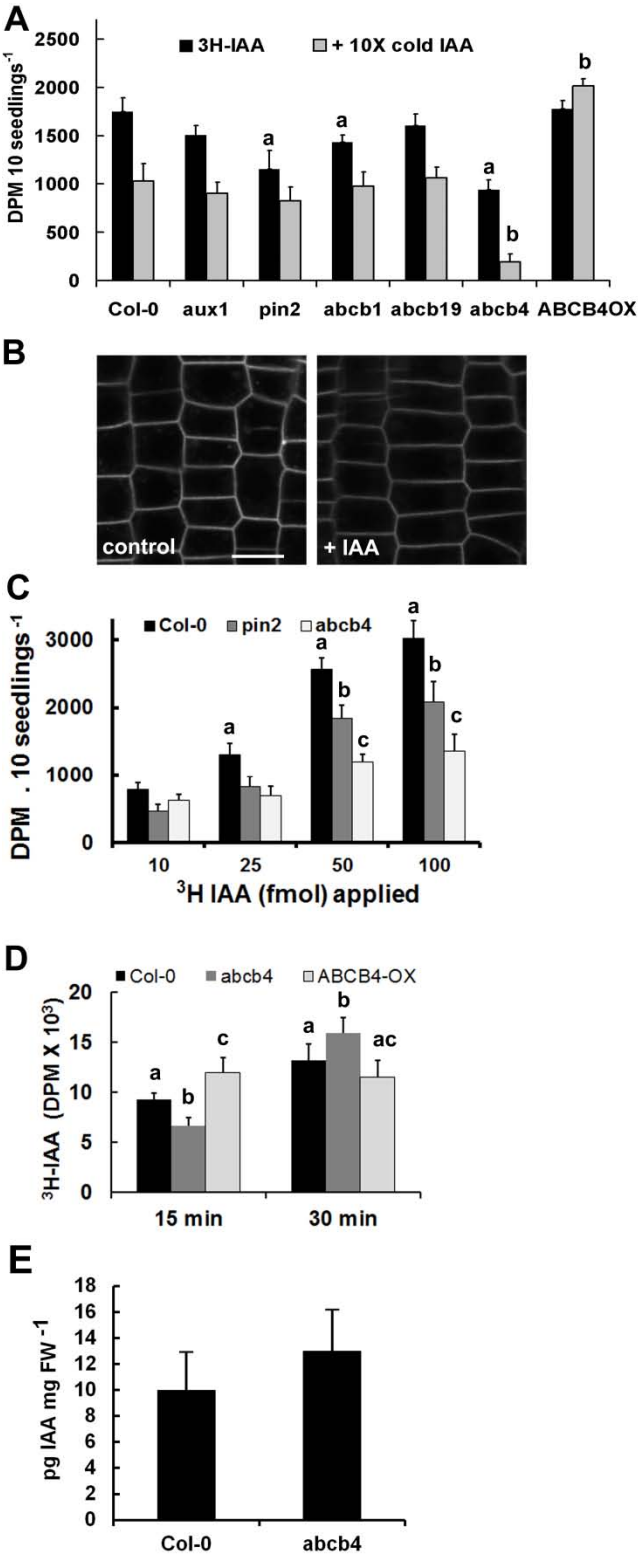

Figure 1. ABCB4-mediated auxin transport is activated by IAA

A. Shootward ^{3}H-IAA (20 nL [25 fmol] placed on root cap/S3 columella) transport from the quiescent centre in 5-day-old Arabidopsis roots. "a" ^{3}H-IAA, "b"+10X cold IAA, ANOVA, Dunnet's post-hoc, $P<0.05$. **B.** *ABCB4$_{pro}$:*ABCB4-GFP signals in control and 3h after 200 nL 10 nmol IAA placed on root cap/S3 columella. Bar: 15 µm. **C**. Application of increasing ^{3}H-IAA concentrations result in more reduced shootward transport in *abcb4.* **D.** Root tip (0.5mm) net ^{3}H-

IAA accumulation assays decreased in *abcb4* and increased in ABCB4 overexpressor (ABCB4-OX) at 15 min. The pattern is reversed at 30 min. [a,b,c]$P<0.05$. **E.** Free IAA levels in differentiation/maturation zone of root (2mm segment starting 1.5mm from apex). Error bars, SD (n=3 pools of 10 seedlings for assays, except D., n=50 seedlings).

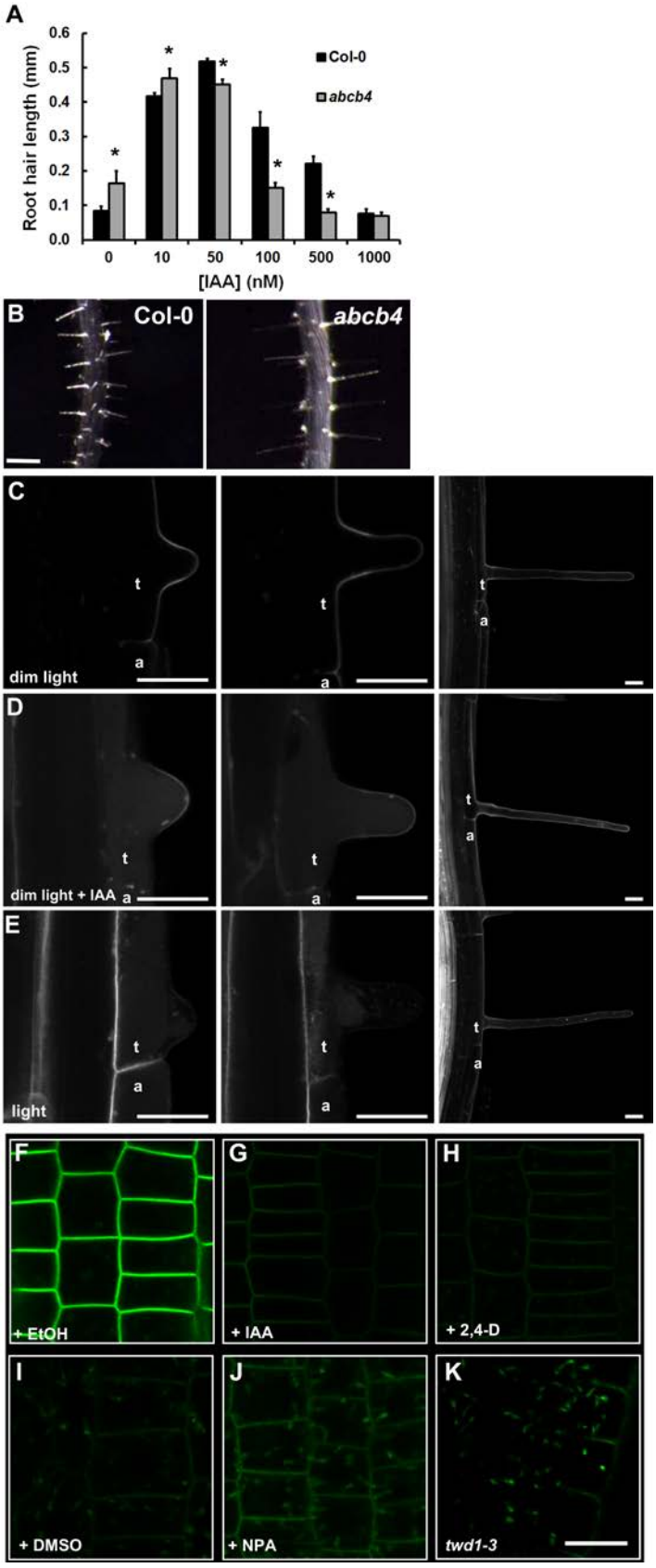

Figure 2. ABCB4 localisation in Arabidopsis root hairs.

5-d Arabidopsis seedlings. **A.** Treatment with increasing IAA concentrations inhibits root hair elongation. Mean lengths and SD from the first ten root hairs measured starting 1.5mm from the

root apex (10 seedling pools, n=3). *P<0.05. **B.** Root hairs in region 1.5mm above the *abcb4* root apex are consistently longer than in wild-type. Bar, 100 µm. **C.** Visualisation of $ABCB4_{pro:}$ABCB4-GFP shows a signal at the plasma membrane in atrichoblast (a) and trichoblast (t) cells in dim light-acclimated light-grown seedlings. **D.** ABCB4-GFP signals in roots hairs after 5h 20 nM IAA treatment in dim light-acclimated light-grown seedlings**. E.** ABCB4-GFP signals in root hairs in light-grown seedlings. Bar, 50 µm (C-E). **(F-K)** $ABCB4_{pro:}$ABCB4-GFP localisation in epidermal cells is sensitive to auxins, NPA, and DMSO. **F.** Ethanol (EtOH), 0.1%, 5h; **G.** IAA, 1 µM, 5h; **H.** 2,4-D, 1 µM, 5h; **I.** DMSO, 0.05%, 5h; **J.** NPA, 10 µM, 5h; **K.** In *twd1-3*. Bar, 10 µm.

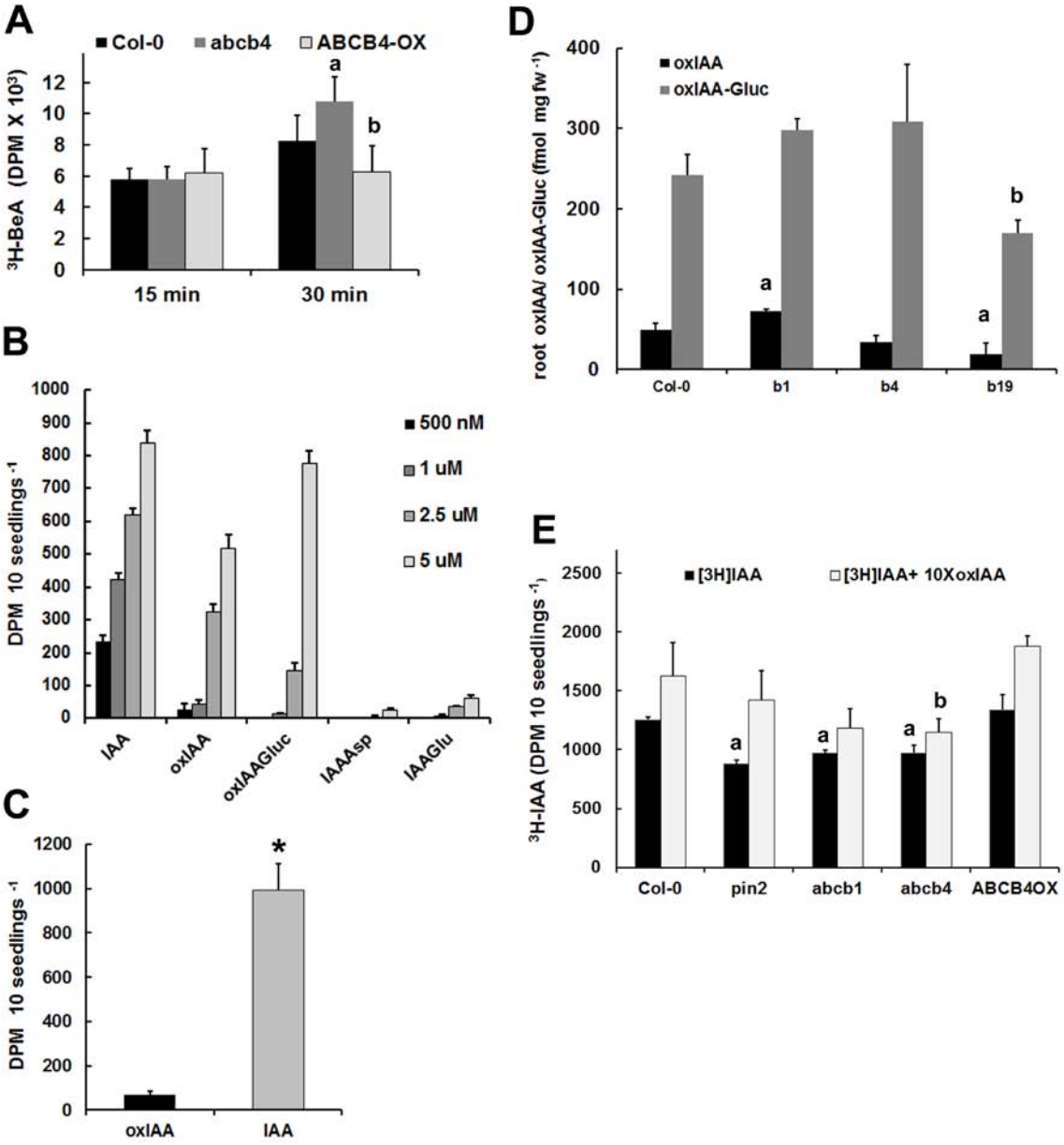

Figure 3. ABCB4 transports benzoic acid, but not oxIAA out of the root.

A. Root tip uptake assays indicate that ABCB4 mediates ^{3}H-benzoic acid (BeA) efflux. **B.** Application of increasing amounts of ^{3}H-IAA to the shoot apex results in increased oxIAA and oxIAA-Gluc accumulation in the root. (50 seedling pools, n=3, error bars, SD). **C.** ^{3}H-oxIAA purified from extracts (see Methods) is not polarly transported in Arabidopsis seedlings. **D.** oxIAA and oxIAA-Gluc levels are not increased in *abcb4.* oxIAA-Gluc levels are normalized against a ^{13}C-IAA standard so are relative values. **E.** oxIAA does not compete with shootward transport of ^{3}H-IAA from the root apex and activates ABCB4-mediated ^{3}H-IAA transport *in planta.* (10 seedling pools, n=3). Error bars, SD. $^{*,a,b}P<0.05$.

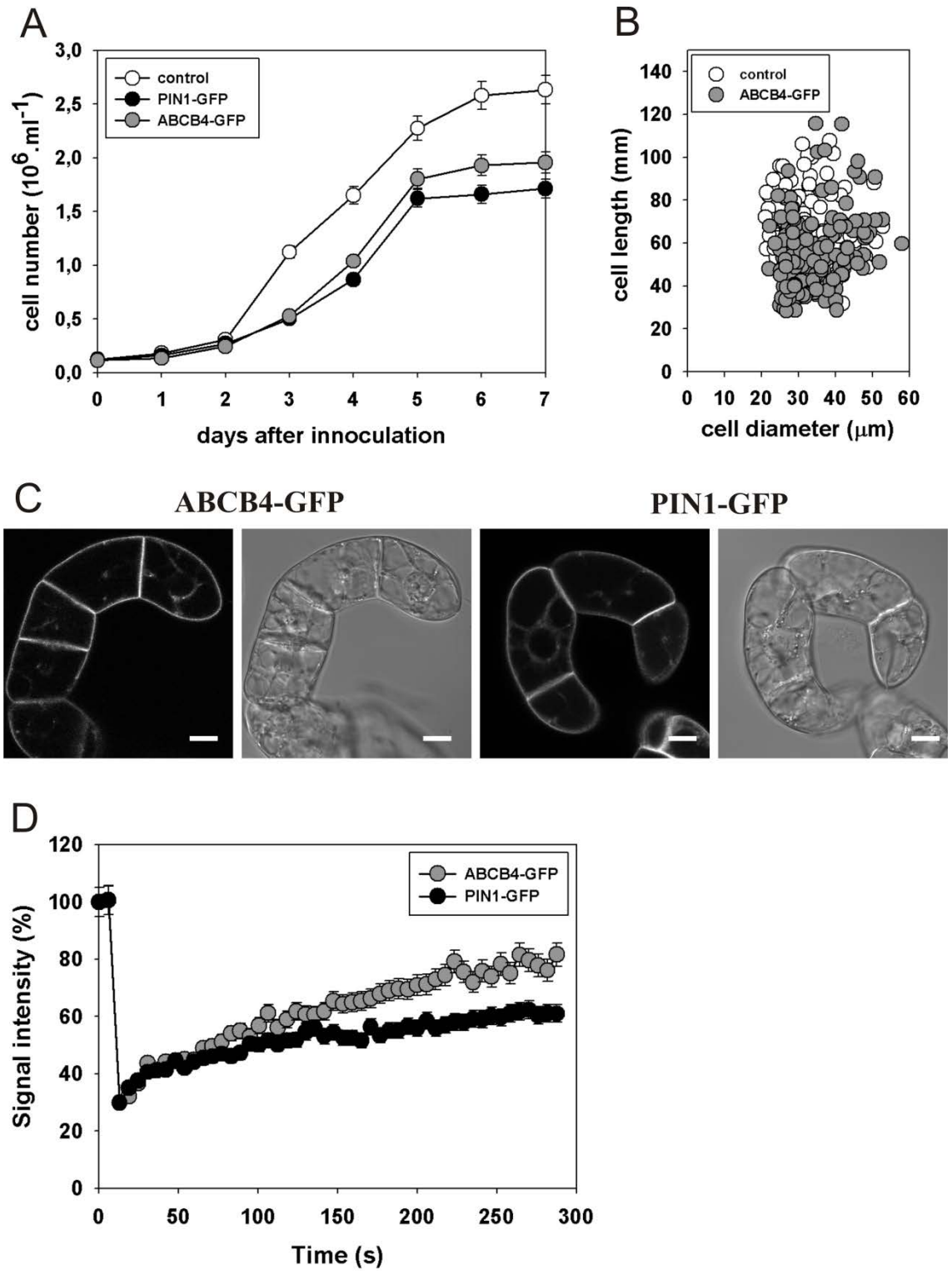

Figure 4. ABCB4 overexpression in BY-2 cells shows auxin related phenotypes.

A. Decreased cell multiplication/density during 7-day sub-cultivation interval in PIN1-GFP and ABCB4-GFP cell lines. Error bars, SE (n=8). **B.** Cell size distribution in control and ABCB4-GFP cells scored 3-day post-inoculation. **C.** ABCB4-GFP and PIN1-GFP fluorescence from single confocal scans and differential interference contrast, DMSO solvent control, 2-day cell cultures. Bars, 40μm. **D.** FRAP dynamics in ABCB4-GFP and PIN1-GFP expressing cells.

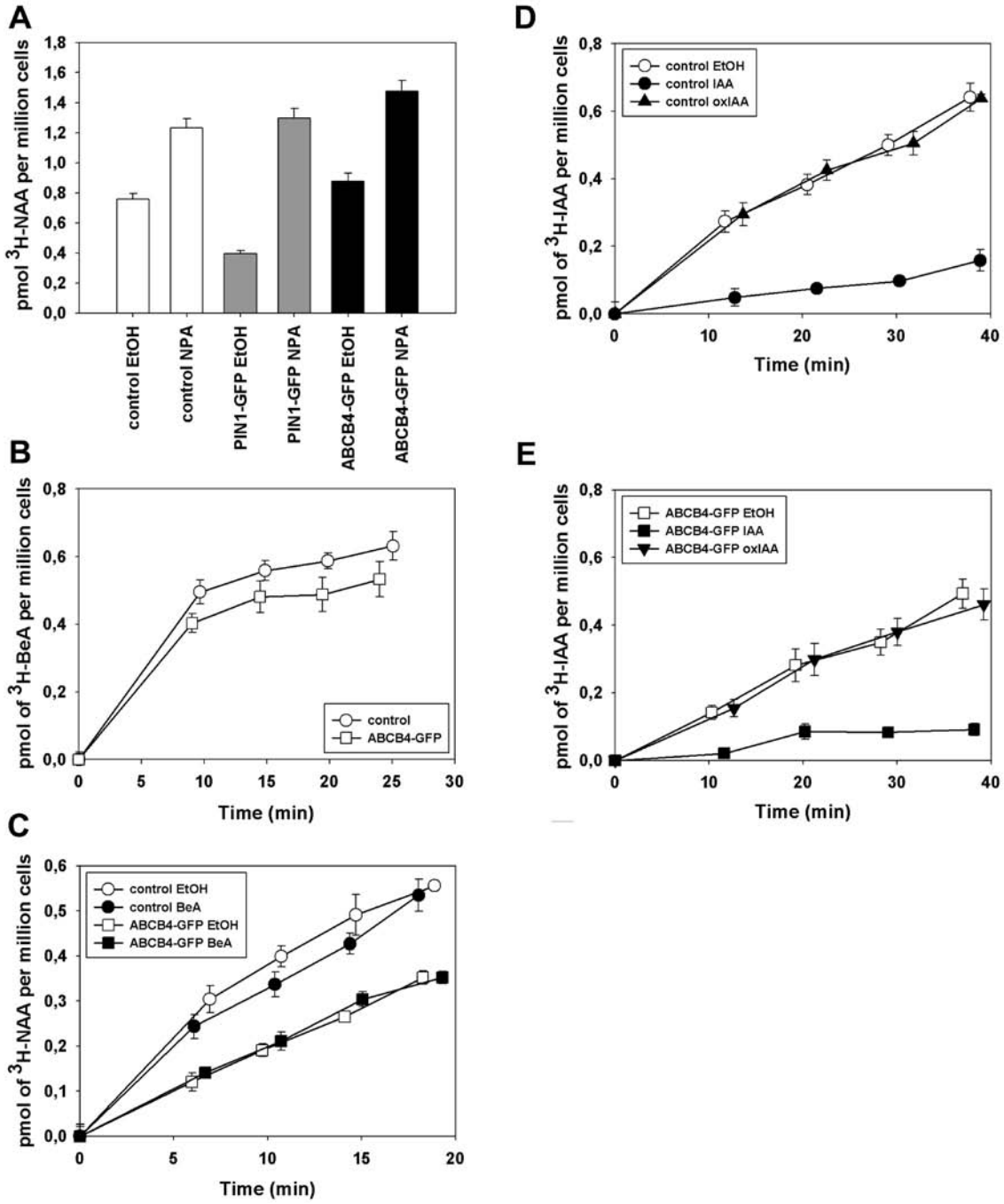

Figure 5. IAA transport by ABCB4 in BY-2 cells.

A. Accumulation of ^{3}H-NAA (2 nM) in control, PIN1-GFP and ABCB4-GFP BY-2 cell lines increased after NPA (10 μM) addition. Error bars, SE (n=3). **B.** ABCB4-GFP expression reduces ^{3}H-BeA retention. **C.** Cold BeA (10μM) does not compete with ^{3}H-2,4-D and ^{3}H-NAA transport in control or ABCB4-GFP cells. **D, E.** 10 μM IAA, but not oxIAA, competes with ^{3}H-IAA net retention in control and ABCB4-GFP cells. Error bars, SE (n=3).

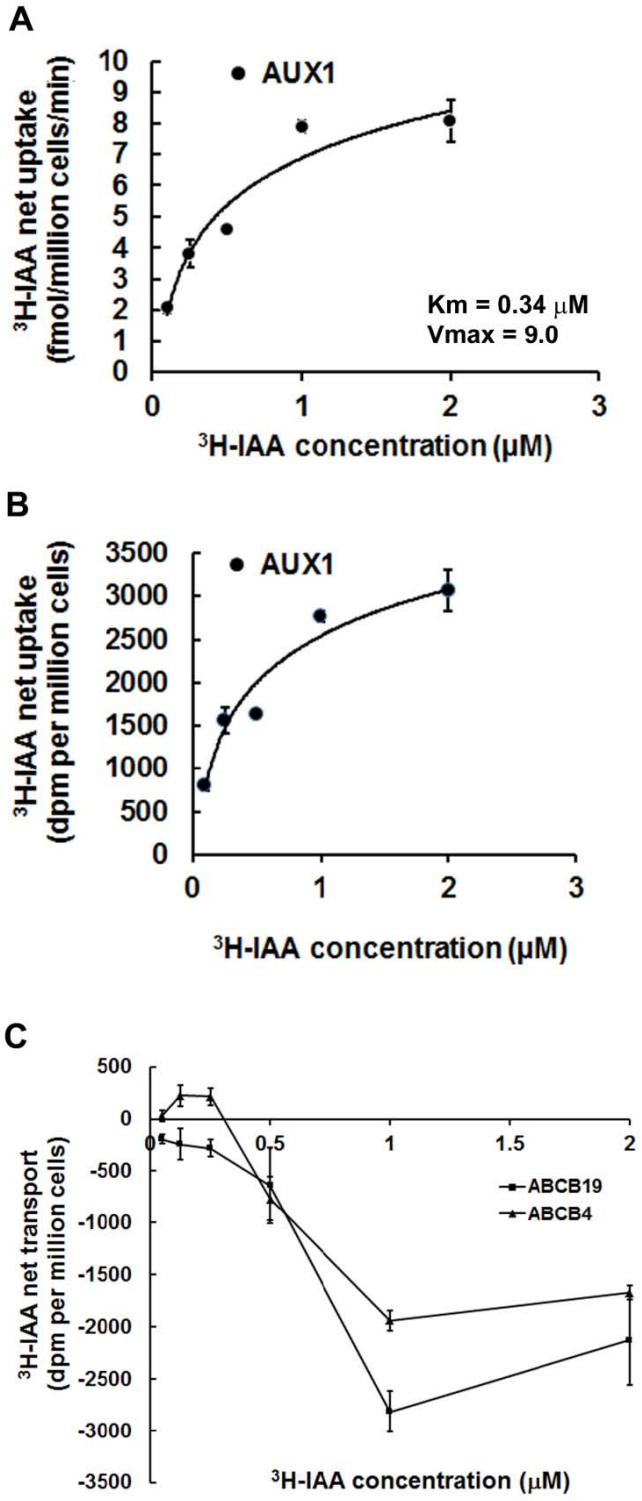

Figure 6. ABCB4-mediated ^{3}H-IAA uptake in *S. pombe*.

A. ^{3}H-IAA uptake by AUX1 (8 min assay). **B.** ^{3}H-IAA uptake by AUX1 saturates at 2 μM (8 min assay). **C.** ^{3}H-IAA efflux by ABCB4 and ABCB19. ^{3}H-IAA uptake by ABCB4 saturates at >250 nM and reverses to efflux after 5 min. Error bars=SD, n=4, 2 independent experiments. Values are subtracted from vector controls (see Fig. S2C for vector).

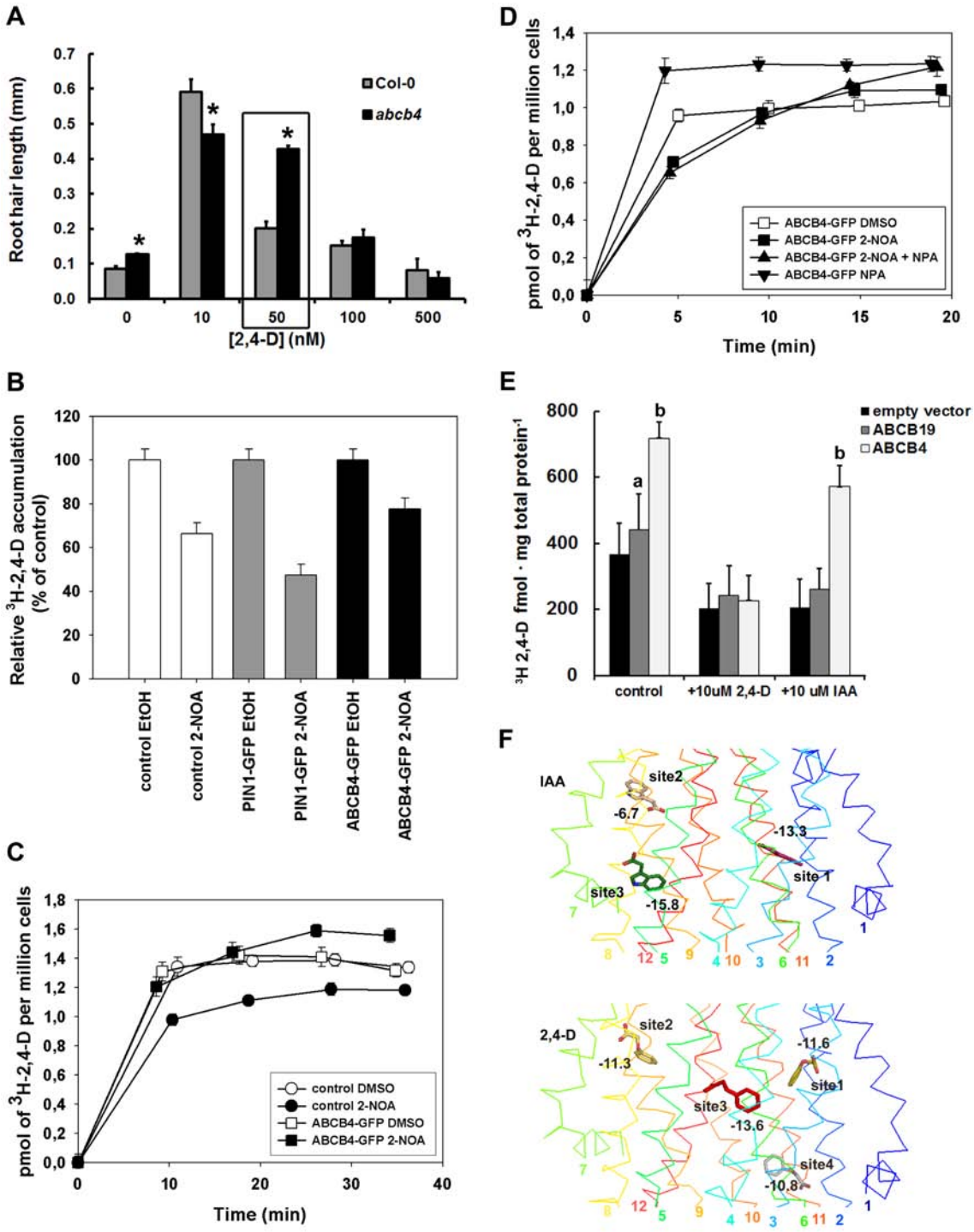

Figure 7. ABCB4 mediates uptake but not efflux of 2,4-D.

A. Root hair responses to increasing concentrations of 2,4-D. **B**. Addition of 2-NOA (10µM) decreased accumulation of ^{3}H-2,4-D in ABCB4-GFP BY-2 cells. Error bars, SE (n=3). **C**. 2-NOA (10µM, 30min pre-treatment) initially blocked ^{3}H-2,4-D accumulation in ABCB4-GFP BY-2 cells but accumulation gradually increased after 15min. Error bars, SE (n=3). **D.** Accumulation of ^{3}H-2,4-D in ABCB4-GFP cell lines pre-treated 30min with 2-NOA or NPA (10µM) was reduced. NPA (10µM, at 13min) applied to 2-NOA pretreated cells increased ^{3}H-2,4-D accumulation compared to 2-NOA only. Error bars, SE (n=3). **E.** In binding assays of

ABCB4 or 19 expressed in HeLa cells, ^{3}H-2,4-D binds ABCB4 with greater affinity than ABCB19 and is not competed away by IAA. Error bars, SD (n=3).*P<0.05. **F.** Modelling of IAA and 2,4-D binding sites to ABCB4.

Supporting Data

Figure S1. *ABCB4* expression in response to stimuli.

Figure S2. Shootward ^{3}H-IAA transport from the root apex in wild-type and auxin transport mutants.

Figure S3. *ABCB4* expression in root cell types and ABCB4-GFP ethanol solvent controls.

Figure S4. oxIAA competition experiments and transport assays controls.

Figure S5. ^{3}H-2,4-D accumulation in BY-2 cells pretreated with cold IAA or 2,4-D.

Figure S6. Gradual reversal of ABCB4 activity in BY-2 cells.

Figure S7. ^{3}H-2,4-D accumulation after washout with uptake buffer.

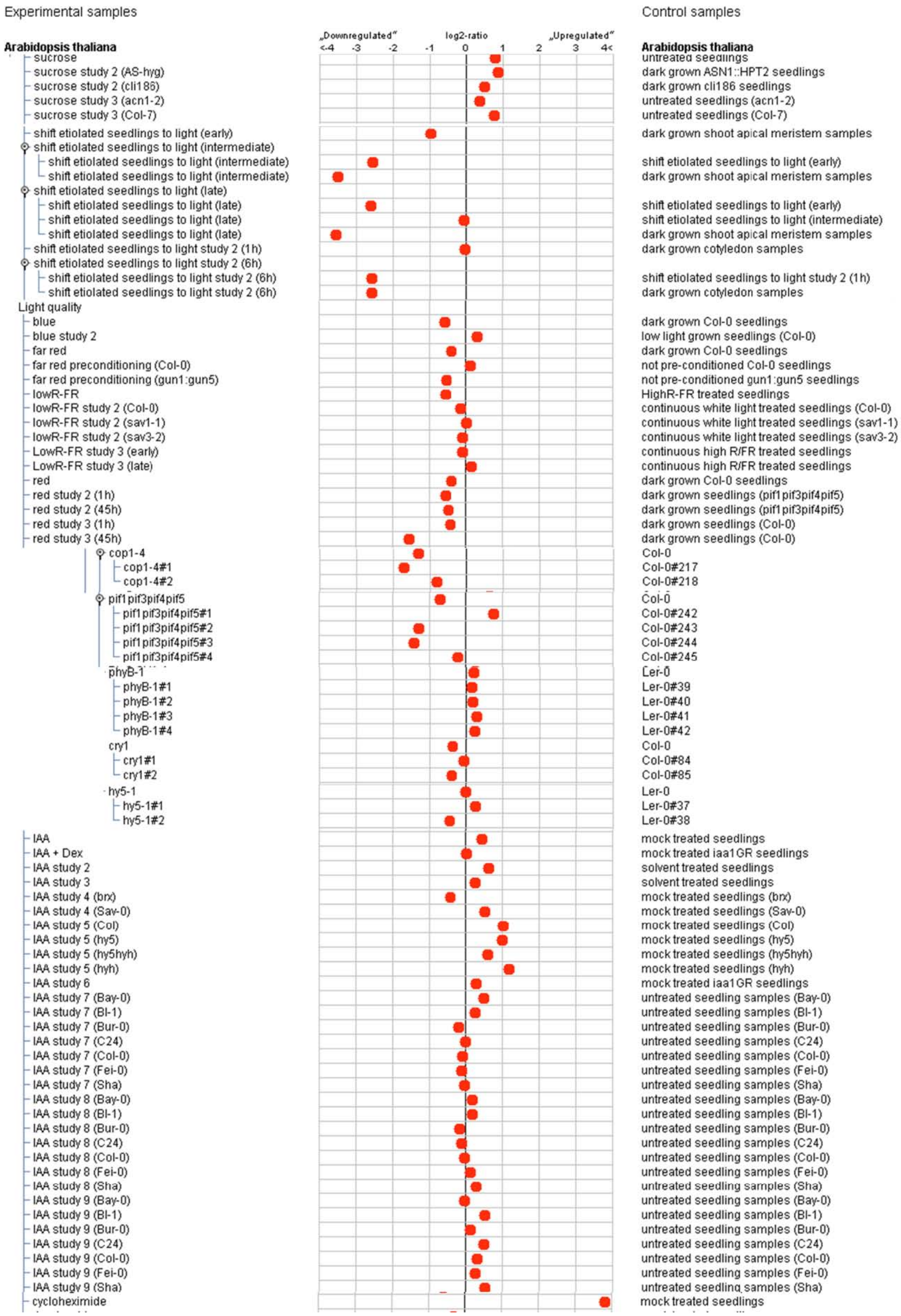

Figure S1. *ABCB4* expression in response to stimuli from Genevestigator (Hruz et al., 2008).

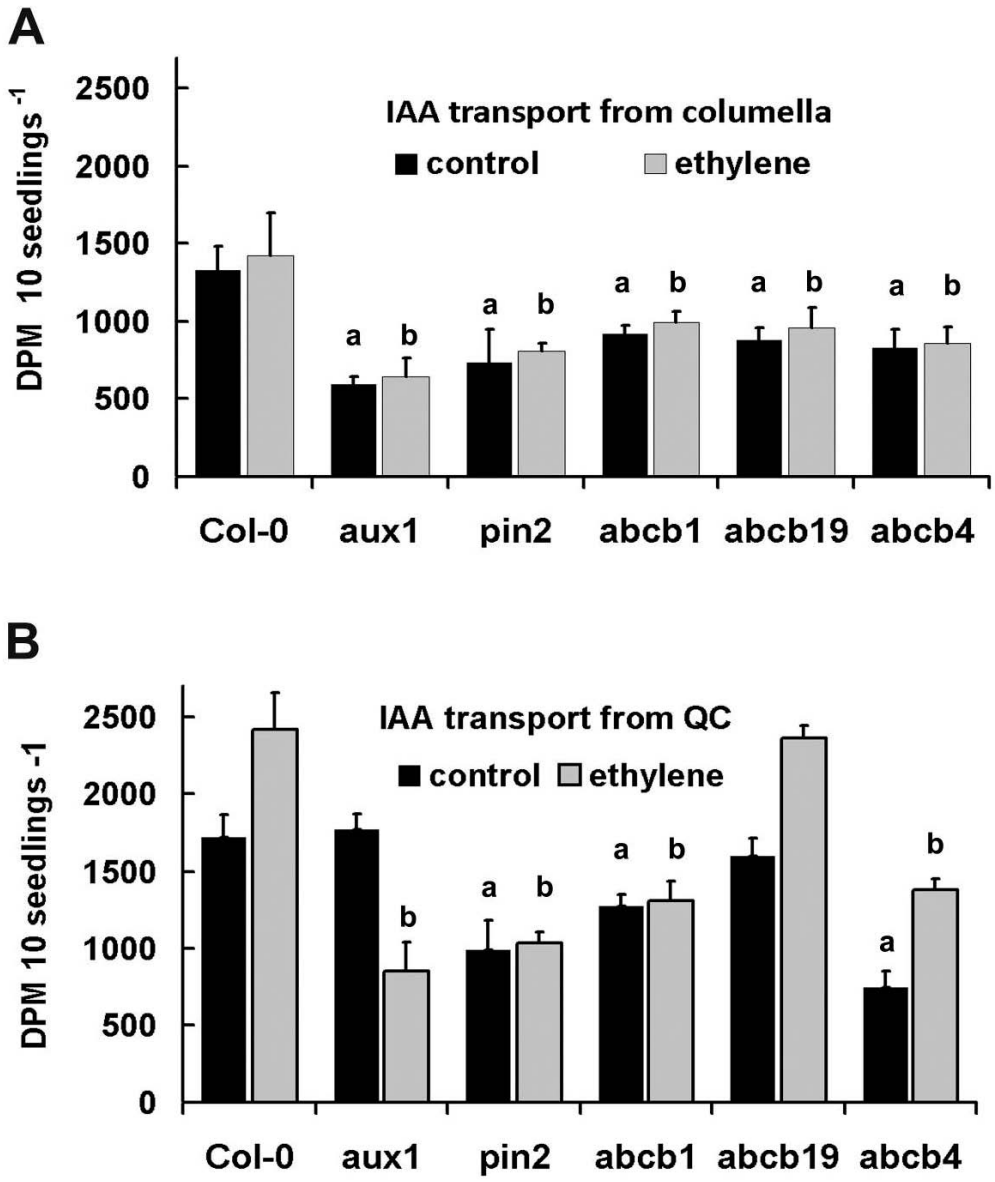

Figure S2. Shootward ^{3}H-IAA transport from the root apex in wild-type and auxin transport mutants. **A.** Transport with 25nL (25fmol) ^{3}H-IAA placed on columella cells (Peer and Murphy, 2007) ± ethylene (0.01% constant rate flow). **B.** Transport with 25nL (25fmol) ^{3}H-IAA placed over quiescent centre (QC) of wild-type or auxin transport mutant roots ± ethylene. Seedlings per assay =10, n=3, error bars are SD. Letters represent statistical difference from wild-type, $P < 0.05$.

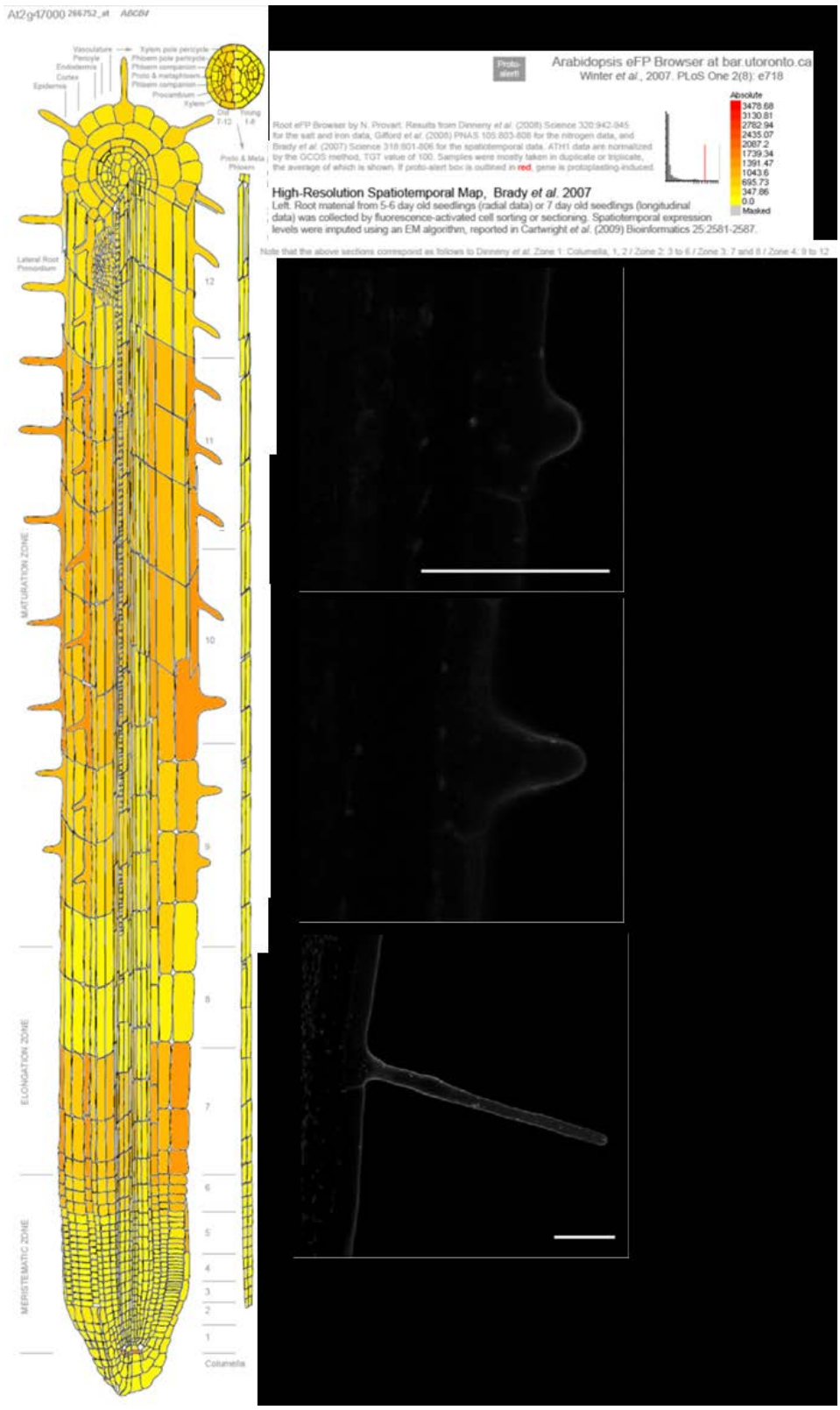

Figure S3. *ABCB4* expression in the root from eFPBroswer (Winter et al., 2007; Brady et al., 2007) (left), and 0.00001 % ethanol solvent control for IAA treatment for ABCB4-GFP localization (right). Bar, 50 μm.

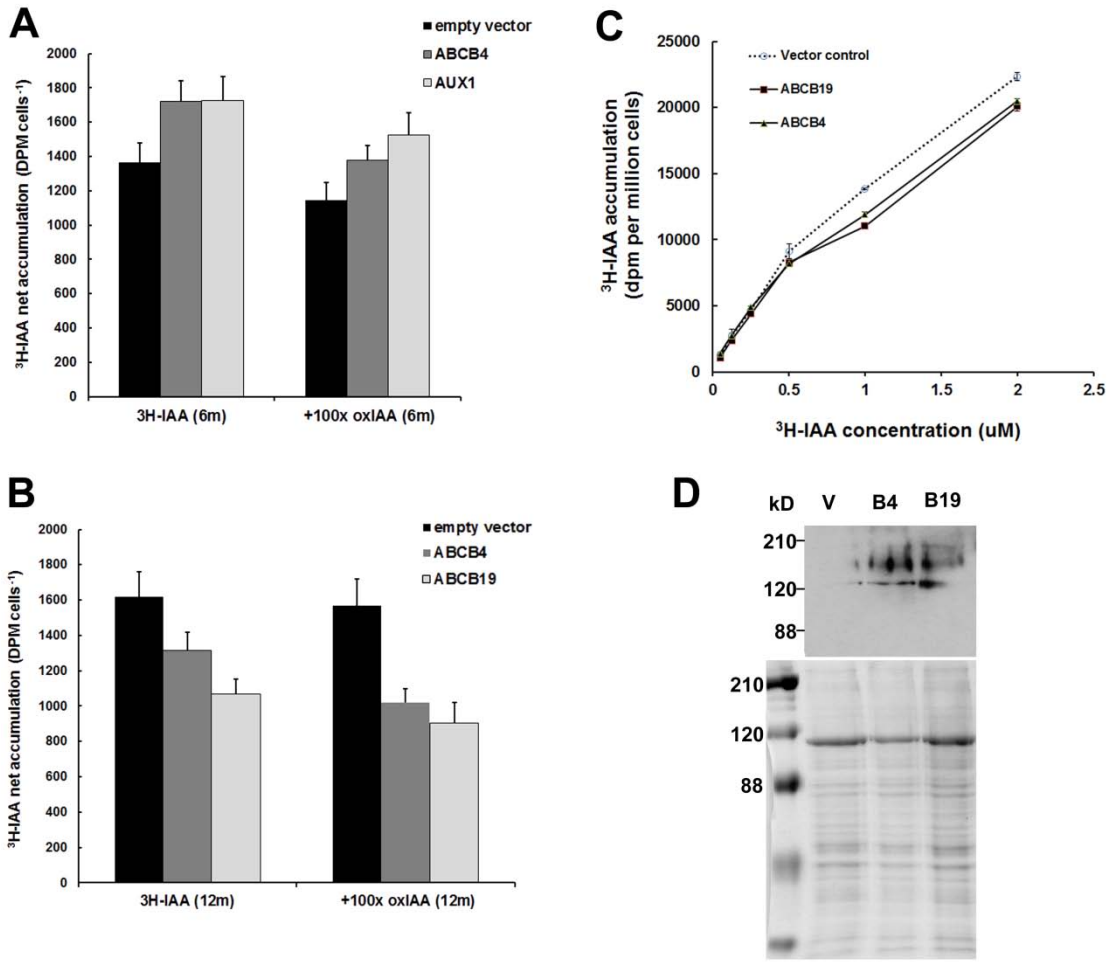

Figure S4. oxIAA competition experiments and transport assays controls.

A-B. oxIAA competition experiments with ^{3}H-IAA uptake (6 minutes) and efflux (12 minutes) of ABCB4, AUX1, and ABCB19 expressed in *S. pombe*. **A.** In six minute uptake assays, a small amount of competition is seen when ^{3}H-IAA is challenged with 100X oxIAA. **B.** No competition is seen when 100X oxIAA is used to challenge ^{3}H-IAA export. N=3, error bars = SD. **C.** Net ^{3}H-IAA accumulation in *S. pombe* expressing vector only, ABCB4 or ABCB19. **D.** Western blot analysis (α-hemaglutinnin, upper panel) of microsomal membranes from *S. pombe* expressing vector only (V), ABCB4 (B4) or ABCB19 (B19). Coomassie stained gel, lower panel.

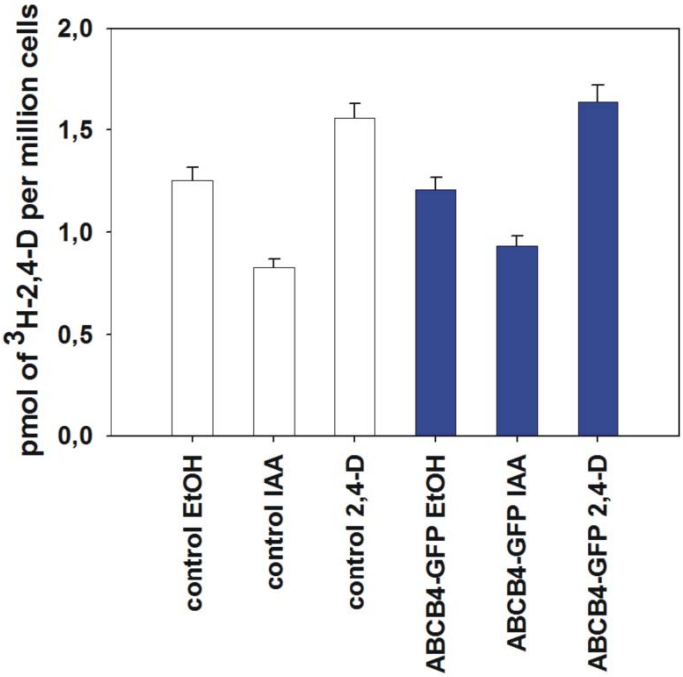

Figure S5. Competition accumulation assays of ^{3}H-2,4-D in BY-2 cells (control, ABCB4-GFP) pretreated with cold IAA or 2,4-D. Both variants (control and ABCB4-GFP) were pretreated for 30 min with 5 μM cold IAA or 2,4-D. In case of cold IAA, slight decrease in ^{3}H-2,4-D uptake while in case of 2,4-D significant increase was observed. We suggest that it is a result of non-competitive 2,4-D inhibition of ABCB4 auxin efflux as similarly described Yang and Murphy (2009) when ABCB4 was expressed in *S. pombe*. Control line (white columns) and ABCB4-GFP line (blue columns).

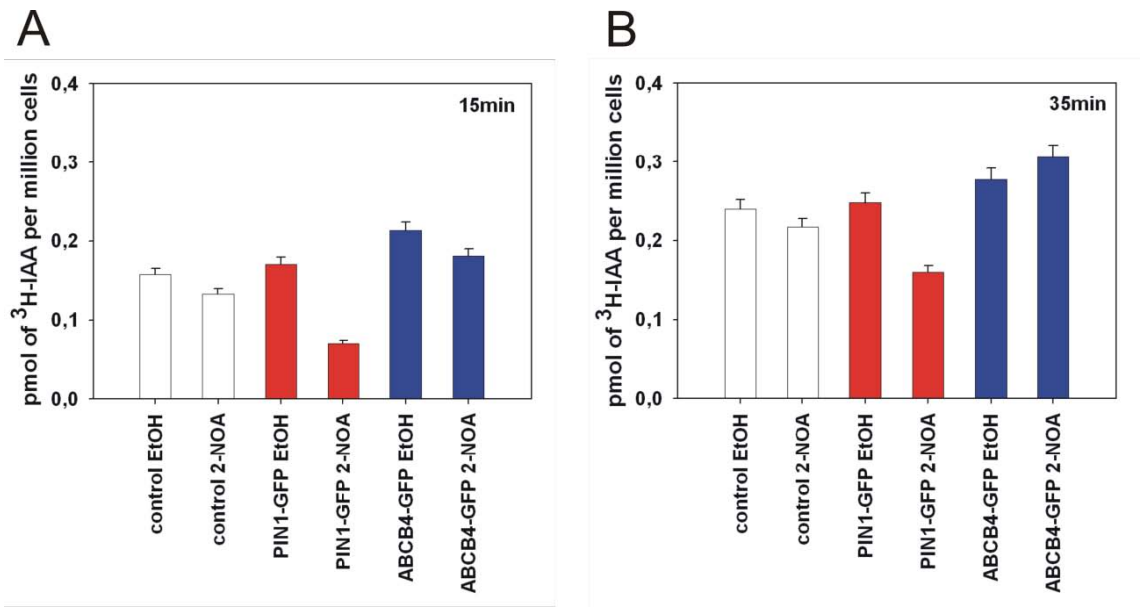

Figure S6. Gradual reversal activity of ABCB4 transporter in early and later time of ^{3}H-IAA accumulation in BY-2 cells (control, PIN1-GFP, ABCB4-GFP) versus 2-NOA.

IAA accumulation in the ABCB4-GFP cell line treated with 2-NOA was lower at 15 min compared to solvent controls, but at 35 min, increased IAA accumulation is observed after 2-NOA application. Non-transformed and lines expressing PIN1 are included as controls. It is important to note that experiments with ^{3}H-IAA in BY-2 cell culture are difficult to interpret due to rapid IAA metabolism and combined uptake and efflux observed with IAA. Control line (white columns), PIN1-GFP line (red column) and ABCB4-GFP line (blue columns).

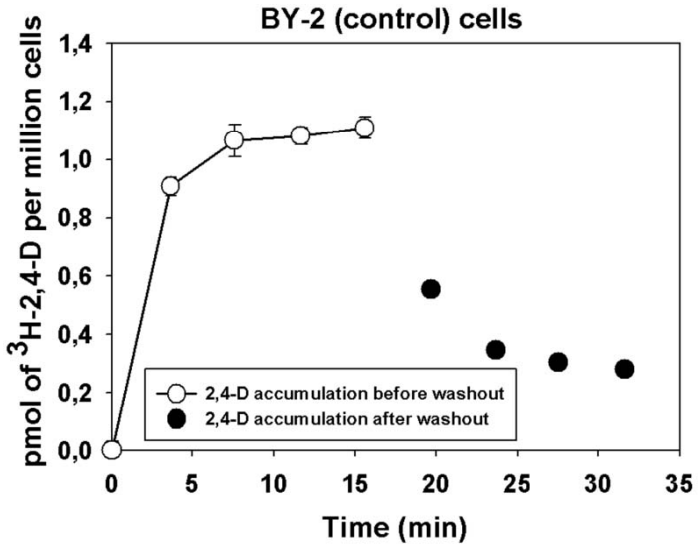

Figure S7. The effect on 3H-2,4-D accumulation after wash out with uptake buffer.

Here we tried to solve whether wash out with uptake buffer is able to removed all 2,4-D from BY-2 cells cultivated on medium supplemented with 2,4-D.

Wash out of BY-2 cells (45 and 90 min) with uptake buffer before radiolabeled auxin accumulation assays is using as a standard procedure. Similarly we did short wash out of BY-2 cells after 16 min of running ^{3}H-2,4-D accumulation experiment. In the time of 16min uptake buffer with 3H-2,4-D was filtered, the cells were flushed, and then fresh uptake buffer without ^{3}H-2,4-D has been added. The results quite clearly showed that even with such rapid wash out there is marked decrease in accumulation of ^{3}H-2,4-D in the cells. So we can conclude that long standard wash out procedure is enough to retain nearly all 2,4-D from BY-2 cells.

(S1) 2,4-D accumulation curve before wash out (white circles) and after wash out (black circles).

Supplementary references

Brady, S.M., Orlando, D.A., Lee, J.Y., Wang, J.Y., Koch, J., Dinneny, J.R., Mace, D., Ohler, U., and Benfey, P.N. (2007) A high-resolution root spatiotemporal map reveals dominant expression patterns. *Science* **318**:801-806.

Hruz, T., Laule, O., Szabo, G., Wessendorp, F., Bleuler, S., Oertle, L., Widmayer, P., Gruissem, W., and Zimmermann, P. (2008) Genevestigator v3: a reference expression database for the meta-analysis of transcriptomes. Adv *Bioinformatics*. **2008**,420747.

Dobrev P. and Kamínek M. (2002) Fast and efficient separation of cytokinins from auxin and abscisic acid and their purification using mixed-mode solid-phase extraction. *J. Chromatography A* **950**, 21-29.

Dobrev P., Havlíček M., Vágner M., Malbeck J. and Kamínek M. (2005) Purification and determination of plant hormones auxin and abscisic acid using solid phase extraction and two-dimensional high performance liquid chromatography. *J.Chromatography A* **1075**,159-166.

Mravec, J., Kubeš, M., Bielach, A., Gaykova, V., Petrášek, J., Skůpa, P., Chand, S., Benková, E., Zažímalová, E., and Friml, J. (2008) Interaction of PIN and PGP transport mechanisms in auxin distribution-dependent development. Development **135**, 3345-3354.

Petrášek, J., Mravec, J., Bouchard, R., Blakeslee, J.J., Abas, M., Seifertová, D., Wisniewska, J., Tadele, Z., Kubeš, M., Čovanová, M., Dhonukshe, P., Skůpa, P., Benková, E., Perry, L., Křeček, P., Lee, O.R., Fink, G.R., Geisler, M., Murphy, A.S., Luschnig, C., Zažímalová, E. and Friml, J. (2006) PIN proteins perform a rate-limiting function in cellular auxin efflux. *Science* **312**, 914-918.

Winter D, Vinegar B, Nahal H, Ammar R, Wilson GV, and Provart, N.J. (2007) An "Electronic Fluorescent Pictograph" Browser for Exploring and Analyzing Large-Scale Biological Data Sets. *PLoS ONE* **2**, e718. doi:10.1371/journal.pone.0000718

Yang, H.B. and Murphy A.S. (2009) Functional expression and characterization of Arabidopsis ABCB, AUX 1 and PIN auxin transporters in *Schizosaccharomyces pombe*. *Plant Journal* **59**, 179-191.

6.6. Chapter 6 - New insights into auxin transport on cellular level by means of mathematical-modelling-motivated research

Petr Hošek*, **Martin Kubeš***, Martina Laňková, Petre I. Dobrev, Petr Klíma, Zdeněk Wimmer, Milada Kohoutová, Jan Petrášek, Eva Zažímalová, Klára Hoyerová, Marcel Jiřina

* These authors contributed equally to this work.

Manuscript in preparation

This manuscript originated from collaboration between Dr. Eva Zažímalová and Dr. Marcel Jiřina laboratories.

My contribution to this article was mainly in characterization of ^{3}H-BeA, ^{3}H-2,4-D and ^{3}H-NAA metabolism in tobacco BY-2 and Xanthi cell cultures together with identification of the main NAA metabolite in BY-2 cells as NAA glucosyl ester based on collaboration with Petre I. Dobrev (HPLC, LC-ESI-MS/MS analysis, confirmation of ester bond in NAA glucosyl ester and discussions), Zdeněk Wimmer (synthesis of NAA metabolite, discussion), Jiří Malbeck and Bedřich Pešek (MS analysis, discussions) and Helena Lipavská (HPLC analysis, discussion). I was partially involved in ^{3}H-2,4-D accumulation assays with auxin transport inhibitors NPA, CHPAA and their combination. I have been involved also in the manuscript preparation and processing of relevant results.

It was indicated that NAA is rapidly metabolized to the major metabolite (identified as NAA glucosyl ester) and after 10 min of incubation this metabolite was predominant in BY-2 cells. All NAA metabolites including predominant NAA glucosyl ester remained in cells and thus confused results of ^{3}H-NAA accumulation assays. Compared to NAA, 2,4-D was only partially metabolized to three unknown products and the analysis of incubation medium also confirmed retention of the 2,4-D metabolites in BY-2 cells. As a control BeA was used and surprisingly it was quickly metabolized to one predominant and one unknown minor products. In incubation medium both metabolites were detected insignificantly, which indicate that these products also remained in cells (Fig. 3A, B, C).
As mentioned above, the main NAA metabolite was identified by HPLC and MS techniques as NAA glucosyl ester (Fig. 4). Simultaneously the presence of ester bond in NAA glucosyl ester was confirmed by its incubation with NH_4OH (Fig. 5). Thanks to the weak 2,4-D metabolism, 2,4-D accumulation data measured under various conditions were used (in presence of auxin

transport inhibitors NPA or CHPAA, Fig. 6) and mathematical model of auxin transport to characterize and validate parameters of 2,4-D transport on cellular level was constructed.

The work was supported by the Ministry of Education, Youth and Sports of the Czech Republic project LC06034 and by the Grant Agency of the Czech Republic, project P305/11/0797.

New insights into auxin transport on cellular level by means of mathematical-modelling-motivated research

Petr Hošek[1,2‡], Martin Kubeš[1‡], Martina Laňková[1], Petre I. Dobrev[1], Petr Klíma[1], Zdeněk Wimmer[1], Milada Kohoutová[2], Jan Petrášek[1], Eva Zažímalová[1], Klára Hoyerová[1*] and Marcel Jiřina[2]

[1] *Institute of Experimental Botany, the Academy of Sciences of the Czech Republic, Rozvojová 263, CZ-165 02 Prague 6, Czech Republic*

[2] *Department of Biomedical Informatics, Faculty of Biomedical Engineering, Czech Technical University in Prague, náměstí Sítná 3105, CZ-272 01 Kladno 2, Czech Republic*

‡These authors contributed to this paper equally.

Authors e-mail addresses:

Petr Hošek - petr.hosek@fbmi.cvut.cz, Martin Kubeš - kubes@ueb.cas.cz, Martina Laňková - lankova@ueb.cas.cz, Petre I. Dobrev - dobrev@ueb.cas.cz, Petr Klíma - klima@ueb.cas.cz, Zdeněk Wimmer - wimmer@ueb.cas.cz, Milada Kohoutová - minuska666@gmail.com, Jan Petrášek - petrasek@ueb.cas.cz, Eva Zažímalová - zazimalova@ueb.cas.cz, Klára Hoyerová - hoyerova@ueb.cas.cz, Marcel Jiřina - jirina@fbmi.cvut.cz

*Corresponding author:

Klára Hoyerová: Institute of Experimental Botany, the Academy of Sciences of the Czech Republic, Rozvojová 263, CZ-165 02 Prague 6, Czech Republic; Telephone +420 225 106 436, fax +420 225 106 446, e-mail: hoyerova@ueb.cas.cz

Key words: auxin, IAA, NAA, 2,4-D, auxin transport, auxin metabolism, auxin transport inhibitors, mathematical modelling, BY-2 tobacco cells

Abstract

During the last fifteen years, polar auxin transport - an important spatial and temporal signalling and coordination mechanism in plant tissues - was thoroughly studied by various approaches. Mathematical modelling as one of these approaches has been frequently used to explore many hypotheses on cell polarization and related regulatory mechanisms, especially on the level of plant tissues. In contrast, auxin transport on the single-cell level has remained much less addressed. Here we describe the transport of auxin at the cellular level using basic techniques of mathematical modelling and characterization of auxin transport mechanisms in tobacco cells.

Our results indicate that naphthalene-1-acetic acid (NAA) is strongly and rapidly metabolized during accumulation experiments in BY-2 tobacco cells. We identified the predominant metabolite as NAA glucosyl ester (NAA-Glc) and thus confirmed assumption made by Delbarre *et al*. (1994). Further, we show that NAA-Glc is retained in the cells, thus raising the apparent intracellular concentration of labelled NAA as measured by accumulation assays and consequently, resulting in serious underestimation of auxin efflux carriers transport capacity. not only for NAA but consequently also for IAA in the past. In contrast, metabolism of 2,4-dichlorophenoxyacetic acid (2,4-D) remains fairly weak in the time span of accumulation assays, making 2,4-D an good tool for probing auxin transport on cellular level. Hence, using 2,4-D accumulation data measured under various conditions including presence of auxin transport inhibitors 1-naphthylphthalamic acid or 3-chloro-4-hydroxyphenylacetic acid, and employing a mathematical model of auxin transport we characterize and validate parameters of 2,4-D transport on cellular level.

Introduction

Auxin is a signal molecule present in plant tissues in nanomolar concentrations (Davies *et al.*, 2010). Fast and tight control of its levels is necessary for proper regulation of plant growth, development and responses to environmental stimuli. Such control is realized on the cellular level via two basic processes – auxin metabolism and auxin transport. Auxin metabolism (biosynthesis, conjugation, de-conjugation, and degradation) (Normanly *et al.*, 2010, Ludwig-Müller, 2011) as well as intercellular (Petrášek and Friml, 2009, Peer *et al*., 2011) and intracellular auxin distribution (Mravec *et al.*, 2009, Tromas *et al*., 2010) determines availability of auxin for transporters. Subsequently the number of plasma membrane auxin transporters facilitates (mostly directional) flow of auxin through plant tissues (Zažímalová and Murphy *et al*., 2010).

Specific physical-chemical nature of auxin molecules underlies the mechanism of their transport across the plasma membrane. Because all auxins – native ones as well as their synthetic analogues – are weak aromatic or heterocyclic acids, their ability to penetrate the plasma membrane depends predominantly on the degree of their dissociation, which corresponds to the dissociation constant of particular auxin and to current pH of the solution. The difference between apoplastic pH (approximately 5.5) and cytoplasmic pH (approximately 7.0) is the basis for the mechanism by which the molecules of weakly dissociated auxins outside the cell are able to penetrate the plasma membrane by diffusion whilst inside the cell auxin molecules dissociate almost entirely and their hydrophilic anionic form cannot leave the cell passively. Therefore, such anions can be excreted only actively through plasma membrane transporters – pumps or carriers. Such transporters, postulated to be asymmetrically localized on plasma membrane of constituent cells, in cooperation with passive diffusive auxin uptake are able to facilitate polar auxin transport through the tissue. This idea is known as chemiosmotic hypothesis (Rubery and Sheldrake, 1974, Raven 1975, Goldsmith 1977).

Despite there is no need for active auxin uptake according to chemiosmotic hypothesis, auxin influx carriers (AUX1/LAX protein family) are indispensable in a number of developmental events. They belong to the subfamily of plasma membrane amino acid permeases (Parry *et al*., 2001b). The efflux of auxin, on the other hand, is facilitated by transporters from PIN and ABCB protein families (Petrášek and Friml, 2009, Titapiwatanakun and Murphy, 2009, Zažímalová and Murphy *et al*., 2010). In Arabidopsis, the PIN family consists of two basic subfamilies, differing in the length of a hydrophilic loop in the middle of their polypeptide chain. The "long" PINs (PIN1–4, and 7) are localized at the plasma membrane, where they act as auxin efflux carriers (Petrášek *et al*., 2006, Mravec *et al*., 2008). These PINs undergo constitutive cycling between the plasma membrane and endosomal compartments (Geldner *et al*., 2001,

Dhonukshe *et al*., 2007, Kleine- Vehn *et al*., 2008). Second group consists of "short" PINs (PIN5, PIN6, and PIN8) (Křeček and Skůpa *et al*., 2009). In contrast to "long" PINs, Arabidopsis PIN5 and PIN8 do not have a direct role in cell-to-cell auxin transport but they regulate intracellular auxin homeostasis and metabolism because of their (predominant) endoplasmic reticulum localization (Mravec *et al*. 2009, Ganguly *et al* 2010, respectively). Besides PIN proteins, ABCB1 and 19 - members of the B-type of ABC protein superfamily - function primarily in auxin export (reviewed in Titapiwatanakun and Murphy, 2009). Interestingly, ABCB4 protein shows ability to switch from influx to efflux mode depending on auxin levels (Yang and Murphy, 2009, Kubeš and Yang et al., submitted). Recently, it was shown that NRT1.1 nitrate transporter/sensor can serve also as an auxin influx carrier (Krouk *et al*., 2010). In addition to the already known auxin carriers, other auxin carriers can exist and/or some of the already known plasma membrane anion transporters may recognize auxin as their substrate at certain circumstances.

Relative contribution of transporters to auxin uptake or auxin efflux was investigated in the past using an elegant cell-based system relying on different substrate specificities of the carriers (Delbarre *et al*., 1996). The competition experiments on auxin uptake or efflux, performed using externally applied radiolabelled tracer and non-labelled competitor, revealed saturable components involved in ^{3}H-2,4-D and ^{3}H-IAA uptake and in ^{3}H-NAA efflux. Besides the non-labelled competitors, specific auxin transport inhibitors can be used to separate influx and efflux activities. These inhibitors include inhibitors of auxin influx carriers (synthetic compounds 1-naphthoxyacetic acid (1-NOA), 2-naphthoxyacetic acid (2-NOA), the most specific representative 3-chloro-4-hydroxyphenylacetic acid (CHPAA) and natural chromosaponin (Imhoff *et al*., 2000, Rahman *et al*., 2001, Laňková *et al*., 2010)) and inhibitors of auxin efflux carriers (synthetic phytotropins 1-naphthylphthalamic acid (NPA) and 2-(1-pyrenoyl)benzoic acid (PBA), cyclopropyl propane dione (CPD) and 2,3,5-triiodobenzoic acid (TIBA), and natural flavonoids) (Rubery, 1990, Petrášek *et al.*, 2003, Peer *et al.*, 2007). In general, it was postulated (Delbarre et al., 1996) that NAA enters cells predominantly by diffusion and its accumulation level is controlled by efflux carriers. NAA was metabolized effectively during 15 min incubation to one dominant metabolite assumed to be a glucose ester conjugate. Conversely, 2,4-D was mostly transported into the cell by the influx carriers and it was found to be a substrate for the auxin efflux carriers only at concentration higher than 100 μM. Moreover, 2,4-D remained non-metabolized during the tested period. Natural auxin IAA was concluded to be a "substrate" for both groups of carriers as well as being able to enter cell passively at considerable amount. IAA metabolism was approximately two times less rapid compared to NAA metabolism in tobacco cells (Delbarre *et al*., 1996). Such characteristics were

confirmed in Arabidopsis root cells of *aux1-7* mutant deficient in AUX1 influx carrier function. In such plants, only NAA that can enter cells by diffusion, was able to rescue agravitropic phenotype (Parry *et al*., 2001a), and the inhibition of root elongation by IAA and 2,4-D in *aux1* mutant require 10 times higher auxin concentrations than wild-type (Yamamoto and Yamamoto, 1998),). Further, the *aux1* mutant root tips accumulate IAA 50% less efficiently than those of wild-type (Rahman *et al*., 2001). From these data Kramer and Bennett (2006) calculated that the contribution of carrier mediated uptake is about 10 times higher than the one of diffusion in Arabidopsis root cells. Gradually, based on increasing amount of experimental data and to explore and validate various hypotheses on auxin transport, cell polarization and related regulatory mechanisms especially in context of tissues, the need for mathematical modelling emerged.

Since one of the well known auxin effects was initiation of vein formation, Sachs (1969) suggested that the flow of the hormone itself serves as the signal that induces such morphogenic changes. His canalization hypothesis suggested positive feedback between the flow of a signal molecule – auxin – and the capacity of its flow. The first mathematical model of auxin flow based on canalization hypothesis was constructed by Mitchison (1980a, b) and Mitchison *et al*. (1981). The key assumption of this model was that auxin transport between adjacent cells depends on its concentration gradient and on the value of the auxin diffusion constant which increases in response to auxin flow. Such mechanism, therefore, represented a positive feedback between the auxin flow and the membrane permeability restricted by efflux capacity (i.e. number or activity of efflux carriers). This prerequisite still remains the core of current models of plant leaf venation. Since the PIN1 was found to be asymmetrically distributed on plasma membrane (Gälweiler *et al.*, 1998) it became the most promising candidate transporter responsible for oriented auxin flow. The dependence of PIN1 efflux carrier's localization on auxin flow was incorporated into models of Feugier *et al*. (2005) and Fujita and Mochizuki (2006).

Another approach was chosen by modellers dealing with phyllotactic patterns, which occurs in response to specifically localized tissue regions with high auxin concentrations. In these models, auxin concentration in neighbouring cells was usually used as the signal modulating carrier localization. Several models of phyllotaxis were able to reproduce specific patterns of auxin concentration maxima in shoot apical meristem in correspondence with experimental data (Jönsson *et al*., 2006, de Reuille *et al*., 2006, Smith *et al*., 2006). Nevertheless, the question of precise PIN carrier's localization mechanism and the nature of its controlling signal remained unanswered.

Since the two distinct regulatory mechanisms of PIN polarization are not as likely to develop as a single one, several models attempting to find a unifying auxin related signal

modulating the localization of PINs emerged. Such model has to be able to reproduce both the generation of auxin concentration maxima during phyllotaxis and the auxin flow canalization (leaf venation patterns or midvein formation in shoot apex) – the phenomena seeming to require almost opposing regulatory mechanism. Several approaches were used to accomplish this challenging task. Merks *et al*. (2007) managed to reproduce venation patterning with use of concentration-based PIN regulation (the number of active PINs on a particular side of a cell increased in response to high auxin concentration in appropriate neighbouring cell). The model incorporated a detailed subsystem of carrier cycling leading to a "travelling wave" of high auxin concentration, leaving polarized channels behind. In contrast, Stoma *et al*. (2008) introduced a flux-based polarization model of phyllotactic patterning relying mainly on the assumption that once certain threshold concentration of auxin is reached, the cells of such concentration maximum turn into a primordium acting as an unlimited auxin sink. Bayer and Smith *et al*. (2009) proposed a combined model integrating both principles of carrier localization, alternating (either smoothly or instantly) independently for each cell based on its internal auxin concentration. Wabnik and Kleine-Vehn *et al*. (2010) newly implemented cell wall compartments where mobile molecules of hypothetical auxin receptor mediate the response of PIN localization to extracellular auxin concentration, providing a model capable of reproducing many venation related phenomena. Even though mathematical description of auxin transport on the single-cell level was the basis of formulation of the 'tissue' models described above, the representation of a cell in these models did not change much since Mitchison derived basic differential equations for auxin flow between a cell and apoplast and between two neighbouring cells (Mitchison *et al*., 1981). Due to the lack of quantitative experimental data, these equations were fairly simplified and required some strong assumptions. To overcome some of their shortcomings, only subtle modifications of these equations were implemented during the construction of the tissue models. Now, the rigorous methodology of cell-based radiolabelled-auxin-accumulation assays (Delbarre *et al.* 1996, Petrášek *et al.* 2006) combined with other analytical approaches (HPLC, GC-MS etc.) are able to generate required but so far scarce qualitative and also quantitative data on the cellular level. Based on such data we have constructed a complex single-cell level model of auxin transport. Our model reveals the parameters of cellular auxin transport that are consistent with auxin transport characteristics observed and provides valuable insight into the regulation of auxin transport.

Material and Methods

Plant material

Cells of tobacco line BY-2 (*Nicotiana tabacum* L., cv. Bright Yellow-2) (Nagata *et al*., 1992) were cultured in liquid medium (3% (w/v) sucrose, 4.3 $g.l^{-1}$ Murashige and Skoog salts, 100 $mg.l^{-1}$ inositol, 1 $mg.l^{-1}$ thiamin, 0.2 $mg.l^{-1}$ 2,4-D, and 200 $mg.l^{-1}$ KH_2PO_4 (pH 5.8)). Cells of tobacco line Xanthi (*Nicotiana tabacum* L., cv. Xanthi XHFD8) (Muller *et al*., 1985) were cultured in Gamborg B5 liquid medium (Gamborg *et al*., 1968) containing 0.176 $mg.l^{-1}$ 2,4-D and 0.1 $mg.l^{-1}$ kinetin. Both cell lines were cultivated in darkness at 26°C on an orbital incubator (Sanyo Gallenkamp, Schöeller Instruments Inc., Prague, Czech Republic; 150 rpm, 32 mm orbit) and subcultured weekly. Stock BY-2 or Xanthi calli were maintained on media solidified with 0.6% (w/v) agar and subcultured monthly.

Chemicals

3-chloro-4-hydroxyphenylacetic acid (CHPAA), 2,4-dichlorophenoxy acetic acid (2,4-D) and all commonly used chemicals were supplied by Sigma-Aldrich, Inc. (St. Louis, USA) and Duchefa (Haarlem, The Netherlands). 1-naphthylphthalamic acid (NPA) was supplied by OlChemIm Ltd. (Olomouc, Czech Republic). ^{3}H-benzoic acid (BeA[4^{3H}]) and ^{3}H-2,4-dichlorophenoxyacetic acid (^{3}H-2,4-D) (both of specific radioactivity 20 $Ci.mmol^{-1}$), as well as ^{3}H-naphthalene-1-acetic acid (^{3}H-NAA) (specific radioactivity 25 $Ci.mmol^{-1}$) were supplied by American Radiolabeled Chemicals, Inc. (St. Louis, USA).

Auxin accumulation assays

Auxin accumulation by two-day old cells was measured according to the Delbarre *et al.* (1996) as modified by Petrášek *et al.* (2006). Inhibitors CHPAA, NPA or their combination were added as required from 50 mM DMSO stock solutions to give final concentration of 10 μM in 2 min pre-treatment before the beginning of the accumulation assay. The radiolabeled auxins were added to give a final concentration of 2 nM. Treatments with particular inhibitor were repeated at least three times. Accumulation results were expressed as pmols of particular auxin or BeA accumulated per 10^6 cells. The 0.5-ml aliquots of cell suspension were collected every 10 seconds (approximately 60 samples per one run) and accumulation of label was terminated by rapid filtration under reduced pressure on 22-mm-diameter cellulose filters. The cell cakes and filters were transferred to scintillation vials, extracted in 0.5 ml of 96% ethanol for 30 min, and afterwards 4 ml of scintillation solution (EcoLite Liquid Scintilation Fluid, MP Biomedicals, Solon, USA) were added. Radioactivity was determined by liquid scintillation counter Packard Tri-Carb 2900TR (Packard-Canberra, Meridian, CT, USA), with automatic correction for quenching.

HPLC metabolic profiling

Two days old BY-2 or Xanthi cells were prepared for the experiment by equilibration in uptake buffer as already described for accumulation assays (Petrášek *et al.*, 2006). Experiments were done in uptake buffer and under standard cultivation conditions. Cells were incubated with addition of 20 nM ^{3}H-BeA, ^{3}H-NAA and ^{3}H-2,4-D for a period of 0, 10 and 20 min. Cells and media (uptake buffer) were collected and frozen in liquid nitrogen (200 mg of fresh weight and 10 ml per sample). Extraction and purification of auxin metabolites in cells and media were performed as described (Dobrev and Kamínek, 2002, Dobrev *et al.*, 2005). The metabolites were separated on HPLC consisting of diode array detector (Perkin Elmer, Shelton, USA), column Luna C18(2), 150 × 4.6 mm, 3 μm (Phenomenex, Torrance, USA), mobile phase A: 40 mM CH_3COONH_4, (pH 4.0) and mobile phase B: CH_3CN/CH_3OH, 1/1, (v/v). Flow rate was 0.6 ml.min^{-1} with linear gradient 30–50% B for 10 min, 50–100% B for 1 min, 100% B for 2 min, 10–30% B for 1 min. The column eluate was monitored on 235C DAD followed by Ramona 2000 flow-through radioactivity detector (Raytest GmbH, Straubenhardt, Germany) after online mixing with three volumes (1.8 ml.min^{-1}) of liquid scintillation cocktail (Flo-Scint III, Perkin Elmer). The radioactive metabolites were identified on the basis of comparison of their retention times with authentic standards. For the results presentation the total integrated area of chromatogram plots has been normalized based on the equalization of total accumulated radiolabel.

Identification of the unknown NAA metabolite

BY-2 cells were incubated with 1-100 μM NAA for 2 hours. The main NAA metabolite M1 (RT 14.8 min) was purified after extraction, purification and HPLC as for the metabolite profiling of radioactive NAA, (see above). M1 was then applied to LC-ESI-MS/MS, which consisted of HPLC Ultimate 3000 (Dionex, Sunnyvale, USA) coupled to hybrid triple quadrupole/ linear ion trap 3200 Q TRAP (AB Sciex, Foster City, USA). MS was set at negative mode. Solution of M1, in 1 mM CH_3COOH in 50% methanol was infused into MS and full scan mass spectra, product ion and precursor ion scans were recorded. To study the stability of M1 under mild alkaline conditions, M1 was poured into 0.1 M NH_4OH and incubated at room temperature. Every 5 minutes, an aliquot was injected into the LC/MS separated on column Luna C18(2)-HST, 50×3 mm, 2.5 μm (Phenomenex, Torrance, USA), isocratic 60% A: 2 mM CH_3COOH and 40% B: CH_3CN at flow rate of 0.3 ml.min^{-1}. MS was set at multiple reaction monitoring mode with records of Q1>Q3 transitions of NAA (185>141), M1 (347>141), glucose (179>89) and 2,4-D (219>161, internal standard).

Mathematical modelling

The mathematical model of 2,4-D transport between cell and apoplast was defined and mathematically formalized by a set differential equations for each experiment setup (various inhibitor combinations, see Figs. 1 and 2). These sets were analytically solved for intracellular concentration, giving a formula of a function describing the time course of auxin (2,4-D) concentration inside the cell. Parameter optimization was then performed by altering parameter values in order to minimize the value of objective function defined as summed squares of residuals (differences between measured and simulated values of intracellular 2,4-D concentration). Each set of parameters was used to simulate all experimental variants (all inhibitor combinations and repetitions) at a time and all squared residuals were summed with equal weights to get a single value of the objective function. Since the objective function had many local minima the optimization problem was solved using a combination of gradient-based and enumerative numerical methods. Over three millions of initial parameter sets were randomly generated within probable parameter value range and from all these starting points a gradient-based optimization algorithm was initiated. From the obtained results, the set of parameters appropriate to the deepest minimum of the objective function was then declared to be the final parameter estimate. The estimates of parameter value standard deviations were calculated from different parameter values optimized independently for each essay repetition. Sensitivity analysis was performed by plotting relative change of objective function value against relative change of the value of each parameter, while the other parameters remained constant at their optimal estimates. Resulting curves, therefore, represent sections through the objective function near its minimum.

Results

^{3}H-NAA metabolites occur immediately after ^{3}H-NAA uptake and remain inside BY-2 cells

To describe auxin transport on cellular level by mathematical model of relations between auxin diffusion, its active uptake and efflux, we re-evaluated importance of NAA metabolism using exogenously applied ^{3}H-NAA in a well-established model system of BY-2 tobacco cells. Conversion of ^{3}H-NAA into corresponding metabolites was observed immediately after ^{3}H-NAA addition to the cells, i.e. at zero time, and after 10 and 20 min of incubation. Accumulated ^{3}H-NAA was rapidly - within a few seconds - metabolised to one major metabolite M1 (approximately 50% of the overall sample radioactivity) and five minor metabolites. Retention time of the major metabolite was 7.7 min (see below). After another 10 and 20 min, the relative content of free ^{3}H-NAA decreased while the content of M1 further increased up to 80% after 20 min. (Fig. 3A).

Besides a trace of unknown polar metabolite in retention time 10.88 min, no metabolites were found in the incubation medium. This observation indicates that products of NAA metabolism including predominant metabolite M1 are unable to translocate across plasma membrane either passively or actively and thus remain inside the cells (Fig. 3A).

To determine whether such enzymatic machinery is specific for cellular auxin management or it is common cell mechanism designated to eliminate undesired amount of diffusible organic elements, ^{3}H-BeA, a weak organic acid lacking auxin activity, has been used at the same experimental setup. Similarly to ^{3}H-NAA, ^{3}H-BeA was metabolised immediately after its uptake to one predominant metabolite acquired at retention time 2.52 min. Minor amount of another metabolite occurred at retention time 4.75 min (Fig. 3C). In incubation medium, only traces of ^{3}H-BeA metabolites with retention times 2.52 min and 4.75 min were detected. Thus the metabolites of ^{3}H-BeA are trapped inside the cells as well as those of ^{3}H-NAA (Fig. 3C).

Similar trends in metabolic profiles were detected under the same experimental conditions in Xanthi cell suspension for ^{3}H-NAA which showed slightly decreased metabolism up to 10 min while ^{3}H-BeA was metabolised almost identically in both types of cells (Suppl. Fig. 1A, 1C).

We have obtained similar results also for IAA (data not shown), and so we assume that fast metabolic conversion of active auxins (IAA, NAA, but not 2,4-D - see below) as well as non-auxin compounds such as BeA to physiologically inactive conjugates is a typical mechanism by which cells manage excessive amounts of weak organic acids to maintain intracellular ionic equilibrium.

NAA is predominantly metabolised to its glucosyl ester

The major metabolite M1 appearing immediately upon incubation of BY-2 cell suspension with ^{3}H-NAA has been identified as glucosyl ester of NAA based on the following observations:

On reversed phase HPLC, M1 had shorter retention time (RT 14.8 min) than NAA itself (RT 16.9 min), suggesting its more polar nature. When BY-2 cells were incubated with cold NAA at 1-100 μM, a UV absorbing peak with identical UV spectrum as NAA (UVmax = 280 nm) appeared at RT of 14.8 min (M1). This implied that firstly, M1 kept the chromophore of NAA - i.e. the naphthalene double ring - and secondly, that no chromophore was added to the molecule of NAA during the metabolic modification.

M1 purified by HPLC and applied on LC-negative ESI-MS/MS, showed three major peaks: m/z347, m/z393 and m/z407. Product ion spectra of all three peaks contained mostly the

same fragments, including the NAA characteristic m/z185 (NAA>$C_{12}H_{10}O_2$ = MW186) and m/z141 (m/z185 - CO_2). Precursor ion scans of fragments m/z185 and m/z141 confirmed that they derive from m/z347, m/z393 and m/z407 (Fig. 4).

We speculate that all three peaks represent one compound of m/z347 and adducts with acetic acid (MW60, m/z407 = 347 + 60) and with formic acid (MW46, m/z393 = 347 + 46). Adducts presumably formed since M1 was in solution containing 1 mM acetic acid added for better ionization, and formic acid is its common contaminant. This was further proved, because both m/z407 and m/z393 contained fragment m/z347 and their major product ion fragments were m/z59 (acetate) and m/z45 (formate), respectively. Product ion spectrum of m/z347 is shown in Fig 4. There are several fragments with mass difference of 18 (corresponds to H_2O): 347 - 329, 227 - 209, 257 - 239, 89 - 71, 119-101, suggesting the presence of several hydroxyl groups. Fragments with mass difference of 30 (corresponds to CH_2O): 257 - 227, 239 - 209, 119 - 89 - 59, 101 – 71, are also characteristic. Very similar fragmentation pattern with several mass differences of 18 and 30, and several identical fragments like: 59, 71, 89, 101, 113, 119 were observed in the product ion spectra of monosaccharides, typically glucose (Fig. 4, MW180). The fragmentation pattern and molecular mass of M1 (MW348), as implied by negative ion m/z347, suggests that it is ester of NAA with hexose: NAA + $C_6H_{12}O_6$ – H_2O = 186 + 180 – 18 = 348.

Ester bond was confirmed, when M1 was quickly degraded to NAA and hexose under mild alkaline conditions (0.1M NH_4OH at 25^{o}C) (Fig. 5). The hexose was consecutively identified as glucose by monosaccharide HPLC, where M1 derived hexose co-eluted with glucose (data not shown).

We have also synthesized NAA glucosyl ester standard (analogically to the procedure published by Kai *et al.,* 2007, for synthesis of IAA glucosyl ester) and on reversed phase HPLC this synthetic NAA glucosyl ester showed the same retention time (RT 14.8 min) like the native endogenous metabolite M1 detected in BY-2 cells (data not shown).

Based on the analyses above, we conclude that the predominant NAA metabolite M1 is identical with NAA glucosyl ester (NAA-Glc).

2,4-D is metabolised very slowly in tobacco BY-2 cells

Besides different substrate specificities of auxin carriers for synthetic auxins NAA and 2,4-D (Depta and Rubery 1984, Sabater and Sabater 1986, Hertel 1987, and later quantified by Delbarre *et al*. 1996), 2,4-D and NAA differ significantly also in their metabolic rates. In comparison with rapid metabolic conversion of ^{3}H-NAA to one predominant metabolite NAA-Glc, ^{3}H-2,4-D was only partially metabolised to three unknown metabolites in minor amounts after 0, 10 and 20 min of incubation (Fig. 3B), and the relative levels of ^{3}H-2,4-D slightly

decreased during 20 min incubation with parallel increase of one of the minor metabolites (RT 10.87 min).

In incubation medium relative levels of 2,4-D remained constant and only traces of three metabolites were observed; this indicates that products of ^{3}H-2,4-D metabolism remain in cells, as the metabolites of other tested weak acids do (mentioned above and Fig. 3B).

As shown above, 2,4-D is more resistant to metabolic conversions in comparison to IAA and NAA. Such minor contribution of metabolism to the changes of intracellular 2,4-D concentration makes the 2,4-D a promising tool for probing cellular auxin transport characteristics and thus offers an opportunity for application of quantitative data-based mathematical modelling.

Characterization of the dynamics of 2,4-D transport at cellular level

Since the metabolism of 2,4-D in BY-2 cells during 10 min is negligible and thus it does not affect intracellular 2,4-D levels, we have investigated the dynamics of 2,4-D transport in BY-2 using accumulation assays within this time span. The cells rapidly accumulated ^{3}H-2,4-D from media with gradually decreasing accumulation speed (Fig. 6A).

Because 2,4-D is a good substrate for auxin influx carriers it was not surprising that CHPAA - a specific auxin influx inhibitor (Imhoff et al., 2000, Laňková et al., 2010) - effectively decreased the accumulation of 2,4-D compared to non-treated control (Fig. 6A,B).

Surprisingly, the use of auxin efflux inhibitor NPA led to the increased accumulation of ^{3}H-2,4-D (Fig. 6C). Although 2,4-D is poorly transported *in planta* (Ito and Gray, 2006) and 2,4-D was demonstrated to be a poor substrate for auxin efflux carriers ABCB1 and ABCB19 (Titapiwatanakun et al., 2009), evidently a significant portion of ^{3}H-2,4-D is transported out of cells actively, probably using other auxin efflux carriers which are sensitive to NPA (Petrášek et al., 2006, Yang and Murphy, 2009, Kubeš and Yang et al., submitted).

Interestingly, the combination of both CHPAA and NPA resulted in strikingly slower rate of ^{3}H-2,4-D (2nM) accumulation in contrast to control ^{3}H-2,4-D accumulation course (Fig. 6D). It is probable that both influx and efflux carriers were effectively blocked by CHPAA and NPA, respectively, and resulting 2,4-D accumulation course reflects rate of the net diffusive uptake resulting from diffusive influx and diffusive efflux.

To describe the auxin transport characteristics on a single-cell level and to check them for consistency, we have designed a mathematical model of 2,4-D transport on cellular level, using quantitative experimental data on 2,4-D accumulation for its construction and validation.

Mathematical model of cellular 2,4-D transport

The model of cellular 2,4-D transport was constructed based on following assumptions:

1. BY-2 cell suspension consists of individual and identical cells of constant volume. Number of the cells (suspension density) does not change during the accumulation assay.

2. Once inside the cell, 2,4-D is distributed homogeneously over the whole cell volume. Although inner cell compartmentation can hardly be neglected from biological point of view, the experimental data does not require any inner cell compartments to be incorporated in the model and thus it does not even allow any cell compartment related parameters to be identified.

3. Based on the results presented above **we assume that 2,4-D is not metabolised in the cells within the 10 min period of accumulation assay.**

4. Number and activity of carriers do not change during the accumulation.

5. Influx and efflux carrier kinetics is linear. Based on the results of Delbarre *et al.* (1996), auxin carriers do not exhibit saturating behaviour until micromolar concentrations of auxins are reached. Since the extracellular concentration of ^{3}H-2,4-D used during the accumulation experiments was only 2 nmol/l and its intracellular concentration did not exceed 100 nmol/l (see Fig. 6), we can assume that just the linear part of carrier kinetics applies under conditions used, i.e., the 2,4-D flux through particular type of carriers is linearly proportional to the concentration of 2,4-D in its source compartment (extracellular concentration for influx and *vice versa*). Application of this assumption also solves potential difficulties related to the presence of endogenous 2,4-D as it will not interfere with the transport of ^{3}H-2,4-D as long sum of their concentrations is within the limits of quasi-linear carrier kinetics.

6. Carrier inhibitors block the activity of carriers entirely and do not affect other cell characteristics. In other words, we assume complete inhibition of active influx when CHPAA is applied as well as complete inhibition of active efflux in case of NPA application.

For further details on the model construction see Fig. 1 and 2.

Biological validity of the above assumptions will be discussed below.

Various carrier inhibitor combinations were used to alter the experimental setup in order to get the data for characterization of various participating transport mechanisms. When CHPAA and NPA were applied simultaneously, only the passive diffusion of ^{3}H-2,4-D is supposed to contribute to its net uptake. Resulting data, therefore, contained the information about the parameters of 2,4-D diffusion and allowed their values to be identified. Individual application of CHPAA or NPA enabled the values of efflux or influx parameters, respectively, to be optimized. Although the optimization could be performed in such stepwise manner, simultaneous parameter optimization algorithm was employed instead, in order to achieve greater precision (see Materials and Methods).

Besides the proper parameters of the model, a constant vertical offset was added to the

model solution as another parameter and it was optimized to let the model compensate the experimental data for the auxin contaminating the cells' surface and thus causing an apparent shift of the accumulation curve. However, final value of this offset parameter provided by the optimization process was relatively low compared to the levels of ^{3}H-2,4-D accumulation (see Tab. 1 and Fig. 6), suggesting the cell surface contamination during accumulation assays to be significantly less important than that observed earlier by Delbarre *et al.* (1996).

Table 1.

Directly identified model parameters

label	meaning	value	unit	variant value	variant unit
p_I	Intracellular fraction of protonated 2,4-D	5,56E-05	-	5,56E-03	%
k_D	difusion parameter	2,45E+03	min^{-1}	4,08E+01	s^{-1}
k_E	parameter of efflux	1,80E-01	min^{-1}	3,00E-03	s^{-1}
k_I	parameter of influx	1,46E+01	min^{-1}	2,44E-01	s^{-1}
offset	average contamination of cells - the apparent increase in accumulation	1,43E-06	$mol.m^{-3}$	5,05E-02	pmol /mil.b.

Calculated membrane parameters

label	meaning	value	unit	variant value	variant unit
k_{Diff}	diffusion permeability of the membrane	1,41E-02	$m.min^{-1}$	2,35E-04	$m.s^{-1}$
k_{Eff}	efflux carrier activity of the membrane	1,04E-06	$m.min^{-1}$	1,73E-08	$m.s^{-1}$
k_{Inf}	influx carrier activity of the membrane	8,45E-05	$m.min^{-1}$	1,41E-06	$m.s^{-1}$

Discussion *(not yet completed)*

The molecular basis of cellular auxin transport and its regulation is still not fully understood. Even if a number of carriers have been identified and proved to be directly involved in auxin transport (Petrášek *et al*., 2006, Yang and Murphy, 2009) their regulation and possible activities of other, so far unknown transporters under certain conditions remain unclear. Nevertheless, it is possible to track a course of auxin accumulation into the cells and to specify and quantify some auxin transport parameters.

Synthetic auxins NAA and 2,4-D represent useful tools for a single-cell based auxin transport studies, because of the distinct specificity of auxin influx and efflux carriers towards them (Delbarre et al., 1996, Petrášek et al., 2006). The short-term auxin transport characteristics comprise auxin metabolism and activities of auxin transporters; the impact of genomic (gene expression-based) regulation of auxin carriers can be omitted here.

Our study of metabolism of radiolabeled NAA, IAA, 2,4-D and non-auxin weak acid BeA during 20 min incubation period revealed surprisingly fast metabolism of NAA and BeA followed by IAA. Glucosyl ester conjugates represent the major form of their metabolites - as shown here for NAA and by Kai *et al.* (2007) for IAA. Presence of glucose as a common monosaccharide in cells together with common ester bond represents an easy mechanism how the cell can deal with excessive amount of auxin. We have shown that glucose-ester conjugates (as well as their other metabolites) stay trapped inside the cells and they decrease accessibility of free NAA or IAA for auxin efflux carriers. This finding has an important consequence for radiolabelled auxins-based accumulation assays: As auxin molecules are preferably labelled on the ring structures, the label stays inside cells in the form of auxin conjugate(s) and thus the real accumulation of free (labelled) auxins is lower than presumed. Therefore, the true capacity of PIN and/or ABCB efflux transporters must be higher than expected previously, and neither NAA nor IAA is reliable tool for precise measurements of auxin efflux.

On the other hand, metabolism of ^{3}H-2,4-D is fairly weak and slow up to 20 min. So, because of its relative high metabolic stability, 2,4-D was used here for probing transport characteristics of auxin influx and efflux carriers.

Such experimental data were then used for construction of mathematical model of cellular auxin transport.

Separately defined parameters for active 2,4-D uptake and efflux correlated well with the measured characteristics suggesting that the particular parameters are sufficient for reliable description of 2,4-D active influx, efflux and the role of neglected factors is unimportant.

Interestingly, in case of simultaneous contribution of diffusive as well as active uptake and efflux, slight disproportion between measured data and model prediction is noticeable after 8 min of accumulation.

Biological effects of auxins are usually detected after their application to plant material in nM concentrations. Observed physiological responses are then referred to direct effect of applied chemicals. The model proves that metabolism, as well as specific transport characteristics of auxins are indispensable in the assessment of their physiological effects.

We propose a single-cell level auxin transport model that could not only provide valuable insights into the regulation of auxin transport and its cellular concentration levels, but also validate mathematical basis of many models of auxin transport in tissues.

Acknowledgements

The work was supported by the Ministry of Education, Youth and Sports of the Czech Republic project LC06034, by the Grant Agency of the Czech Republic, project P305/11/0797 and by project MSM6840770012 Transdisciplinary Research in the Field of Biomedical Engineering II. We thank Markéta Pařezová and Jana Žabová for technical assistance.

References

Davies PJ. 2010. The plant hormones: Biosynthesis, Signal Transduction, Action!*, Third Edition* Davies, P.J. ed: Springer, Dordrecht, The Netherlands, 700 pp.

Delbarre A, Muller P, Imhoff V, Morgat JL, Barbier-Brygoo H. 1994. Uptake, accumulation and metabolism of auxins in tobacco leaf protoplasts. *Planta* **195,** 159-167.

Delbarre A, Muller P, Imhoff V, Guern J. 1996. Comparison of mechanisms controlling uptake and accumulation of 2,4-dichlorophenoxy acetic acid, naphthalene-1-acetic acid, and indole-3-acetic acid in suspension-cultured tobacco cells. *Planta* **198,** 532-541.

Depta H, Rubery PH. 1984. A comparative study of carrier participation in the transport of 2,3,5-trriodobenzoic acid, indole-3-acetic acid, and 2,4-dichlorophenoxyacetic acid by *Cucurbita pepo* L. hypocotyl segments. *J. Plant Physiol* **115**, 371-387.

de Reuille PB, Bohn-Courseau I, Ljung K, Morin H, Carraro N, Godin C, Traas J. 2006. Computer simulations reveal properties of the cell–cell signaling network at the shoot apex in Arabidopsis. *Proceedings of the NationalAcademy of Sciences of the United States of America* **103,** 1627–1632.

Dhonukshe P, Aniento F, Hwang I, Robinson DG, Mravec J, Stierhof YD, Friml J. 2007. Clathrin-mediated constitutive endocytosis of PIN auxin efflux carriers in Arabidopsis. *Current Biology* **17**, 520-527.

Feugier FG, Mochizuki A, Iwasa Y. 2005. Self-organization of the vascular system in plant leaves: inter-dependent dynamics of auxin flux and carrier proteins. *J Theor Biol* **236,** 366–375.

Fujita H, Mochizuki A. 2006. Pattern formation by the positive feedback regulation between flow of diffusible signal molecule and localization of its carrier. *J Theoret Biol* **241**, 541–555.

Galweiler L, Guan CH, Muller A, Wisman E, Mendgen K, Yephremov A, Palme K. 1998. Regulation of polar auxin transport by AtPIN1 in Arabidopsis vascular tissue. *Science* **282**, 2226-2230.

Gamborg OL, Miller RA, Ojima K. 1968. Nutrient requirements of suspension cultures of soybean root cells. *Experimental Cell Research* **15,** 148-151.

Ganguly A, Lee SH, Cho M, Lee OR, Yoo H, Cho HT. 2010. Differential Auxin-Transporting Activities of PIN-FORMED Proteins in Arabidopsis Root Hair Cells. *Plant Physiology* **153**, 1046-1061.

Geldner N, Friml J, Stierhof YD, Jurgens G, Palme K. 2001. Auxin transport inhibitors block PIN1 cycling and vesicle traficking. *Nature* **413**, 425-428.

Goldsmith MHM. 1977. The Polar Transport of Auxin. *Annual Review of Plant Physiology* **28**, 439-478.

Hertel R. 1987. Auxin transport: binding of auxins and phytotropins to the carriers. Accumulation into and efflux from membrane vesicles. *In: Klämbt D. (ed) Plant hormone receptors (NATO ASI Series, vol H10). Springer-Verlag, Berlin, Heidelberg,* 81-92.

Imhoff V, Muller P, Guern J, Delbarre A. 2000. Inhibitors of the carrier-mediated influx of auxin in suspension-cultured tobacco cells. *Planta* **210**, 580–588.

Ito H, Gray WM. 2006. A gain-of-function mutation in the Arabidopsis pleiotropic drug resistance transporter PDR9 confers resistance to auxinic herbicides. *Plant Physiol* **142**, 63–74.

Jönsson H, Heisler MG, Shapiro BE, Meyerowitz EM, Mjolsness E. 2006. An auxin-driven polarized transport model for phyllotaxis. *Proc Natl Acad Sci* **103**, 1633–1638.

Kai K, Nakamura S, Wakasa K, Miyagawa H. 2007. Facile preparation of deuterium-labeled of indole-3-acetic acid (IAA) and its metabolites to quantitatively analyze the disposition of exogenous IAA in *Arabidopsis thaliana*. *Biosci. Biotech. Biochem.* **71,** 1946-1954.

Kleine-Vehn J, Dhonukshe P, Sauer M, Brewer PB, Wisniewska J, Paciorek T, Benková E, Friml J. 2008. ARF GEF-dependent transcytosis and polar delivery of PIN auxin carriers in Arabidopsis. *Current Biology* **18**, 526-531.

Kramer EM, Bennett MJ. 2006. Auxin transport: A field in flux. *Trends Plant Sci* **11,** 382–386.

Krouk G, Lacombe B, Bielach A, Perrine-Walker F, Malinská K, Mounier E, Hoyerová K, Tillard P, Leon S, Ljung K, Zažímalová E, Benková E, Nacry P, Gojon A. 2010. Nitrate-Regulated Auxin Transport by NRT1.1 Defines a Mechanism for Nutrient Sensing in Plants. *Developmental Cell* **18**, 927-937.

Křeček P, Skůpa P, Libus J, Naramoto S, Tejos R, Friml J, Zažímalová E. 2009. The PIN-FORMED (PIN) protein family of auxin transporters. *Genome Biol* **10**, 249.

Laňková M, Smith RS, Pešek B, Kubeš M, Zažímalová E, Petrášek J, Hoyerová K. 2010. Auxin influx inhibitors 1-NOA, 2-NOA, and CHPAA interfere with membrane dynamics in tobacco cells. *Journal of Experimental Botany* **61**, 3589-3598.

Ludwig-Muller J. 2011. Auxin conjugates: their role for plant development and in the evolution of land plants. *Journal of Experimental Botany* **62**, 1757-1773.

Merks RMH, Van de Peer Y, Inzé D, Beemster GTS. 2007. Canalization without flux sensors: a traveling-wave hypothesis. *Trends Plant Sci* **12**, 384–390.

Mitchison GJ. 1980. A model for vein formation in higher plants. *Proc R Soc Lond B* **207**, 79–109.

Mitchison GJ. 1980. The dynamics of auxin transport. *Proc R Soc Lond B* **209**, 489–511.

Mitchison GJ, Hanke DE, Sheldrake AR. 1981.The polar transport of auxin and vein patterns in plants. *Philos Trans R Soc Lond B* **295**, 461–471.

Mravec J, Kubeš M, Bielach A, Gaykova V, Petrášek J, Skůpa P, Chand S, Benková E, Zažímalová E, Friml J. 2008. Interaction of PIN and PGP transport mechanisms in auxin distribution-dependent development. *Development* **135**, 3345-3354.

Mravec J, Skůpa P, Bailly A, Hoyerová K, Křeček P, Bielach A, Petrášek J, Zhang J, Gaykova V, Stierhof YD, Dobrev PI, Schwarzerová K, Rolčík J, Seifertová D, Luschnig, C, Benková E, Zažímalová E, Geisler M, Friml J. 2009. Subcellular homeostasis of

phytohormone auxin is mediated by the ER-localized PIN5 transporter. *Nature* **459**, 1136-1140.

Muller JF, Goujaud J, Caboche M. 1985. Isolation in vitro of naphthalene-acetic-tolerant mutants of *Nicotiana tabacum*, which are impaired in root morphogenesis. *Molecular and General Genetics* **199,** 194–200.

Nagata T, Nemoto Y, Hasezava S. 1992. Tobacco BY-2 cell line as the 'Hela' cell in the cell biology of higher plants. *International Review of Cytology* **132,** 1-30.

Normanly J. 2010. Approaching Cellular and Molecular Resolution of Auxin Biosynthesis and Metabolism. *Cold Spring Harbor Perspectives in Biology* **2**.

Parry G, Delbarre A, Marchant A, Swarup R, Napier R, Perrot-Rechenmann C, Bennett MJ. 2001a. Novel auxin transport inhibitors phenocopy the auxin influx carrier mutation aux1. *Plant Journal* **25**, 399-406.

Parry G, Marchant A, May S, Swarup R, Swarup K, James N, Graham N, Allen T, Martucci T, Yemm A, Napier R, Manning K, King G, Bennett M. 2001b. Quick on the uptake: Characterization of a family of plant auxin influx carriers. *Journal of Plant Growth Regulation* **20**, 217-225.

Peer WA, Blakeslee JJ, Yang H, Murphy AS. 2011. Seven Things We Think We Know about Auxin Transport. *Molecular Plant* **4**, 487-504.

Peer WA, Murphy AS. 2007. Flavonoids and auxin transport: modulators or regulators? *Trends in Plant Science* **12**, 556-563.

Petrášek J, Černá A, Schwarzerová K, Elčkner M, Morris DA, Zažímalová E. 2003. Do phytotropins inhibit auxin efflux by impairing vesicle traffic? *Plant Physiology* **131**, 254-263.

Petrášek J. and Friml J. 2009. Auxin transport routes in plant development. *Development* **136**, 2675-2688.

Petrášek J, Mravec J, Bouchard R, Blakeslee JJ, Abas M, Seifertová D, Wiśniewska J, Tadele Z, Kubeš M, Čovanová M, Dhonukshe P, Skůpa P, Benková E, Perry L, Křeček P, Lee OR, Fink GR, Geisler M, Murphy AS, Luschnig C, Zažímalová E, Friml J. 2006. PIN proteins perform a rate-limiting function in cellular auxin efflux. *Science* **312,** 914-918.

Rahman A, Ahamed A, Amakawa T, Goto N, Tsurumi S. 2001. Chromosaponin I specifically interacts with AUX1 protein in regulating the gravitropic response of arabidopsis roots. *Plant Physiology* **125,** 990-1000.

Raven J. 1975. Transport of indoleacetic acid in plant cells in relation to pH and electrical potential gradients, and its significance for polar IAA transport. *New Phytologist* **74**, 163-172.

Rubery P. and Sheldrake A. 1974. Carrier-mediated auxin transport. *Planta* **118**, 101-121.

Rubery P.H. 1990. Phytotropins: receptors and endogenous ligands. In: Roberts J, Kirk C, Venis M (eds) Hormone perception and signal transduction in animals and plants. The Company of Biologists Ltd, Cambridge, pp 119±145.

Sabater M, Sabater F. 1986. Auxin carriers in membranes of lupin hypocotyls *Planta* **167**, 76-80.

Sachs T. 1969. Polarity and the induction of organized vascular tissues. *Ann Bot Lond* **33,** 263.

Smith RS, Bayer EM. 2009. Auxin transport-feedback models of patterning in plants. *Plant, Cell and Environment* **32**, 1258-1271.

Smith RS, Guyomarch S, Mandel T, Reinhardt D, Kuhlemeier C, Prusinkiewicz P. 2006. A plausible model of phyllotaxis. *Proc Natl Acad Sci* **103**, 1301–1306.

Smulders MJM, Van de Ven ETWM, Croes AF, Wullems GJ. 1990. Metabolism of 1-naphthalene acetic acid in explants of tobacco: evidence for release of free hormone from conjugates. *J. Plant Growth Regul.* **9,** 27-34.

Stoma S, Lucas M, Chopard J, Schaedel J, Traas J, Godin C. 2008. Flux-based transport enhancement as a plausible unifying mechanism for auxin transport in meristem development. *PLoS Computational Biology* **4**, e1000207.

Titapiwatanakun B, Blakeslee JJ, Bandyopadhyay A, Yang H, Mravec J, Sauer M, Cheng Y, Adamec J, Nagashima A, Geisler M, Sakai T, Friml J, Peer WA, Murphy AS. 2009. ABCB19/PGP19 stabilises PIN1 in membrane microdomains in Arabidopsis. *Plant Journal* **57**, 27-44.

Titapiwatanakun B and Murphy AS. 2009. Post-transcriptional regulation of auxin transport proteins: cellular trafficking, protein phosphorylation, protein maturation, ubiquitination, and membrane composition. *Journal of Experimental Botany* **60,** 1093-1097.

Tromas A, Paponov I and Perrot-Rechenmann C. 2010. AUXIN BINDING PROTEIN 1: functional and evolutionary aspects. *Trends in Plant Science* **15**, 436-446.

Wabnik K, Kleine-Vehn J, Balla J, Bauer M, Naramoto S, Reinöhl V, Merks RMH, Goaverts W, Friml J. 2010 Emergence of tissue polarization from synergy of intracellular and extracellular auxin signaling. *Molecular Systems Biology* **6**,447.

Yamamoto M, Yamamoto KT. 1998. Differential effects of 1- naphthalene acetic acid, indole-3-acetic acid and 2,4-dichlorophenoxyacetic acid on the gravitropic response of roots in an auxin resistant mutant of Arabidopsis, Aux1. *Plant Cell Physiol* **39**, 660–664.

Yang HB and Murphy AS. 2009. Functional expression and characterization of Arabidopsis ABCB, AUX 1 and PIN auxin transporters in Schizosaccharomyces pombe. *Plant Journal* **59**, 179-191.

Zažímalová E, Murphy A, Yang H, Hoyerová K, Hošek P. 2010. Auxin transporters-why so many? *Cold Spring Harb Perspect Biol* **2**, a001552.

Figure legends

Figure 1 Mathematical model of ^{3}H-2,4-D uptake by diffusion (A) and both diffusion and efflux (B).

A. In presence of CHPAA and NPA, we assume active influx and efflux (respectively) of ^{3}H-2,4-D to be completely blocked as indicated in the scheme by expressions stating that the density of ^{3}H-2,4-D flux through plasma membrane (the amount of ^{3}H-2,4-D transported by influx carriers – dn_{Inf} – or efflux carriers – dn_{Eff} – in the cell per unit of time – dt – and unit of plasma membrane area – dS) is null. The only non-zero flux of ^{3}H-2,4-D is, therefore, caused by diffusion. In appropriate equation, dn_{Diff} represents the amount of transported ^{3}H-2,4-D, k_{Diff} is diffusion permeability of plasma membrane, p_e and p_i represent the fraction (relative amount) of protonated (not dissociated) ^{3}H-2,4-D in extracellular and intracellular space respectively. Since both extracellular (C_E) and intracellular (C_I) concentrations of ^{3}H-2,4-D change during accumulation, we expressed the extracellular concentration using initial extracellular concentration ($C_E(0)$), the intracellular concentration, cell suspension density (number of cells in unit of suspension volume –*dens*) and cell volume (volume of single cell - V_C) as indicated in the bottom. This expression was then used to substitute for the ^{3}H-2,4-D extracellular concentration in the equation of diffusion. To get the final differential equation of the model (1), the diffusion permeability of plasma membrane (k_{Diff}), which is a universal property of the membrane independent of cell dimensions, was replaced by the diffusion parameter (k_D), which is simply a rate constant specific to particular cell geometry represented by its volume (V_C) and surface area (S_C).

B. In presence of CHPAA, we assume active ^{3}H-2,4-D influx to be completely inhibited, while active efflux and diffusion of ^{3}H-2,4-D being unaffected. Therefore, mathematical representation of ^{3}H-2,4-D flux by diffusion remains identical to the one derived in A. In case of active efflux, we assume the flux of ^{3}H-2,4-D to be proportional to the source (intracellular) concentration of dissociated ^{3}H-2,4-D (i.e., we assume a linear kinetics of efflux carriers). The appropriate parameter – efflux carrier activity of the membrane (k_{Eff}) – is again transformed in the cell-specific rate constant k_E – the efflux parameter, according to the same principle used for diffusion parameters described above in A. The efflux parameter (k_E) is then used in the final differential equation (2) of the model.

Figure 2 Mathematical model of ^{3}H-2,4-D uptake by diffusion and influx (A) and diffusion, influx and efflux (B).

A. In presence of NPA, we assume active ^{3}H-2,4-Defflux to be completely inhibited, while active influx and diffusion of ^{3}H-2,4-D being unaffected. Therefore, mathematical representation

of ^{3}H-2,4-D flux by diffusion remains unchanged. In case of active influx, we assume the flux of ^{3}H-2,4-D to be proportional to the source (extracellular) concentration of dissociated ^{3}H-2,4-D (i.e., we assume a linear kinetics of influx carriers). The appropriate parameter – influx carrier activity of the membrane (k_{Inf}) – is again transformed in the cell-specific rate constant k_I – the influx parameter – to obtain the final differential equation (3) of the model.

B. With no inhibitor of ^{3}H-2,4-Dactive transport present in the medium, all of the three transport mechanisms (i.e., diffusion, active influx and active efflux) take part in the uptake of ^{3}H-2,4-D in the cell. Therefore, the contributions of all these three processes are combined in the final differential equation (4) of the model.

Figure 3 Metabolism of ^{3}H-NAA, ^{3}H-2,4-D and ^{3}H-BeA in BY-2 tobacco cells and media at time of 0, 10 and 20 min of incubation.

A. NAA is rapidly metabolised to major metabolite (identified as NAA glucosyl ester with retention time 7.7 min) and in 10 and 20 min this metabolite is predominant in cells. The levels of NAA in 0, 10 and 20 min stayed constant. 2-NAA was also determined with constant level in all time points of incubation and other four unknown metabolites (more polar than NAA itself). In incubation medium were observed any changes of NAA levels and only one minor metabolite peak, which indicate that products of NAA metabolism (including predominant NAA glucosyl ester) remained in cells.

B. 2,4-D is partially metabolised to three unknown products and in 10 and 20 min this metabolite (retention time 10.87 min) is minority in cells. The levels of 2,4-D during 20 min incubation slightly decreased with contemporary increase of unknown metabolite (retention time 10.87 min). In incubation medium the levels of 2,4-D stayed constant and three minority metabolites were observed, which indicate that products of 2,4-D metabolism also remained in cells.

C. BeA was quickly metabolised to one predominant (retention time 2.52 min) and one unknown minor product (retention time 4.75 min). In incubation medium was observed slight decrease of BeA itself. Both metabolite products were detected here only as insignificant products, which indicate that these products remained in cells.

Percentage of individual peaks activities were determined and normalized according to respective total samples activities (100 %).

Figure 4 Identification of the main NAA metabolite (NAA glucosyl ester), precursor ion scans of fragments m/z 141, 179, 185, 347, 393 and 407.

Product ion scan revealed three major peaks: m/z347, m/z393, m/z407 and their fragments were NAA characteristic. Precursor ion scans of fragments m/z185 and m/z141confirmed that they

derive from m/z347, m/z393 and m/z407. The fragmentation pattern and molecular mass of NAA major metabolite MW348 suggests that it is ester of NAA (MW186) with hexose (MW180).

Figure 5 Confirmation of ester bond in NAA major metabolite (identified as NAA glucosyl ester) by its incubation with 0.1 M NH_4OH at 25°C.
NAA major metabolite (identified as NAA glucosyl ester) was quickly degraded to NAA and glucose. After 5 min nearly 60 % of NAA major metabolite has been degraded to NAA and glucose, in later time (30 min and more) of incubation with 0.1 M NH_4OH less than 10 % of NAA major metabolite has been detected.

Figure 6 Accumulation of ^{3}H-2,4-D (2 nM) vs. auxin transport inhibitors CHPAA, NPA and their combination (10 μM in EtOH) in BY-2 tobacco cells.
A. Control line with EtOH.
B. CHPAA (10 μM in EtOH) decreased 2,4-D accumulation by effective influx blockage.
C. NPA (10 μM in EtOH) increased 2,4-D accumulation by effective efflux blockage.
D. Combination of both inhibitors (CHPAA and NPA) revealed the real diffusion of 2,4-D into the cells.

Figure 7 Sensitivity of model-data fit quality to parameter change.

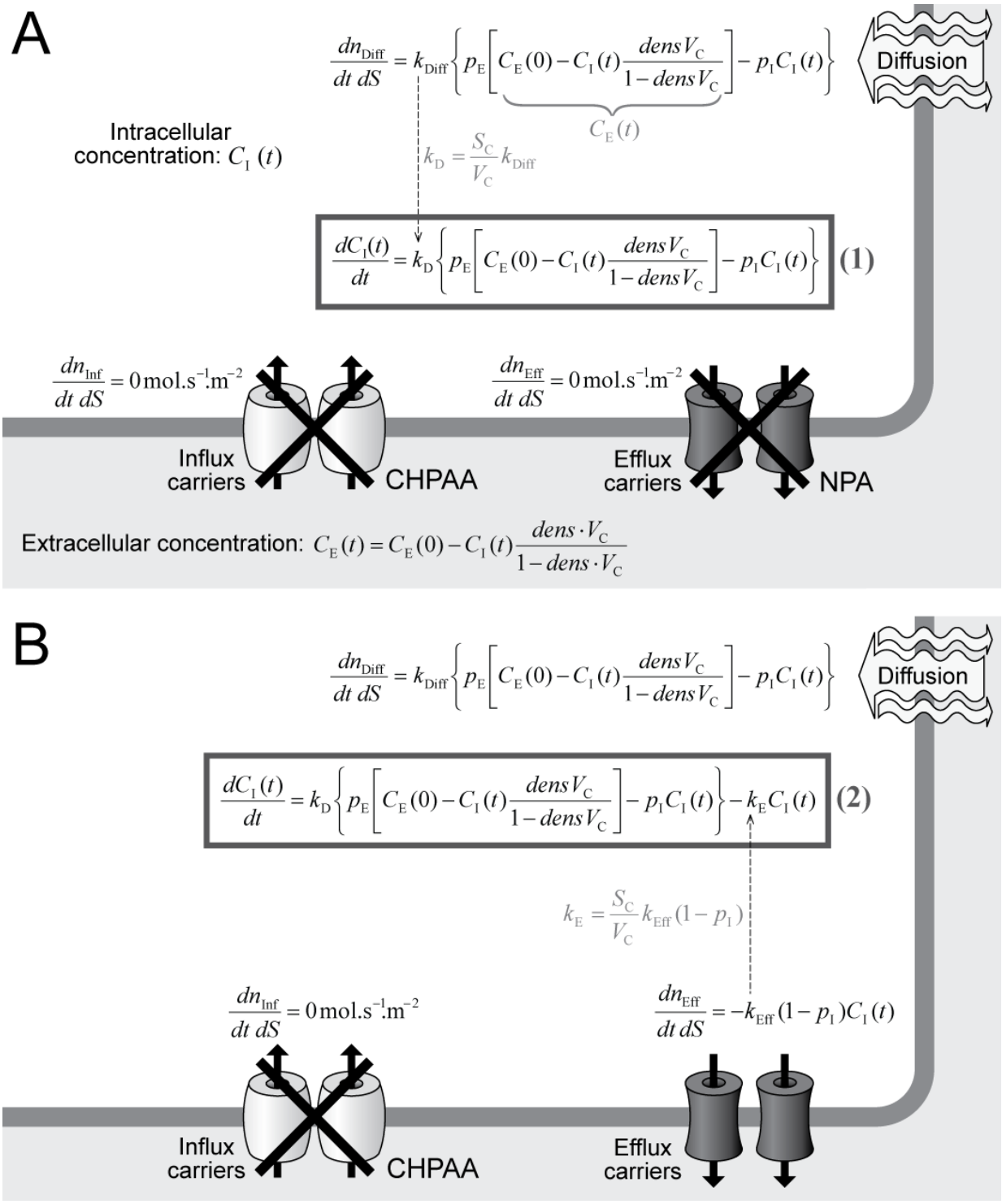

Figure 1 Mathematical model of ^{3}H-2,4-D uptake by diffusion (A) and both diffusion and efflux (B).

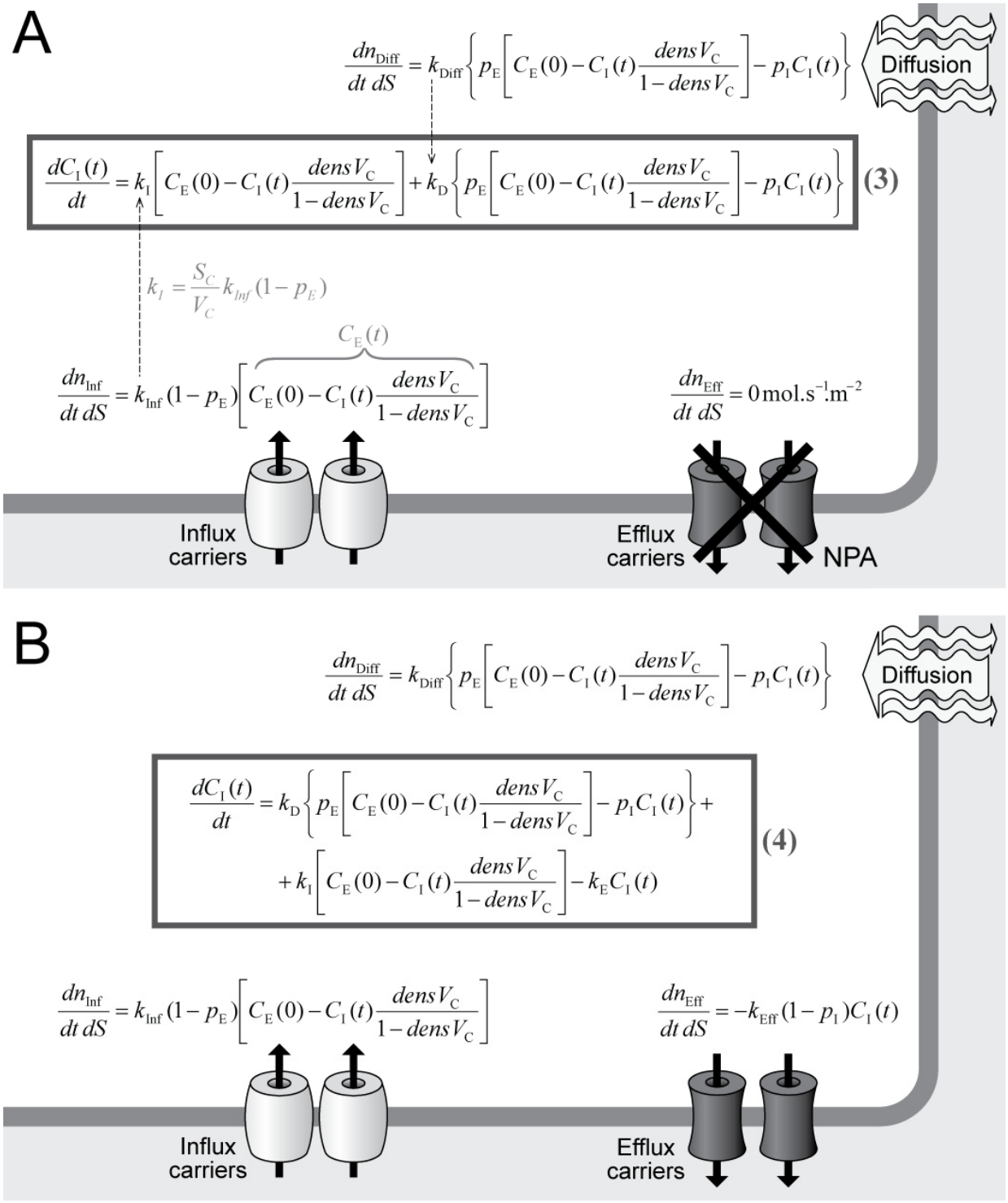

Figure 2 Mathematical model of ^{3}H-2,4-D uptake by diffusion and influx (A) and diffusion, influx and efflux (B).

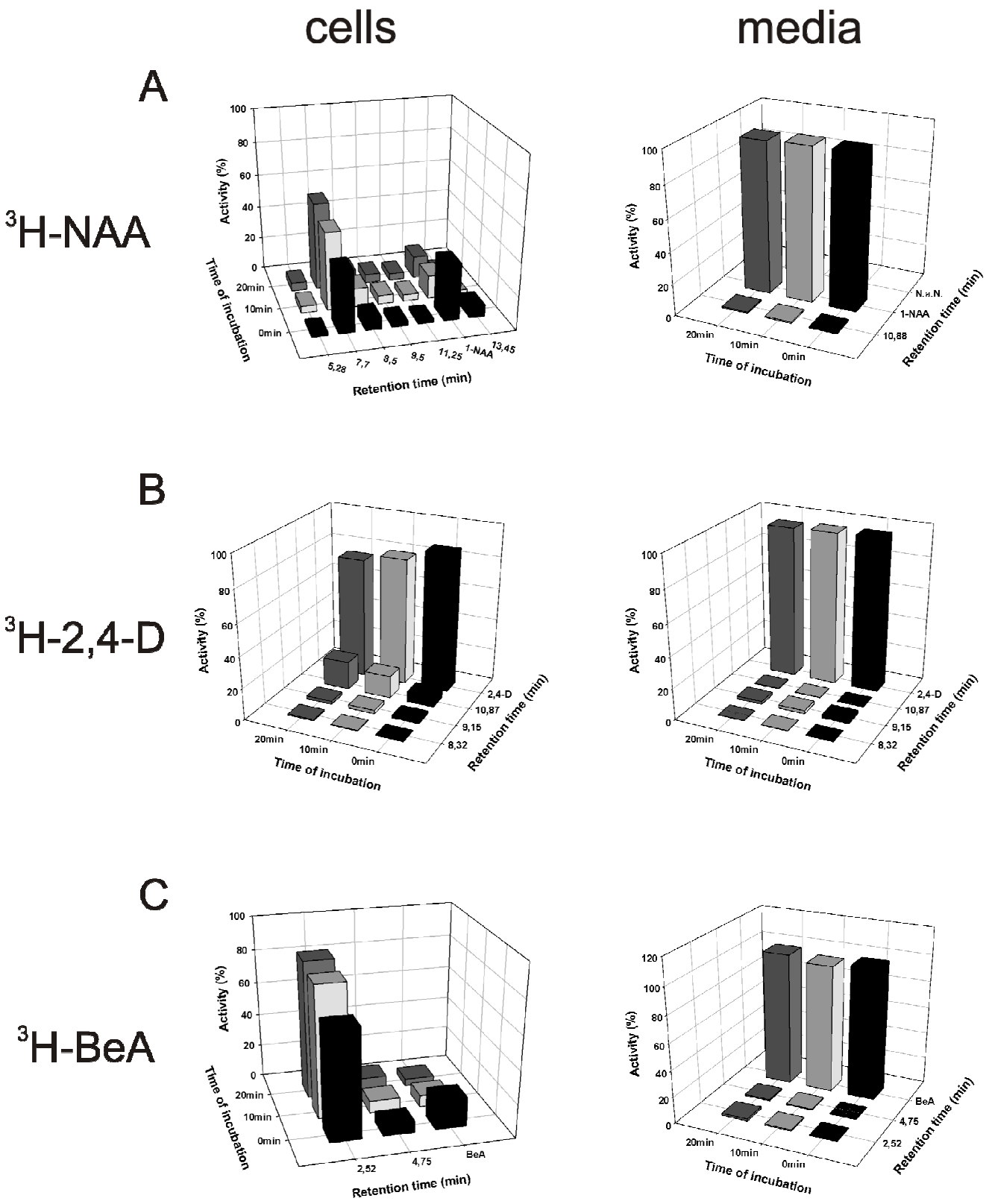

Figure 3 Metabolism of ^{3}H-NAA, ^{3}H-2,4-D and ^{3}H-BeA in BY-2 tobacco cells and media at time of 0, 10 and 20 min of incubation.

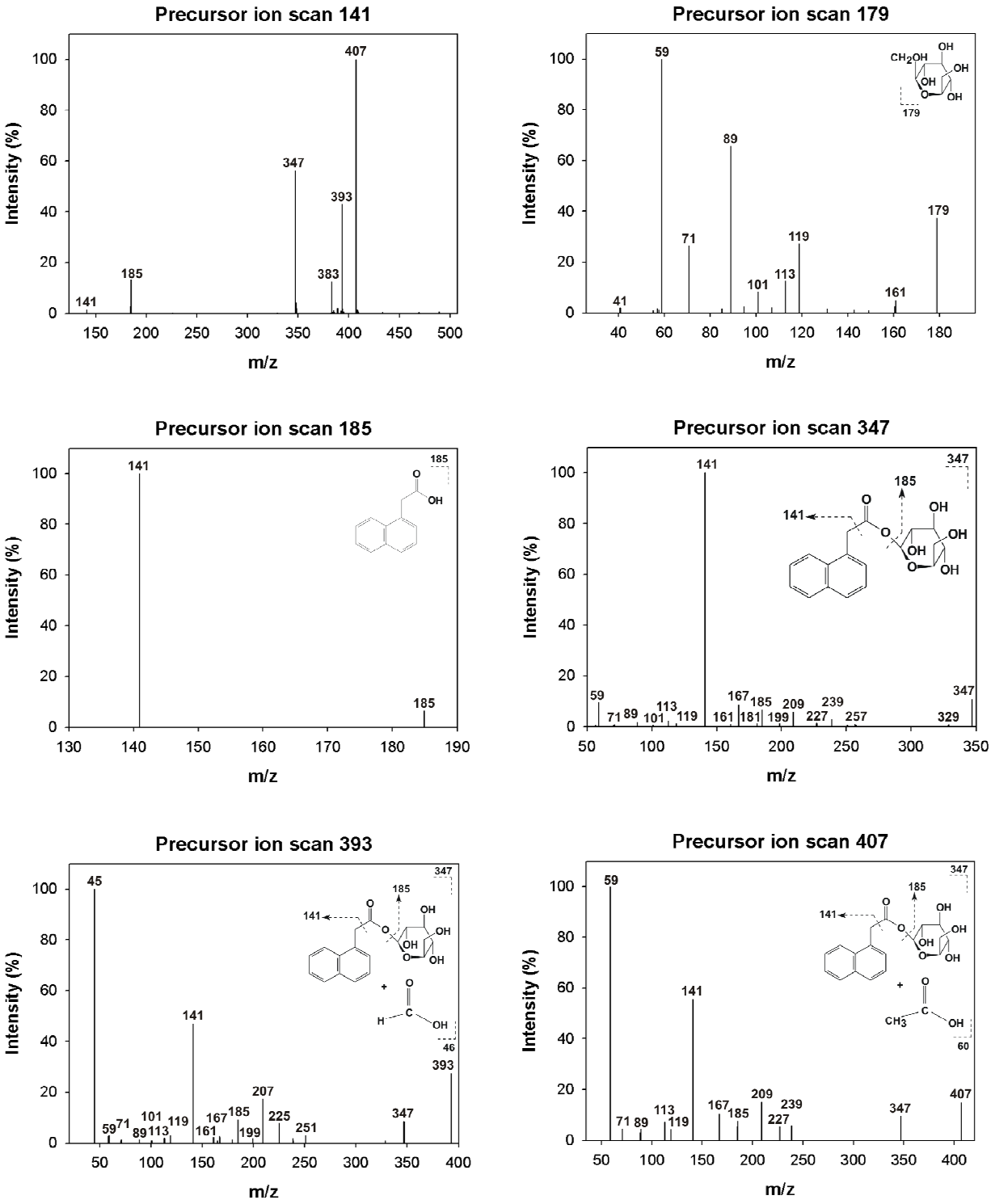

Figure 4 Identification of the main NAA metabolite (NAA glucosyl ester), precursor ion scans of fragments m/z 141, 179, 185, 347, 393 and 407.

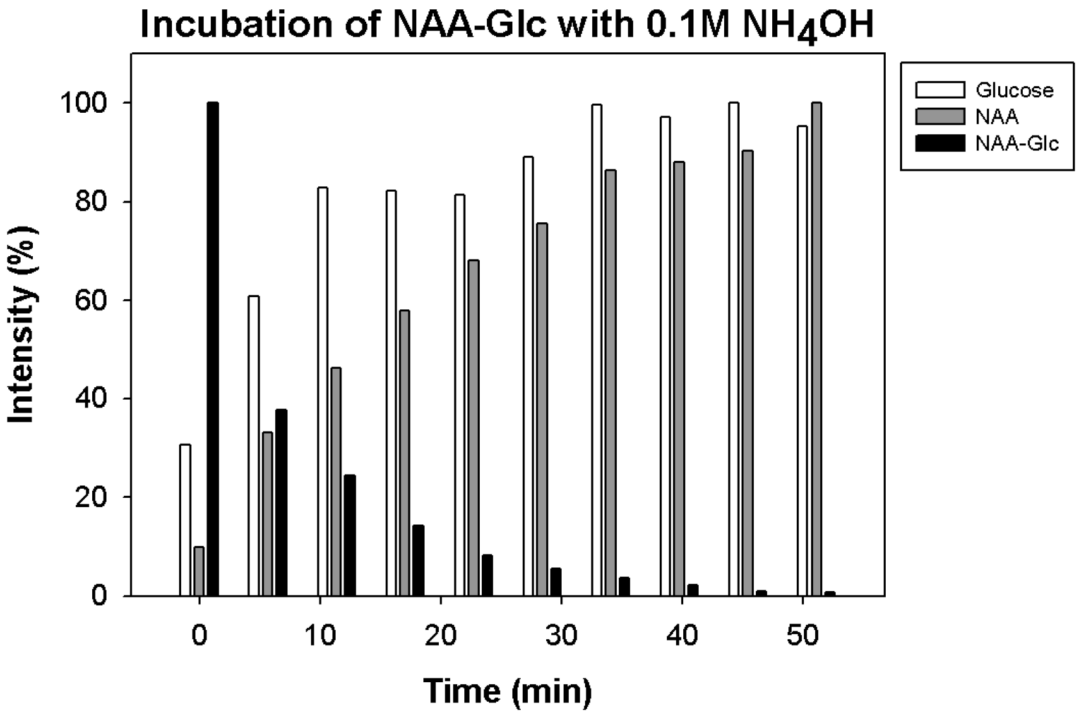

Figure 5 Confirmation of ester bond in NAA major metabolite (identified as NAA glucosyl ester) by its incubation with 0.1 M NH_4OH at 25°C.

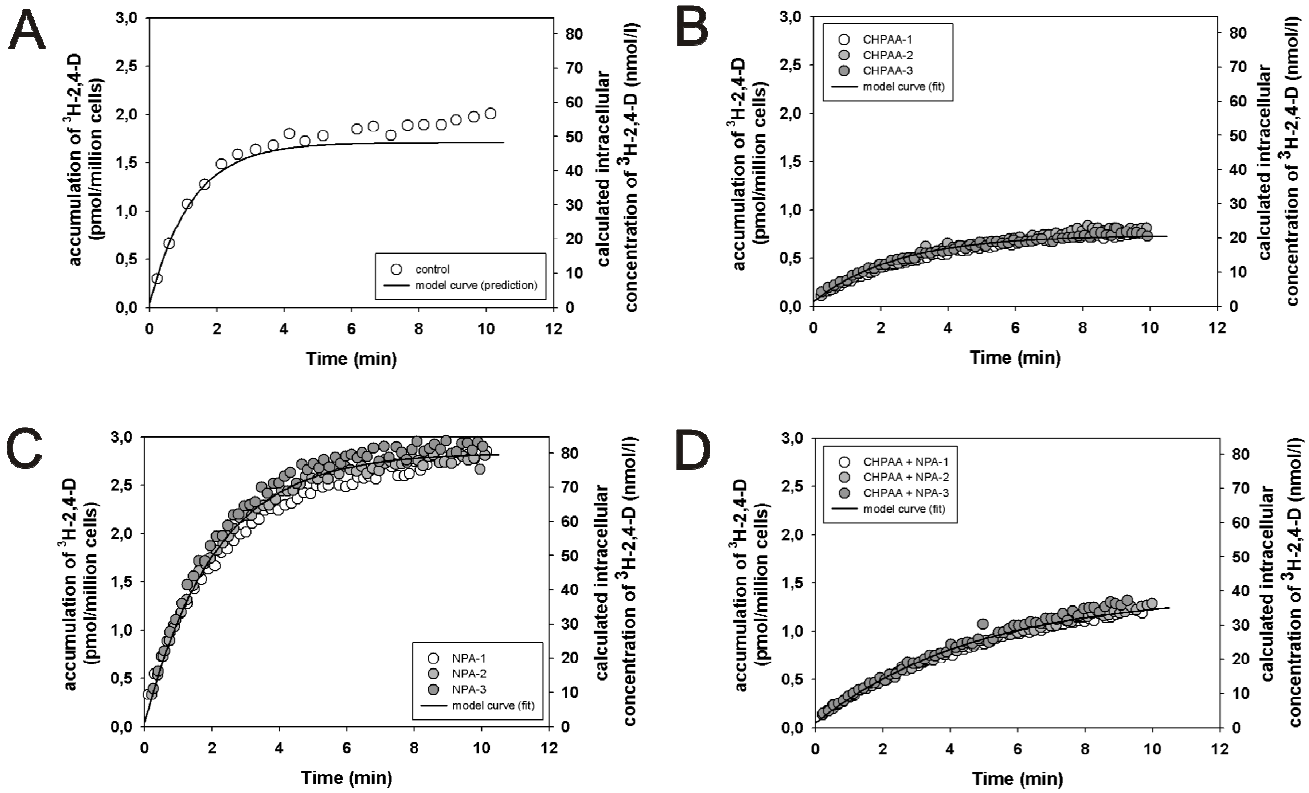

Figure 6 Accumulation of ^{3}H-2,4-D (2 nM) vs. auxin transport inhibitors CHPAA, NPA and their combination (10 μM in EtOH) in BY-2 tobacco cells.

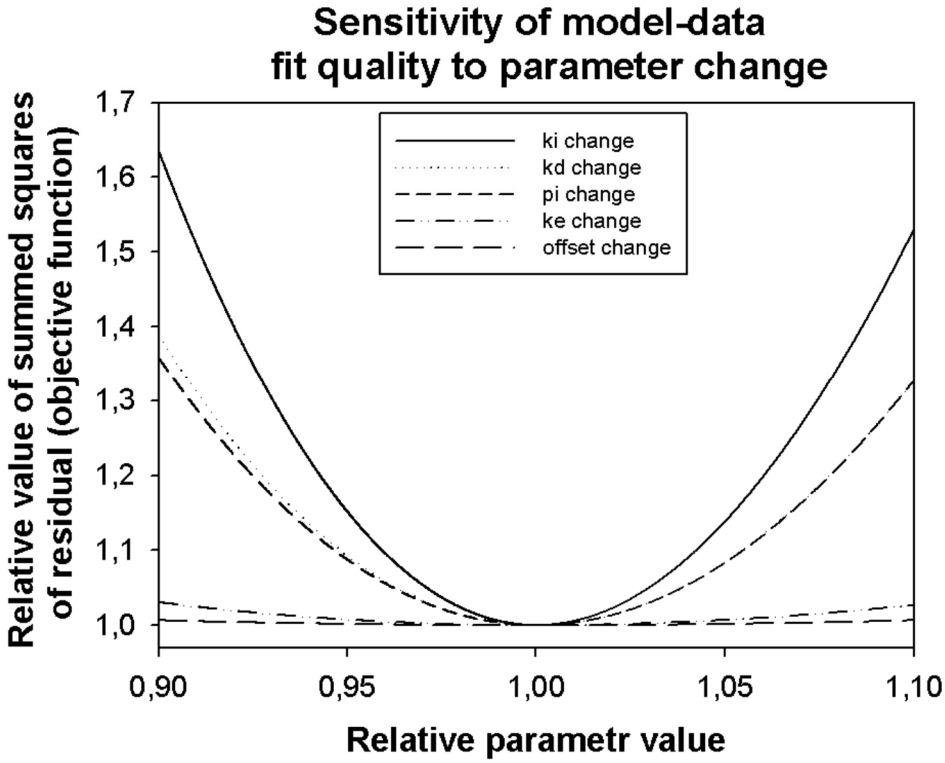

Figure 7 Sensitivity of model-data fit quality to parameter change.

Supplementary material

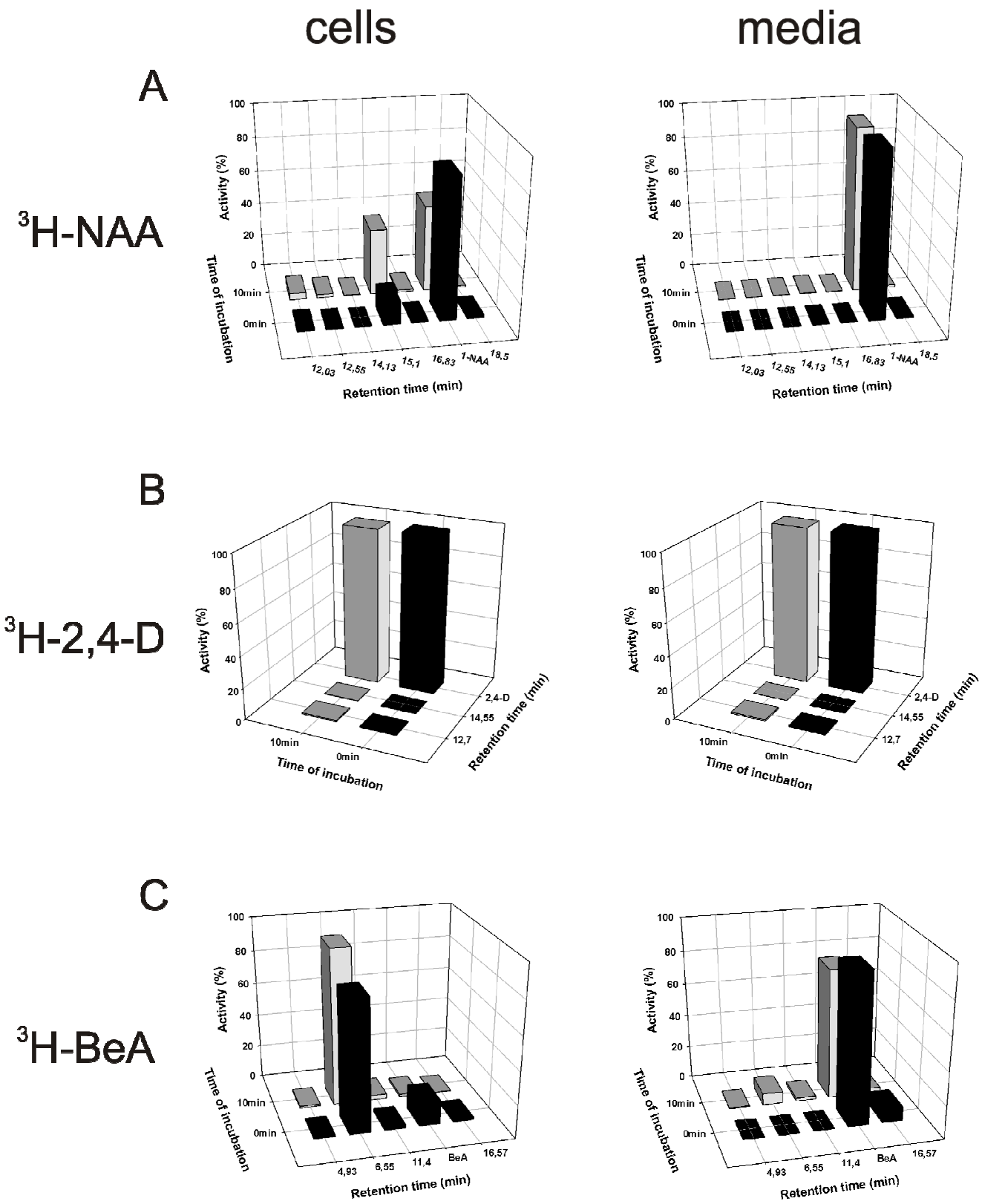

Supplementary figure 1 Metabolism of ^{3}H-NAA, ^{3}H-2,4-D, ^{3}H-BeA in Xanthi tobacco cells and media in time 0 and 10 min of incubation.

A. NAA is metabolized to unknown product (retention time 15.1 min; not identical with NAA glucosyl ester) and at 10 min this metabolite is remarkable in cells. The levels of NAA during 10 min incubation decreased (by about 20 %). Other five unknown and minor metabolites were observed. In incubation medium no changes of NAA and other six minor metabolites were observed, which indicates that products of NAA metabolism remained in cells.

B. 2,4-D is metabolized only very weakly at time 0 and 10 min, and 2,4-D levels in cells and medium stayed constant during incubation.

C. BeA was rapidly metabolized to one predominant (retention time 6.55 min) and other three minor unknown products at 0 and 10 min. BeA level in cells after 10 min incubation decreased significantly. In incubation medium gradual decrease of BeA level was observed. All metabolites detected in cells were also detected in incubation medium, and comparedto BeA peak they were minor. In case of BeA the retention of its metabolites was greater compared to NAA and 2,4-D.

Percentage of individual peaks activities were determined and normalized according to respective total samples activities (100 %).

7. Discussion

ABCB proteins as a plant orthologues of the mammalian multidrug-resistance proteins MDRs have been proved to participate in auxin transport (Martinoia et al., 2002; Verrier et al., 2008). Phenotypic defects caused by loss of ABCB function are most pronounced in vegetative organs and include dwarfism, curly wrinkled leaves, twisted stems and reduced apical dominance, supporting their role in auxin-based development (Bandyopadhyay et al., 2007). Auxin transport defects and dwarf phenotypes are more exaggerated in *Arabidopsis thaliana abcb1/abcb19* double mutants (Noh et al., 2001; Geisler et al., 2003). A direct role for ABCB1 and ABCB19 in cellular efflux was demonstrated when increased auxin retention was observed in mesophyll protoplasts from *Arabidopsis thaliana* and in heterologous systems of yeast, mammalian HeLa or tobacco BY-2 cells (Geisler et al., 2005; Petrášek et al., 2006). Similarly, as it was observed in case of PIN proteins, enhanced auxin efflux in HeLA or yeast cells with heterologously expressed *ABCB1* and *ABCB19* was inhibited by NPA (Geisler et al., 2005; Bouchard et al., 2006). However, contrary to PIN expression, the efflux mediated by the ABCBs in mammalian HeLa cells was insensitive to inhibitors of mammalian organic anion transporters (Geisler et al., 2005; Petrášek et al., 2006).

As shown in Chapter 1 of this thesis (Petrášek et al., 2006), we used inducible ABCB19-transformed BY-2 cell line to compare the roles of PINs and ABCBs in auxin efflux. The induction of ABCB19 led to a decrease in ^{3}H-NAA accumulation, similar to that observed in the PIN4, PIN6 and PIN7 lines. However, compared to PIN-mediated auxin efflux, the ABCB19-mediated NAA efflux was notably less sensitive to NPA. Whereas PIN-mediated transport was completely inhibited by NPA, about 20% of ABCB19-dependent transport was NPA insensitive. It is well known that NPA affinity chromatography was initially used to isolate the ABCB1, 4 and 19 proteins (Murphy et al., 2002; Geisler et al., 2003; Terasaka et al., 2005). Therefore, it is possible that NPA and other auxin efflux inhibitors are able to bind multiple binding and regulatory sites on various proteins with different affinities. Some evidence suggests that there are at least two distinct NPA-binding sites in *Arabidopsis thaliana* membranes. A high affinity site is associated with the inhibition of auxin transport at the PM and with an integral membrane protein. A low affinity site is thought to be a membrane-anchored or peripheral amidase (Murphy et al., 2002). Other non-specific sites of NPA action have been associated with membrane trafficking (Geldner et al., 2001). Moreover, auxin efflux inhibitors might have multiple effects, including modification of actin-based subcellular dynamics (Dhonukshe et al., 2008) or of the ABCB-PIN interaction (Blakeslee et al., 2007). Importantly, NPA has been shown to regulate ABCB-mediated auxin transport by influencing the interaction of ABCB with TWD1

immunophilin (Bailly et al., 2008; Wu et al., 2010) providing the mechanistic explanation for the various sensitivity of plant tissues to NPA.

To address whether PIN action *in planta* requires ABCB1 and ABCB19 proteins, the effect of *PIN1* overexpression on plant development was analyzed in *Arabidopsis abcb1/abcb19* double mutants (Petrášek et al., 2006). The *PIN1* overexpression led to pronounced defects in root gravitropism. Quantitative evaluation of reorientation of root growth revealed that *PIN1* overexpression in *abcb1/abcb19* had the same effects. These data showed that PIN1 action on plant development does not strictly require function of ABCB1 and ABCB19 proteins. This is also supported by evidence that PIN2 mediates auxin efflux in yeast, which is known to lack homologs to *Arabidopsis thaliana* ABCB proteins (Geisler and Murphy, 2006; Yang and Murphy, 2009). However, it was still unclear whether these two auxin transport machineries act *in planta* entirely independently or in a coordinated fashion.

This is partially addressed in the Chapter 2 of this thesis (Mravec et al., 2008), where the effect of increased auxin efflux in BY-2 cells was examined on the level of cell growth and morphology of non-induced and induced PIN7 and ABCB19 cell lines (already used in Petrášek et al., 2006). After induction of *PIN7* or *ABCB19* expression, analogous phenotypical changes occurred: cells ceased to divide, started to elongate, and formed and accumulated starch granules. Similar morphological changes were observed in induced PIN4 and PIN6 lines or constitutive PIN1 line which also showed increased auxin efflux. These results imply that the enhanced auxin efflux leads to depletion of auxin from cells, resulting in a change in the developmental program reflected by the switch from cell division to cell elongation. The auxin starvation phenotype in induced PIN7 cell line was rescued by the application of auxin efflux inhibitor NPA. However, similarly as shown in Petrášek et al. (2006) in less NPA-sensitive ABCB19 cell line, NPA was ineffective thus pointing to possible NPA-mediated regulation of ABCB19 with TWD1 (Bailly et al., 2008; Wu et al., 2010).

Further, results presented in Mravec et al. (2008) allowed propose the model for *Arabidopsis* roots, where ABCBs control auxin transport in auxin channel-forming cells and thus controlling the amount of auxin for directional PIN-dependent auxin transport. In the model, the proportions of ABCBs that do not colocalize with PINs act multilaterally in auxin efflux and thus regulate the effective cellular auxin concentration available for PIN-mediated transport. This combined action of PIN and ABCB determines how much auxin flows through auxin channels. Observation of a higher cellular auxin concentration in *abcb* mutants (Bouchard et al., 2006) that might enhance PIN-mediated transport directly supports this scenario. It is likely that for long-distance transport, e.g. in stems, another mode of ABCB and PIN interaction functions as suggested by strong auxin transport defects in *abcb* mutant stems (Noh et al., 2001; Geisler et al.,

2005). It is important to note that different internal or external cues, such as light, can influence the extent and mode of PIN-ABCB interactions, for instance at the level of functional pairing of PINs and ABCBs (Blakeslee et al., 2007; Titapiwatanakun et al., 2009). Also, the activity of previously uncharacterized ABCBs may significantly contribute to auxin transport. In summary, our model could provide an explanation of the existence of two auxin transport mechanisms (PIN-based and ABCB-based) that ensure precise and proper formation of spatial and temporal auxin distribution in plants.

Like the PIN proteins, ABCBs exhibit both the polar and apolar distribution on the PM. Both ABCB1 and ABCB4 exhibit polar localisations in elongating and mature epidermal and/or cortical root cells and apolar localisations in the lateral root cap (Geisler et al., 2005; Terasaka et al., 2005; Cho et al., 2007). ABCB19 exhibits a predominantly polar localisation on the plasma membrane in immature vascular cells and apolar distribution in mature vascular, cortical and epidermal cells at the root apex (Blakeslee et al., 2007; Wu et al., 2007). Blakeslee et al. (2007) showed by comparisons with the cytokinesis marker KNOLLE that the polar localisation of ABCB19 seen in immature vascular tissues coincides with cell wall maturation, but not with early cell plate formation. In Chapters 1, 3, 4 and 5 (Petrášek et al., 2006; Jelínková and Malínská et al., 2010; Laňková et al., 2010) of this thesis the localization of ABCB19 and ABCB4 is characterized in BY-2 cells. For ABCB19 (Petrášek et al., 2006) the localization was shown to be not predominantly at transversal plasma membranes within the cell chain as it was shown for PIN proteins. This is in agreement with mostly non-polarly localized ABCB19 in various tissues of *Arabidopsis thaliana* (Petrášek and Friml, 2009). Moreover, in Chapter 3 (Jelínková and Malínská et al., 2010), ABCB4-transformed cell line was shown to be transiently re-localized from the plasma membrane with routinely used concentrations of FM 4-64 and FM 5-95. The active process of re-localization is blocked neither by inhibitors of endocytosis (BFA - which in plants act as an inhibitor of anterograde vesicle trafficking) nor by cytoskeletal drugs (wortmannin - which have all been successfully shown to block endocytosis in plants (Emans et al., 2002; Dettmer et al., 2006)). The formation of FM-induced ABCB4 patches was blocked only after sodium azide treatment, which suggests that the process of FM-induced PM protein re-localization is energy-dependent, possibly via an ATP-driven step.

Interestingly, in Laňková et al. (2010) we showed that after the application of putative auxin transport inhibitors 1-NOA, 2-NOA and CHPAA, ABCB4 is more stable on PM than AUX1 or PIN1 proteins. While in AUX1- and PIN1-transformed BY-2 cell lines fast redistribution of proteins from PM inside the cells was induced, ABCB4 in form of a few membrane aggregates appeared only after long inhibitors treatment. Both NOAs (1-NOA being more effective) can induce the formation of endosomes containing auxin carriers. At least partly

this may be the reason for the decrease in auxin influx or efflux after the 1-NOA or 2-NOA treatments. The fact that NOA was not able to induce fast redistribution of ABCB4 (as observed for AUX1 and PIN1) and that this ABCB4 appeared in membrane aggregates after longer treatment suggests a membrane composition-dependent NOA effect. The most important in this respect seems to be sterol composition, namely the presence of sterols and sterol-associated proteins (Borner et al., 2005); since ABCB4 was reported to be present in these compartments (Titapiwatanakun and Murphy, 2009), thus the ABCB4 could be more resistant to 1-NOA treatment.

Further in Chapter 5 (Kubeš and Yang et al., submitted), we provided evidence that ABCB4 functions as a homeostatic switch on the PM for regulation of cellular auxin levels. We confirmed that ABCB4 function in shootward auxin movement from the root apex increases with auxin concentration, but it is evident in regulating root hair elongation at lower concentrations. It seems that ABCB4 plays a more important role in controlling auxin movement out of the elongation zone as previously proposed (Peer and Murphy, 2007). Expression of *Arabidopsis thaliana* ABCB4::ABCB4-GFP in BY-2 resulted in abundance and localisation similar to that reported for *35S*-driven expression of ABCB4 in BY-2 (Cho et al., 2007) as well as a partial inhibition of cell division compared to untransformed cells. This inhibition was similar to *PIN1pro*:PIN1-GFP expression, but it was less severe than in auxin-starved BY-2 cells or in cells expressing *Arabidopsis thaliana PIN4*, *PIN6*, *PIN7* and *ABCB19* (Petrášek et al., 2006; Mravec et al., 2008). Further, cell elongation observed with expression of *Arabidopsis thaliana ABCB19* or *PIN1* (Mravec et al., 2008) was not observed in 3-day ABCB4-GFP cells, perhaps due to decreased transversal PM localisation of ABCB4-GFP (Cho et al., 2007) compared to PIN1-GFP. This decrease in transversal localisation may be a consequence of faster lateral diffusion or trafficking of ABCB4 compared to PIN1-GFP as indicated by FRAP analysis. As reported previously (Petrášek et al., 2002, 2006), PIN1 expression in BY-2 resulted in increased ^{3}H-NAA efflux, and NPA treatment increased NAA retention. Similarly, BY-2 cells expressing *ABCB4pro*:ABCB4-GFP exhibited increased retention of NAA after NPA treatment, which is in agreement with results in BY-2 cells overexpressing *ABCB4* under the control of a *35S* promoter (Cho et al., 2007). 2,4-D is often used as a substitute for IAA in growth assays, as it is highly stable (Delbarre et al., 1996) and is poorly distributed through the plant by auxin polar transport mechanisms (Pitts et al., 1998). This synthetic auxin taken up via AUX1/LAX permeases (Bennett et al., 1996; Yang et al., 2006; Yang and Murphy, 2009) was shown to be an uptake substrate for ABCB4 expressed in *Schizosaccharomyces pombe,* and to non-competitively inhibit ABCB4 ^{3}H-IAA efflux activity (Yang and Murphy, 2009). 2,4-D is a weak efflux substrate for all ABCB and PIN proteins expressed in non-plant heterologous systems, but it is a preferred

efflux substrate for the ABCG37/PDR9 pleiotropic substrate transporter (Titapiwatanakun et al., 2009; Růžička et al., 2010). Our analysis of 2,4-D effects on root hair elongation confirmed that this compound is an ABCB4 uptake substrate *in planta*. Low concentrations of 2,4-D compensated for differences in *abcb4* root hair elongation in a manner similar to what is seen with IAA, and higher 2,4-D concentrations inhibited root hair elongation equally in both *abcb4* and wild-type. However, unlike IAA, an intermediate concentration of 2,4-D (50 nM) inhibited wild-type root hair elongation to a greater extent than in *abcb4*, suggesting a direct role of ABCB4 in 2,4-D uptake. This result cannot be attributed to enhanced AUX1-driven uptake in *abcb4* root hairs, as *AUX1* is not expressed in trichoblasts (Jones et al., 2009). 2,4-D is also the preferred substrate for native 2-NOA-sensitive auxin influx assays in BY-2, and ABCB4 is resistant to 2-NOA inhibition (Laňková et al., 2010). As expected, 2-NOA decreased the net uptake of ^{3}H-2,4-D in control and PIN1-expressing cells, but had a lesser effect on the accumulation of 2,4-D in ABCB4-overexpressing cells. However, 2,4-D uptake was enhanced in cells expressing *ABCB4* after background auxin uptake was blocked with 2-NOA, suggesting a non-competitive interaction of 2,4-D with the ABCB4-based auxin efflux activity. This notion was further supported by the fact that pre-treatment of cells expressing *ABCB4* with cold 2,4-D, but not cold IAA, resulted in an enhanced net uptake of ^{3}H-2,4-D. An enhancement of auxin influx in BY-2 expressing ABCB4 was also observed following addition of NPA to 2-NOA-pretreated cells. This treatment resulted in an increase in 2,4-D accumulation, consistent with continued 2,4-D import by ABCB4 in combination with inhibition of the weak PIN and ABCB (including ABCB4) efflux activity. One explanation for the lack of ^{3}H-NAA efflux seen in BY-2 cells expressing ABCB4 might be that the cells are routinely maintained on medium containing the synthetic auxin 2,4-D (Nagata et al., 1992). Although routinely washed out with uptake buffer before auxin transport assays are conducted (Cho et al., 2007), 2,4-D from the BY-2 cell culturing medium bound to ABCB4 may be difficult to completely eliminate, especially as 2,4-D is poorly metabolized in tobacco cells compared to IAA and NAA (Delbarre et al. 1994, 1996). In short term yeast assays, ABCB4 showed influx activity at lower IAA concentrations and ABCB4 transport activity switched to efflux at concentrations >250 nM or after longer exposure to IAA. Conversion to efflux rather than conventional saturation suggests that IAA uptake mediated by ABCB4 is an indirect effect of transporter activity and suggests that ABCB4 could mobilise other substrates. Our results presented here indicate that ABCB4 regulates cellular auxin levels in the *Arabidopsis thaliana* root epidermis by enhancing auxin uptake when cellular levels are low and catalyzing auxin efflux when internal levels rise. Alternatively, the combination of more hydrophobic anchoring and additional IAA binding sites in ABCB4 may provide a mechanism for substrate uptake that would not occur in ABCB1 or 19 during the

conformational change associated with the first of two ATP hydrolysis steps required for ABC transport function (Knöller and Murphy, 2010). Substrate activation and conformational change has been shown for other ABC transporters (Loo et al., 2003; Terasaka et al., 2005; Sauna et al., 2008), and apparent drug-induced reversal of mammalian ABCB1 and ABCG22 activity has recently been reported (Shi et al., 2011). Finally, we confirmed that ABCB4 enhances 2,4-D uptake, but not efflux, and thus ABCB4 appears to be a direct herbicidal target of 2,4-D. Binding of 2,4-D to ABCB4 results in increased accumulation of both 2,4-D and other auxins in root epidermal cells and so it is likely to amplify the herbicidal effects of the compound. As such, tissue-specific manipulation of *ABCB4* expression may be a useful tool for decreasing damage to crop plants caused by 2,4-D drift.

The mathematical modelling of auxin transport at the cellular level revealed and confirmed the parameters for better and more precise characterization of auxin transport mechanisms in tobacco BY-2 cells. In Chapter 6 (Hošek and Kubeš et al., in preparation), we indicated that NAA is strongly and rapidly metabolized during accumulation experiments in BY-2 cells. We identified the predominant metabolite as NAA glucosyl ester (NAA-Glc). Further, we showed that NAA-Glc is retained in the cells, thus raising apparent intracellular concentration of NAA previously measured during accumulations of radiolabeled auxins. This might have led to serious underestimation of auxin efflux carriers transport capacity for NAA as well as IAA in the past. In contrast, metabolism of 2,4-D remains fairly weak in the time span of accumulation assays, making 2,4-D an ideal tool for probing auxin transport on cellular level, at least on the level of auxin uptake. Hence, using 2,4-D accumulation data measured under various conditions (in presence of auxin transport inhibitors NPA or CHPAA) and employing mathematical model of auxin transport we characterize and validate parameters of 2,4-D transport on cellular level.

Obtained experimental data provides a basis for mathematical description of characteristics of transport of particular auxins, including their metabolism. Making use of relevant mutants and overexpressors, this data can also serve as a basis for further modelling related to contributions of particular auxin transport proteins and for construction of detailed mathematical model of auxin transport on the cellular level.

8. Conclusion

In the papers and manuscripts forming this thesis it was shown that:

- The overexpression of ABCB19 results in a decrease of ^{3}H-NAA accumulation in BY-2 cells, similar to that observed in the PIN7-overexpressing line, and produces the auxin starvation phenotype.
- Compared to PIN7-mediated auxin efflux, the ABCB19-mediated NAA efflux is less sensitive to auxin efflux inhibitor NPA, and the ABCB19-dependent auxin starvation phenotype cannot be rescued by NPA.
- Auxin transporters ABCB1, ABCB4 and ABCB19 display non-polar localization on PM in BY-2 cells.
- ABCB4 protein is more stable and resistant to auxin transport inhibitors 1-NOA, 2-NOA and CHPAA in the plasma membrane of BY-2 cells.
- Routinely used concentrations of FM styryl dyes FM 4-64 trigger transient re-localization of ABCB4.
- ABCB4 functions as a homeostatic switch on the PM for regulation of cellular auxin levels. There is a non-competitive interaction of 2,4-D with the ABCB4-based auxin efflux activity. ABCB4 enhances 2,4-D uptake, but not efflux, and ABCB4 appears to be a direct herbicidal target of 2,4-D.
- NAA is strongly and rapidly metabolized during accumulation assays in BY-2 cells and the predominant metabolite is NAA glucosyl ester, which is retained in the cells. In contrast, metabolism of 2,4-D remains fairly weak in the time span of accumulation assays, making 2,4-D good tool for probing auxin transport on cellular level. Using 2,4-D accumulation data measured under various conditions and exploring the modified mathematical model of auxin transport, the parameters of 2,4-D transport on cellular level were characterized and validated.

Altogether, results presented in this thesis further clarified the role of ABC-transporters in translocation of auxin across plasma membrane and pointed at their involvement in establishment and maintenance of cellular auxin homeostasis in a way different from that of PIN5.

9. References

Analysis of the genome sequence of the flowering plant *Arabidopsis thaliana*. (2000) *Nature*, **408**, 796-815.

Abas, L., Benjamins, R., Malenica, N., Paciorek, T., Wirniewska, J., Moulinier-Anzola, J.C., Sieberer, T., Friml, J. and Luschnig, C. (2006) Intracellular trafficking and proteolysis of the Arabidopsis auxin-efflux facilitator PIN2 are involved in root gravitropism. *Nature Cell Biology*, **8**, 249-256.

Abel, S., Nguyen, M.D. and Theologis, A. (1995) THE PS-IAA4/5-LIKE FAMILY OF EARLY AUXIN-INDUCIBLE MESSENGER-RNAS IN ARABIDOPSIS-THALIANA. *Journal of Molecular Biology*, **251**, 533-549.

Alvarez, A.I., Real, R., Perez, M., Mendoza, G., Prieto, J.G. and Merino, G. (2010) Modulation of the Activity of ABC Transporters (P-Glycoprotein, MRP2, BCRP) by Flavonoids and Drug Response. *Journal of Pharmaceutical Sciences*, **99**, 598-617.

Ambudkar, S.V., Kimchi-Sarfaty, C., Sauna, Z.E. and Gottesman, M.M. (2003) P-glycoprotein: from genomics to mechanism. *Oncogene*, **22**, 7468-7485.

Ames, G.F., Mimura, C.S., Holbrook, S.R. and Shyamala, V. (1992) TRAFFIC ATPASES - A SUPERFAMILY OF TRANSPORT PROTEINS OPERATING FROM ESCHERICHIA-COLI TO HUMANS. *Advances in Enzymology and Related Areas of Molecular Biology*, **65**, 1-47.

An, G., Watson, B.D., Stachel, S., Gordon, M.P. and Nester, E.W. (1985) NEW CLONING VEHICLES FOR TRANSFORMATION OF HIGHER-PLANTS. *Embo Journal*, **4**, 277-284.

Aoyama, T. and Chua, N.H. (1997) A glucocorticoid-mediated transcriptional induction system in transgenic plants. *Plant Journal*, **11**, 605-612.

Bailly, A., Sovero, V. and Geisler, M. (2006) The TWISTED DWARF's ABC - How Immunophilins Regulate Auxin Transport. *Plant Signaling & Behavior*, **1**, 277-280.

Bailly, A., Sovero, V., Vincenzetti, V., Santelia, D., Bartnik, D., Koenig, B.W., Mancuso, S., Martinoia, E. and Geisler, M. (2008) Modulation of P-glycoproteins by auxin transport inhibitors is mediated by interaction with immunophilins. *Journal of Biological Chemistry*, **283**, 21817-21826.

Bainbridge, K., Guyomarc'h, S., Bayer, E., Swarup, R., Bennett, M., Mandel, T. and Kuhlemeier, C. (2008) Auxin influx carriers stabilize phyllotactic patterning. *Genes & Development*, **22**, 810-823.

Bais, H.P., Weir, T.L., Perry, L.G., Gilroy, S. and Vivanco, J.M. (2006) The role of root exudates in rhizosphere interations with plants and other organisms. *Annual Review of Plant Biology*, **57**, 233-266.

Bajguz, A. and Piotrowska, A. (2009) Conjugates of auxin and cytokinin. *Phytochemistry*, **70**, 957-969.

Bandyopadhyay, A., Blakeslee, J.J., Lee, O.R., Mravec, J., Sauer, M., Titapiwatanakun, B., Makam, S.N., Bouchard, R., Geisler, M., Martinoia, E., Friml, J., Peer, W.A. and Murphy, A.S. (2007) Interactions of PIN and PGP auxin transport mechanisms. *Biochemical Society Transactions*, **35**, 137-141.

Barlier, I., Kowalczyk, M., Marchant, A., Ljung, K., Bhalerao, R., Bennett, M., Sandberg, G. and Bellini, C. (2000) The SUR2 gene of Arabidopsis thaliana encodes the cytochrome P450CYP83B1, a modulator of auxin homeostasis. *Proceedings of the National Academy of Sciences of the United States of America*, **97**, 14819-14824.

Bartel, B. (1997) Auxin biosynthesis. *Annual Review of Plant Physiology and Plant Molecular Biology*, **48**, 49-64.

Bauly, J.M., Sealy, I.M., Macdonald, H., Brearley, J., Droge, S., Hillmer, S., Robinson, D.G., Venis, M.A., Blatt, M.R., Lazarus, C.M. and Napier, R.M. (2000) Overexpression of auxin-binding protein enhances the sensitivity of guard cells to auxin. *Plant Physiology*, **124**, 1229-1238.

Bell, C.J. and Maher, E.P. (1990) Mutants of *Arabidopsis thaliana*with abnormal gravitropic responses. *Molecular and General Genetics*, **220**, 289-293.

Benjamins, R., Quint, A., Weijers, D., Hooykaas, P. and Offringa, R. (2001) The PINOID protein kinase regulates organ development in Arabidopsis by enhancing polar auxin transport. *Development*, **128**, 4057-4067.

Benjamins, R. and Scheres, B. (2008) Auxin: The looping star in plant development. *Annual Review of Plant Biology*, **59**, 443-465.

Benková, E., Michniewicz, M., Sauer, M., Teichmann, T., Seifertová, D., Jurgens, G. and Friml, J. (2003) Local, efflux-dependent auxin gradients as a common module for plant organ formation. *Cell*, **115**, 591-602.

Bennett, M.J., Marchant, A., Green, H.G., May, S.T., Ward, S.P., Millner, P.A., Walker, A.R., Schulz, B. and Feldmann, K.A. (1996) Arabidopsis AUX1 gene: A permease-like regulator of root gravitropism. *Science*, **273**, 948-950.

Blakeslee, J.J., Bandyopadhyay, A., Lee, O.R., Mravec, J., Titapiwatanakun, B., Sauer, M., Makam, S.N., Cheng, Y., Bouchard, R., Adamec, J., Geisler, M., Nagashima, A., Sakai, T., Martinoia, E., Friml, J., Peer, W.A. and Murphy, A.S. (2007) Interactions among PIN-FORMED and P-glycoprotein auxin transporters in Arabidopsis. *Plant Cell*, **19**, 131-147.

Blakeslee, J.J., Peer, W.A. and Murphy, A.S. (2005) Auxin transport. *Current Opinion in Plant Biology*, **8**, 494-500.

Blancaflor, E.B. and Masson, P.H. (2003) Plant gravitropism. Unraveling the ups and downs of a complex process. *Plant Physiology*, **133**, 1677-1690.

Blilou, I., Xu, J., Wildwater, M., Willemsen, V., Paponov, I., Friml, J., Heidstra, R., Aida, M., Palme, K. and Scheres, B. (2005) The PIN auxin efflux facilitator network controls growth and patterning in Arabidopsis roots. *Nature*, **433**, 39-44.

Boerjan, W., Cervera, M.T., Delarue, M., Beeckman, T., Dewitte, W., Bellini, C., Caboche, M., Vanonckelen, H., Vanmontagu, M. and Inze, D. (1995) SUPERROOT, A RECESSIVE MUTATION IN ARABIDOPSIS, CONFERS AUXIN OVERPRODUCTION. *Plant Cell*, **7**, 1405-1419.

Borner, G.H.H., Sherrier, D.J., Weimar, T., Michaelson, L.V., Hawkins, N.D., MacAskill, A., Napier, J.A., Beale, M.H., Lilley, K.S. and Dupree P. (2005) Analysis of detergent-resistant membranes in Arabidopsis. Evidence for plasma membrane lipid rafts. *Plant Physiology*, **137**, 104–116.

Bouchard, R., Bailly, A., Blakeslee, J.J., Oehring, S.C., Vincenzetti, V., Lee, O.R., Paponov, I., Palme, K., Mancuso, S., Murphy, A.S., Schulz, B. and Geisler, M. (2006) Immunophilin-like TWISTED DWARF1 modulates auxin efflux activities of Arabidopsis P-glycoproteins. *Journal of Biological Chemistry*, **281**, 30603-30612.

Bradley, G., Javanta, P.F. and Ling, V. (1988) Mechanism of multigdrug resistance. *Biochmica et Biophysica Acta*, **948**, 87-128.

Breiman, A., Fawcett, T.W., Ghirardi, M.L. and Mattoo, A.K. (1992) PLANT ORGANELLES CONTAIN DISTINCT PEPTIDYLPROLYL CIS, TRANS-ISOMERASES. *Journal of Biological Chemistry*, **267**, 21293-21296.

Brown, D.E., Rashotte, A.M., Murphy, A.S., Normanly, J., Tague, B.W., Peer, W.A., Taiz, L. and Muday, G.K. (2001) Flavonoids act as negative regulators of auxin transport in vivo in Arabidopsis. *Plant Physiology*, **126**, 524-535.

Buer, C.S., Imin, N. and Djordjevic, M.A. (2010) Flavonoids: New Roles for Old Molecules. *Journal of Integrative Plant Biology*, **52**, 98-111.

Buer, C.S. and Muday, G.K. (2004) The transparent testa4 mutation prevents flavonoid synthesis and alters auxin transport and the response of Arabidopsis roots to gravity and light. *Plant Cell*, **16**, 1191-1205.

Buer, C.S., Sukumar, P. and Muday, G.K. (2006) Ethylene modulates flavonoid accumulation and gravitropic responses in roots of Arabidopsis. *Plant Physiology*, **140**, 1384-1396.

Calderon-Villalobos, L.I., Tan, X., Zheng, N. and Estelle, M. (2010) Auxin Perception-Structural Insights. *Cold Spring Harbor Perspectives in Biology*, **2**.

Chang, G. (2003) Structure of MsbA from Vibrio cholera: A multidrug resistance ABC transporter homolog in a closed conformation. *Journal of Molecular Biology*, **330**, 419-430.

Chang, G. and Roth, C.B. (2001) Structure of MsbA from E-coli: A homolog of the multidrug resistance ATP binding cassette (ABC) transporters (Retracted Article. See vol 314, pg 1875, 2006). *Science*, **293**, 1793-1800.

Chen, J.G., Shimomura, S., Sitbon, F., Sandberg, G. and Jones, A.M. (2001a) The role of auxin-binding protein 1 in the expansion of tobacco leaf cells. *Plant Journal*, **28**, 607-617.

Chen, L.S., Ortiz-Lopez, A., Jung, A. and Bush, D.R. (2001b) ANT1, an aromatic and neutral amino acid transporter in Arabidopsis. *Plant Physiology*, **125**, 1813-1820.

Chen, R.J., Hilson, P., Sedbrook, J., Rosen, E., Caspar, T. and Masson, P.H. (1998) The Arabidopsis thaliana AGRAVITROPIC 1 gene encodes a component of the polar-auxin-transport efflux carrier. *Proceedings of the National Academy of Sciences of the United States of America*, **95**, 15112-15117.

Cho, M., Lee, S.H. and Cho, H.T. (2007) P-glycoprotein4 displays auxin efflux transporter-like action in Arabidopsis root hair cells and tobacco cells. *Plant Cell*, **19**, 3930-3943.

Chou, I.T. and Gasser, C.S. (1997) Characterization of the cyclophilin gene family of Arabidopsis thaliana and phylogenetic analysis of known cyclophilin proteins. *Plant Molecular Biology*, **35**, 873-892.

Christensen, S.K., Dagenais, N., Chory, J. and Weigel, D. (2000) Regulation of auxin response by the protein kinase PINOID. *Cell*, **100**, 469-478.

Cohen, J.D. and Bandurski, R.S. (1982) CHEMISTRY AND PHYSIOLOGY OF THE BOUND AUXINS. *Annual Review of Plant Physiology and Plant Molecular Biology*, **33**, 403-430.

Cohen, J.D., Slovin, J.P. and Hendrickson, A.M. (2003) Two genetically discrete pathways convert tryptophan to auxin: more redundancy in auxin biosynthesis. *Trends in Plant Science*, **8**, 197-199.

Conner, T.W., Goekjian, V.H., Lafayette, P.R. and Key, J.L. (1990) STRUCTURE AND EXPRESSION OF 2 AUXIN-INDUCIBLE GENES FROM ARABIDOPSIS. *Plant Molecular Biology*, **15**, 623-632.

Cooke, T.J., Poli, D., Sztein, A.E. and Cohen, J.D. (2002) Evolutionary patterns in auxin action. *Plant Molecular Biology*, **49**, 319-338.

Cooper, W.C. (1935) Hormones in relation to root formation on stem cuttings. *Plant Physiology*, **10**, 789-794.

Crouzet, J., Trombik, T., Fraysse, A.S. and Boutry, M. (2006) Organization and function of the plant pleiotropic drug resistance ABC transporter family. *Febs Letters*, **580**, 1123-1130.

Darwin, C. (1880) *The power of movements in plants* London: John Murray.

David, K.M., Couch, D., Braun, N., Brown, S., Grosclaude, J. and Perrot-Rechenmann, C. (2007) The auxin-binding protein 1 is essential for the control of cell cycle. *Plant Journal*, **50**, 197-206.

Davidson, A.L. and Chen, J. (2004) ATP-binding cassette transporters in bacteria. *Annual Review of Biochemistry*, **73**, 241-268.

Davidson, A.L., Dassa, E., Orelle, C. and Chen, J. (2008) Structure, function, and evolution of bacterial ATP-binding cassette systems. *Microbiology and Molecular Biology Reviews*, **72**, 317-364.

Davidson, A.L., Laghaeian, S.S. and Mannering, D.E. (1996) The maltose transport system of Escherichia coli displays positive cooperativity in ATP hydrolysis. *Journal of Biological Chemistry*, **271**, 4858-4863.

Davies, P.J. (2004) The plant hormones: Their nature, occurrence and function. In *Plant hormones: Biosynthesis, Signal Transduction, Action!* (Davies, P.J. ed: Springer, Dordrecht, The Netherlands, pp. pp. 1-15.

Davies, T.G.E. and Coleman, J.O.D. (2000) The Arabidopsis thaliana ATP-binding cassette proteins: an emerging superfamily. *Plant Cell and Environment*, **23**, 431-443.

Davies, T.G.E., Theodoulou, F.L., Hallahan, D.L. and Forde, B.G. (1997) Cloning and characterisation of a novel P-glycoprotein homologue from barley. *Gene*, **199**, 195-202.

Dawson, R.J.P. and Locher, K.P. (2006) Structure of a bacterial multidrug ABC transporter. *Nature*, **443**, 180-185.

Dawson, R.J.P. and Locher, K.P. (2007) Structure of the multidrug ABC transporter Sav1866 from Staphylococcus aureus in complex with AMP-PNP. *Febs Letters*, **581**, 935-938.

De Smet, I., Voss, U., Lau, S., Wilson, M., Shao, N., Timme, R.E., Swarup, R., Kerr, I., Hodgman, C., Bock, R., Bennett, M., Jurgens, G. and Beeckman, T. (2011) Unraveling the Evolution of Auxin Signaling. *Plant Physiology*, **155**, 209-221.

Dean, M. and Annilo, T. (2005) Evolution of the ATP-binding cassette (ABC) transporter superfamily in vertebrates. *Annual Review of Genomics and Human Genetics*, **6**, 123-142.

Dean, M., Rzhetsky, A. and Allikmets, R. (2001) The human ATP-binding cassette (ABC) transporter superfamily. *Genome Research*, **11**, 1156-1166.

Delarue, M., Prinsen, E., Van Onckelen, H., Caboche, M. and Bellini, C. (1998) Sur2 mutations of Arabidopsis thaliana define a new locus involved in the control of auxin homeostasis. *Plant Journal*, **14**, 603-611.

Delbarre, A., Muller, P., Imhoff, V. and Guern, J. (1996) Comparison of mechanisms controlling uptake and accumulation of 2,4-dichlorophenoxy acetic acid, naphthalene-1-acetic acid, and indole-3-acetic acid in suspension-cultured tobacco cells. *Planta*, **198**, 532-541.

Delbarre, A., Muller, P., Imhoff, V., Morgat, J.L. and Barbierbrygoo, H. (1994) UPTAKE, ACCUMULATION AND METABOLISM OF AUXINS IN TOBACCO LEAF PROTOPLASTS. *Planta*, **195**, 159-167.

Dettmer, J., Hong-Hermesdorf, A., Stierhof, Y.D. and Schumacher, K. (2006) Vacuolar H+-ATPase activity is required for endocytic and secretory trafficking in Arabidopsis. *Plant Cell*, **18**, 715–730.

Dharmasiri, N., Dharmasiri, S. and Estelle, M. (2005a) The F-box protein TIR1 is an auxin receptor. *Nature*, **435**, 441-445.

Dharmasiri, N., Dharmasiri, S., Weijers, D., Lechner, E., Yamada, M., Hobbie, L., Ehrismann, J.S., Jurgens, G. and Estelle, M. (2005b) Plant development is regulated by a family of auxin receptor F box proteins. *Developmental Cell*, **9**, 109-119.

Dharmasiri, S., Swarup, R., Mockaitis, K., Dharmasiri, N., Singh, S.K., Kowalchyk, M., Marchant, A., Mills, S., Sandberg, G., Bennett, M.J. and Estelle, M. (2006) AXR4 is required for localization of the auxin influx facilitator AUX1. *Science*, **312**, 1218-1220.

Dhonukshe, P., Aniento, F., Hwang, I., Robinson, D.G., Mravec, J., Stierhof, Y.D. and Friml, J. (2007) Clathrin-mediated constitutive endocytosis of PIN auxin efflux carriers in Arabidopsis. *Current Biology*, **17**, 520-527.

Dhonukshe, P., Baluška, F., Schlicht, M., Hlavačka, A., Šamaj, J., Friml, J. and Gadella, T.W.J. (2006) Endocytosis of cell surface material mediates cell plate formation during plant cytokinesis. *Developmental Cell*, **10**, 137-150.

Dhonukshe, P., Tanaka, H., Goh, T., Ebine, K., Mahonen, A.P., Prasad, K., Blilou, I., Geldner, N., Xu, J., Uemura, T., Chory, J., Ueda, T., Nakano, A., Scheres, B. and Friml, J. (2008) Generation of cell polarity in plants links endocytosis, auxin distribution and cell fate decisions. *Nature*, **456**, 962-U975.

Dobrev, P.I., Havlíček, L., Vágner, M., Malbeck, J. and Kamínek, M. (2005) Purification and determination of plant hormones auxin and abscisic acid using solid phase extraction and two-dimensional high performance liquid chromatography. *Journal of Chromatography A*, **1075**, 159-166.

Dobrev, P.I. and Kamínek, M. (2002) Fast and efficient separation of cytokinins from auxin and abscisic acid and their purification using mixed-mode solid-phase extraction. *Journal of Chromatography A*, **950**, 21-29.

Dudler, R. and Hertig, C. (1992) STRUCTURE OF AN MDR-LIKE GENE FROM ARABIDOPSIS-THALIANA - EVOLUTIONARY IMPLICATIONS. *Journal of Biological Chemistry*, **267**, 5882-5888.

Emans, N., Zimmermann, S. and Fischer, R. (2002) Uptake of a fluorescent marker in plant cells is sensitive to brefeldin A and wortmannin. *Plant Cell*, **14**, 71–86.

Endicott, J.A. and Ling, V. (1989) THE BIOCHEMISTRY OF P-GLYCOPROTEIN-MEDIATED MULTIDRUG RESISTANCE. *Annual Rev of Biochemistry*, **58**, 137-171.

Fetsch, E.E. and Davidson, A.L. (2002) Vanadate-catalyzed photocleavage of the signature motif of an ATP-binding cassette (ABC) transporter. *Proceedings of the National Academy of Sciences of the United States of America*, **99**, 9685-9690.

Friml, J. (2003) Auxin transport - shaping the plant. *Current Opinion in Plant Biology*, **6**, 7-12.

Friml, J. (2010) Subcellular trafficking of PIN auxin efflux carriers in auxin transport. *Eur J Cell Biol*, **89**, 231-235.

Friml, J., Benková, E., Blilou, I., Wisniewska, J., Hamann, T., Ljung, K., Woody, S., Sandberg, G., Scheres, B., Jurgens, G. and Palme, K. (2002a) AtPIN4 mediates sink-driven auxin gradients and root patterning in Arabidopsis. *Cell*, **108**, 661-673.

Friml, J., Vieten, A., Sauer, M., Weijers, D., Schwarz, H., Hamann, T., Offringa, R. and Jurgens, G. (2003) Efflux-dependent auxin gradients establish the apical-basal axis of Arabidopsis. *Nature*, **426**, 147-153.

Friml, J., Wisniewska, J., Benková, E., Mendgen, K. and Palme, K. (2002b) Lateral relocation of auxin efflux regulator PIN3 mediates tropism in Arabidopsis. *Nature*, **415**, 806-809.

Friml, J., Yang, X., Michniewicz, M., Weijers, D., Quint, A., Tietz, O., Benjamins, R., Ouwerkerk, P.B.F., Ljung, K., Sandberg, G., Hooykaas, P.J.J., Palme, K. and Offringa, R. (2004) A PINOID-dependent binary switch in apical-basal PIN polar targeting directs auxin efflux. *Science*, **306**, 862-865.

Gälweiler, L., Guan, C.H., Muller, A., Wisman, E., Mendgen, K., Yephremov, A. and Palme, K. (1998) Regulation of polar auxin transport by AtPIN1 in Arabidopsis vascular tissue. *Science*, **282**, 2226-2230.

Ganguly, A., Lee, S.H., Cho, M., Lee, O.R., Yoo, H. and Cho, H.T. (2010) Differential Auxin-Transporting Activities of PIN-FORMED Proteins in Arabidopsis Root Hair Cells. *Plant Physiology*, **153**, 1046-1061.

Garcia, O., Bouige, P., Forestier, C. and Dassa, E. (2004) Inventory and comparative analysis of rice Arabidopsis ATP-binding cassette (ABC) systems. *Journal of Molecular Biology*, **343**, 249-265.

Geisler, M., Blakeslee, J.J., Bouchard, R., Lee, O.R., Vincenzetti, V., Bandyopadhyay, A., Titapiwatanakun, B., Peer, W.A., Bailly, A., Richards, E.L., Ejenda, K.F.K., Smith, A.P., Baroux, C., Grossniklaus, U., Muller, A., Hrycyna, C.A., Dudler, R., Murphy, A.S. and Martinoia, E. (2005) Cellular efflux of auxin catalyzed by the Arabidopsis MDR/PGP transporter AtPGP1. *Plant Journal*, **44**, 179-194.

Geisler, M., Girin, M., Brandt, S., Vincenzetti, V., Plaza, S., Paris, N., Kobae, Y., Maeshima, M., Billion, K., Kolukisaoglu, U.H., Schulz, B. and Martinoia, E. (2004) Arabidopsis immunophilin-like TWD1 functionally interacts with vacuolar ABC transporters. *Molecular Biology of the Cell*, **15**, 3393-3405.

Geisler, M., Kolukisaoglu, H.U., Bouchard, R., Billion, K., Berger, J., Saal, B., Frangne, N., Koncz-Kalman, Z., Koncz, C., Dudler, R., Blakeslee, J.J., Murphy, A.S., Martinoia, E. and Schulz, B. (2003) TWISTED DWARF1, a unique plasma membrane-anchored immunophilin-like protein, interacts with Arabidopsis multidrug resistance-like transporters AtPGP1 and AtPGP19. *Molecular Biology of the Cell*, **14**, 4238-4249.

Geisler, M. and Murphy, A.S. (2006) The ABC of auxin transport: The role of p-glycoproteins in plant development. *Febs Letters*, **580**, 1094-1102.

Geldner, N., Anders, N., Wolters, H., Keicher, J., Kornberger, W., Muller, P., Delbarre, A., Ueda, T., Nakano, A. and Jurgens, G. (2003) The Arabidopsis GNOM ARF-GEF mediates endosomal recycling, auxin transport, and auxin-dependent plant growth. *Cell*, **112**, 219-230.

Geldner, N., Friml, J., Stierhof, Y.D., Jurgens, G. and Palme, K. (2001) Auxin transport inhibitors block PIN1 cycling and vesicle traficking. *Nature*, **413**, 425-428.

Gerber, S., Comellas-Bigler, M., Goetz, B.A. and Locher, K.P. (2008) Structural basis of trans-inhibition in a molybdate/tungstate ABC transporter. *Science*, **321**, 246-250.

Goda, H., Sawa, S., Asami, T., Fujioka, S., Shimada, Y. and Yoshida, S. (2004) Comprehensive comparison brassinosteroid-regulated of auxin-regulated and brassinosteroid-regulated genes in arabidopsis. *Plant Physiology*, **134**, 1555-1573.

Gojon, A., Krouk, G., Perrine-Walker, F. and Laugier, E. (2011) Nitrate transceptor(s) in plants. *Journal of Experimental Botany*, **62**, 2299-2308.

Goldsmith, M.H.M. (1977) The Polar Transport of Auxin. *Annual Review of Plant Physiology*, **28**, 439-478.

Goldsmith, M.H.M. (1982) A saturable site responsible for polar transport of indole-3-acetic acid in sectoins of maize coleoptiles. *Planta*, **155**, 68-75.

Goldsmith, M.H.M. (1993) CELLULAR SIGNALING - NEW INSIGHTS INTO THE ACTION OF THE PLANT-GROWTH HORMONE AUXIN. *Proceedings of the National Academy of Sciences of the United States of America*, **90**, 11442-11445.

Gray, W.M., del Pozo, J.C., Walker, L., Hobbie, L., Risseeuw, E., Banks, T., Crosby, W.L., Yang, M., Ma, H. and Estelle, M. (1999) Identification of an SCF ubiquitin-ligase complex required for auxin response in Arabidopsis thaliana. *Genes & Development*, **13**, 1678-1691.

Gray, W.M., Kepinski, S., Rouse, D., Leyser, O. and Estelle, M. (2001) Auxin regulates SCFTIR1-dependent degradation of AUX/IAA proteins. *Nature*, **414**, 271-276.

Guilfoyle, T.J. and Hagen, G. (2007) Auxin response factors. *Current Opinion in Plant Biology*, **10**, 453-460.

Harrar, Y., Bellini, C. and Faure, J.D. (2001) FKBPs: at the crossroads of folding and transduction. *Trends in Plant Science*, **6**, 426-431.

He, Z.Y., Li, L.G. and Luan, S. (2004) Immunophilins and parvulins. Superfamily of peptidyl prolyl isomerases in Arabidopsis. *Plant Physiology*, **134**, 1248-1267.

Hertel, R., Russo, V.E.A. and Thomson, K.S. (1972) IN-VITRO AUXIN BINDING TO PARTICULATE CELL FRACTIONS FROM CORN COLEOPTILES. *Planta*, **107**, 325-&.

Higgins, C.F. (1992) ABC TRANSPORTERS - FROM MICROORGANISMS TO MAN. *Annual Review of Cell Biology*, **8**, 67-113.

Higgins, C.F. (1995) THE ABC OF CHANNEL REGULATION. *Cell*, **82**, 693-696.

Higgins, C.F. (2007) Multiple molecular mechanisms for multidrug resistance transporters. *Nature*, **446**, 749-757.

Higgins, C.F. and Linton, K.J. (2004) The ATP switch model for ABC transporters. *Nature Structural & Molecular Biology*, **11**, 918-926.

Hollenstein, K., Dawson, R.J.P. and Locher, K.P. (2007a) Structure and mechanism of ABC transporter proteins. *Current Opinion in Structural Biology*, **17**, 412-418.

Hollenstein, K., Frei, D.C. and Locher, K.P. (2007b) Structure of an ABC transporter in complex with its binding protein. *Nature*, **446**, 213-216.

Hunke, S., Drose, S. and Schneider, E. (1995) VANADATE AND BAFILOMYCIN A(1) ARE POTENT INHIBITORS OF THE ATPASE ACTIVITY OF THE RECONSTITUTED BACTERIAL ATP-BINDING CASSETTE TRANSPORTER FOR MALTOSE (MALFGK(2)). *Biochemical and Biophysical Research Communications*, **216**, 589-594.

Hvorup, R.N., Goetz, B.A., Niederer, M., Hollenstein, K., Perozo, E. and Locher, K.P. (2007) Asymmetry in the structure of the ABC transporter-binding protein complex BtuCD-BtuF. *Science*, **317**, 1387-1390.

Jacobs, M. and Rubery, P.H. (1988) NATURALLY-OCCURRING AUXIN TRANSPORT REGULATORS. *Science*, **241**, 346-349.

Jaillais, Y., Santambrogio, M., Rozier, F., Fobis-Loisy, I., Miege, C. and Gaude, T. (2007) The retromer protein VPS29 links cell polarity and organ initiation in plants. *Cell*, **130**, 1057-1070.

Jasinski, M., Ducos, E., Martinoia, E. and Boutry, M. (2003) The ATP-binding cassette transporters: Structure, function, and gene family comparison between rice and Arabidopsis. *Plant Physiology*, **131**, 1169-1177.

Jelínková, A., Malinská, K., Simon, S., Kleine-Vehn, J., Pařezová, M., Pejchar, P., Kubeš, M., Martinec, J., Friml, J., Zažímalová, E. and Petrášek, J. (2010) Probing plant membranes with FM dyes: tracking, dragging or blocking? *Plant Journal*, **61**, 883-892.

Jones, A.R., Kramer, E.M., Knox, K., Swarup, R., Bennett, M.J., Lazarus, C.M., Leyser, H.M.O. and Grierson, C.S. (2009) Auxin transport through non-hair cells sustains root-hair development. *Nature Cell Biology*, **11**, 78-U156.

Kadaba, N.S., Kaiser, J.T., Johnson, E., Lee, A. and Rees, D.C. (2008) The high-affinity E-coli methionine ABC transporter: Structure and allosteric regulation. *Science*, **321**, 250-253.

Kamphausen, T., Fanghanel, R., Neumann, D., Schulz, B. and Rahfeld, J.U. (2002) Characterization of Arabidopsis thaliana AtFKBP42 that is membrane-bound and interacts with Hsp90. *Plant Journal*, **32**, 263-276.

Kepinski, S. and Leyser, O. (2005) The Arabidopsis F-box protein TIR1 is an auxin receptor. *Nature*, **435**, 446-451.

Kerr, I.D. and Bennett, M.J. (2007) New insight into the biochemical mechanisms regulating auxin transport in plants. *Biochemical Journal*, **401**, 613-622.

Kim, J.Y., Henrichs, S., Bailly, A., Vincenzetti, V., Sovero, V., Mancuso, S., Pollmann, S., Kim, D., Geisler, M. and Nam, H.G. (2010) Identification of an ABCB/P-glycoprotein-specific Inhibitor of Auxin Transport by Chemical Genomics. *Journal of Biological Chemistry*, **285**, 23307-23315.

King, J.J., Stimart, D.P., Fisher, R.H. and Bleecker, A.B. (1995) A mutation altering auxin homeostasis and plant morphology in Arabidopsis. *Plant Cell*, **7**, 2023-2037.

Kleine-Vehn, J., Dhonukshe, P., Sauer, M., Brewer, P.B., Wisniewska, J., Paciorek, T., Benkova, E. and Friml, J. (2008) ARF GEF-dependent transcytosis and polar delivery of PIN auxin carriers in Arabidopsis. *Current Biology*, **18**, 526-531.

Kleine-Vehn, J., Dhonukshe, P., Swarup, R., Bennett, M. and Friml, J. (2006) Subcellular trafficking of the Arabidopsis auxin influx carrier AUX1 uses a novel pathway distinct from PIN1. *Plant Cell*, **18**, 3171-3181.

Knöller, A.S., Blakeslee, J.J., Richards, E.L., Peer, W.A. and Murphy, A.S. (2010) Brachytic2/*Zm*ABCB1 functions in IAA export from intercalary meristems. *Journal of Experimental Botany*, **61**, 3689-3696.

Knöller, A.S., and Murphy, A.S. (2010). "ABC transporters and their function at the plasma membrane." In *The Plant Plasma Membrane*. (2010) Murphy AS, Schulz B, and Peer WA, eds. Springer-Verlag, Berlin. pp. 353-377.

Koepfli, J.B., Thimann, K.V. and Went, F.W. (1938) Phytohormones: Structure and physiological activity I. *Jour. Biol. Chem.*, **122**, 763-780.

Kogl, F. and Haagen-Smit, A.J. (1931) Uber die Chemie des Wuchsstoffs K. Akad. Wetenschap. Amsterdam. *Proc. Sect. Sci.*, **34**, 1411-1416.

Kolukisaoglu, H.U., Bovet, L., Klein, M., Eggmann, T., Geisler, M., Wanke, D., Martinoia, E. and Schulz, B. (2002) Family business: the multidrug-resistance related protein (MRP) ABC transporter genes in Arabidopsis thaliana. *Planta*, **216**, 107-119.

Kos, V. and Ford, R.C. (2009) The ATP-binding cassette family: a structural perspective. *Cellular and Molecular Life Sciences*, **66**, 3111-3126.

Kramer, E.M. and Bennett, M.J. (2006) Auxin transport: a field in flux. *Trends in Plant Science*, **11**, 382-386.

Krouk, G., Lacombe, B., Bielach, A., Perrine-Walker, F., Malinska, K., Mounier, E., Hoyerova, K., Tillard, P., Leon, S., Ljung, K., Zazimalova, E., Benkova, E., Nacry, P. and Gojon, A. (2010) Nitrate-Regulated Auxin Transport by NRT1.1 Defines a Mechanism for Nutrient Sensing in Plants. *Developmental Cell*, **18**, 927-937.

Krouk, G., Ruffel, S., Gutierrez, R.A., Gojon, A., Crawford, N.M., Coruzzil, G.M. and Lacombe, B. (2011) A framework integrating plant growth with hormones and nutrients. *Trends in Plant Science*, **16**, 178-182.

Kurek, I., Aviezer, K., Erel, N., Herman, E. and Breiman, A. (1999) The wheat peptidyl prolyl cis-trans-isomerase FKBP77 is heat induced and developmentally regulated. *Plant Physiology*, **119**, 693-703.

Křeček, P., Skůpa, P., Libus, J., Naramoto, S., Tejos, R., Friml, J. and Zažímalová, E. (2009) The PIN-FORMED (PIN) protein family of auxin transporters. *Genome Biol*, **10**, 249.

Laňková, M., Smith, R.S., Pešek, B., Kubeš, M., Zažímalová, E., Petrášek, J. and Hoyerová, K. (2010) Auxin influx inhibitors 1-NOA, 2-NOA, and CHPAA interfere with membrane dynamics in tobacco cells. *Journal of Experimental Botany*, **61**, 3589-3598.

Leblanc, N., David, K., Grosclaude, J., Pradier, J.M., Barbier-Brygoo, H., Labiau, S. and Perrot-Rechenmann, C. (1999) A novel immunological approach establishes that the auxin-binding protein, Nt-abp1, is an element involved in auxin signaling at the plasma membrane. *Journal of Biological Chemistry*, **274**, 28314-28320.

Lee, M., Choi, Y., Burla, B., Kim, Y.Y., Jeon, B., Maeshima, M., Yoo, J.Y., Martinoia, E. and Lee, Y. (2008) The ABC transporter AtABCB14 is a malate importer and modulates stomatal response to CO2. *Nature Cell Biology*, **10**, 1217-1223.

Lee, S.H. and Cho, H.T. (2006) PINOID positively regulates auxin efflux in Arabidopsis root hair cells and tobacco cells. *Plant Cell*, **18**, 1604-1616.

Lewis, D.R., Miller, N.D., Splitt, B.L., Wu, G.S. and Spalding, E.P. (2007a) Separating the roles of acropetal and basipetal auxin transport on gravitropism with mutations in two Arabidopsis Multidrug Resistance-Like ABC transporter genes. *Plant Cell*, **19**, 1838-1850.

Li, J.S., Yang, H.B., Peer, W.A., Richter, G., Blakeslee, J., Bandyopadhyay, A., Titapiwantakun, B., Undurraga, S., Khodakovskaya, M., Richards, E.L., Krizek, B., Murphy, A.S., Gilroy, S. and Gaxiola, R. (2005) Arabidopsis H+-PPase AVP1 regulates auxin-mediated organ development. *Science*, **310**, 121-125.

Lin, R.C. and Wang, H.Y. (2005) Two homologous ATP-binding cassette transporter proteins, AtMDR1 and AtPGP1, regulate Arabidopsis photomorphogenesis and root development by mediating polar auxin transport. *Plant Physiology*, **138**, 949-964.

Ljung, K., Bhalerao, R.P. and Sandberg, G. (2001) Sites and homeostatic control of auxin biosynthesis in Arabidopsis during vegetative growth. *Plant Journal*, **28**, 465-474.

Ljung, K., Hull, A.K., Celenza, J., Yamada, M., Estelle, M., Nonmanly, J. and Sandberg, G. (2005) Sites and regulation of auxin biosynthesis in Arabidopsis roots. *Plant Cell*, **17**, 1090-1104.

Locher, K.P. (2009) Structure and mechanism of ATP-binding cassette transporters. *Philosophical Transactions of the Royal Society B-Biological Sciences*, **364**, 239-245.

Locher, K.P., Lee, A.T. and Rees, D.C. (2002) The E-coli BtuCD structure: A framework for ABC transporter architecture and mechanism. *Science*, **296**, 1091-1098.

Loe, D.W., Oleschuk, C.J., Deeley, R.G. and Cole, S.P.C. (2000) Structure-activity studies of verapamil analogs that modulate transport of leukotriene C-4 and reduced glutathione by multidrug resistance protein MRP1. *Biochemical and Biophysical Research Communications*, **275**, 795-803.

Loo, T.W., Bartlett, M.C., and Clarke, D.M. (2003) Methanethiosulfonate derivatives of rhodamine and verapamil activate human P-glycoprotein at different sites. *J Biol Chem*., **278**, 50136-50141.

Luan, S., Albers, M.W. and Schreiber, S.L. (1994) LIGHT-REGULATED, TISSUE-SPECIFIC IMMUNOPHILINS IN A HIGHER-PLANT. *Proceedings of the National Academy of Sciences of the United States of America*, **91**, 984-988.

Ludwig-Müller, J. (2011) Auxin conjugates: their role for plant development and in the evolution of land plants. *Journal of Experimental Botany*, **62**, 1757-1773.

Lupas, A., Vandyke, M. and Stock, J. (1991) PREDICTING COILED COILS FROM PROTEIN SEQUENCES. *Science*, **252**, 1162-1164.

Luschnig, C., Gaxiola, R.A., Grisafi, P. and Fink, G.R. (1998) EIR1, a root-specific protein involved in auxin transport, is required for gravitropism in Arabidopsis thaliana. *Genes & Development*, **12**, 2175-2187.

Maher, E.P. and Martindale, S.J.B. (1980) MUTANTS OF ARABIDOPSIS-THALIANA WITH ALTERED RESPONSES TO AUXINS AND GRAVITY. *Biochemical Genetics*, **18**, 1041-1053.

Marchant, A., Bhalerao, R., Casimiro, I., Eklof, J., Casero, P.J., Bennett, M. and Sandberg, G. (2002) AUX1 promotes lateral root formation by facilitating indole-3-acetic acid distribution between sink and source tissues in the Arabidopsis seedling. *Plant Cell*, **14**, 589-597.

Marchant, A., Kargul, J., May, S.T., Muller, P., Delbarre, A., Perrot-Rechenmann, C. and Bennett, M.J. (1999) AUX1 regulates root gravitropism in Arabidopsis by facilitating auxin uptake within root apical tissues. *Embo Journal*, **18**, 2066-2073.

Marigo, G. and Boudet, A.M. (1977) POLYPHENOLS AND GROWTH - INHIBITION OF POLAR AUXIN TRANSPORT BY PHENOLIC COMPOUNDS. *Physiologia Plantarum*, **41**, 197-202.

Martinoia, E., Klein, M., Geisler, M., Bovet, L., Forestier, C., Kolukisaoglu, U., Muller-Rober, B. and Schulz, B. (2002) Multifunctionality of plant ABC transporters - more than just detoxifiers. *Planta*, **214**, 345-355.

Martinoia, E., Massonneau, A. and Frangne, N. (2000) Transport processes of solutes across the vacuolar membrane of higher plants. *Plant and Cell Physiology*, **41**, 1175-1186.

Mathesius, U. (2008) Auxin: at the root of nodule development? *Functional Plant Biology*, **35**, 651-668.

Men, S.Z., Boutte, Y., Ikeda, Y., Li, X.G., Palme, K., Stierhof, Y.D., Hartmann, M.A., Moritz, T. and Grebe, M. (2008) Sterol-dependent endocytosis mediates post-cytokinetic acquisition of PIN2 auxin efflux carrier polarity. *Nature Cell Biology*, **10**, 237-244.

Michniewicz, M., Zago, M.K., Abas, L., Weijers, D., Schweighofer, A., Meskiene, I., Heisler, M.G., Ohno, C., Zhang, J., Huang, F., Schwab, R., Weigel, D., Meyerowitz, E.M., Luschnig, C., Offringa, R. and Friml, J. (2007) Antagonistic regulation of PIN phosphorylation by PP2A and PINOID directs auxin flux. *Cell*, **130**, 1044-1056.

Mockaitis, K. and Estelle, M. (2008) Auxin Receptors and Plant Development: A New Signaling Paradigm. *Annual Review of Cell and Developmental Biology*, **24**, 55-80.

Morris, D.A., Friml, J., and Zažímalová, E. (2004) The transport of auxins. In *Plant hormones: Biosynthesis, Signal Transduction, Action!* (Davies, P.J. ed: Springer, Dordrecht, The Netherlands, pp. pp. 437-470.

Morris, M.E. and Zhang, S.Z. (2006) Flavonoid-drug interactions: Effects of flavonoids on ABC transporters. *Life Sciences*, **78**, 2116-2130.

Mravec, J., Kubeš, M., Bielach, A., Gaykova, V., Petrasek, J., Skůpa, P., Chand, S., Benková, E., Zažímalová, E. and Friml, J. (2008) Interaction of PIN and PGP transport mechanisms in auxin distribution-dependent development. *Development*, **135**, 3345-3354.

Mravec, J., Skůpa, P., Bailly, A., Hoyerová, K., Křeček, P., Bielach, A., Petrášek, J., Zhang, J., Gaykova, V., Stierhof, Y.D., Dobrev, P.I., Schwarzerová, K., Rolčík, J., Seifertová, D., Luschnig, C., Benková, E., Zažímalová, E., Geisler, M. and Friml, J. (2009) Subcellular homeostasis of phytohormone auxin is mediated by the ER-localized PIN5 transporter. *Nature*, **459**, 1136-1142.

Müller, A., Guan, C.H., Galweiler, L., Tanzler, P., Huijser, P., Marchant, A., Parry, G., Bennett, M., Wisman, E. and Palme, K. (1998) AtPIN2 defines a locus of Arabidopsis for root gravitropism control. *Embo Journal*, **17**, 6903-6911.

Multani, D.S., Briggs, S.P., Chamberlin, M.A., Blakeslee, J.J., Murphy, A.S. and Johal, G.S. (2003) Loss of an MDR transporter in compact stalks of maize br2 and sorghum dw3 mutants. *Science*, **302**, 81-84.

Murakami, S., Nakashima, R., Yamashita, E., Matsumoto, T. and Yamaguchi, A. (2006) Crystal structures of a multidrug transporter reveal a functionally rotating mechanism. *Nature*, **443**, 173-179.

Murphy, A., Peer, W.A. and Taiz, L. (2000) Regulation of auxin transport by aminopeptidases and endogenous flavonoids. *Planta*, **211**, 315-324.

Murphy, A.S., Hoogner, K.R., Peer, W.A. and Taiz, L. (2002) Identification, purification, and molecular cloning of N-1-naphthylphthalmic acid-binding plasma membrane-associated aminopeptidases from Arabidopsis. *Plant Physiology*, **128**, 935-950.

Nagata, T., Nemoto, Y. and Hasezawa, S. (1992) TOBACCO BY-2 CELL-LINE AS THE HELA-CELL IN THE CELL BIOLOGY OF HIGHER-PLANTS. *International Review of Cytology-a Survey of Cell Biology*, **132**, 1-30.

Napier, R.M., David, K.M. and Perrot-Rechenmann, C. (2002) A short history of auxin-binding proteins. *Plant Molecular Biology*, **49**, 339-348.

Nemhauser, J.L., Hong, F.X. and Chory, J. (2006) Different plant hormones regulate similar processes through largely nonoverlapping transcriptional responses. *Cell*, **126**, 467-475.

Noh, B., Bandyopadhyay, A., Peer, W.A., Spalding, E.P. and Murphy, A.S. (2003) Enhanced gravi- and phototropism in plant mdr mutants mislocalizing the auxin efflux protein PIN1. *Nature*, **423**, 999-1002.

Noh, B., Murphy, A.S. and Spalding, E.P. (2001) Multidrug resistance-like genes of Arabidopsis required for auxin transport and auxin-mediated development. *Plant Cell*, **13**, 2441-2454.

Normanly, J. (2010) Approaching Cellular and Molecular Resolution of Auxin Biosynthesis and Metabolism. *Cold Spring Harbor Perspectives in Biology*, **2**.

Okada, K. and Shimura, Y. (1990) REVERSIBLE ROOT-TIP ROTATION IN ARABIDOPSIS SEEDLINGS INDUCED BY OBSTACLE-TOUCHING STIMULUS. *Science*, **250**, 274-276.

Okada, K., Ueda, J., Komaki, M.K., Bell, C.J. and Shimura, Y. (1991) REQUIREMENT OF THE AUXIN POLAR TRANSPORT-SYSTEM IN EARLY STAGES OF ARABIDOPSIS FLORAL BUD FORMATION. *Plant Cell*, **3**, 677-684.

Oldham, M.L., Khare, D., Quiocho, F.A., Davidson, A.L. and Chen, J. (2007) Crystal structure of a catalytic intermediate of the maltose transporter. *Nature*, **450**, 515-U517.

Ortiz-Lopez, A., Chang, H.C. and Bush, D.R. (2000) Amino acid transporters in plants. *Biochimica Et Biophysica Acta-Biomembranes*, **1465**, 275-280.

Overvoorde, P.J., Okushima, Y., Alonso, J.M., Chan, A., Chang, C., Ecker, J.R., Hughes, B., Liu, A., Onodera, C., Quach, H., Smith, A., Yu, G.X. and Theologis, A. (2005) Functional genomic analysis of the AUXIN/INDOLE-3-ACETIC ACID gene family members in Arabidopsis thaliana. *Plant Cell*, **17**, 3282-3300.

Paciorek, T. and Friml, J. (2006) Auxin signaling. *Journal of Cell Science*, **119**, 1199-1202.

Paciorek, T., Zazimalova, E., Ruthardt, N., Petrasek, J., Stierhof, Y.D., Kleine-Vehn, J., Morris, D.A., Emans, N., Jurgens, G., Geldner, N. and Friml, J. (2005) Auxin inhibits endocytosis and promotes its own efflux from cells. *Nature*, **435**, 1251-1256.

Parry, G., Delbarre, A., Marchant, A., Swarup, R., Napier, R., Perrot-Rechenmann, C. and Bennett, M.J. (2001a) Novel auxin transport inhibitors phenocopy the auxin influx carrier mutation aux1. *Plant Journal*, **25**, 399-406.

Parry, G., Marchant, A., May, S., Swarup, R., Swarup, K., James, N., Graham, N., Allen, T., Martucci, T., Yemm, A., Napier, R., Manning, K., King, G. and Bennett, M. (2001b) Quick on the uptake: Characterization of a family of plant auxin influx carriers. *Journal of Plant Growth Regulation*, **20**, 217-225.

Pastan, I. and Gottesman, M.M. (1991) MULTIDRUG RESISTANCE. *Annual Review of Medicine*, **42**, 277-286.

Peer, W.A., Bandyopadhyay, A., Blakeslee, J.J., Makam, S.I., Chen, R.J., Masson, P.H. and Murphy, A.S. (2004) Variation in expression and protein localization of the PIN family of auxin efflux facilitator proteins in flavonoid mutants with altered auxin transport in Arabidopsis thaliana. *Plant Cell*, **16**, 1898-1911.

Peer, W.A., Brown, D.E., Tague, B.W., Muday, G.K., Taiz, L. and Murphy, A.S. (2001) Flavonoid accumulation patterns of transparent testa mutants of Arabidopsis. *Plant Physiology*, **126**, 536-548.

Peer, W.A. and Murphy, A.S. (2007) Flavonoids and auxin transport: modulators or regulators? *Trends in Plant Science*, **12**, 556-563.

Pekker, I., Alvarez, J.P. and Eshed, Y. (2005) Auxin response factors mediate Arabidopsis organ asymmetry via modulation of KANADI activity. *Plant Cell*, **17**, 2899-2910.

Perez-Perez, J.M., Ponce, M.R. and Micol, J.L. (2004) The ULTRACURVATA2 gene of Arabidopsis encodes an FK506-binding protein involved in auxin and brassinosteroid signaling. *Plant Physiology*, **134**, 101-117.

Petrášek, J., Černá, A., Schwarzerová, K., Elčkner, M., Morris, D.A. and Zažímalová, E. (2003) Do phytotropins inhibit auxin efflux by impairing vesicle traffic? *Plant Physiology*, **131**, 254-263.

Petrášek, J., Elčkner, M., Morris, D.A., and Zažímalová, E. (2002). Auxin efflux carrier activity and auxin accumulation regulate cell division and polarity in tobacco cells. *Planta* **216**, 302-308.

Petrášek, J. and Friml, J. (2009) Auxin transport routes in plant development. *Development*, **136**, 2675-2688.

Petrášek, J., Mravec, J., Bouchard, R., Blakeslee, J.J., Abas, M., Seifertová, D., Wisniewska, J., Tadele, Z., Kubeš, M., Čovanová, M., Dhonukshe, P., Skůpa, P., Benková, E., Perry, L., Křeček, P., Lee, O.R., Fink, G.R., Geisler, M., Murphy, A.S., Luschnig, C., Zažímalová, E. and Friml, J. (2006) PIN proteins perform a rate-limiting function in cellular auxin efflux. *Science*, **312**, 914-918.

Pinkett, H.W., Lee, A.T., Lum, P., Locher, K.P. and Rees, D.C. (2007) An inward-facing conformation of a putative metal-chelate-type ABC transporter. *Science*, **315**, 373-377.

Pitts, J.R., Cernac, A. and Estelle M. (1998) Auxin and ethylene promote root hair elongation in *Arabidopsis*. *Plant Journal,* **16**, 553–560.

Pohl, A., Devaux, P.F. and Herrmann, A. (2005) Function of prokaryotic and eukaryotic ABC proteins in lipid transport. *Biochimica Et Biophysica Acta-Molecular and Cell Biology of Lipids*, **1733**, 29-52.

Porter, W.L. and Thimann, K.V (1965) Molecular requirements for auxin action – I. Halogenated indoles and indoleacetic acids. *Phytochemistry*, **4**, 229-243.

Raven, J. (1975) Transport of indoleacetic acid in plant cells in relation to pH and electrical potential gradients, and its significance for polar IAA transport. *New Phytologist*, **74**, 163-172.

Rea, P.A. (2007) Plant ATP-Binding cassette transporters. *Annual Review of Plant Biology*, **58**, 347-375.

Rea, P.A., Li, Z.S., Lu, Y.P., Drozdowicz, Y.M. and Martinoia, E. (1998) From vacuolar GS-X pumps to multispecific ABC transporters. *Annual Review of Plant Physiology and Plant Molecular Biology*, **49**, 727-760.

Rea, P.A., Sánchez-Férnandez, R., Chen, S., Peng, M., Klein, M., Geisler, M. and Martinoia, E. (2002) The plant ABC transporter superfamily: the functions of a few and the identity of many. In *ABC Transporters: From Bacteria to Man* (Cole, S.P., Kuchler, K., Higgins, C., Holland, B. and eds. eds). Amsterdam, The Netherlands: Elsevier, pp. 335-355.

Rees, D.C., Johnson, E. and Lewinson, O. (2009) ABC transporters: the power to change. *Nature Reviews Molecular Cell Biology*, **10**, 218-227.

Reinhardt, D., Pesce, E.R., Stieger, P., Mandel, T., Baltensperger, K., Bennett, M., Traas, J., Friml, J. and Kuhlemeier, C. (2003) Regulation of phyllotaxis by polar auxin transport. *Nature*, **426**, 255-260.

Reyes, C.L. and Chang, G. (2005) Structure of the ABC transporter MsbA in complex with ADP-vanadate and lipopolysaccharide. *Science*, **308**, 1028-1031.

Richter, S., Geldner, N., Schrader, J., Wolters, H., Stierhof, Y.D., Rios, G., Koncz, C., Robinson, D.G. and Jurgens, G. (2007) Functional diversification of closely related ARF-GEFs in protein secretion and recycling. *Nature*, **448**, 488-492.

Robert, S., Kleine-Vehn, J., Barbez, E., Sauer, M., Paciorek, T., Baster, P., Vanneste, S., Zhang, J., Simon, S., Čovanová, M., Hayashi, K., Dhonukshe, P., Yang, Z., Bednarek, S.Y., Jones, A.M., Luschnig, C., Aniento, F., Zažímalová, E. and Friml, J. (2010) ABP1 Mediates Auxin Inhibition of Clathrin-Dependent Endocytosis in Arabidopsis. *Cell*, **143**, 111-121.

Rojas-Pierce, M., Titapiwatanakun, B., Sohn, E.J., Fang, F., Larive, C.K., Blakeslee, J., Cheng, Y., Cuttler, S., Peer, W.A., Murphy, A.S. and Raikhel, N.V. (2007) Arabidopsis P-glycoprotein19 participates in the inhibition of Gravitropism by gravacin. *Chemistry & Biology*, **14**, 1366-1376.

Roman, G., Lubarsky, B., Kieber, J.J., Rothenberg, M. and Ecker, J.R. (1995) GENETIC-ANALYSIS OF ETHYLENE SIGNAL-TRANSDUCTION IN ARABIDOPSIS-THALIANA - 5 NOVEL MUTANT LOCI INTEGRATED INTO A STRESS-RESPONSE PATHWAY. *Genetics*, **139**, 1393-1409.

Romano, P., He, Z.Y. and Luan, S. (2004a) Introducing immunophilins. From organ transplantation to plant biology. *Plant Physiology*, **134**, 1241-1243.

Romano, P.G.N., Horton, P. and Gray, J.E. (2004b) The Arabidopsis cyclophilin gene family. *Plant Physiology*, **134**, 1268-1282.

Rubery, P. and Sheldrake, A. (1974) Carrier-mediated auxin transport. *Planta*, **118**, 101-121.

Sachs, v.J. (1868) *Lehrbuch der Botanik* 1st Edition edn. Leipzig: Verlag von Wilhelm Engelmann.

Růžička, K., Strader, L., Bailly, A., Yang, H. Blakeslee, J., Langowski, L., Nejedlá, E., Fujita, H., Itoh, H., Syono, K., Hejátko, J., Gray, W., Martinoia, E., Geisler, M., Bartel, B., Murphy, A.S. and Friml, J. (2010) Arabidopsis PIS1 encodes the ABCG37 transporter of auxinic compounds including the auxin precursor indole-3-butyric acid. *PNAS,* **107**, 10749-10753.

Salkowski, E. (1885) Ueber das Verhalten der Skatolcarbonsäure im Organismus. *Zeitschrift für physiologische Chemie*, **9**, 23-33.

Sanchez-Fernandez, R., Davies, T.G.E., Coleman, J.O.D. and Rea, P.A. (2001a) The Arabidopsis thaliana ABC protein superfamily, a complete inventory. *Journal of Biological Chemistry*, **276**, 30231-30244.

Sanchez-Fernandez, R., Rea, P.A., Davies, T.G.E. and Coleman, J.O.D. (2001b) Do plants have more genes than humans? Yes, when it comes to ABC proteins. *Trends in Plant Science*, **6**, 347-348.

Santelia, D., Vincenzetti, V., Azzarello, E., Bovet, L., Fukao, Y., Duchtig, P., Mancuso, S., Martinoia, E. and Geisler, M. (2005) MDR-like ABC transporter AtPGP4 is involved in auxin-mediated lateral root and root hair development. *Febs Letters*, **579**, 5399-5406.

Santner, A., Calderon-Villalobos, L.I.A. and Estelle, M. (2009) Plant hormones are versatile chemical regulators of plant growth. *Nature Chemical Biology*, **5**, 301-307.

Santner, A. and Estelle, M. (2009) Recent advances and emerging trends in plant hormone signalling. *Nature*, **459**, 1071-1078.

Sauer, M., Balla, J., Luschnig, C., Wisniewska, J., Reinohl, V., Friml, J. and Benkova, E. (2006) Canalization of auxin flow by Aux/IAA-ARF-dependent feedback regulation of PIN polarity. *Genes & Development*, **20**, 2902-2911.

Sauna, Z.E., Bohn, S.S., Rutledge, R., Dougherty, M.P., Cronin, S., May, L., Xia, D., Ambudkar, S.V., and Golin, J. (2008) Mutations define cross-talk between the N-terminal nucleotide-binding domain and transmembrane helix-2 of the yeast multidrug transporter Pdr5: possible conservation of a signaling interface for coupling ATP hydrolysis to drug transport. *J Biol Chem*., **283**, 35010-35022.

Scarpella, E., Marcos, D., Friml, J. and Berleth, T. (2006) Control of leaf vascular patterning by polar auxin transport. *Genes & Development*, **20**, 1015-1027.

Scheres, B. and Xu, L. (2006) Polar auxin transport and patterning: grow with the flow. *Genes & Development*, **20**, 922-926.

Schiene-Fischer, C. and Yu, C. (2001) Receptor accessory folding helper enzymes: the functional role of peptidyl prolyl cis/trans isomerases. *Febs Letters*, **495**, 1-6.

Schmitt, L., Benabdelhak, H., Blight, M.A., Holland, B.I. and Stubbs, M.T. (2003) Crystal structure of the nucleotide-binding domain of the ABC-transporter haemolysin B: Identification of a variable region within ABC helical domains. *Journal of Molecular Biology*, **330**, 333-342.

Schreiber, S.L. (1991) CHEMISTRY AND BIOLOGY OF THE IMMUNOPHILINS AND THEIR IMMUNOSUPPRESSIVE LIGANDS. *Science*, **251**, 283-287.

Schuldiner, S. (2006) The ins and outs of drug transport. *Nature*, **443**, 156-157.

Schulz, B. and Kolukisaoglu, H.Ü. (2006) Genomics of plant ABC transporters: The alphabet of photosynthetic life forms or just holes in membranes? *FEBS Letters*, **580**, 1010-1016.

Seeger, M.A., Schiefner, A., Eicher, T., Verrey, F., Diederichs, K. and Pos, K.M. (2006) Structural asymmetry of AcrB trimer suggests a peristaltic pump mechanism. *Science*, **313**, 1295-1298.

Sekimoto, H., Seo, M., Kawakami, N., Komano, T., Desloire, S., Liotenberg, S., Marion-Poll, A., Caboche, M., Kamiya, Y. and Koshiba, T. (1998) Molecular cloning and characterization of aldehyde oxidases in Arabidopsis thaliana. *Plant and Cell Physiology*, **39**, 433-442.

Seo, M., Akaba, S., Oritani, T., Delarue, M., Bellini, C., Caboche, M. and Koshiba, T. (1998) Higher activity of an aldehyde oxidase in the auxin-overproducing superroot1 mutant of Arabidopsis thaliana. *Plant Physiology*, **116**, 687-693.

Shi, Z., Tiwari, A.K., Shukla, S., Robey, R.W., Singh, S., Kim, I.W., Bates, S.E., Peng, X., Abraham, I., Ambudkar, S.V., Talele, T.T., Fu, L.W., and Chen, Z.S. (2011) Sildenafil Reverses ABCB1- and ABCG2-Mediated Chemotherapeutic Drug Resistance. *Cancer Res*., **71**, 3029-3041.

Shitan, N., Bazin, I., Dan, K., Obata, K., Kigawa, K., Ueda, K., Sato, F., Forestier, C. and Yazaki, K. (2003) Involvement of CjMDR1, a plant multidrug-resistance-type ATP-binding cassette protein, in alkaloid transport in Coptis japonica. *Proceedings of the National Academy of Sciences of the United States of America*, **100**, 751-756.

Sidler, M., Hassa, P., Hasan, S., Ringli, C. and Dudler, R. (1998) Involvement of an ABC transporter in a developmental pathway regulating hypocotyl cell elongation in the light. *Plant Cell*, **10**, 1623-1636.

Smith, R.S., Guyomarc'h, S., Mandel, T., Reinhardt, D., Kuhlemeier, C. and Prusinkiewicz, P. (2006) A plausible model of phyllotaxis. *Proceedings of the National Academy of Sciences of the United States of America*, **103**, 1301-1306.

Steinmann, T., Geldner, N., Grebe, M., Mangold, S., Jackson, C.L., Paris, S., Galweiler, L., Palme, K. and Jurgens, G. (1999) Coordinated polar localization of auxin efflux carrier PIN1 by GNOM ARF GEF. *Science*, **286**, 316-318.

Stenlid, G. (1976) EFFECTS OF FLAVONOIDS ON POLAR TRANSPORT OF AUXINS. *Physiologia Plantarum*, **38**, 262-266.

Stone, B.B., Stowe-Evans, E.L., Harper, R.M., Celaya, R.B., Ljung, K., Sandberg, R. and Liscum, E. (2008) Disruptions in AUX1-dependent auxin influx alter hypocotyl phototropism in Arabidopsis. *Molecular Plant*, **1**, 129-144.

Subramanian, S., Stacey, G. and Yu, O. (2007) Distinct, crucial roles of flavonoids during legume nodulation. *Trends in Plant Science*, **12**, 282-285.

Sugiyama, A., Shitan, N., Sato, S., Nakamura, Y., Tabata, S. and Yazaki, K. (2006) Genome-wide analysis of ATP-binding cassette (ABC) proteins in a model legume plant, Lotus japonicus: comparison with Arabidopsis ABC protein family. *DNA Research*, **13**, 205-228.

Sukumar, P., Edwards, K.S., Rahman, A., DeLong, A. and Muday, G.K. (2009) PINOID Kinase Regulates Root Gravitropism through Modulation of PIN2-Dependent Basipetal Auxin Transport in Arabidopsis. *Plant Physiology*, **150**, 722-735.

Surpin, M., Rojas-Pierce, M., Carter, C., Hicks, G.R., Vasquez, J. and Raikhel, N.V. (2005) The power of chemical genomics to study the link between endomembrane system components and the gravitropic response. *Proceedings of the National Academy of Sciences of the United States of America*, **102**, 4902-4907.

Swarup, K., Benková, E., Swarup, R., Casimiro, I., Peret, B., Yang, Y., Parry, G., Nielsen, E., De Smet, I., Vanneste, S., Levesque, M.P., Carrier, D., James, N., Calvo, V., Ljung, K., Kramer, E., Roberts, R., Graham, N., Marillonnet, S., Patel, K., Jones, J.D.G., Taylor, C.G., Schachtman, D.P., May, S., Sandberg, G., Benfey, P., Friml, J., Kerr, I., Beeckman, T., Laplaze, L. and Bennett, M.J. (2008) The auxin influx carrier LAX3 promotes lateral root emergence. *Nature Cell Biology*, **10**, 946-954.

Swarup, R., Friml, J., Marchant, A., Ljung, K., Sandberg, G., Palme, K. and Bennett, M. (2001) Localization of the auxin permease AUX1 suggests two functionally distinct hormone transport pathways operate in the Arabidopsis root apex. *Genes & Development*, **15**, 2648-2653.

Tanaka, H., Dhonukshe, P., Brewer, P.B. and Friml, J. (2006) Spatiotemporal asymmetric auxin distribution: a means to coordinate plant development. *Cellular and Molecular Life Sciences*, **63**, 2738-2754.

Taylor, L.P. and Grotewold, E. (2005) Flavonoids as developmental regulators. *Current Opinion in Plant Biology*, **8**, 317-323.

Teh, O.K. and Moore, I. (2007) An ARF-GEF acting at the Golgi and in selective endocytosis in polarized plant cells. *Nature*, **448**, 493-496.

Terasaka, K., Blakeslee, J.J., Titapiwatanakun, B., Peer, W.A., Bandyopadhyay, A., Makam, S.N., Lee, O.R., Richards, E.L., Murphy, A.S., Sato, F. and Yazaki, K. (2005) PGP4, an ATP binding cassette P-glycoprotein, catalyzes auxin transport in Arabidopsis thaliana roots. *Plant Cell*, **17**, 2922-2939.

Terasaka, K., Shitan, N., Sato, F., Maniwa, F., Ueda, K. and Yazaki, K. (2003) Application of vanadate-induced nucleotide trapping to plant cells for detection of ABC proteins. *Plant and Cell Physiology*, **44**, 198-200.

Theodoulou, F.L. (2000) Plant ABC transporters. *Biochimica Et Biophysica Acta-Biomembranes*, **1465**, 79-103.

Tian, Q., Uhlir, N.J. and Reed, J.W. (2002) Arabidopsis SHY2/IAA3 inhibits auxin-regulated gene expression. *Plant Cell*, **14**, 301-319.

Timpte, C. (2001) Auxin binding protein: curiouser and curiouser. *Trends in Plant Science*, **6**, 586-590.

Titapiwatanakun, B., Blakeslee, J.J., Bandyopadhyay, A., Yang, H., Mravec, J., Sauer, M., Cheng, Y., Adamec, J., Nagashima, A., Geisler, M., Sakai, T., Friml, J., Peer, W.A. and Murphy, A.S. (2009) ABCB19/PGP19 stabilises PIN1 in membrane microdomains in Arabidopsis. *Plant Journal*, **57**, 27-44.

Titapiwatanakun, B. and Murphy, A.S. (2009) Post-transcriptional regulation of auxin transport proteins: cellular trafficking, protein phosphorylation, protein maturation, ubiquitination, and membrane composition. *Journal of Experimental Botany*, **60**, 1093-1107.

Tiwari, S.B., Hagen, G. and Guilfoyle, T. (2003) The roles of auxin response factor domains in auxin-responsive transcription. *Plant Cell*, **15**, 533-543.

Tiwari, S.B., Wang, X.J., Hagen, G. and Guilfoyle, T.J. (2001) AUX/IAA proteins are active repressors, and their stability and activity are modulated by auxin. *Plant Cell*, **13**, 2809-2822.

Treml, B.S., Winderl, S., Radykewicz, R., Herz, M., Schweizer, G., Hutzler, P., Glawischnig, E. and Ruiz, R.A.T. (2005) The gene ENHANCER OFPINOID controls cotyledon development in the Arabidopsis embryo. *Development*, **132**, 4063-4074.

Treutter, D. (2005) Significance of flavonoids in plant resistance and enhancement of their biosynthesis. *Plant Biology*, **7**, 581-591.

Tromas, A., Paponov, I. and Perrot-Rechenmann, C. (2010) AUXIN BINDING PROTEIN 1: functional and evolutionary aspects. *Trends in Plant Science*, **15**, 436-446.

Ugartechea-Chirino, Y., Swarup, R., Swarup, K., Peret, B., Whitworth, M., Bennett, M. and Bougourd, S. (2010) The AUX1 LAX family of auxin influx carriers is required for the establishment of embryonic root cell organization in Arabidopsis thaliana. *Annals of Botany*, **105**, 277-289.

Utsuno, K., Shikanai, T., Yamada, Y. and Hashimoto, T. (1998) AGR, an Agravitropic locus of Arabidopsis thaliana, encodes a novel membrane-protein family member. *Plant and Cell Physiology*, **39**, 1111-1118.

van den Brule, S. and Smart, C.C. (2002) The plant PDR family of ABC transporters. *Planta*, **216**, 95-106.

Vandenbussche, F., Petrášek, J., Žádníková, P., Hoyerová, K., Pešek, B., Raz, V., Swarup, R., Bennett, M., Zažímalová, E., Benková, E. and Van Der Straeten, D. (2010) The auxin influx carriers AUX1 and LAX3 are involved in auxin-ethylene interactions during apical hook development in Arabidopsis thaliana seedlings. *Development*, **137**, 597-606.

Vanderbliek, A.M. and Borst, P. (1989) MULTIDRUG RESISTANCE. *Advances in Cancer Research*, **52**, 165-203.

Vanneste, S. and Friml, J. (2009) Auxin: a trigger for change in plant development. *Cell*, **136**, 1005-1016.

Venis, M.A. (1977a) AFFINITY LABELS FOR AUXIN BINDING-SITES IN CORN COLEOPTILE MEMBRANES. *Planta*, **134**, 145-149.

Venis, M.A. (1977b) SOLUBILIZATION AND PARTIAL-PURIFICATION OF AUXIN-BINDING SITES OF CORN MEMBRANES. *Nature*, **266**, 268-269.

Verrier, P.J., Bird, D., Buria, B., Dassa, E., Forestier, C., Geisler, M., Klein, M., Kolukisaoglu, U., Lee, Y., Martinoia, E., Murphy, A., Rea, P.A., Samuels, L., Schulz, B., Spalding, E.P., Yazaki, K. and Theodoulou, F.L. (2008) Plant ABC proteins - a unified nomenclature and updated inventory. *Trends in Plant Science*, **13**, 151-159.

Vieten, A., Sauer, M., Brewer, P.B. and Friml, J. (2007) Molecular and cellular aspects of auxin-transport-mediated development. *Trends in Plant Science*, **12**, 160-168.

Ward, A., Reyes, C.L., Yu, J., Roth, C.B. and Chang, G. (2007) Flexibility in the ABC transporter MsbA: Alternating access with a twist. *Proceedings of the National Academy of Sciences of the United States of America*, **104**, 19005-19010.

Weijers, D., Benkova, E., Jager, K.E., Schlereth, A., Hamann, T., Kientz, M., Wilmoth, J.C., Reed, J.W. and Jurgens, G. (2005) Developmental specificity of auxin response by pairs of ARF and Aux/IAA transcriptional regulators. *Embo Journal*, **24**, 1874-1885.

Weijers, D. and Jurgens, G. (2004) Funneling auxin action: specificity in signal transduction. *Current Opinion in Plant Biology*, **7**, 687-693.

Weijers, D. and Jurgens, G. (2005) Auxin and embryo axis formation: the ends in sight? *Current Opinion in Plant Biology*, **8**, 32-37.

Weijers, D., van Hamburg, J.P., van Rijn, E., Hooykaas, P.J.J. and Offringa, R. (2003) Diphtheria toxin-mediated interregional communication seed development. *Plant Physiology*, **133**, 1882-1892.

Went, F.W. (1926) On growth-accelerating substances in the coleoptile of *Avena sativa*. *Proc. Kon. Ned. Akad. Wet.*, **30**, 10-19.

Went, F.W. and Thimann, K.V. (1937) *Phytohormones* New York: The Macmillan Company.

Willemsen, V., Friml, J., Grebe, M., van den Toorn, A., Palme, K. and Scheres, B. (2003) Cell polarity and PIN protein positioning in Arabidopsis require STEROL METHYLTRANSFERASE1 function. *Plant Cell*, **15**, 612-625.

Windsor, B., Roux, S.J. and Lloyd, A. (2003) Multiherbicide tolerance conferred by AtPgp1 and apyrase overexpression in Arabidopsis thaliana. *Nature Biotechnology*, **21**, 428-433.

Winkel-Shirley, B. (2002) Biosynthesis of flavonoids and effects of stress. *Current Opinion in Plant Biology*, **5**, 218-223.

Wisniewska, J., Xu, J., Seifertová, D., Brewer, P.B., Růžička, K., Blilou, I., Rouquie, D., Scheres, B. and Friml, J. (2006) Polar PIN localization directs auxin flow in plants. *Science*, **312**, 883-883.

Woodward, A.W. and Bartel, B. (2005) Auxin: Regulation, action, and interaction. *Annals of Botany*, **95**, 707-735.

Wu, G., Lewis, D.R. and Spalding, E.P. (2007) Mutations in Arabidopsis multidrug resistance-like ABC transporters separate the roles of acropetal and basipetal auxin transport in lateral root development. *Plant Cell*, **19**, 1826-1837.

Wu, G., Otegui, M.S. and Spalding, E.P. (2010) The ER-Localized TWD1 Immunophilin Is Necessary for Localization of Mulitdrug Resistance-Like Proteins Required for Polar Auxin Transport in *Arabidopsis* Roots. *Plant Cell*, **22**, 3295-3304.

Xu, J., Hofhuis, H., Heidstra, R., Sauer, M., Friml, J. and Scheres, B. (2006) A molecular framework for plant regeneration. *Science*, **311**, 385-388.

Yang, H.B. and Murphy, A.S. (2009) Functional expression and characterization of Arabidopsis ABCB, AUX 1 and PIN auxin transporters in Schizosaccharomyces pombe. *Plant Journal*, **59**, 179-191.

Yang, Y.D., Hammes, U.Z., Taylor, C.G., Schachtman, D.P. and Nielsen, E. (2006) High-affinity auxin transport by the AUX1 influx carrier protein. *Current Biology*, **16**, 1123-1127.

Yazaki, K. (2006) ABC transporters involved in the transport of plant secondary metabolites. *Febs Letters*, **580**, 1183-1191.

Young, G.B., Jack, D.L., Smith, D.W. and Saier, M.H. (1999) The amino acid/auxin : proton symport permease family. *Biochimica Et Biophysica Acta-Biomembranes*, **1415**, 306-322.

Zažímalová, E., Murphy, A., Yang, H., Hoyerová, K. and Hošek, P. (2010) Auxin transporters-why so many? *Cold Spring Harb Perspect Biol*, **2**, a001552.

Zažímalová, E. and Napier, R. (2003) Points of regulation for auxin action. *Plant Cell Rep*, **21**, 625-634.

Zhang, J., Nodzynski, T., Pencik, A., Rolcik, J. and Friml, J. (2010) PIN phosphorylation is sufficient to mediate PIN polarity and direct auxin transport. *Proceedings of the National Academy of Sciences of the United States of America*, **107**, 918-922.

Zhang, S.H. and Morris, M.E. (2003) Effects of the flavonoids biochanin A, morin, phloretin, and silymarin on P-glycoprotein-mediated transport. *Journal of Pharmacology and Experimental Therapeutics*, **304**, 1258-1267.

Zhao, J. and Dixon, R.A. (2010) The 'ins' and 'outs' of flavonoid transport. *Trends in Plant Science*, **15**, 72-80.

Zhao, Y.D., Christensen, S.K., Fankhauser, C., Cashman, J.R., Cohen, J.D., Weigel, D. and Chory, J. (2001) A role for flavin monooxygenase-like enzymes in auxin biosynthesis. *Science*, **291**, 306-309.

Zhao, Y.D., Hull, A.K., Gupta, N.R., Goss, K.A., Alonso, J., Ecker, J.R., Normanly, J., Chory, J. and Celenza, J.L. (2002) Trp-dependent auxin biosynthesis in Arabidopsis: involvement of cytochrome P450s CYP79B2 and CYP79B3. *Genes & Development*, **16**, 3100-3112.

Zhou, H.W., Nussbaumer, C., Chao, Y. and DeLong, A. (2004) Disparate roles for the regulatory A subunit isoforms in Arabidopsis protein phosphatase 2A. *Plant Cell*, **16**, 709-722.